

TERMOMECCANICA CENTRIFUGAL PUMP HANDBOOK

**TM.P S.p.A. - Termomeccanica Pompe**

Via del Molo, 3 - 19126 La Spezia - Italy  
Tel. +39(0)187 552.512 - fax +39(0)187 552.506  
<http://www.termomeccanica.com>  
e-mail: [pumps@termomeccanica.com](mailto:pumps@termomeccanica.com)



**TERMOMECCANICA**  
**CENTRIFUGAL PUMP**  
**HANDBOOK**

ISBN 88-900996-0-7



Nº 00423

TERMOMECCANICA  
**CENTRIFUGAL PUMP  
HANDBOOK**

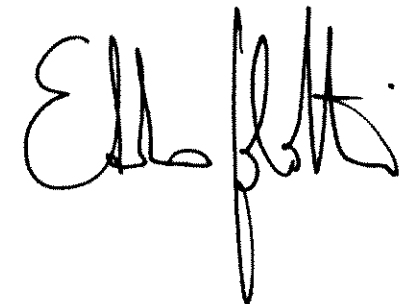
..... *dedicated to those who believe  
in our Company,  
in work and innovation.*

This Handbook has been published to celebrate the ninetieth anniversary of the Termomeccanica foundation.

The aim is to provide newcomers with an instrument to help them approach the field of centrifugal pumps, and more experienced people with an effective support in their daily work.

We would like to take the opportunity to express our thanks to the members of the Design, Engineering, Product Development, Quality Assurance and After Sales Service Departments, who have made an essential contribution in transferring and condensing the experience of the Company into this Handbook.

**The Managing Director**  
Edoardo Garibotti



Published by:

TM.P. S.p.A. Termomeccanica Pompe - La Spezia - Italy

**First edition 2003**

*Copyright TM.P. S.p.A. Termomeccanica Pompe  
All right reserved. No parts of this publication may be reproduced  
stored in a retrieval system or transmitted in any form or by  
any means, electronic, electrostatic, magnetic tape, mechanical,  
photocopying, recording or otherwise, without permission in writing  
form the publishers.*

ISBN 88-900996-0-7

# CONTENTS

Preface	iii
<b>A. Hydraulic fundamentals</b>	<b>1</b>
<i>A.1. Hydraulic principles of centrifugal pumps</i>	1
<i>A.2. Specific speed</i>	3
<i>A.3. Total head of the pump</i>	4
<i>A.4. Power required by the pump</i>	6
<i>A.5. Losses in the pump</i>	6
<i>A.6. Pump efficiency</i>	11
<b>B. Operation of centrifugal pumps</b>	<b>12</b>
<i>B.1. Characteristics</i>	12
B.1.1. Centrifugal pump characteristics	12
B.1.2. System characteristics	13
B.1.3. Matching of pump system characteristics	15
<i>B.2. Control possibilities</i>	17
B.2.1. Throttling control	17
B.2.2. By-pass control	18
B.2.3. Inlet guide vane control	20
B.2.4. Impeller blade adjustment	21
B.2.5. Speed control	23
B.2.6. Adjustment of impeller	24
B.2.7. Pumps working in series	26
B.2.8. Pumps working in parallel	28
<i>B.3. Start-up and shut-down of centrifugal pumps</i>	30
B.3.1. Starting torque of centrifugal pumps	30
B.3.2. Start-up time of a centrifugal pump	32
B.3.3. Run-out of centrifugal pump-motor system	33
B.3.4. Start-up against a closed valve	36
B.3.5. Start-up against an open delivery valve	37
B.3.6. Start-up against a closed non-return (check) valve	38
<i>B.4. Operating range of centrifugal pumps</i>	40
B.4.1. Power required by zero flow as a function of the specific speed	41
B.4.2. Poor hydraulic behaviour in the part-load range	41
B.4.3. Minimum flow determination by admissible temperature rise	42

<b>c. Cavitation in pump</b>	48
<i>C.1. Physical principles</i>	48
<i>C.2. Cavitation at the impeller inlet</i>	51
<i>C.3. NPSH characteristics</i>	52
<i>C.4. Types of cavitation</i>	57
<i>C.5. Recirculation at the pump inlet</i>	59
<i>C.6. Suction specific speed</i>	61
<i>C.7. Cavitation erosion</i>	63
<i>C.8. Cavitation safety values</i>	66
<i>C.9. Methods for improving the pump-system cavitation performance</i>	70
<b>d. Basic pump designs</b>	72
<i>D.1. Designs of hydraulic elements</i>	72
<i>D.2. Mechanical design</i>	73
D.2.1. Centrifugal pump types – Overhung	73
D.2.2. Centrifugal pump types – Between Bearings	74
D.2.3. Centrifugal pump types – Vertically Suspended	75
<i>D.3. Main application areas</i>	76
D.3.1. Water	76
D.3.2. Power generation	76
D.3.3. Oil and gas	76
D.3.4. Industry	76
<b>e. Mechanical components of a centrifugal pump</b>	77
<i>E.1 Bearings</i>	77
E.1.1. Rolling contact bearings	78
E.1.2. Hydrodynamic radial bearings	83
E.1.3. Hydrodynamic thrust bearings	87
E.1.4. Product-lubricated hydrodynamic bearings	90
E.1.5. Hydrostatic and combined bearings	93
<i>E.2. Seals</i>	94
E.2.1. Static seals	94
E.2.1.1. Flat gaskets	94
E.2.1.2. O-rings and C-rings	96
E.2.2. Dynamic seals – shaft seals	97
E.2.2.1. Stuffing box packings	97
E.2.2.2. Mechanical seals	99
E.2.2.3. Hydrodynamic seals	104
E.2.3. Canned motor pumps	105

<i>E.3. Couplings</i>	106
E.3.1. Rigid couplings	106
E.3.2. Flexible couplings	107
E.3.2.1. Permanent elastic couplings	108
E.3.2.2. Torsional-stiff flexible couplings	109
E.3.3. Hydrodynamic couplings	112
E.3.4. Magnetic couplings	113
<b>F. Hydraulic thrust</b>	114
<i>F.1. Axial thrust</i>	114
F.1.1. Origins of axial thrust	114
F.1.2. Calculation of the hydraulic axial thrust	115
F.1.3. Design possibilities for reducing axial thrust	117
F.1.4. Axial thrust in pump start regimes	122
<i>F.2. Radial thrust</i>	123
F.2.1. Origins of radial thrust	123
F.2.2. Reduction of radial thrust	123
F.2.3. Determination of radial thrust	126
<b>g. Noise emission from centrifugal pumps</b>	128
<i>G.1. Basic acoustic terminology</i>	128
<i>G.2. Origin of noise in pumps</i>	129
G.2.1. Liquid (hydraulic) noise sources	130
G.2.2. Mechanical noise sources	131
<i>G.3. Measuring noise</i>	132
G.3.1. Standard EN 12693	133
G.3.2. Examples of SPL measurement results	134
<i>G.4. Ways of abating noise</i>	135
G.4.1. Noise reduction at sources	135
G.4.2. Interruption of noise transmission	138
<b>H. Vibration in centrifugal pumps</b>	139
<i>H.1. Introduction</i>	139
<i>H.2. Forces acting on the pump rotor</i>	140
H.2.1. Steady forces	140
H.2.2. Excitation forces	142
H.2.3. Interaction forces	144

<b>H.3. Rotordynamic behaviour of pumps</b>	145
H.3.1. Rotordynamic analysis	145
H.3.2. Possibilities for improved rotordynamic behaviour in centrifugal pumps	148
<b>H.4. Measuring bearing and shaft vibration</b>	150
H.4.1. General	150
H.4.2. Measurement of vibration	150
H.4.3. Standards related to vibration	152
H.4.4. Vibration limits	153
<b>i. Monitoring, diagnostic and early failure detection</b>	157
<b>I.1. General</b>	157
<b>I.2. Monitoring of large and high speed pumps</b>	158
<b>I.3. Monitoring of process pumps</b>	159
<b>I.4. Diagnostic based on vibration analysis</b>	160
<b>J. Pump intake and suction piping design</b>	162
<b>J.1. Open sump intakes</b>	162
J.1.1. Individual installation	163
J.1.2. Multiple parallel installation	163
<b>J.2. Can-type intakes</b>	167
J.2.1. Open bottom can intakes	168
J.2.2. Closed bottom can intakes	169
<b>J.3. Wet pits for solid-bearing liquids</b>	169
<b>J.4. Pump suction piping</b>	172
J.4.1. Common intakes for suction piping	173
J.4.2. Suction tank intakes with vortex breakers	174
J.4.3. Suction pipe configuration	175
<b>J.5. Model study of intake structures</b>	176
J.5.1. Need for model study	176
J.5.2. Hydraulic similarity	176
J.5.3. Instrumentation and measuring techniques	177
J.5.4. Acceptance criteria	178
<b>k. Pumping special liquids</b>	179
<b>K.1. Pumping viscous liquids</b>	179
K.1.1. Definition of viscosity	179

K.1.2. Description of a Newtonian fluid	179
K.1.3. Effects of fluid viscosity on pump characteristics	180
K.1.4. Instructions for determining viscous fluid pump characteristics	183
<b>K.2. Pumping gas-liquid mixtures</b>	185
K.2.1. Capabilities of standard pump designs	185
K.2.2. Possible improvements and special designs	187
<b>K.3. Pumping solid-bearing fluids</b>	188
K.3.1. General description of flow regimes	188
K.3.2. Non-settling solid-bearing fluids	189
K.3.3. Settling solid-bearing fluids	189
K.3.4. Design guidelines and speed limitation	192
<b>K.4. Pumping hydrocarbons</b>	192
<b>L. Corrosion and material selection</b>	195
<b>L.1. General</b>	195
<b>L.2. Factors influencing corrosion</b>	195
<b>L.3. Corrosive properties of the liquid being pumped</b>	197
<b>L.4. Types of corrosion</b>	198
L.4.1. Inhomogeneities in a material: galvanic corrosion	198
L.4.2. Pitting corrosion	199
L.4.3. Crevice corrosion	200
L.4.4. Intergranular corrosion	200
L.4.5. Corrosion caused by interaction with cavitation	201
L.4.6. Uniform corrosion and the influence of flow velocity	201
<b>L.5. Selection of materials selection for a pump</b>	203
L.5.1. Optimising the life cycle costs	203
L.5.2. Influence of the fluid properties on corrosion fatigue	204
L.5.3. Influence of material properties on pitting resistance equivalent	204
L.5.4. Choice of materials for important pump elements	205
L.5.4.1. Pump shaft	205
L.5.4.2. Impellers	205
L.5.4.3. Casing	206
L.5.4.4. Wearing rings	206
L.5.5. Materials frequently used for the wetted parts of the pump	207
<b>m. Quality assurance</b>	212
<b>M.1. General</b>	212
<b>M.2. Quality Assurance of Termomeccanica Pumps S.p.A.</b>	212

<b>N. Testing</b>	215
<b><i>N.1. Hydrostatic tests</i></b>	215
<b><i>N.2. Performance and NPSH tests</i></b>	215
N.2.1. General	215
N.2.2. Testing arrangements	217
N.2.3. Measuring accuracy, permissible reading fluctuations and performance tolerances	221
N.2.4. Fulfilment of guarantee	223
N.2.5. Conversion of test results	224
<b><i>N.3. Optional tests</i></b>	226
<b>o. Life cycle costs</b>	227
<b><i>O.1. Introduction</i></b>	227
<b><i>O.2. Elements of LCC and their definitions</i></b>	228
O.2.1. Calculation of life cycle costs	228
O.2.2. Description of LCC elements	228
<b>P. General tables</b>	234
<b>Nomenclature</b>	240
<b>Graphical symbols</b>	244
<b>Literature</b>	245



# A. HYDRAULIC FUNDAMENTALS

## A.1. Hydraulic principles of centrifugal pumps

Centrifugal pumps are hydrodynamic machines, in which a rotating impeller continually transmits mechanical work from the driving machine to the fluid. The energy process takes place in two successive stages. In the first stage, the rotational motion of the impeller causes the growth of the kinetic energy of the fluid. In the second stage, where the fluid passes through several channels of different cross-section, the kinetic energy is converted into potential pressure energy. The flow through the impeller is usually represented by velocity triangles (vector diagrams). Fig.A.1. shows the flow through the impeller of a radial pump, and Fig.A.2. the flow through an axial impeller.

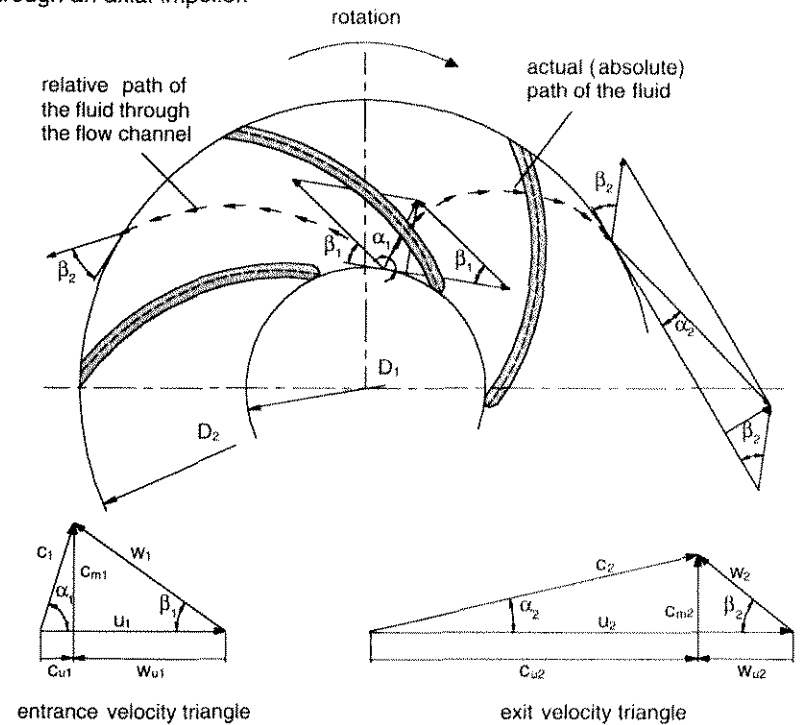


Fig.A.1 Velocity diagrams for radial-flow impellers

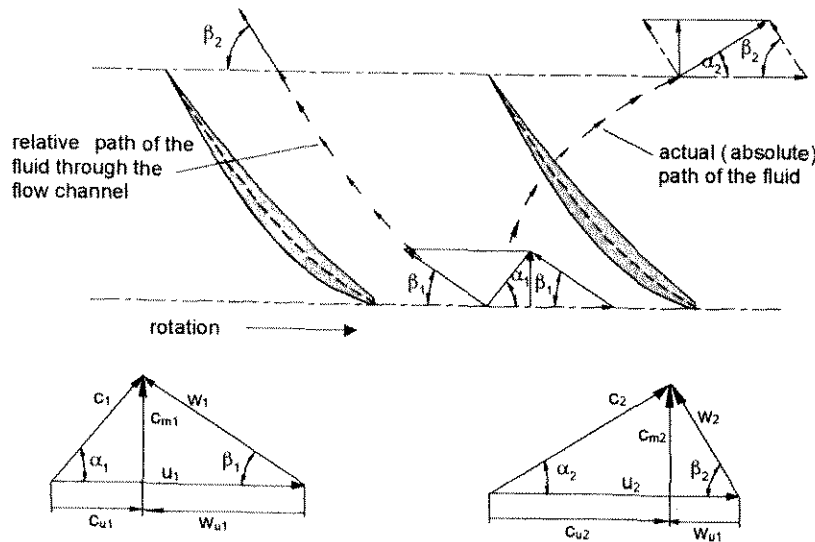


Fig.A.2 Velocity diagrams for axial-flow impellers

The basic equation which describes the relationship between the flow of an ideal fluid (assuming no friction, and an incompressible fluid) and the external energy is Euler's turbine equation. It can be written as Euler's momentum equation in the following way.

$$M_{imp} = \rho \cdot Q_{imp} \cdot (c_{u2} \cdot r_2 - c_{u1} \cdot r_1)$$

In the case of a pump,  $M_{imp}$  is the blade torque transferred from the impeller to the fluid. If the shaft rotates with an angular speed  $\omega$ , the increase of energy in the impeller is:

$$P_{imp} = M_{imp} \cdot \omega = \rho \cdot Q_{imp} \cdot (c_{u2} \cdot u_2 - c_{u1} \cdot u_1)$$

Power transferred to the fluid by the impeller per unit mass flow is defined as useful specific work done by the impeller:

$$Y_{imp} = \frac{P_{imp}}{\rho \cdot Q_{imp}} = c_{u2} \cdot u_2 - c_{u1} \cdot u_1$$

Another way of expressing Euler's equation is from the velocities:

$$Y_{imp} = \frac{1}{2} \left( (c_2^2 - c_1^2) + (u_2^2 - u_1^2) + (w_1^2 - w_2^2) \right)$$

where the first and the second parts represent the increase of kinetic energy, while the third part represents the increase of pressure energy. After some trigonometric work Euler's equation becomes:

$$Y_{imp} = (u_2 \cdot c_{u2} - u_1 \cdot c_{u1})$$

The energy transferred to the fluid by the pump impeller  $Y_{imp}$  can be divided into useful pump specific work  $Y$  and hydraulic losses  $Y_{loss}$ :

$$Y_{imp} = Y + Y_{loss}$$

The hydraulic losses are expressed as pump hydraulic efficiency by the ratio:

$$\eta_h = \frac{Y}{Y_{imp}} = \frac{Y}{Y + Y_{loss}}$$

Hydraulic efficiency includes hydraulic losses in all pump elements between the suction and discharge flanges (intake, impeller, diffuser, outlet).

## A.2. Specific speed

Pump specific speed  $nq$  is a numeric value, which defines roughly the pump geometry and the shape of the pump characteristics. It includes the pump flow rate, head and rotational speed at the best efficiency point. It is not a dimensionless number and depends strongly on used units. There are many different definitions of specific speed. The two most frequently used expressions are given here.

In Europe the most frequently used expression for pump specific speed is:

$$nq = \frac{n \cdot \sqrt{Q}}{H^{0.75}}; \quad Q \text{ (m}^3\text{/s)}, H \text{ (m)}, n \text{ (rpm)}$$

In the USA the most frequently used expression is:

$$ns = \frac{n \cdot \sqrt{Q}}{H^{0.75}}; \quad Q \text{ (gpm)}, H \text{ (ft)}, n \text{ (rpm)}$$

The relationship between both is:

$$nq = \frac{1}{51.65} * ns$$

In the case of a double suction impeller, a half flow rate has to be used in the formula. H is the total head for one stage in the case of multi-stage pumps.

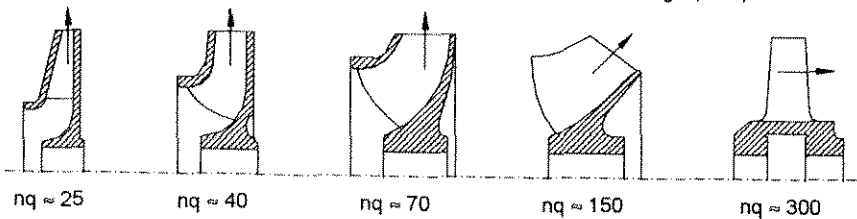


Fig.A.3 Typical shapes of different specific speed pump impellers

The value is the same for geometrically similar types of pumps regardless of the pump's size and speed. Considering the impeller meridional cross-section, the ratio of the outlet width to the outer diameter increases with nq. As the nq increases, the direction of the flow passing the impeller changes from a radial flow, where the fluid is discharged radially to the pump axis, through a mixed-flow (semi-axial, diagonal), to an axial direction. Fig.A.3. shows the relationship between the impeller geometry in meridional cross-section and the specific speed. The ranges are approximate and cannot be strictly applied. At some specific speeds two types of pump can be designed. For example, at nq=80, radial or mixed-flow pumps can be designed, and at nq=180 mixed-flow or axial type pumps can be designed.

### A.3. Total head of the pump (specific energy)

The pump specific energy is the useful total energy in the mass unit, which is supplied to the fluid by the pump. It is measured between the discharge and suction flanges. Usually the specific energy is expressed as the pump total head:

$$H = \frac{Y}{g}$$

The pump total head is independent of the density i.e. of the kind of fluid pumped. Theoretically a pump has the same total head, whether it pumps water, air or mercury. But it does not have the same pressure rise, which does depend on density:

$$\Delta p = \rho \cdot g \cdot H$$

Pressure rise  $Dp$  is measured with manometers. In addition to the pressure differences, all powers and thrusts are also proportional to the density.

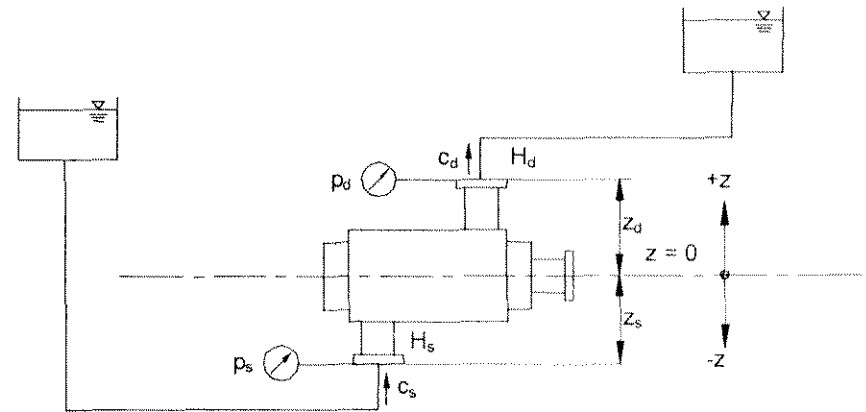


Fig.A.4 Total head of a pump

The total head consists of a static head ( $p/\rho \cdot g$ ), a geodetic head ( $z$ ), and a dynamic head ( $c^2/2 \cdot g$ ). The total head of the pump is the difference between the total heads at the discharge and at the suction flanges and is expressed by the Bernoulli equation (Fig.A.4.):

$$H = H_d - H_s = \left( \frac{p_d}{\rho \cdot g} + z_d + \frac{c_d^2}{2 \cdot g} \right) - \left( \frac{p_s}{\rho \cdot g} + z_s + \frac{c_s^2}{2 \cdot g} \right) = \frac{p_d - p_s}{\rho \cdot g} + (z_d - z_s) + \frac{c_d^2 - c_s^2}{2 \cdot g}$$

The first part of the equation represents the difference of the potential pressure energies between the discharge and suction flanges, the second part is the difference of the geodetic potential energies between the two flanges and the third part is the difference of the kinetic energies.

Usually the head is represented by the dimensionless head coefficient  $\psi$ . It is the ratio between the head per stage H and the head due to the circumferential velocity  $H_{u2}$ :

$$\psi = \frac{H}{H_{u2}} = \frac{2 \cdot g \cdot H}{u_2^2}$$

Fig.A.5. shows the range of the head coefficient  $\psi$  for the best efficiency point as a function of specific speed. The curve decreases with nq due to the fact that with the increase of nq the centrifugal part of the total head decreases (see Euler's equation for velocities in section A.1.) and is zero in axial pumps. If the head coefficient lies near the upper limit curve, the pump head characteristic is probably unstable in the case of low specific speed pumps. For getting stable characteristics, the head coefficient must lie near or even below the lower limit curve.

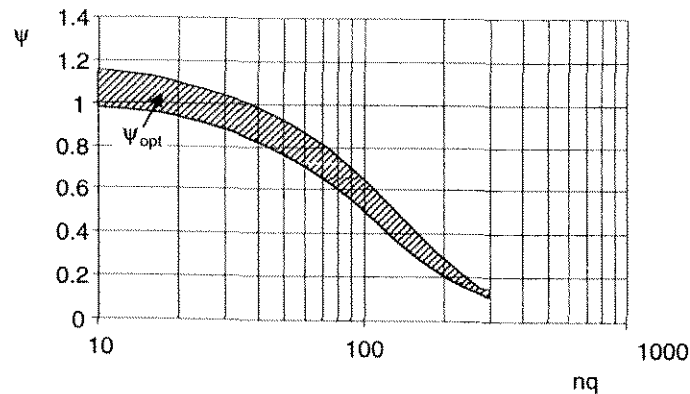


Fig.A.5 Pump head coefficient  $\psi$  for best efficiency point versus pump specific speed

#### A.4. Power required by the pump

The effective energy given to the fluid by a pump in a unit of time is called fluid power  $P_u$  (also pumping power, useful hydraulic power).

$$P_u = \rho \cdot Y \cdot Q = \rho \cdot g \cdot H \cdot Q$$

The power required by the pump (pump shaft power)  $P$  is higher, because in addition to the fluid power it also covers all the losses in the pump. The ratio between fluid power and pump shaft power is pump efficiency (pump total efficiency):

$$\eta = \frac{\rho \cdot g \cdot H \cdot Q}{P}$$

#### A.5. Losses in the pump

Losses can be divided into external and internal losses.

**External losses** are mechanical losses  $P_m$ , which are generated by friction in bearings and shaft seals. They cause no direct-warming up of the pumped fluid. Mecha

nical losses depend on mechanical efficiency.

$$\eta_m = \frac{P - P_m}{P}$$

**Internal losses** have many sources. They cause the warming-up of the pumped fluid.

**Volumetric losses**  $Q_v$  are the result of all leakage flows in the pump. In addition to the useful flow  $Q$ , the impeller pumps leakage flows:

$$Q_{imp} = Q + Q_v$$

Volumetric losses are:

- Volumetric losses through the sealing ring at the impeller inlet -  $Q_{sr}$
- Volumetric losses through the axial balancing device, if there is one (piston, disc, impeller holes) -  $Q_{bd}$
- In extreme cases, additional volumetric losses for auxiliary purposes such as feeding hydrostatic bearings, cooling pump elements, flushing, quenching the seal etc. -  $Q_a$

Volumetric losses can be expressed as volumetric efficiency:

$$\eta_v = \frac{Q}{Q_{imp}} = \frac{Q}{Q + Q_v}; \quad Q_v = Q_{sr} + Q_{bd} + Q_a$$

The power required to overcome all the volumetric losses is:

$$P_v = \rho \cdot g \cdot H_{th} \cdot (Q_{sr} + Q_{bd} + Q_a)$$

In multi-stage pumps there are additional volumetric losses through the sealing rings between the stages -  $P_{2s}$ . These volumetric losses do not go through the impeller.

**Hydraulic losses** are the result of friction and flow irregularities in all parts of the pump flow duct, from the suction to the discharge flanges. They are expressed as hydraulic efficiency:

$$\eta_h = \frac{H}{H_{th}} \quad \left( = \frac{Y}{Y_{imp}} \right)$$

$H_{th}$  is the theoretical pump head without hydraulic losses.

The power required to overcome the hydraulic losses is:

$$P_h = \rho \cdot g \cdot H \cdot Q \cdot (1/\eta_h - 1)$$

Friction losses rise with the square of the flow rate. The losses caused by incorrect inflow (shock losses) are zero at the best efficiency point, and rise to the left and right of it.

**Disc friction losses**  $P_{df}$  are also part of the hydraulic losses, and are induced by the rotational movement of the impeller outer walls in the fluid against the casing walls.

Similar frictional losses are generated by the rotation of the surfaces of the axial **thrust balancing devices** – pistons and discs,  $P_{bdf}$ .

At part load, flow recirculation occurs and **recirculation losses**  $P_{rec}$  are generated (see section C.4.). If the impeller inlet is designed correctly, the recirculation losses are zero at the best efficiency point. At shut-off and at part load the recirculation losses are the biggest consumer of shaft power.

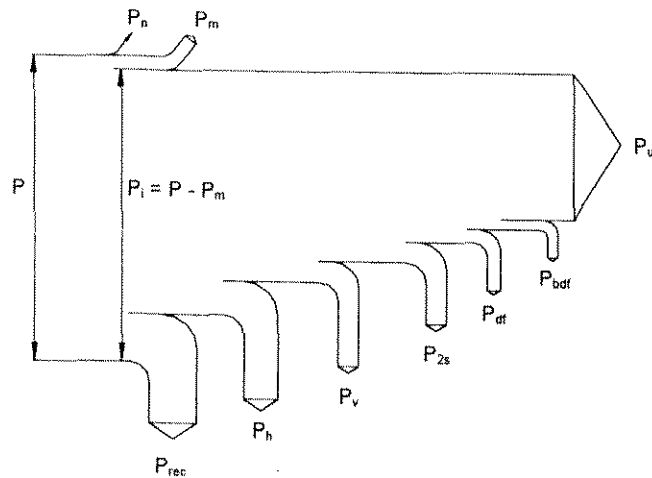


Fig.A.6 Centrifugal pump power balance

In pump operation a certain level of noise is induced depending on the circumferential speed, power input, pump type and fluid, and which also represents power losses  $P_n$ . They are very small compared to others and can be ignored. However, they are disturbing for the environment (see section G).

All the losses are presented graphically as the power balance in Fig.A.6.

The magnitudes of the different losses vary as a function of the flow rate. A typical distribution of the latter in a radial pump is given in Fig.A.7. It can be seen that hydraulic and volumetric losses reduce the pump head curve, while other losses affect directly only the pump power. Some losses (mechanical, disc friction, friction losses in balancing devices, volumetric losses between two stages) are practically independent of the flow rate. Recirculation losses appear only at part load.

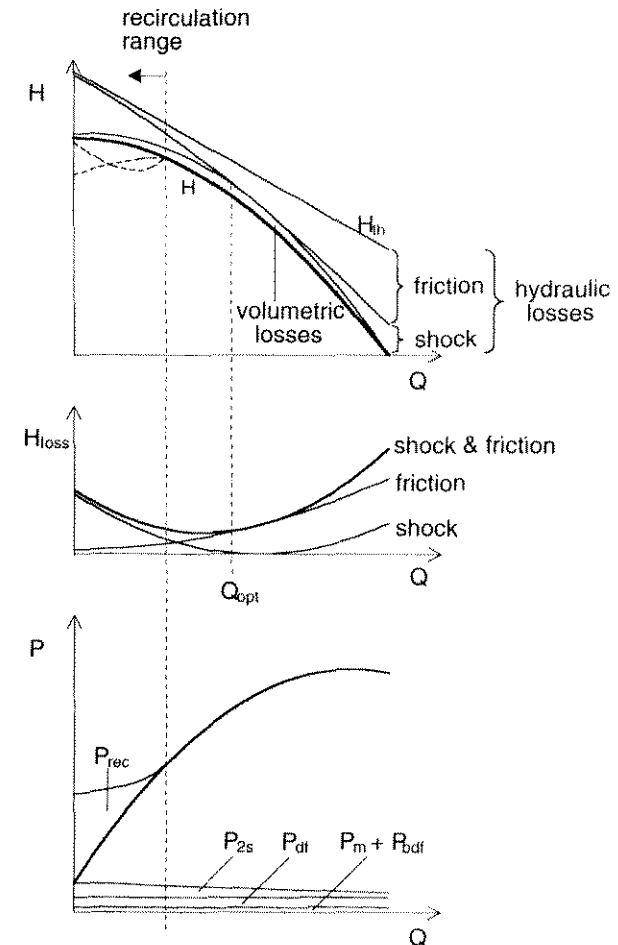


Fig.A.7 Effects of losses on pump characteristics

The magnitude of the different losses depends on the pump specific speed and the pump type. For the best efficiency point, the influence of the various main losses on the pump efficiency of radial volute pumps is shown schematically in Fig.A.8:

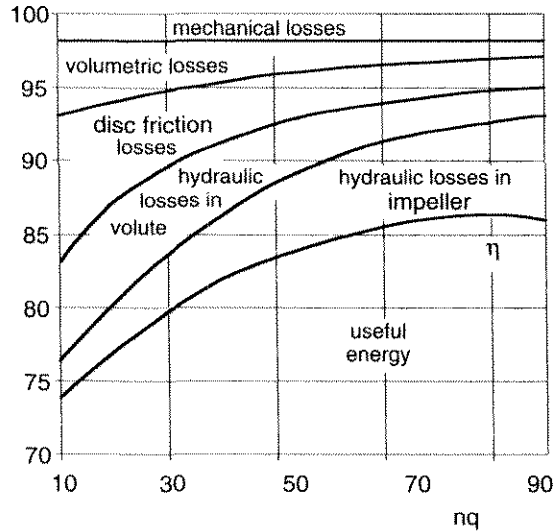


Fig.A.8 Approximate structure of losses in single-stage radial volute pump versus specific speed

Sometimes, especially in model tests, the expression "internal efficiency" is used. This is the ratio between fluid power and pump shaft power, reduced for mechanical losses.

$$\eta_i = \frac{\rho \cdot g \cdot H \cdot Q}{P - P_m}$$

### A.6. Pump efficiency

Many efficiency charts have been plotted on the basis of the statistics of published test results for actual centrifugal pumps of "good" designs. Some of them are very general and involve all types of pumps with specific speeds  $nq$  from 10 to 300. Others are more or less specialised. The diagram in Fig.A.9. shows an efficiency chart for radial pumps with specific speeds  $nq$  between appr. 5 and 60.

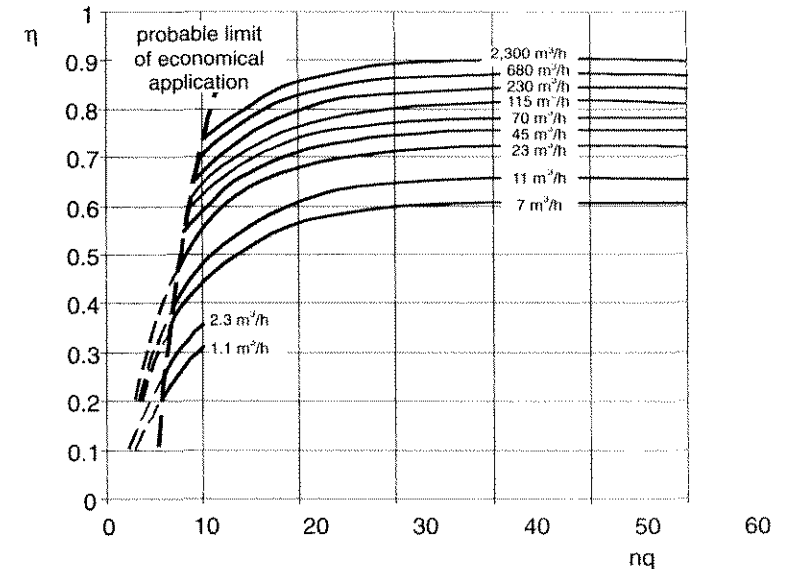


Fig.A.9 Efficiency of radial pumps as a function of specific speed and flow rate

The total pump efficiency is a function of pump geometry (specific speed) and of flow rate (Reynolds number). It can be seen that there is a certain specific speed at which the maximal efficiency can be reached: for radial pumps it is between  $nq=40$  and  $50$ . Left from the maximum, the pump efficiency decreases because of the rise of the proportion of losses, such as mechanical, disc friction, volumetric and hydraulic (friction) losses. Right from optimum the efficiency decreases because of the increase of hydraulic losses, influenced by flow irregularities in relatively wide flow channels.

The total pump efficiency increases with the flow rate, which is a function of pump size (impeller diameter) and pump speed, i.e. of Reynolds number. The proportion of friction, hydraulic and mechanical losses decreases with the increase of the flow rate at the same specific speed and absolute roughness. From the diagram it can be concluded that the efficiency of a small pump at high speed can be the same as of a large pump at low speed, if both have the same specific speed and optimal flow rate.

## B. OPERATION OF CENTRIFUGAL PUMPS

### B.1. Characteristics

#### B.1.1. Centrifugal pump characteristics

Characteristic curves showing on the vertical axis the pump total head  $H$ , power consumption  $P$ , total pump efficiency  $\eta$ , cavitation parameter  $NPSH_{3\%}$  and on the horizontal axis the flow rate  $Q$ , are called pump characteristics. These characteristics indicate the behaviour of a pump under changing flow conditions and are dependent on specific speed  $nq$ . For a comparison of characteristics, the dimensionless form of diagrams is used where the value 1,0 is at the best efficiency point (BEP). In Fig.B.1.1. the pump characteristics are shown for three different specific speeds. Curves 1 represent radial-flow pumps, curves 2 mixed-flow pumps and curves 3 axial-flow pumps. The following differences can be noted:

**Q-H chart:** The slope of the pump characteristic increases with specific speed. At higher specific speeds (axial-flow pumps) the pump characteristic becomes unstable.

**Q-P chart:** In radial-flow pumps, power consumption increases with the flow rate. Shut-off power (at  $Q=0$ ) increases with specific speed, and in pumps with  $nq$  80-100 the power consumption is practically independent of the flow rate. In axial-flow pumps the biggest power consumption is at shut-off, and decreases with the flow rate.

**Q- $\eta$  chart:** The region of high efficiency is wider in low specific speed pumps (in radial-flow pumps).

**Q-NPSH chart:** The NPSH characteristics shown in diagram Fig B.1.1. are  $NPSH_{3\%}$  (at 3% head drop). More favourable characteristics from the operating point of view are in pumps with a low specific speed, especially in the range of a flow rate higher than the BEP.

When recalculating pump characteristics to different speeds and sizes, equations called affinity law equations are used:

$$Q^*/Q = (n^*/n) \cdot (D^*/D)^3$$

$$H^*/H = (n^*/n)^2 \cdot (D^*/D)^2$$

$$P^*/P = (n^*/n)^3 \cdot (D^*/D)^5$$

$$NPSH^*/NPSH = (n^*/n)^2 \cdot (D^*/D)^2$$

These equations are valid when the total pump hydraulic geometry is scaled-up in the size ratio  $D^*/D$  and geometrical similarity is fulfilled.

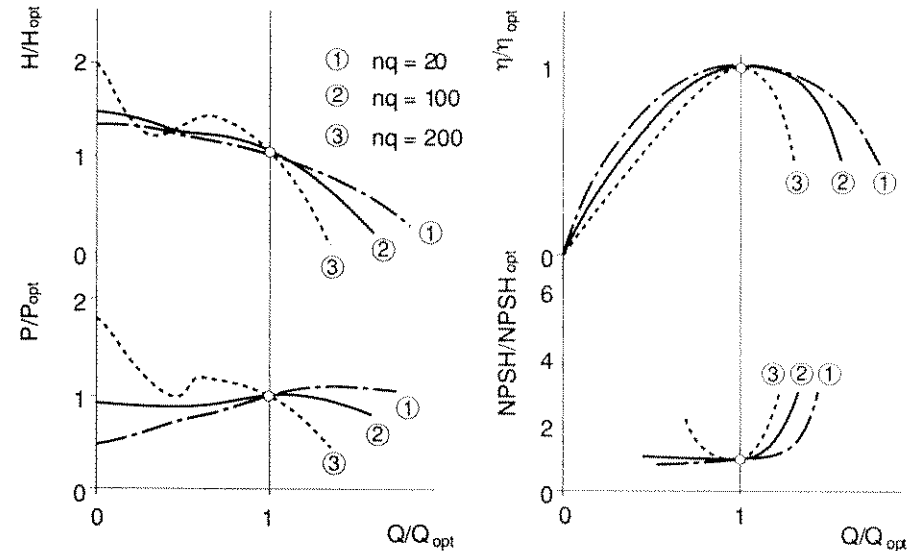


Fig.B.1.1 Pump characteristics in dimensionless form

#### B.1.2. System characteristics

The main task of the pump-motor unit is to transfer the energy to the fluid flowing through the pump. The total energy increase is presented as a sum of the static and dynamic heads and is called the system characteristic:

$$H_{sys} = H_{st} + H_{dyn}$$

The static head consists of the geodetic head and the static pressure difference between the suction and delivery vessels:

$$H_{st} = H_{geo} + (p_d - p_s) / \rho \cdot g$$

When the kinetic energies on the pump suction and delivery sides are identical, the dynamic head consists of the pressure losses in the pipeline  $H_{pip}$  and the losses in the control valve  $H_{cv}$ :

$$H_{dyn} = H_{pip} + H_{cv} = k \cdot Q^2$$

Pressure losses in the pipeline,  $H_{pip}$ , depend on the pipeline layout, the pipe length and diameter, and the resistance of other elements installed in the system.

The static part of the system characteristic is independent of flow rate  $Q$ , and the dynamic part of the system head increases with the square of flow rate  $Q$ . The resulting curve of the static and dynamic parts is a system characteristic which intersects the pump characteristic at the pump operating point. Three basic examples of a pumping system and its characteristics are shown in Figs.B.1.2. – B.1.4.

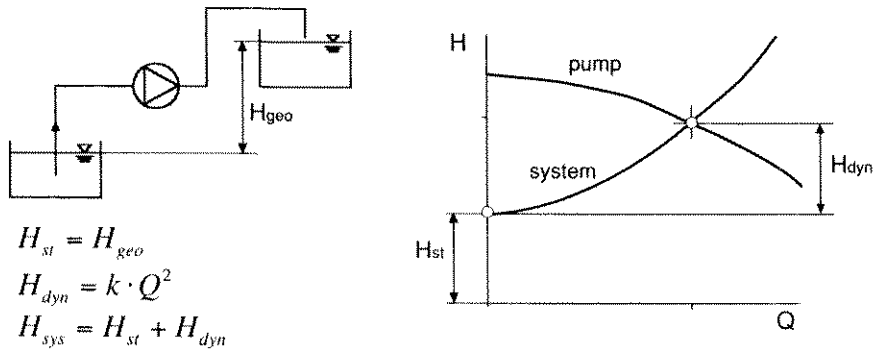


Fig.B.1.2 Fluid transport between two open reservoirs at different geodetic levels

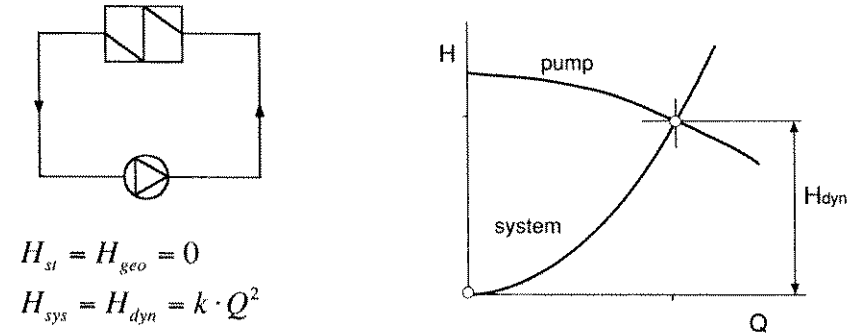


Fig.B.1.3 Fluid circulation in a closed system with installed heat exchanger

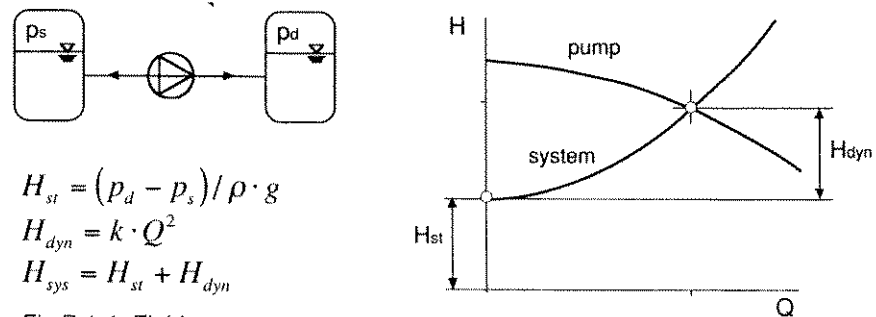


Fig.B.1.4 Fluid transport between two closed vessels

### B.1.3. Matching of pump and system characteristics

The pump operating point is represented as the intersection of the pump and system characteristics. With time, some pump or system parameters can change, and as a consequence the operating point is shifted along the pump Q-H curve. In Fig.B.1.5. an example with a changed geodetic head is shown. From the controllability point of view the slopes of the characteristics are also important. A pump with a flat Q-H characteristic causes a much bigger flow difference for the same geodetic change as a pump with a steep characteristic. When the system characteristic is nearly horizontal and the pump characteristic is flat great care is needed because flow rate control is very difficult.

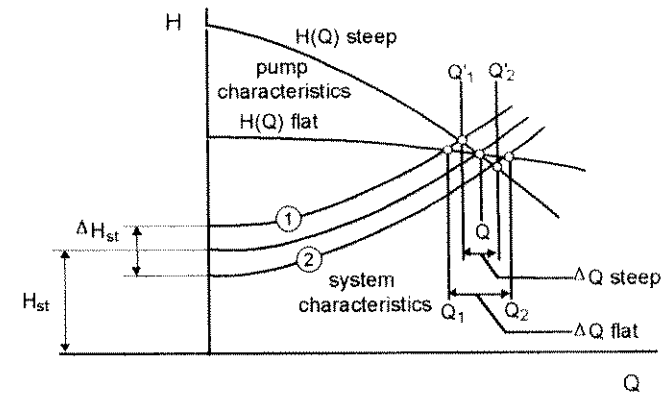


Fig.B.1.5 Operating points for flat and steep pump characteristics

Centrifugal pump characteristics are stable when the Q-H curve rises steadily with flow reduction. In low specific speed pumps with large impeller blade angles it can happen that the pump total head at zero flow is not the maximal. The part of the characteristic from  $Q=0$  to  $Q$  (at  $H_{max}$ ) is called the unstable part of the pump characteristic. Another type of unstable pump characteristic can be observed in axial-flow pumps (high specific speed pumps). This type of unstable Q-H curve is called a "saddle type" and can be seen in Fig.B.1.1. The characteristic is unstable at part flows and becomes stable again near  $Q=0$ .

A typical unstable characteristic is shown in Fig.B.1.6. where the system characteristic intersects the pump characteristic twice (operating points  $Q_{1-1}$  and  $Q_{1-2}$ ). It can happen therefore that the pump flow rate fluctuates between both operating points, which can also result in water hammer problems. In some extreme cases the left operating point is so close to  $Q=0$  that a danger exists of the pump overheating, because the total energy transferred to the pump is converted into heat. Starting a pump with an unstable pump characteristic is only possible when  $H_{st} < H_0$ .



Unstable Q-H curves should be avoided when pumps are operating in systems with a high proportion of static head and flat system curves. The same is valid when more pumps are running in parallel.

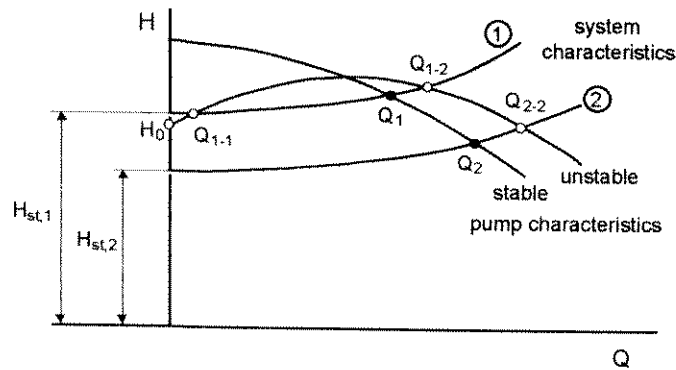
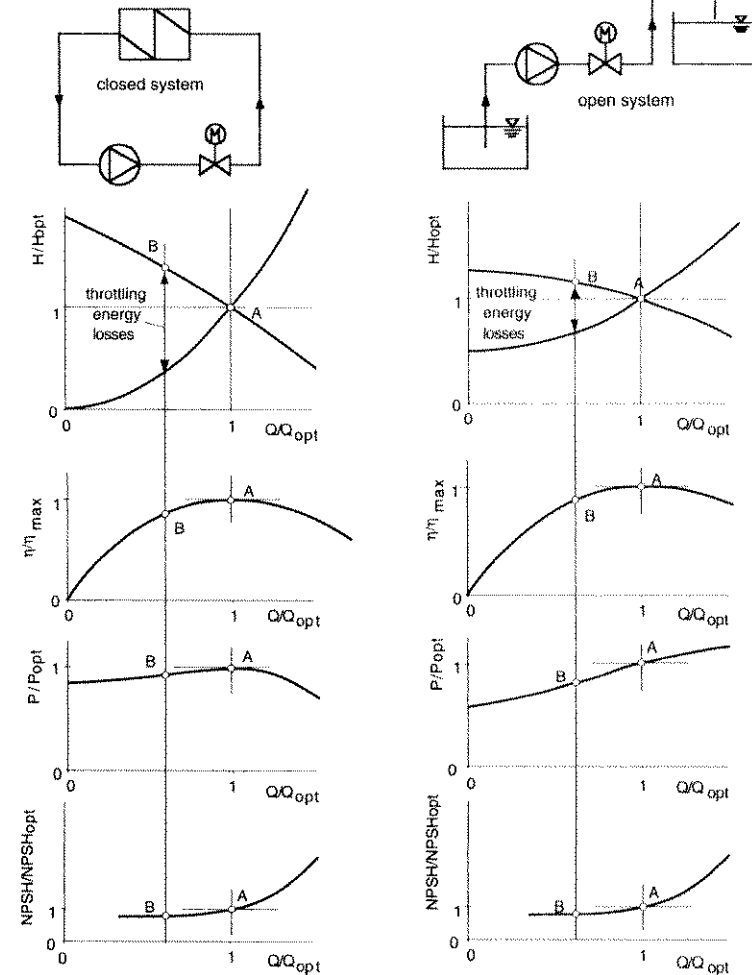


Fig.B.1.6 Operating points for stable and unstable pump characteristics

## B.2. Control possibilities

### B.2.1. Throttling control



A – operating points without throttling  
 B – operating points when applying throttling

Fig.B.2.1 Throttling control: schematic system layout and characteristics

The partial closing of a throttling device installed in a delivery pipeline changes the system characteristics, and as a consequence the required reduced flow rate is achieved. Throttling in a suction pipeline is not applicable due to excessive dete-

rioration of the NPSH available. Throttling control is used in many applications, especially in pumping systems with a lower installed power, due to simple operation and low investment costs. When applying throttling, it is important to choose the appropriate throttling device to avoid excessive vibration, noise and even cavitation in the latter (in the case of low back-pressure in the delivery pipeline).

Two examples of a system layout and its characteristics are shown in Fig.B.2.1. In throttling, the flow rate is reduced but, as a disadvantage of this control, energy losses occur in the throttling device. How big the energy losses are depends on the desired flow reduction, the slope of the Q-H curve and the ratio of the static/dynamic heads in the system characteristic. It can be seen from the diagrams in Fig.B.2.1. that lower losses occurs at a flat Q-H characteristic, a flat system characteristic and at a high percentage of static head in the total system head. Logically, throttling is applied in systems where pumps with a low specific speed are installed. The reason is because of the decrease in pump power when throttling is applied.

**B.2.2. By-pass control**

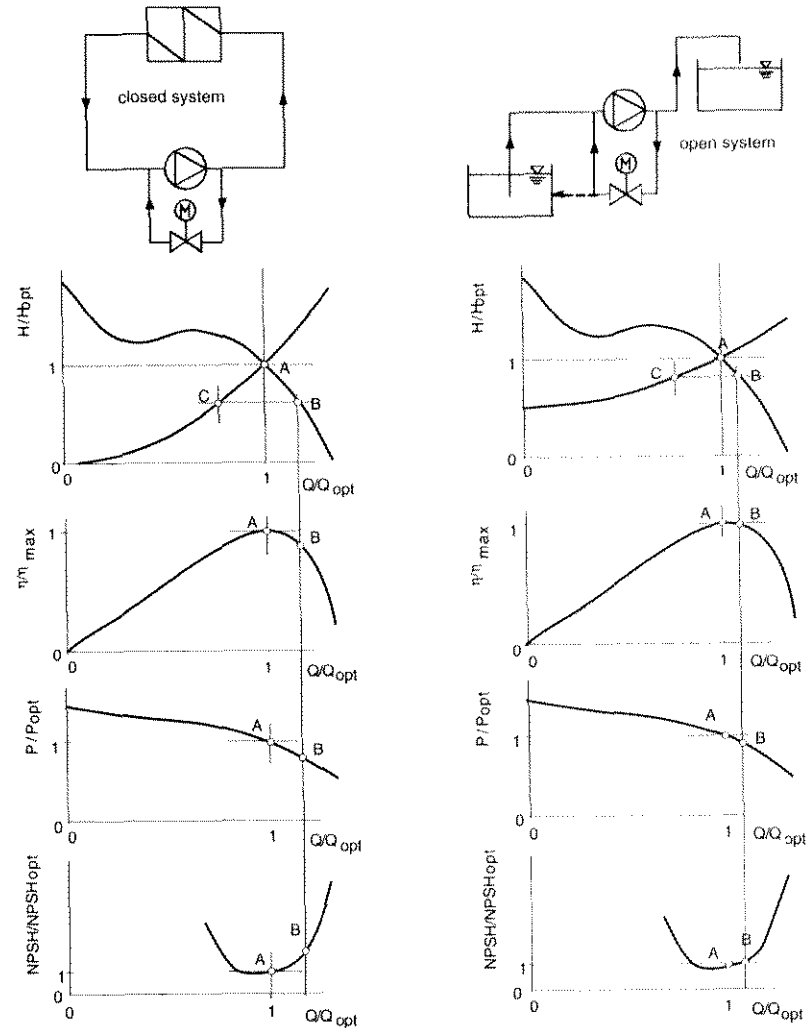
In pumps with a high specific speed, where power consumption decreases with an increased flow rate, by-pass control is more economical than throttling control. When a reduced flow rate is required in the system, one part of the flow is directed back to the pump suction side via a by-pass pipeline, which is installed parallel with the pump. As can be observed from the diagrams in Fig.B.2.2., the operating point on the pump characteristic is transferred from point A (without applying by-pass) to the higher flow rates B (with by-pass) but the operating point on the system characteristic is represented by point C in this case:

- $Q_c$  – flow rate in the system
- $Q_B$  – flow rate in the pump
- $(Q_B - Q_c)$  – flow rate in the by-pass pipeline

The distance to the right of the best efficiency point at which a pump will still operate when using by-pass control depends on the required flow reduction and the slope of the system characteristics (see diagrams in Fig.B.2.2.). In particular in systems where the dynamic part of the total system head is dominant, a possible danger of cavitation in the pump has to be taken into account.

The disadvantage of by-pass control is that it is a quite expensive and space-consuming installation, especially at higher flow rates.

One of the cases where by-pass control is also applied in pumps with a low specific speed, is to protect a pump with a closed delivery valve from overheating (when the pump volume is small, and longer operation with a closed delivery valve is expected). But in this case the by-pass pipeline leads to the suction reservoir and not to the front of the pump.



- A – operating points without applying by-pass
- B – operating points on pump characteristics with by-pass control
- C – operating points on system characteristic with by-pass control

Fig.B.2.2 Discharge control with by-pass: schematic system layout and characteristics

### B.2.3. Inlet guide vane control

A controllable inlet guide vane cascade can be installed in front of an impeller with fixed blades (Fig.B.2.3.). Inlet guide vanes can have stationary adjustment or be movable during pump operation, in accordance with changing flow requirements. The main function of the inlet guide vanes is to impose a peripheral velocity component to the fluid entering the impeller. With pre-rotation (peripheral velocity component in the same direction as impeller rotation) the pump total head is reduced, and with counter-rotation (peripheral velocity component in opposite direction to impeller rotation) the pump total head is increased (see diagram in Fig.B.2.5. and velocity triangles in Fig.A.1. and Fig.A.2.). Control in counter-rotation is limited due to an excessive impeller blade pressure loading and thus to a worsening of the pump cavitation characteristic.

An inlet guide vane control has an optimal effect with mixed-flow and axial-flow pumps ( $nq > 50$ ). It is applied mostly with bigger pumps and vertical wet pit installations. In comparison with impeller blade control, a system with inlet guide vanes is simpler and cheaper. On the other hand the range of high efficiency and acceptable cavitation characteristics is narrower than with impeller blade adjustment.

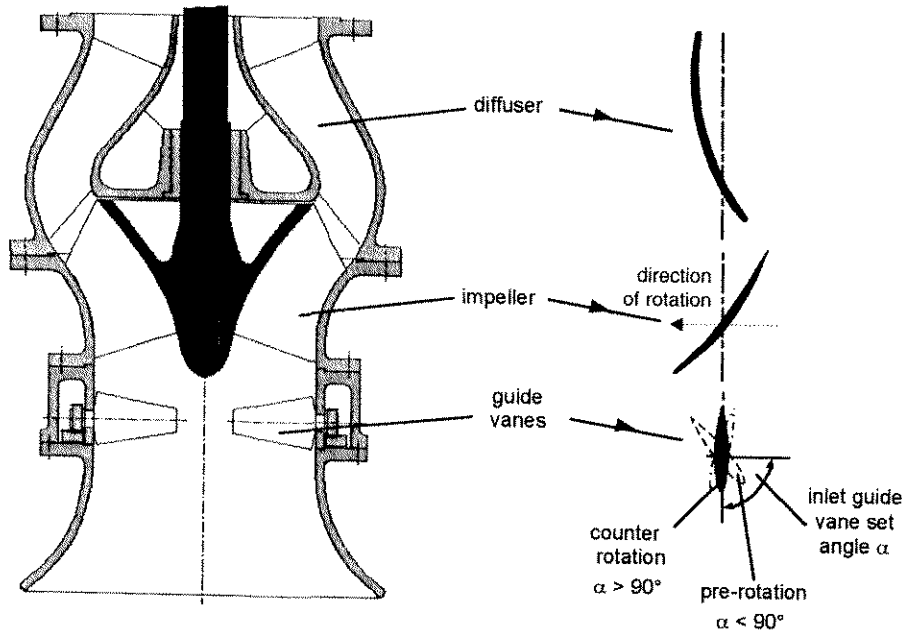


Fig.B.2.3 Mixed flow pump with inlet guide vanes

Fig.B.2.4 Schematic pump cascade layout – pre-rotation control

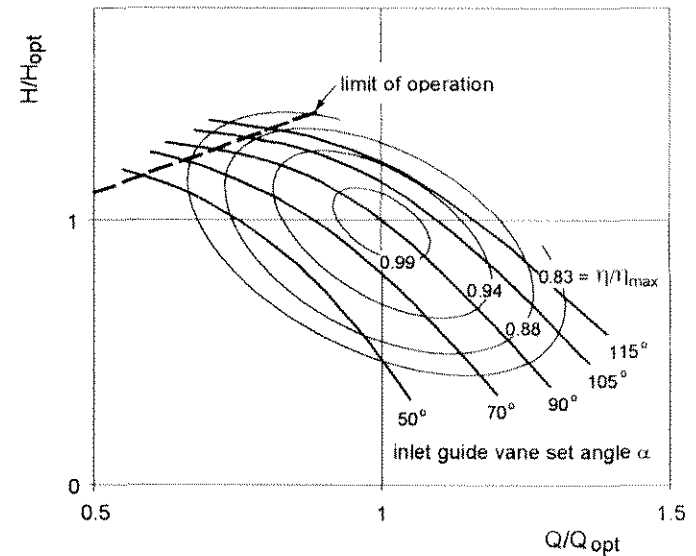


Fig.B.2.5 Pump characteristics with pre-rotation control

### B.2.4. Impeller blade adjustment

In bigger mixed-flow and axial-flow pumps ( $nq$  50-250), when the flow rate requirements vary within wider limits, impeller blade control is frequently applied (Fig.B.2.6.). A pump construction is adopted which allows the pivoting of the impeller blades in the pump hub at standstill or during operation. By changing the impeller blade setting angle, the velocity triangles shown in the Fig.A.2. change, and as a consequence the optimal flow rate is altered. Permanent operation is limited in the area of higher efficiencies because at part flows the Q-H characteristics can become unstable and the cavitation characteristics unfavourable (see diagram Fig.B.1.1.). The area of high efficiency is wider than in pre-rotation control but the mechanical operation of impeller blade control is more expensive. For a rough estimate of the flow rate variation, the linear relationship between flow rate and impeller blade angle setting can be applied.

Axial flow pumps with fixed impeller vanes are difficult to operate at low flows due to unstable characteristics, but with impeller blade control this disadvantage is eliminated.

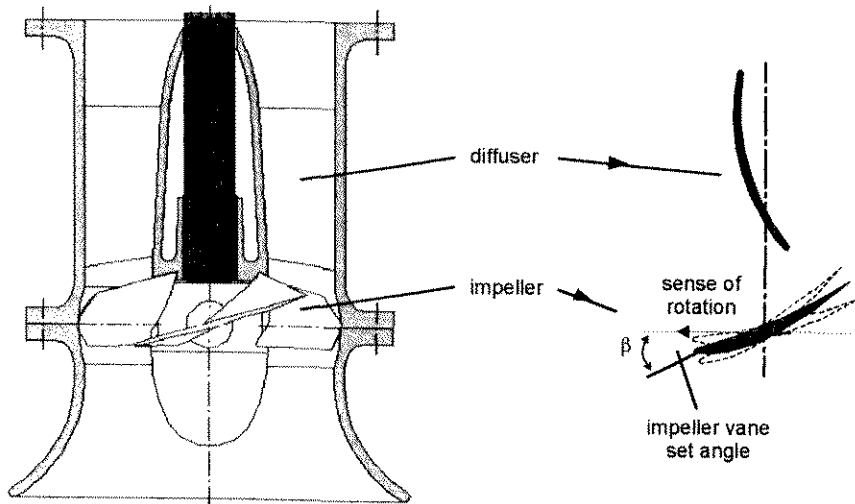


Fig.B.2.6. Axial flow pump with impeller blade control

Fig.B.2.7. Schematic pump cascade layout – impeller blade control

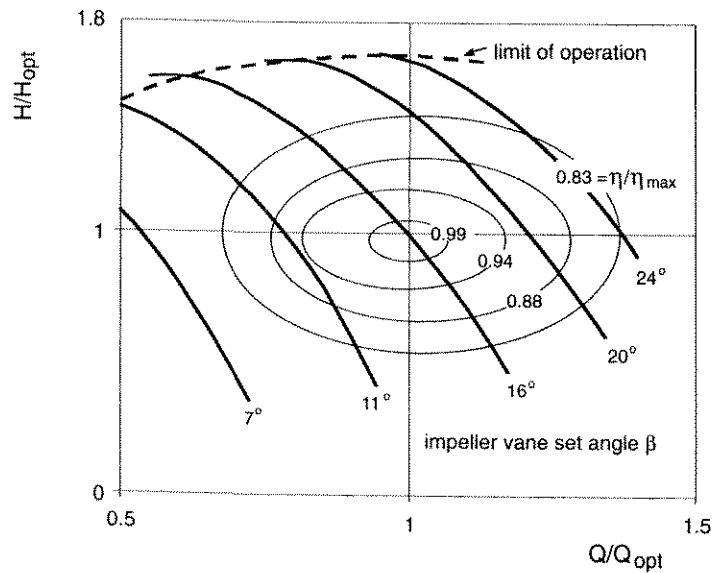


Fig.B.2.8 Pump characteristics with impeller blade adjustment

B.2.5. Speed control

With speed control, the main disadvantage of throttling control, energy losses, is eliminated or at least reduced. Speed control can be effected by additional equipment or a different drive motor. The most frequent applications are: variable speed electric motors, variable speed gears, hydraulic couplings, internal combustion engines, and steam or gas turbines. In small and middle size pumps the combination of a standard low-voltage squirrel cage motor and a frequency converter represents an efficient and also economical solution. Although speed control is accompanied by more expensive equipment and increased space requirements, this is in most cases balanced by reduced energy consumption (see also the chapter Life Cycle Cost – LCC).

The advantages of speed control are highest when the system characteristic is composed completely of the dynamic head, and the operating point is in the region of maximum efficiency (curve 1 in diagram Fig.B.2.9.).

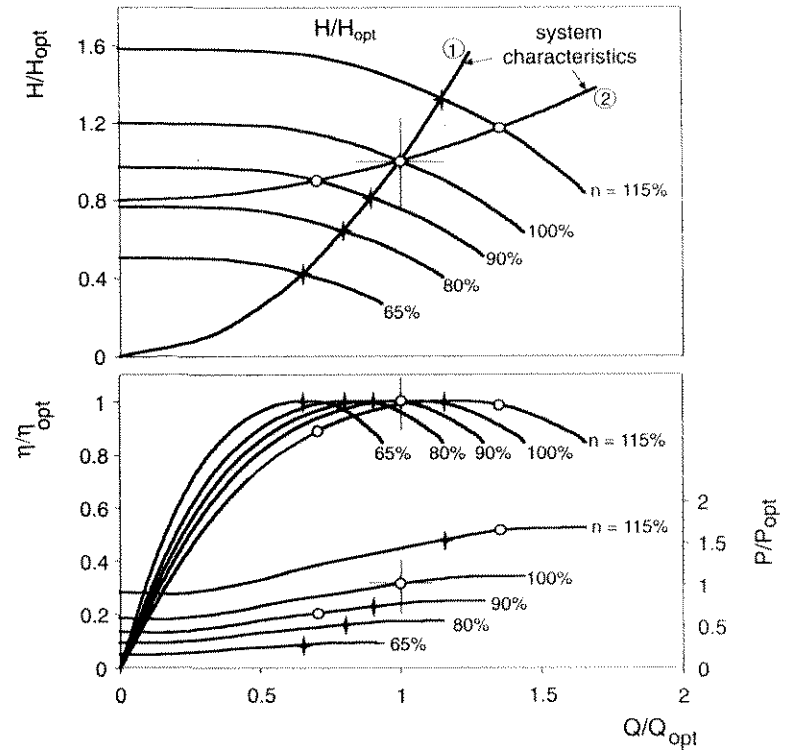


Fig.B.2.9 Speed control: pump and system characteristics

The higher the static part of the system head, the lower is the energy saving. Another disadvantage of a system characteristic with a high proportion of static head (curve 2 in diagram Fig.B.2.9.) is due to the low slope of the system curve at reduced flow. Flow control is difficult due to the flat intersection of the pump and system characteristics. In the region of low operating speeds the possibility of flow interruption and the danger of overheating have to be taken into account.

When varying pump speed, the pump characteristic can be calculated in accordance with the following relationships:

$$Q_x / Q_{des} = n_x / n_{des} \quad H_x / H_{des} = (n_x / n_{des})^2$$

$$P_x / P_{des} = (n_x / n_{des})^3 \quad NPSH_x / NPSH_{des} = (n_x / n_{des})^2$$

When increasing speed above the design speed, it is important to consider the absorbed pump power and total head, because of pump elements stress limitation, and the NPSH available, because of a possible danger of cavitation.

In addition to lowering energy consumption, speed control also has an important advantage in the system operation behaviour. Due to soft start and stop procedures the operation is gentle, water hammer problems are greatly reduced, there are no throttling functions in the valves, and as a consequence the lifetime of all the mechanical equipment increases.

**B.2.6. Adjustment of impeller**

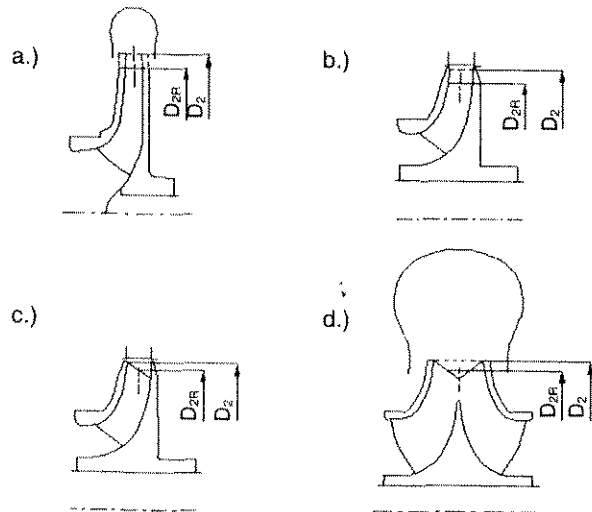


Fig.B.2.10 Impeller reduction variants

Quite often pump characteristics are overestimated in the project phase of the pumping system, and after putting the pumps into operation a need for a reduction of pump characteristics appears. This can be achieved in a simple but effective way: reduction of the impeller diameter. Different ways of doing this can be applied (see Fig.B.2.10.):

- for spiral casing pumps: variant a.
- for diffuser pumps: variants b. and c.
- for double suction pumps: variant d.

The exact change in the pump characteristics achieved by reducing the impeller diameter is established by testing, and is often given by pump manufacturers in diagram form. Nevertheless, the change in pump characteristics can also be defined in the following way (see diagram in Fig.B.2.11.):

$$Q_R = Q \cdot (D_{2R} / D_2)^m$$

$$H_R = H \cdot (D_{2R} / D_2)^m$$

$$m \approx 2 - 3$$

- exponent near 3: for small corrections of diameter and additional sharpening of impeller blade outlet on pressure side
- exponent near 2: for corrections of diameter larger than 5%

When for example seasonal changes in pump flow rates are required, this demand can be met by using alternately two impellers with different diameters. Performance change is stepwise, and stopping time is needed for impeller disassembly and reassembly.

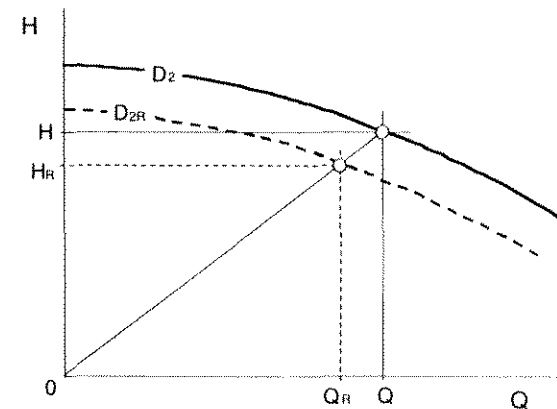
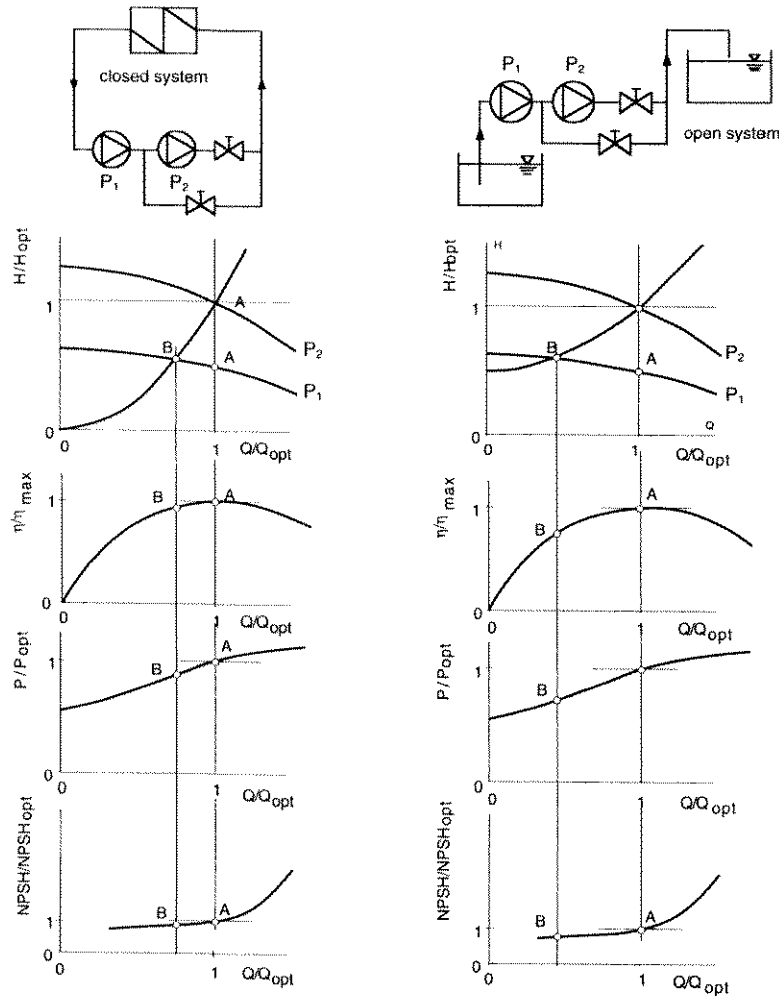


Fig.B.2.11 Pump characteristics with impeller diameter reduction

**B.2.7. Pumps working in series**



A – operating points in pump characteristics: two pumps working in series  
 B – operating points in pump characteristics: single pump P1 in operation

Fig.B.2.12 Pumps working in series: schematic system layout and characteristics

Pumps are installed in series when a high head variation is required or when head requirements cannot be covered by a single pump. This type of control is simple but stepwise. Sometimes the pumps are dispersed along a long-distance pipeline to cover the total system losses more uniformly, and additionally the pipeline wall thickness can be optimised (see Fig.B.2.13.). Another special application is when a booster pump is installed in front of the main pump to increase the available NPSH of the main pump (application: boiler feed pumps, injection pumps). Two examples with the same pump but different system characteristics are shown in Fig.B.2.12. An equal flow rate flows through both pumps connected in series, and operating point A corresponds to the best efficiency point. When a single pump is running (operating point B), the operating point is shifted to the left of the best efficiency point. In installations with low specific speed pumps the NPSH required and the power consumption shift towards lower values, which is not a problem. On the other hand it has to be taken into account that the pump which is installed as second or third in a series has to be designed for higher system pressures (casing, flanges, sealing system).

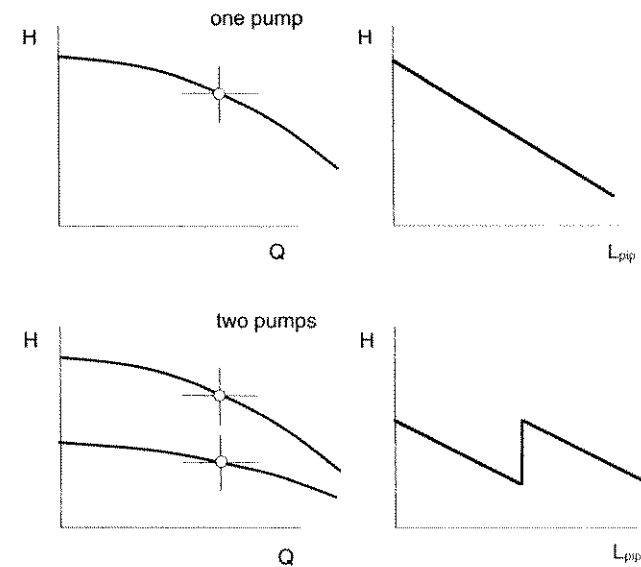
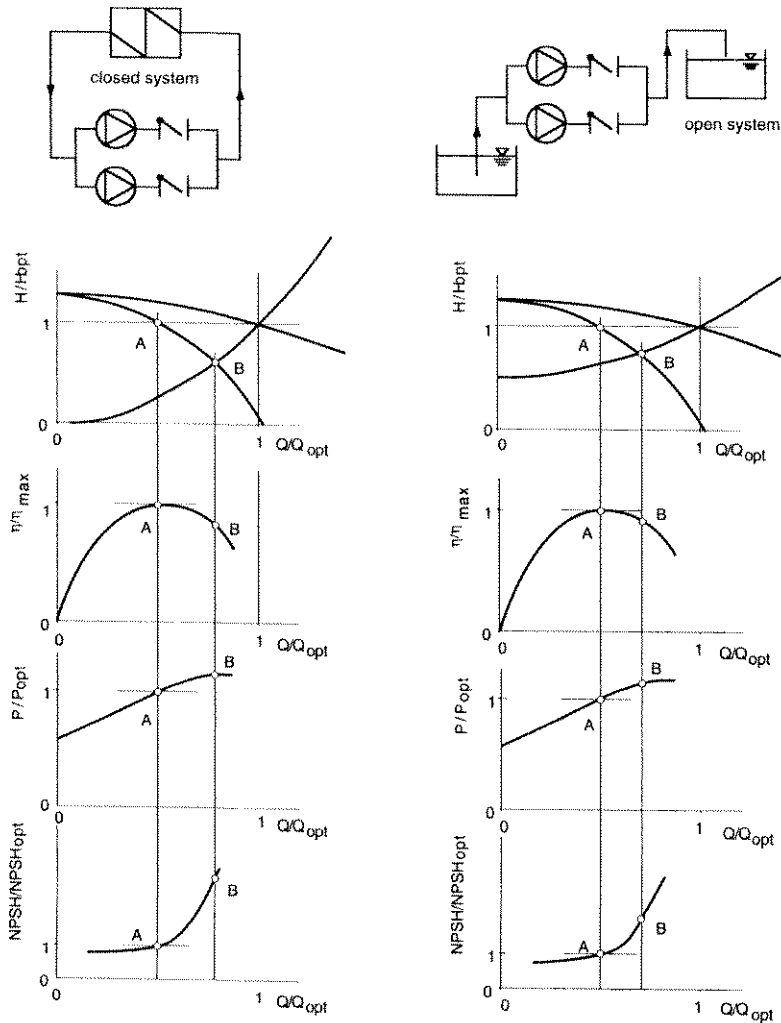


Fig.B.2.13 Two examples of a long-distance pipeline: with one pump, and with two pumps in series

It can be concluded that the serial installation of pumps is mainly suitable for applications when a higher proportion of dynamic head occurs in the total system head. Some general rules have to be taken into account: on starting, put pump P1 into operation first, with pump P2 at a standstill.

**B.2.8. Pumps working in parallel**



A – operating points in pump characteristics: parallel operation  
 B – operating points in pump characteristics: single pump operation

Fig.B.2.14 Pumps working in parallel: schematic system layout and characteristics

In systems where flow rate requirements vary greatly, or when the flow rate requirements cannot be met by the installation of a single pump, a solution with two or more pumps in parallel is applied. The control method is simple but the flow rate variation is stepwise. A wrong assumption is that adding one pump of the same size in parallel will double the flow rate. The flow difference between a single pump and two identical pumps running in parallel depends on many factors, the most significant being the static/dynamic head ratio in the system characteristics and the slope of the pump Q-H characteristics. Two system examples are shown in Fig.B.2.14., where the pumps are chosen so as to run at the best efficiency point in parallel operation (operating points A). In the case of single operation, the operating points B are always at higher flow rates, to the right of the best efficiency point. Thus the increased NPSH value and increased power consumption have to be considered in single pump operation.

From the diagrams shown in Fig.B.2.14. it can be concluded that parallel pump operation is mainly suitable for systems with a higher proportion of static head in the total system head. The range of the total head variation should be small, and also the shut-off head of each individual pump should be approximately the same. If not, it can happen that in parallel operation the pump with the lowest shut-off head will operate with a zero flow rate.

### B.3. Start-up and shut-down of centrifugal pumps

#### B.3.1. Starting torque of centrifugal pumps

The first condition for the successful start-up of a centrifugal pump is that it is sufficiently filled with the pumping liquid. Furthermore, an intersection must exist between the pump and system characteristics.

The start-up of a centrifugal pump is a transitory period in which the pump and its driver accelerate from zero speed to operating speed. The acceleration is possible only if the driving torque is higher than the pump torque at each speed (Fig.B.3.1.). Both starting torque curves must be known. The starting torque curve of the driving machine ( $M_M = f(n)$ ) is obtained from its manufacturer.

The pump starting torque curve ( $M_P = f(n)$ ) can be derived from the pump characteristics:

$$M = \frac{P}{2 \cdot \pi \cdot n/60} ; \quad M = f(Q)$$

on the basis of the affinity law:

$$\frac{M}{M_N} = \left( \frac{n}{n_N} \right)^2$$

Before the pump begins to turn, sufficient torque is needed to overcome the static friction in bearings, seals and other sliding parts. The starting torque is between 10 and 15% of pump torque at best efficiency point. Then it is assumed to decrease linearly with speed to nearly zero when the speed reaches 15 to 20% of the nominal.

The pump torque curve depends on its specific speed (see Fig.B.1.1.). Pumps with a low specific speed (radial) have rising  $M_P = f(Q)$  characteristics, while high specific speed pumps (axial) have falling  $M_P = f(Q)$  characteristics. The pump torque curve also depends on the starting procedure. Some starting procedures are described in sections B.3.4 to B.3.6.

When the driving machine is a steam, gas or water turbine, no problems at start-up should be expected, because their torque curves are high and they accelerate a centrifugal pump to its operating speed very quickly. If the pump is driven by an internal combustion engine, the starter must be large enough to bring both engine and pump up to operating speed, or else a clutch must be installed.

The most commonly used driving machine is an electric motor. Depending on their size and type, electric motors have different characteristics (Fig.B.3.1.). Electric

motors can have a low start-up curve, which can drop below the pump curve. In such cases, acceleration stops and the motor absorbs a high current, and the risk of overheating and destroying the windings is high. It is therefore necessary to investigate the start-up thoroughly, especially for cases where pumps have to be started frequently.

If the distribution network conditions allow, the electric motor can be started directly (Fig.B.3.1.). The starting current is then about 4,5 to 6 times the rated current  $I_N$ . Local electricity supply usually limits the direct on-line starting of asynchronous motors above a certain rating, due to unacceptable voltage drops. Different methods are possible to reduce the starting current, such as star-delta starters, slip-ring rotor motors, or auto-transformers.

An example of the start-up of an asynchronous squirrel cage motor with a star-delta (Y- $\Delta$ ) starter is shown in Fig.B.3.2. A star-delta starter is usually used for smaller motors. After start-up, the motor accelerates at first along the  $M_{MY}$  curve and absorbs current  $I_Y$  until the intersection with the pump torque curve (point A).

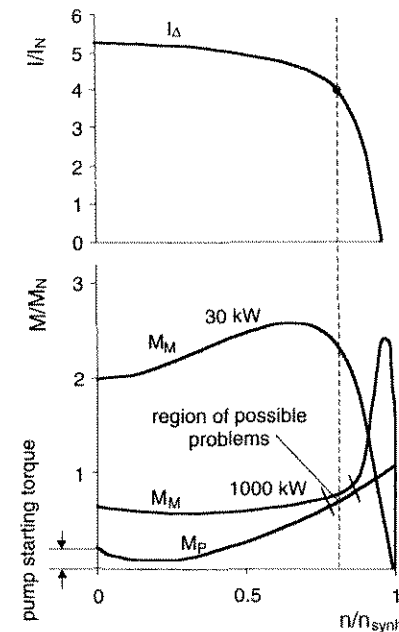


Fig.B.3.1 Starting torque and current of pump and electric motor

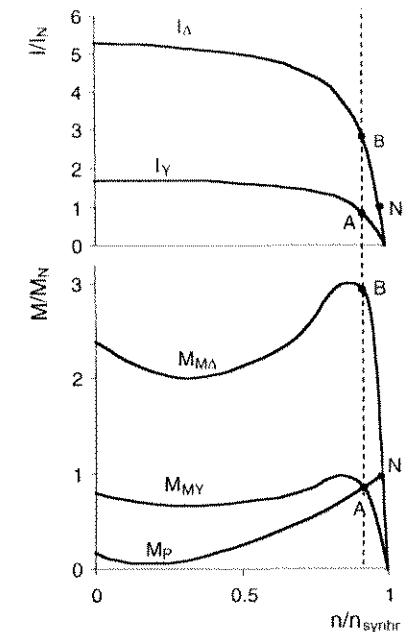


Fig.B.3.2 Starting torque and current of pump and asynchronous electric motor with star-delta starter



At that moment the starter switches to the delta circuit – point B. It runs further along the  $M_{M\Delta}$  curve until the intersection with the pump torque curve at nominal point N. It absorbs current  $I_{\Delta}$ . In the present example the highest absorbed current is at point B and is about three times the nominal current. Compared to a direct start, which is about five times the nominal current, the benefit is obvious. But there are many cases where a star-delta starter does not bring any benefit. Each case must be studied separately.

A schematic presentation of the start-up of a slip-ring motor is given in Fig.B.3.3. The starting rheostat (resistance) is switched into the electric motor rotor circuit, via the slip rings, during the starting period, and is subsequently short-circuited in stages. Slip-ring motors provide a smooth start-up to full speed

An auto-transformer starter enables asynchronous motors with a squirrel cage rotor to start smoothly at a reduced voltage.

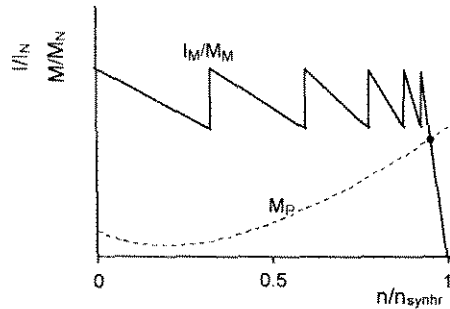


Fig.B.3.3 Starting curves for current and torque  $M$  of a slip-ring rotor motor

### B.3.2. Start-up time of a centrifugal pump

Start-up time, from switching on to the moment of reaching the nominal speed, depends on the difference between the torque of the driving unit  $M_M$  and the pump torque  $M_P$ . The difference is the torque needed for the acceleration of the load: acceleration torque  $M_A$  (Fig.B.3.4). Acceleration torque varies with speed.

If the total mass moment of inertia  $J$  of all unit rotating parts (pump rotor set including liquid, coupling, possible gears, rotor of driving machine) is known, the start-up time can be calculated in the following way:

$$M_A = J \frac{d\omega}{dt} ;$$

where  $\frac{d\omega}{dt}$  is the angular acceleration of the drive shaft.

$$t = \int_0^{\omega} \frac{J}{M_A} d\omega = \frac{\pi \cdot J}{30} \int_0^{n_N} \frac{dn}{M_A}$$

Instead of solving the integral, the sum of all the elements of the sequence must be calculated.

$$t = \sum t_i = \frac{\pi \cdot J}{30} \left( \frac{\Delta n_1}{M_{A1}} + \frac{\Delta n_2}{M_{A2}} + \dots + \frac{\Delta n_i}{M_{Ai}} \right)$$

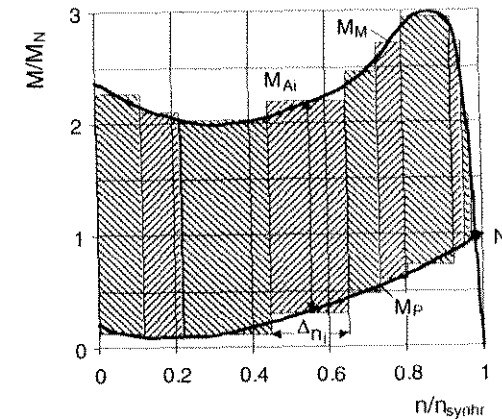


Fig.B.3.4 Calculation of start-up time

### B.3.3. Run-out of centrifugal pump-motor system

After the motor has shut down, the driving torque drops to zero. Usually the valve on the discharge side is closed immediately, and the pump runs out adequately to the total mass moment of inertia and break (run-out) torque. The same procedure can be applied, as in section B.3.2., but instead of the accelerating torque  $M_A$ , the pump run-out torque must be taken into account. The pump run-out torque is equal to the pump start-up torque  $M_P$ .

$$t = \int_0^{\omega} \frac{J}{M_P} d\omega = \frac{\pi \cdot J}{30} \int_0^{n_N} \frac{dn}{M_P}$$

$$t = \sum t_i = \frac{\pi \cdot J}{30} \left( \frac{\Delta n_1}{M_{P1}} + \frac{\Delta n_2}{M_{P2}} + \dots + \frac{\Delta n_i}{M_{Pi}} \right)$$

Run-out time under stationary conditions is normally between 10 and 60 sec., and can be shorter for smaller pumps. A typical run-out diagram is shown in Fig.B.3.5. The pressure surge is disregarded. This procedure is not valid for other stopping procedures, where the run-out time must be calculated differently.

In some systems, after the motor has shut down, the water is allowed to flow from the piping system back through the pump for a certain period, until the valve is closed (Fig.B.3.6.). The pump at first slows down, the flow rate being still positive but decreasing (pump operation). Because of the mass moment of inertia the pump still rotates in a positive direction, while the flow is already increasing in a negative direction (dissipation region). The pump speed decreases and reaches zero speed and then the pump begins to rotate in a negative direction (turbine operation). The pump speed increases until it reaches the stationary run-away speed at  $M_P=0$ . Then, according to the valve characteristics, the flow rate and pump speed decrease to zero.

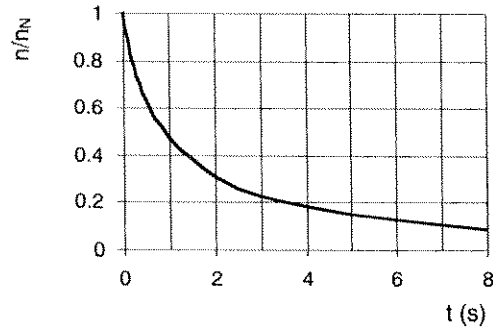


Fig.B.3.5 Run-out time of a centrifugal pump

The stationary run-away speed depends on the pump specific speed and the geodetic head (Fig.B.3.7.). The pump-motor system must be designed in such cases for continuous operation. Due to the water hammer effect, which depends very much on the system, on the closing time of the valve and the inertia of rotating parts, the momentary maximum run-away speed can be greater than the stationary one. The motor also must be able to sustain such a short-period maximum run-away speed.

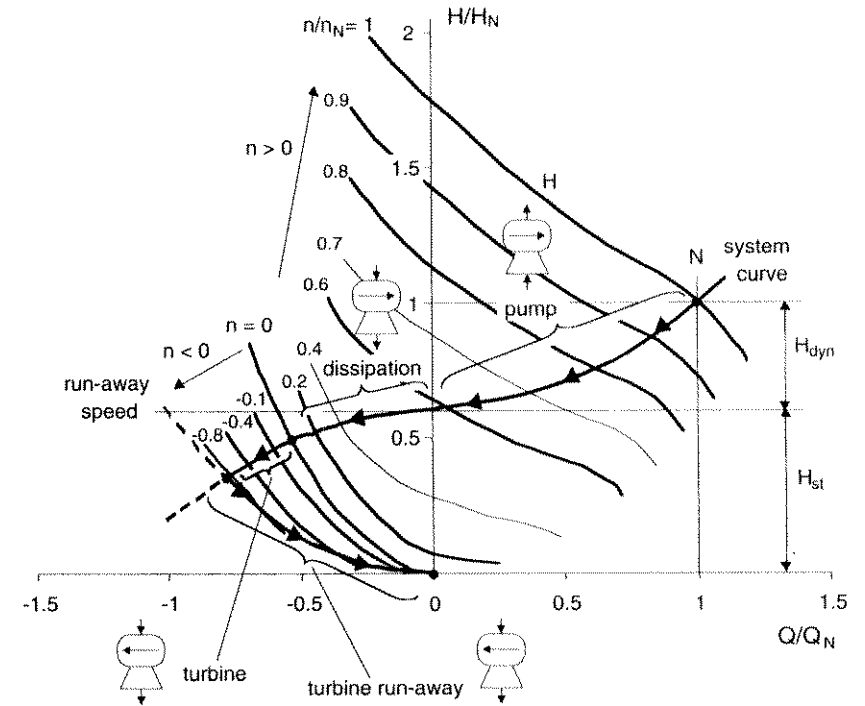


Fig.B.3.6 Run-out of a centrifugal pump with permitted reverse running

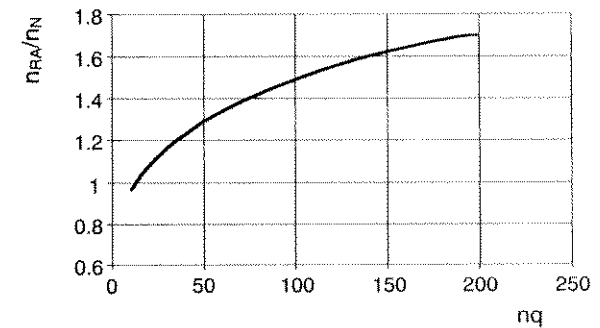


Fig.B.3.7 Stationary run-away speed at pump optimal head

**B.3.4. Start-up against a closed valve**

Low and medium specific speed pumps (radial and mixed-flow pumps with a specific speed  $nq[90]$ ) have a shaft power at shut-off lower than at the best efficiency point. This type of pump usually starts against a closed discharge valve, because the pump starting torque is lowest at shut-off.

During start-up the head and torque rise proportionally to the square of the rotational speed from point 0 (0') to point A (Fig.B.3.8.). As soon as the pump reaches the nominal speed (point A), the valve will start to open, and the head and torque move to nominal point N.

High head pumps are not allowed to run against a closed discharge valve (see section B.4). The pump rotor set can warm up to an unacceptable degree with the risk of it touching the stationary parts. In addition the liquid can evaporate inside the pump. A minimum flow rate valve which opens during pump start-up must be installed. The starting curve is 0(0')-MM-N.

If a pump with a higher specific speed, which has a falling  $P=f(Q)$  curve, must start against a closed valve, it is recommended to open a by-pass valve during start-up.

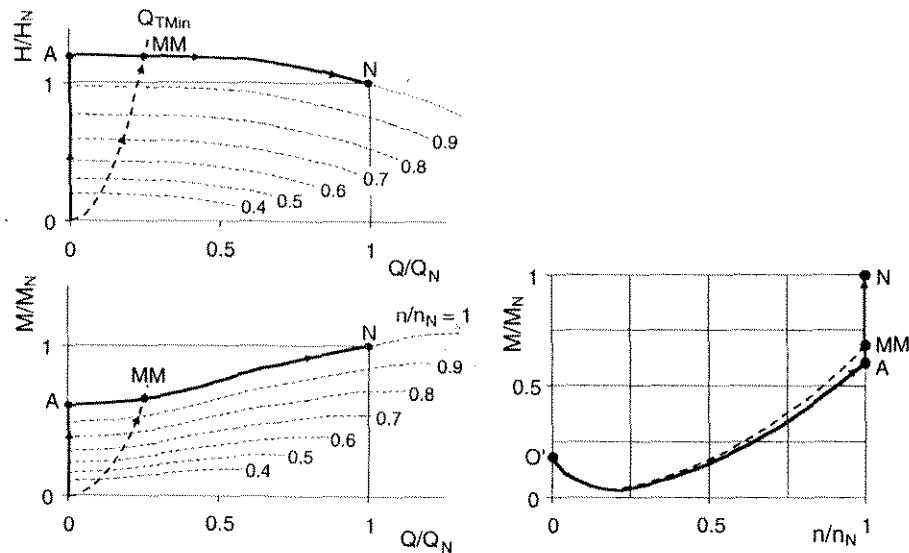


Fig.B.3.8 Start-up against a closed valve

**B.3.5. Start-up against an open delivery valve**

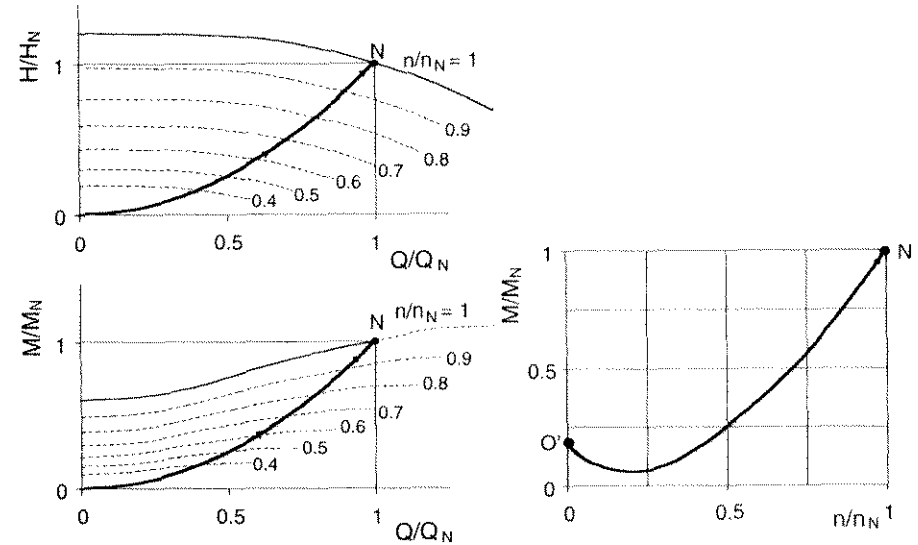


Fig.B.3.9 Start-up against an open delivery valve, no geodetic head

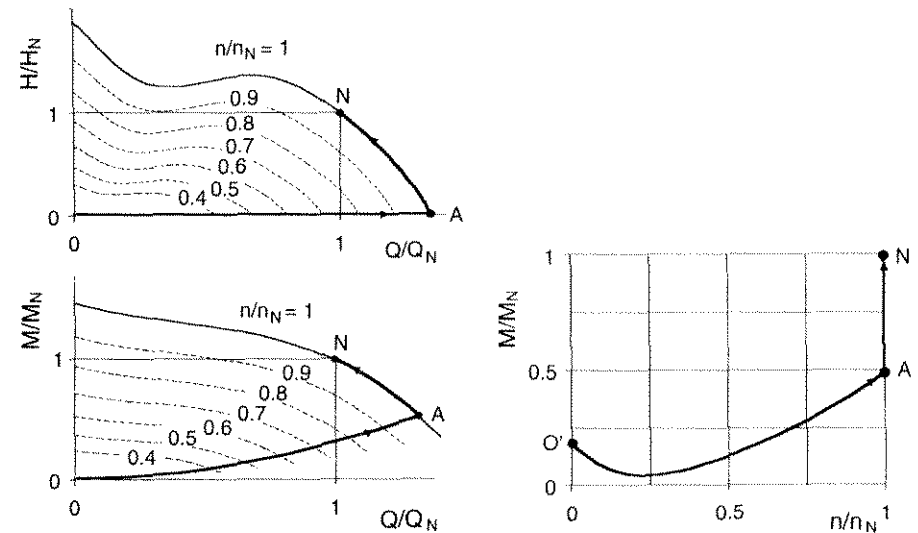


Fig.B.3.10 Start-up against an open delivery valve, system empty

In systems without a static head, the system characteristics represent only the dynamic part. If the system is filled with liquid and the pipeline is short, i.e. that the time needed for accelerating the liquid column is the same as the pump start-up time, the pump head and torque rise along a parabolic curve  $O(O')-N$  (Fig.B.3.9.).

If the pipeline is long, the start-up curve is similar to Fig.B.3.8. The acceleration time of the mass of liquid in the discharge pipeline is much longer than the pump start-up time. The large mass of fluid standing still along the pipeline acts like a closed discharge valve.

If the system is empty (Fig.B.3.10.), the pump runs at  $H=0$  far to the right of the nominal point in a region with strong cavitation (point A). After the system fills with liquid the operating point moves along the system curve to point N. This method of start-up is usually used in high specific speed mixed-flow and axial pumps with a falling  $P=f(Q)$  curve. The counter-pressure must be established as soon as possible to prevent the pump running in a region with strong cavitation and vibration, if necessary using throttling. The maximal flow rate at  $H=0$  (point A) can be reduced to smaller values depending on  $NPSH_{avail}$ . In addition the time needed for filling up the system depends on  $NPSH_{avail}$ .

**B.3.6. Start-up against a closed non-return (check) valve**

The delivery valve is open. After switching on, the pump runs at  $Q=0$  until it overcomes the static pressure on the other side of the check valve (Fig.B.3.11., point A), when the check valve opens. Then the operating point moves along the system curve to nominal point N. If there is another identical pump installed in the same system, and it has to start up when the first pump is already running, the pressure on the check valve corresponds to the pressure at point N. The second pump runs at  $Q=0$  until it overcomes pressure  $H_N$  (point  $A_2$ ). Then both pumps move to point  $N_2$ .

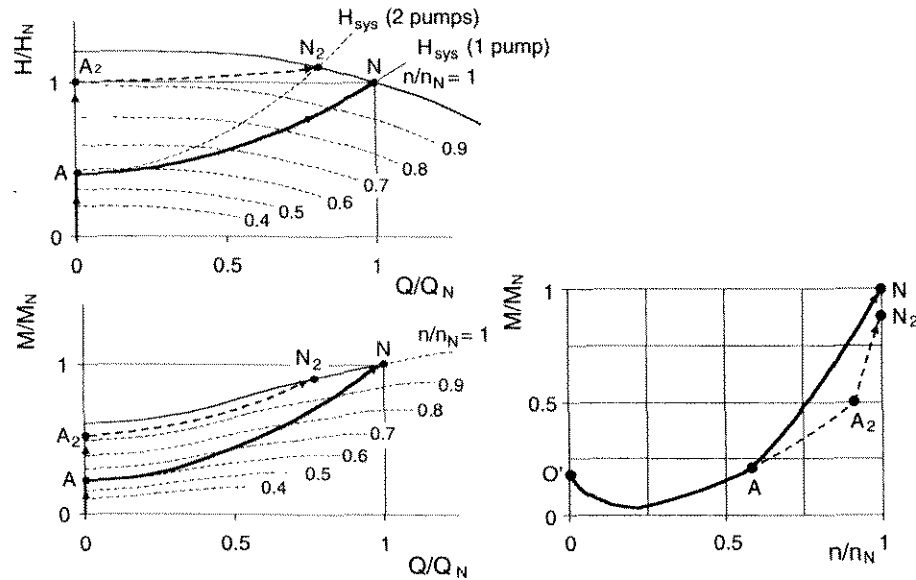


Fig.B.3.11 Start-up against a closed check valve, control valve open

## B.4. Operating range of centrifugal pumps

With regards to the system, the pump must be selected in such a way that it operates as often as possible near the best efficiency point. This is best in relation to the energy and maintenance costs. Usually it is not possible to run the pump all the time at the best efficiency point. The diagram in Fig.B.4.1. shows the guidelines for permitted permanent, short-period and prohibited operating ranges as a function of  $nq$ . The permitted permanent operating range is the range of flow rates, where the pump can operate continuously without any mechanical damage to the pump parts. The limits are not strict and depend on the application, pump size (power concentration), type, energy costs (drive capacity), stability of the head characteristics, onset of recirculation etc. Boiler feed pumps are in many cases required to be capable of operating permanently at flow rates in the range shown in the diagram in Fig.B.4.1. as the short-period operating range, and correspondingly the limit of the short-period operating range shifts to lower flow rates.

For determining the minimum flow rate, the following criteria can be decisive:

- increase in fluid temperature at the pump exit and its balancing system due to internal energy losses in the pump and balancing system
- increase in cavitation
- increase in shaft vibration, caused by an increase in static and dynamic radial thrusts and by recirculation
- increase in pressure pulsation at part-load
- increase in axial thrust (static and dynamic) at part-load
- stability of head characteristics
- power required by zero flow
- physical properties of fluid

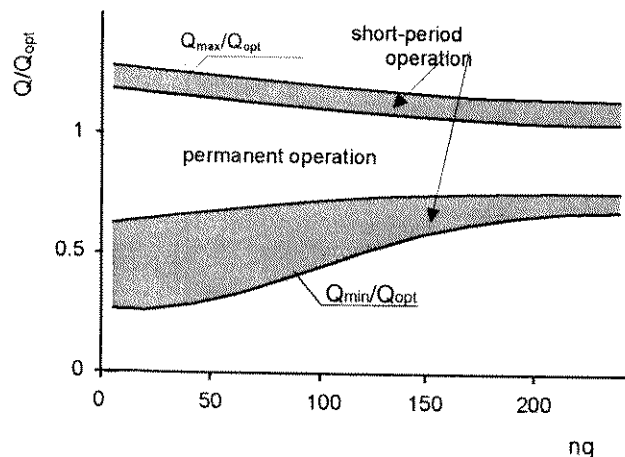


Fig.B.4.1 Recommended operating range of centrifugal pumps

The criteria for limiting the maximum flow rates are in most cases shaft vibration and cavitation.

### B.4.1. Power required by zero flow as a function of the specific speed of the pump

The pump power characteristic depends on its specific speed (section B.1.). The power required at zero flow defines the pump starting process. It can also limit the pump minimum flow so as not to overload the drive. The ratio between power required at zero flow and power at best efficiency point versus specific speed is in Fig.B.4.2. It can be seen that pumps with specific speeds higher than 80 can be problematic, where the shut-off power is greater than the power at best efficiency point.

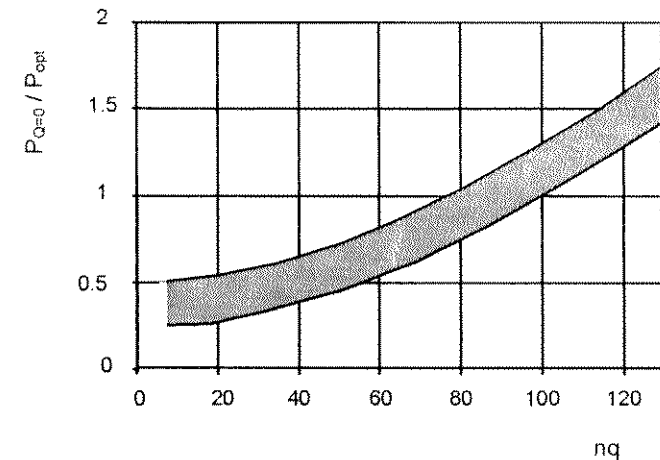


Fig.B.4.2 Power required by zero flow versus specific speed

### B.4.2. Poor hydraulic behaviour in the part-load range

A pump impeller is usually designed so that at the best efficiency point the geometrical and flow angles at the impeller inlet are practically the same, and the flow is smooth. At part flow and overflow, the inflow angle does not coincide with the blade angle any more. It causes an irregular flow at the impeller inlet, and flow separation and recirculation, which are the sources of many effects:

- Efficiency drop: for big pumps with a stage power over 500 kW, the efficiency must not be less than about 70 to 80% of the best efficiency.
- Cavitation: during the planning of the pump system (controlling  $NPSH_{av}$ ), it is important to investigate the cavitation over the whole operating range, and not

only at the best efficiency point, and to check the safety margin against a 3% head drop due to cavitation, or other NPSH criteria (see section C).

- Vibration: a result of recirculation, cavitation, pressure and radial thrust pulsation (see section H)
- Unstable characteristics: a result of recirculation (see section B.1.)
- Also the radial and axial thrusts increase when changing from the best efficiency point to part-load (see section F).

The forces at part-load caused by flow recirculation at the impeller inlet can result in excessive vibration in the pump and system, especially when the impeller inlet geometry is not optimally designed. This phenomenon is more important in pumps with a higher power concentration and with higher specific and suction specific speeds.

#### B.4.3. Minimum flow determination by admissible temperature rise

Only a part of the total shaft power is used as pump useful hydraulic power. Other parts are external (mechanical) and internal losses. A schematic representation of useful hydraulic power, and internal and external losses is given in Fig.B.4.3.

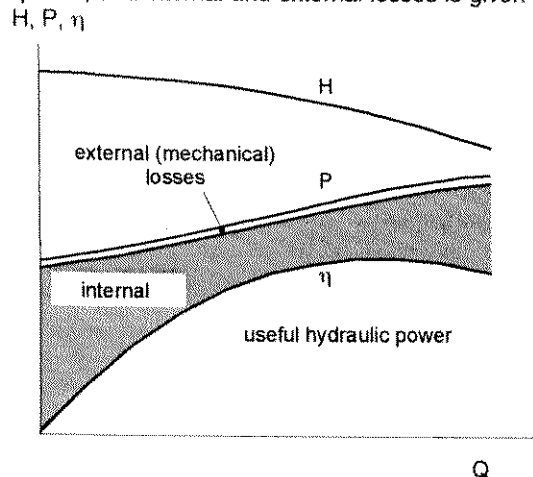


Fig.B.4.3 Useful hydraulic power and losses in a centrifugal pump

External losses are small and do not affect the heating of the fluid in the pump. Internal losses are the result of friction and flow separation, and cause the heating of the fluid as it flows from pump inlet to outlet. They depend strongly on the flow rate. The lower the flow rate, the lower the efficiency, and the greater the propor-

tion of energy which is converted into heat and causes a temperature rise. Additionally, part of the temperature rise is caused by isentropic compression of the fluid in a pump (Fig.B.4.4.).

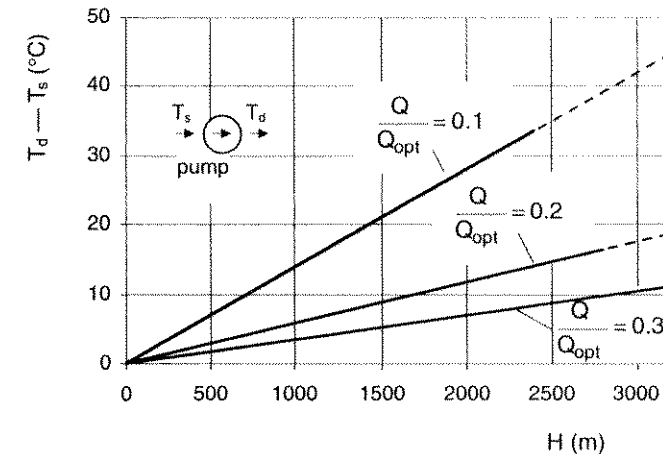


Fig.B.4.4 Temperature rise as a function of pressure and minimum flow rate, (valid only for water)

Because of energy converted into heat, the fluid temperature at the discharge flange is higher than at the suction flange. Temperature rise in the permanent operating range plays a negligible role.

For high-pressure pumps with heads over about 2000 m, the temperature rise at part-load can be high. The determining of the minimum flow, influenced only by the temperature rise, has to be studied carefully. As part of the temperature rise is influenced by the compressibility of the fluid, the physical properties of the latter have to be taken into account. This is especially important for process pumps, which operate near the fluid evaporation pressure.

The most critical points in a pump are the balancing discs or pistons (or labyrinth seals in multi-stage pumps), where the pressure drop occurs, and this can lead to local evaporation of fluid and damage to pump parts. In order to avoid the pump heating above permitted limits, and to avoid the evaporation of fluid in the pump, a minimum flow through the pump must be ensured. The temperature rise in the pump and additionally in the axial thrust balancing system, due to additional throttling effect in the gaps, is the criterion for determining the minimal flow rate. The temperature rises exponentially with the diminishing of the flow rate (Fig.B.4.5.).

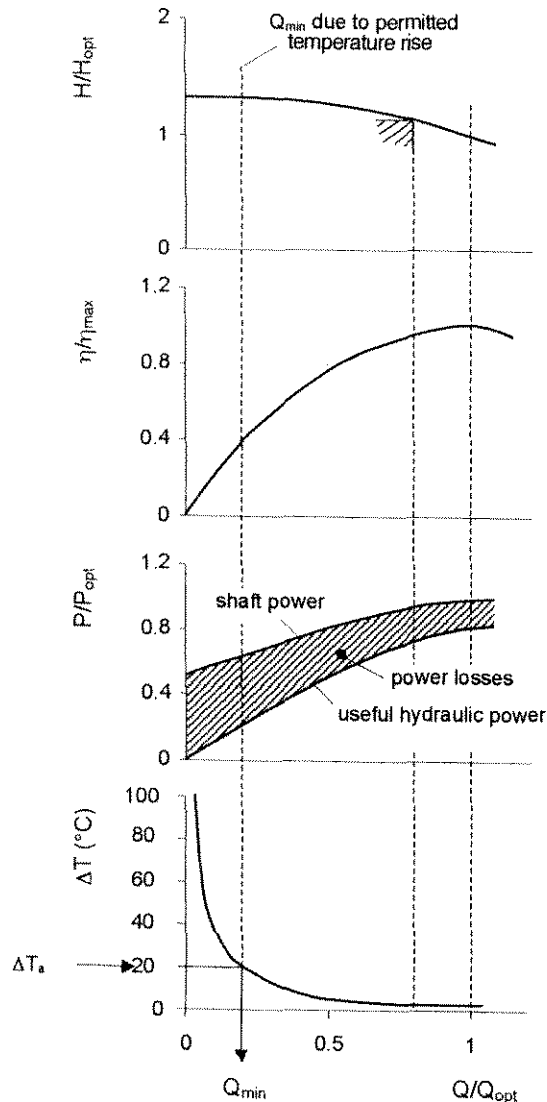


Fig.B.4.5 Example of water temperature rise in a high head 20 MW pump and permitted minimum flow rate

The temperature rise in a pump is the difference between the fluid temperatures at the discharge and suction flanges.

$$\Delta T_p = T_d - T_s = \Delta T_{loss} + \Delta T_{ic}$$

$\Delta T_{loss}$  is the temperature rise due to internal losses

$\Delta T_{ic}$  is the temperature rise due to isentropic compression

$$\Delta T_{loss} = \left( \frac{1}{\eta_i} - 1 \right) \cdot g \cdot \frac{H}{c_p}$$

$c_p$  is the specific heat of the pumped fluid

Isentropic compression is calculated by means of an enthalpy-entropy diagram. A rough estimate for water is given by the following formula:

$$\Delta T_{ic} = 0.7 \cdot \frac{T_s}{T_{ref}} \cdot \frac{H}{H_{ref}}$$

Where  $T_s$  is the fluid temperature at the suction flange,  $T_{ref} = 100 \text{ }^\circ\text{C}$ ,  $H_{ref} = 1000 \text{ m}$ .

Additionally a certain temperature rise occurs in the axial thrust balancing device (disc or piston), which is defined by the formula:

$$\Delta T_{bd} = T_{ebd} - T_d = \frac{g \cdot H}{c_p \cdot \eta_i}$$

Where  $T_{ebd}$  is the temperature of the fluid at the exit of the balancing system.

The pressure behind the balancing system must be sufficiently far from the vapour pressure corresponding to the calculated temperature  $T_{ebd}$ .

The total temperature rise is:

$$\Delta T = \Delta T_p + \Delta T_{bd}$$

Based on experience, the suggested permitted temperature rise is  $20^\circ\text{C}$  and is independent of the fluid.

The minimum flow rate can be determined with following formula:

$$Q_{min} = \frac{P}{\rho \cdot c_p \cdot \Delta T}$$

The minimum flow rate depends basically on the pump power and the type of fluid. Additionally it depends also on the pump volume (power concentration), the operating speed and the type of leak-off valve.

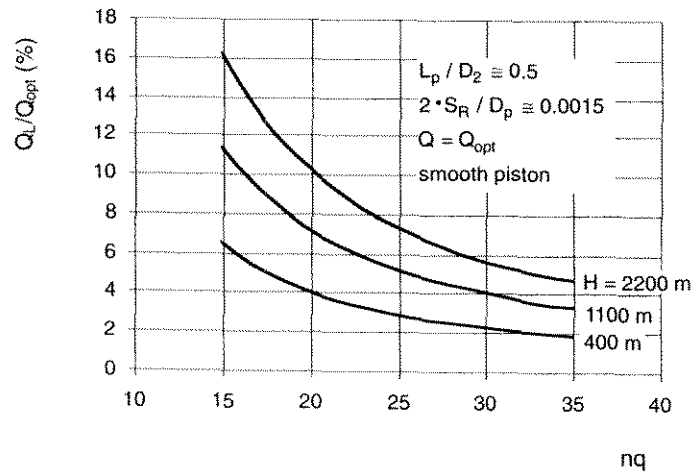


Fig.B.4.6 Flow through the balancing piston as a function of specific speed and pump head

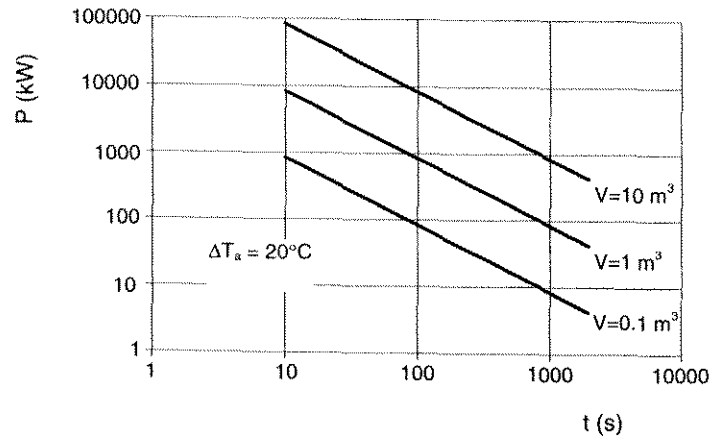


Fig.B.4.7 Time of temperature rise as a function of pump fluid volume and power rating

In relatively small multi-stage pumps the balancing flow through the balancing piston is often adequate as a minimum flow, and no special additional arrangements are needed. In Fig.B.4.6. the relative flow through the balancing piston versus specific speed and pump head is given.

In larger high head and high power rating pumps, the fluid temperature at the pump exit can even rise several degrees per second if the pump operates against a closed valve. During the start-up procedure, evaporation would occur before the main control valve could open and the pump would be damaged. To prevent this, such pumps must be equipped with a minimum-flow bypass to the suction tank with an additional leak-off valve, which automatically open when the discharge valve is closed. A very fast temperature rise is a result of a high ratio between power rating and pump fluid mass (Fig.B.4.7.).



# C. CAVITATION IN A PUMP

## C.1. Physical principles

In hydrodynamics, the expression "cavitation" refers to the conditions where a partial evaporation of the fluid in a hydraulic system occurs. When the static pressure drops to the fluid vapour pressure, a bubble filled with vapour is formed, due to the velocity increase in a given flow area. Part of the fluid evaporates, and in the given area of the flow field a two-phase flow takes place. As the vapour bubble moves to the region where static pressure is higher than fluid vapour pressure, the vapour bubble condenses (collapses) immediately.

Cavitation bubbles are only formed when nuclei are present in the fluid. Nuclei are groups of gas or vapour molecules which are present in the form of microscopic bubbles,  $10^{-3} - 10^{-1}$  mm in size. In practically all technical processes with different types of fluids, a sufficient amount of the nuclei needed for cavitation formation is present.

With the enlargement of the cavitating zone, the effects on the characteristics of the machine or device can be noticed: noise and vibration increase, and cavitation damage can take place.

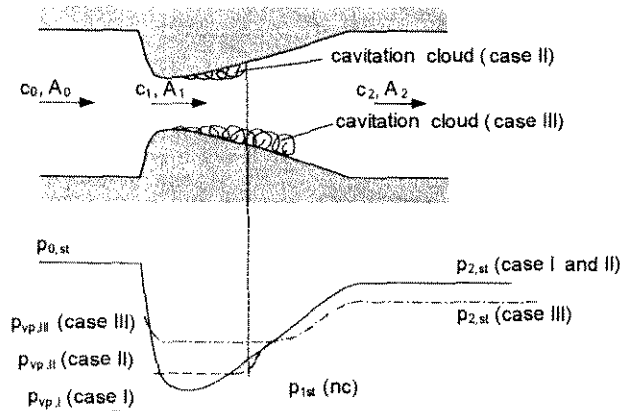


Fig.C.1.1 Pressure distribution in a nozzle

In Fig.C.1.1. the static pressure distribution inside a nozzle is shown. The conditions without cavitation are represented by the curve "case I", and static pressure in the smallest nozzle cross-section can be calculated using the following relationship:

$$p_{0, st} - p_{1, st(nc)} = \rho/2 \cdot (c_1^2 - c_0^2)$$

Pressure recuperation in the exit part of the nozzle (in the diffuser) is not complete due to pressure losses, thus  $p_{2, st} < p_{0, st}$ . When fluid vapour pressure  $p_{vp}$  is lower than  $p_{1, st(nc)}$ , no cavitation takes place in the nozzle. With an increased fluid temperature the vapour pressure also increases. Three characteristic flow conditions are described in Table C.1.1.:

Case	Pressure conditions	Description
I	$p_{vp, I} < p_{1, st(nc)}$	No cavitation
II	$p_{vp, II} > p_{1, st(nc)}$	Fluid vapour pressure is reached and cavitation takes place in the smallest nozzle cross-section. Cavitation region is small and does not influence the pressure recuperation in the diffuser.
III	$p_{vp, III} \gg p_{1, st(nc)}$	Cavitation region extends deep into the diffuser. Due to changed velocity distribution, additional pressure losses take place and pressure recuperation in the diffuser is lower than in the case of a non-cavitating flow.

Table C.1.1 Description of characteristic flow conditions in a nozzle

As the cavitation (vapour) bubble flows into a region where the static pressure is higher than the fluid vapour pressure, the equilibrium of the vapour bubble is terminated and as a consequence the vapour bubble condenses (implodes) immediately. When the spherical form of a bubble (see Fig.C.1.2.) implodes, at the end of the implosion process the implosion pressure reaches the value:

$$p_i = \beta_T^{0.5} \cdot (2/3 \cdot p \cdot ((R_0/R_e)^3 - 1))^{0.5}$$

- $p$  – fluid pressure
- $p_i$  – implosion pressure
- $R_0$  – bubble radius at beginning of implosion
- $R_e$  – bubble radius at end of implosion
- $\beta_T$  – compressibility coefficient

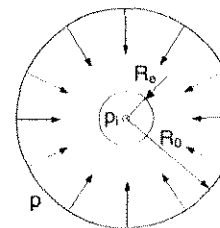


Fig.C.1.2 Spherical bubble form

$R_0/R_e(-)$	$p_i$ (bar)
6	1 800
10	3 900
20	11 100
30	20 300

Table C.1.2 Implosion pressures for spherical bubble

The relationship shown above is valid for ideal conditions but the model itself can be used for understanding the important influencing parameters in an implosion. Implosion pressure increases with the increase of initial vapour bubble volume and fluid pressure, and on the other hand it decreases with the vapour bubble size at the end of the implosion. To get an idea of how big implosion pressures can be, Table C.1.2. shows the values in the case of a spherical vapour bubble in cold water, for fluid pressure ( $p = 1$  bar) and for different ratios of initial and final vapour bubble diameters.

In practice, vapour bubbles implode asymmetrically, and at the end of this process a fluid micro-jet is formed (see Fig.C.1.3.). When the vapour bubble implodes inside the flow channel, the micro-jet is directed towards the area of lower pressure (against flow direction). In most cases this type of implosion has no consequences for the equipment. This type of cavitation is also called "supercavitation". When the implosion process takes place near the wall of the flow channel, the micro-jet is directed towards the wall of the flow channel. High implosion pressures and fluid jets act on the wall, and as a consequence material damage can be expected. It has to be stated also that an important influence on the implosion pressure is the fluid compressibility in the vicinity of the implosion area.

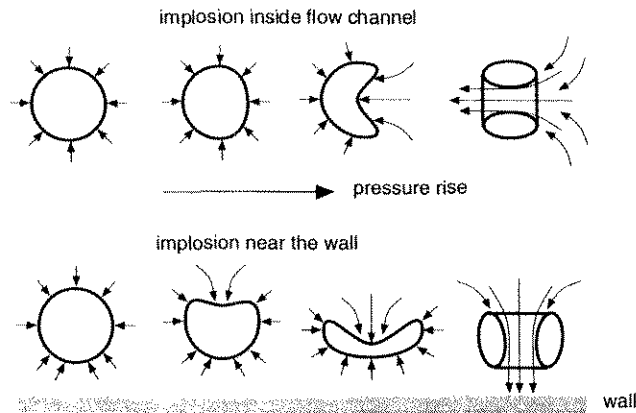


Fig.C.1.3 Bubble implosion process

When describing cavitation behaviour in hydraulic machines, a distinction must be made between different expressions:

- cavitation: localised evaporation, two-phase flow
- cavitation intensity: sum of implosion energies of all bubbles
- cavitation resistance: material property (strength) against bubble implosion
- cavitation erosion: material damage due to implosion of vapour bubbles

### C.2. Cavitation at the impeller inlet

Cavitation zones at the impeller blade leading edge are formed in a similar way to those at the nozzle, as described in the previous section. In Fig.C.2.1. the pressure distributions at the inlet of the impeller blade are shown for cases without and with cavitation.

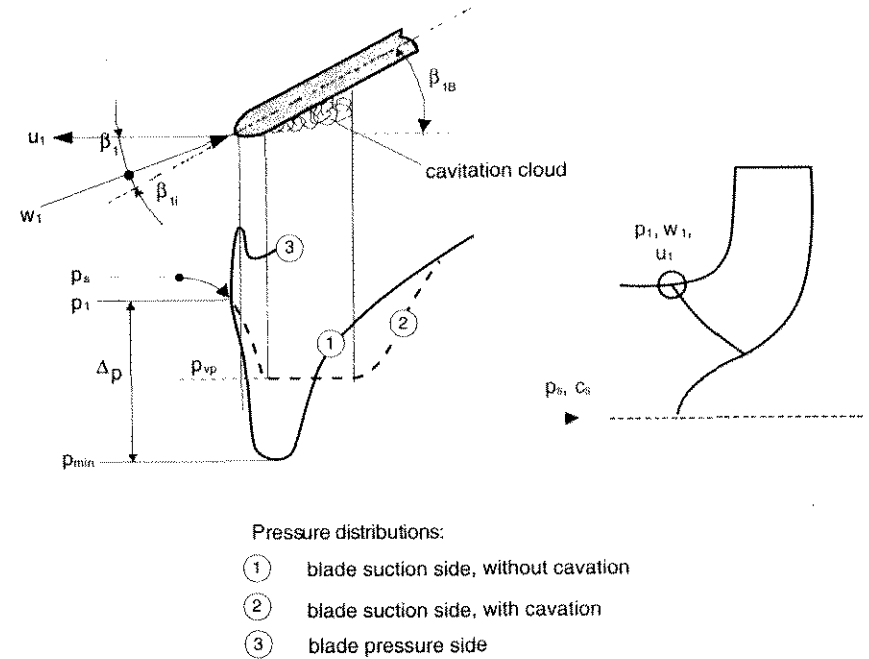


Fig.C.2.1 Pressure distribution on an impeller blade

At the pump suction flange the static pressure has a value  $p_s$  and the absolute velocity is  $c_s$ . Due to hydraulic losses in the pump suction branch and flow acceleration in this area, the static pressure in front of the impeller blade  $p_1$  is lower than  $p_s$ . Flow angle  $\beta_1$  is smaller than blade angle  $\beta_{IB}$ , so the fluid approaches the blade with an angle of incidence  $\beta_{II}$ . When the fluid flows around the profile, the pressure drops near the blade leading edge due to local fluid acceleration. Pressure drop can be defined by the following relationship:

$$\Delta p = 1/2 \cdot \rho \cdot \lambda_{w,i} \cdot w_1^2$$

The pressure drop coefficient  $\lambda_{w,i}$  depends mainly on the angle of incidence  $\beta_{11}$  and on the shape of the blade profile. When the static pressure at the blade inlet is lower than the fluid vapour pressure, cavitation bubbles are formed. The size of the cavitation cloud depends on the level of vapour pressure  $p_{vp}$ . Under the conditions ( $p_{vp} = p_{min}$ ) the first bubbles are observed visually, and so-called "cavitation inception" takes place. As the cavitation cloud becomes larger and thicker, the more significant is its influence on the flow inside the impeller, and on the pressure distribution around the blade. The effect on pump characteristics can be seen by a drop in efficiency, head and flow rate.

With an increased pump flow rate, the flow angle  $\beta_1$  also increases. When the angle of incidence  $\beta_{11}$  becomes negative (flow angle  $\beta_1$  greater than blade angle  $\beta_{1B}$ ), vapour bubbles form on the blade pressure side.

### C.3. NPSH characteristics

According to Standard ISO 3555 (Class B) the NPSH (Net Positive Suction Head) is defined as the total inlet head  $H_1$ , plus the head corresponding to the atmospheric pressure ( $p_b/\rho \cdot g$ ), minus the head corresponding to the vapour pressure ( $p_{vp}/\rho \cdot g$ ):

$$NPSH = H_1 + p_b/\rho \cdot g - p_{vp}/\rho \cdot g$$

$$H_1 = z_1 + p_1/\rho \cdot g + v_1^2/\rho \cdot g$$

For determining NPSH and  $H_1$ , the reference level shown in Fig.C.3.1. for different impeller types and installations has to be taken into account.

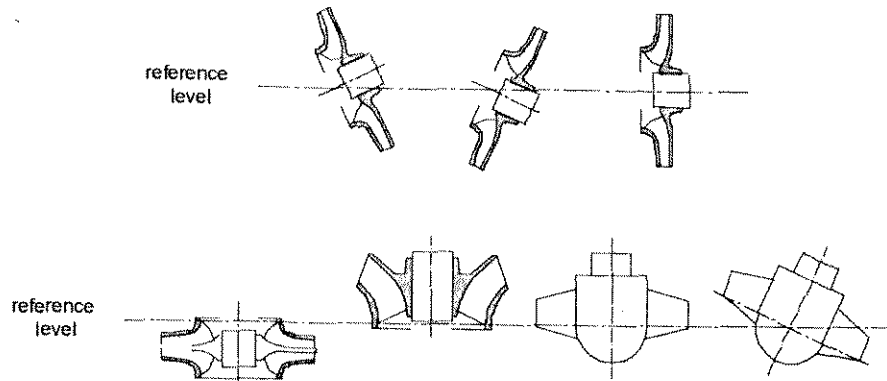


Fig.C.3.1 Definition of reference level

**NPSH required:** The  $NPSH_{req}$  describes by how much the total head should be above the fluid vapour pressure, so that the pump can operate without unacceptable or dangerous consequences. The  $NPSH_{req}$  depends mainly on the impeller inlet geometry, speed of rotation, fluid properties and pump flow rate. It can very often be seen that two different pumps with the same flow rate, head, and speed of rotation have very different  $NPSH_{req}$  characteristics. It is evident that  $NPSH_{req}$  is the characteristic which is defined by the pump.

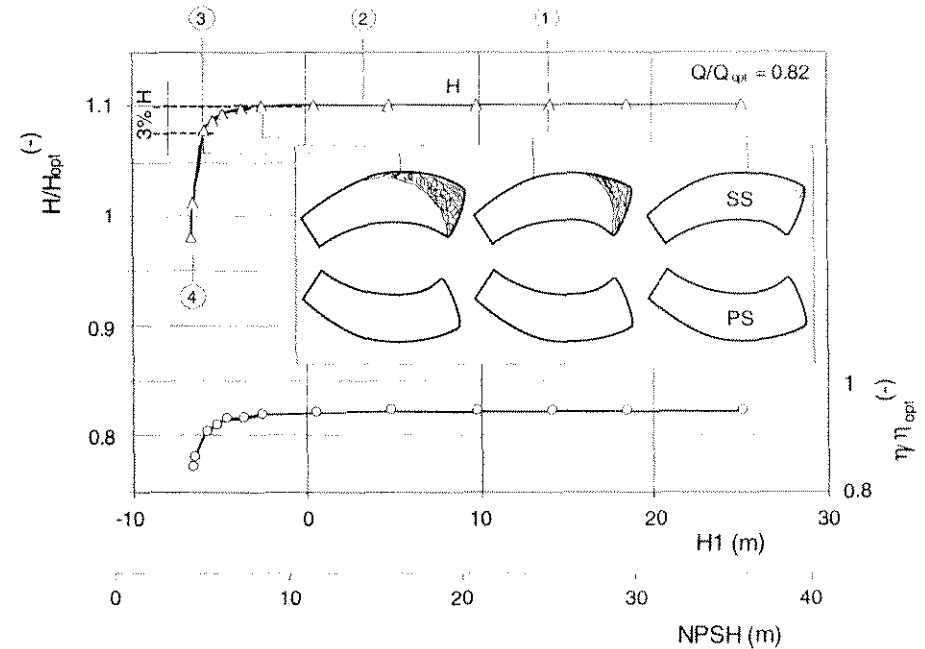


Fig.C.3.2 Influence of the inlet head on pump total head and efficiency

**Cavitation criteria:** Different criteria can be used for determining the extent of cavitation. This is represented by an example in Fig.C.3.2., showing pump characteristics at a constant speed and flow rate, but with different inlet heads  $H_1$ .

The diagram in Fig C.3.2. is obtained by measurement. The inlet head  $H_1$  is reduced in steps at a constant flow rate  $Q$ . The pump total head  $H$  is measured and cavitation phenomena are visually observed. Four characteristic points are identified and described in Table C.3.1.

Point	Criteria	Description
1	onset of cavitation (cavitation incipient)	At this inlet head the first bubbles can be observed on the impeller blade.
2	0% head drop	At this inlet head the pump total head starts to drop (difficult to determine).
3	3% head drop	At this inlet head the pump total head drops by 3%. This is a widely used cavitation criterion because determining is clear. It has to be noted that Standard ISO 3555 defines the criteria $(3 + K/2)\%$ , where the K is type number: $K = 2 \cdot \pi \cdot n \cdot Q^{0.5} \cdot (g \cdot H)^{0.75}$ $n$ (s <sup>-1</sup> ), $Q$ (m <sup>3</sup> /s), $g$ (m/s <sup>2</sup> ), $H$ (m)
4	full cavitation	At a certain inlet head the pump total head starts to fall very steeply.

Table C.3.1. Description of different cavitation criteria

Some other criteria are also sometimes used in special cases: efficiency drop, increase in noise or vibration, material damage, etc.

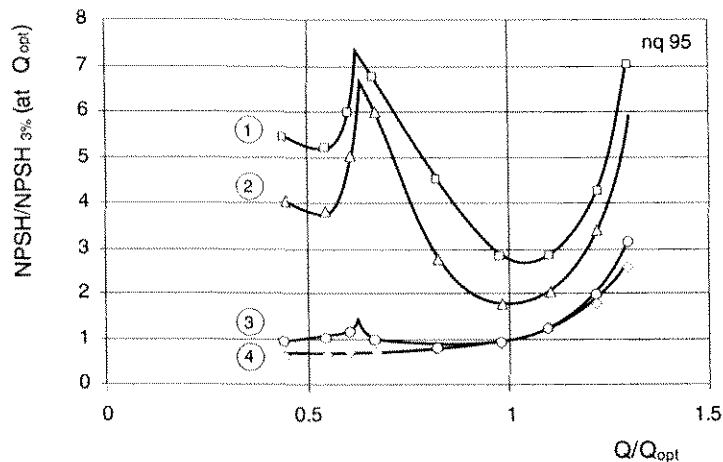
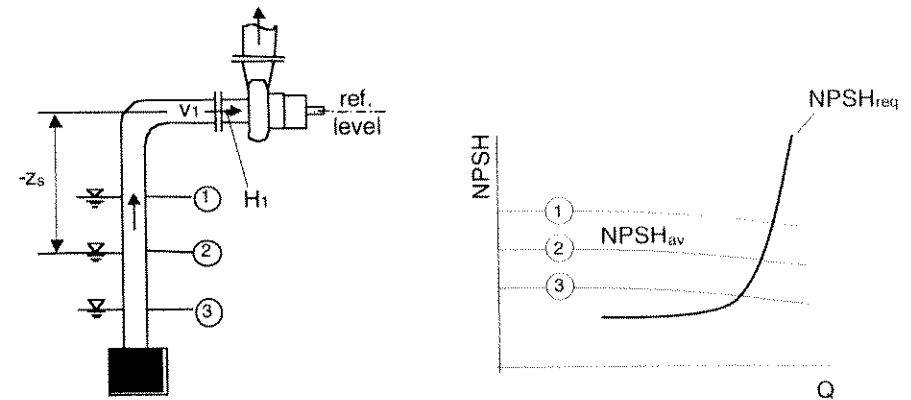


Fig.C.3.3 Determination of  $NPSH = f(Q)$  for different cavitation criteria

**Measurement of NPSH:** For determining the characteristic  $NPSH = f(Q)$  (see example in Fig.C.3.3.) a series of tests should be carried out at different pump flow rates. The pump suction conditions are changed step by step from cavitation-free operation to full cavitation. As described in Standard ISO 3555, there are other possible ways of measuring NPSH, but the most frequent are the following:

- open system: changing the suction head by adjusting the fluid level in the suction reservoir or by throttling in the suction pipe
- closed system: changing the pressure in the suction vessel

**NPSH available:** The  $NPSH_{av}$  is a value of the plant and is independent of the pump itself. It is defined as the total head in the pump suction nozzle.  $NPSH_{av}$  is dependent on the pump installation, submergence, losses in the suction pipeline, and fluid properties. Pump flow rate is not an important influencing parameter on the  $NPSH_{av}$ . It influences only the hydraulic losses in the suction pipeline.



$$H_1 = -z_s - H_{loss,s}$$

$$NPSH_{av} = H_1 + \frac{P_b}{\rho \cdot g} - \frac{P_{vp}}{\rho \cdot g}$$

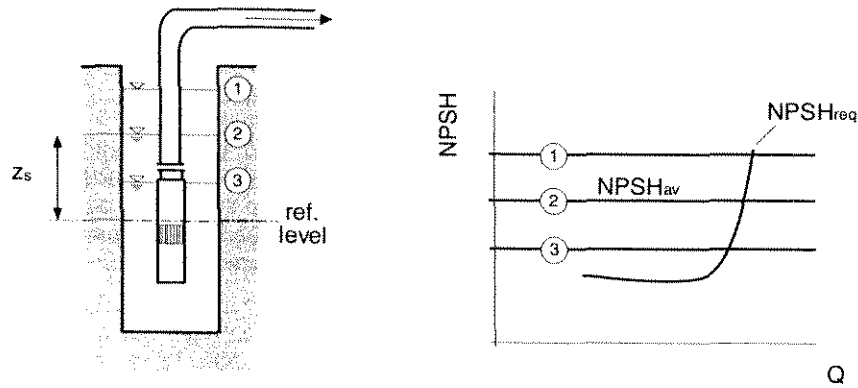
$$H_{loss,s} = f(Q^2)$$

$$NPSH_{av} = \frac{P_b}{\rho \cdot g} - z_s - H_{loss,s} - \frac{P_{vp}}{\rho \cdot g}$$

Fig.C.3.4 Pumping from suction reservoir

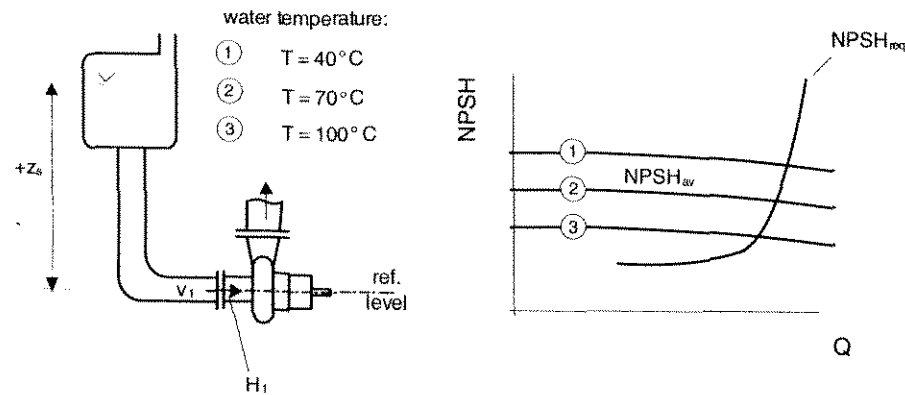
Three different pump installations are shown as examples for determining  $NPSH_{av}$ . Fig.C.3.4. represents pumping from a suction reservoir situated below the pump. Inlet pressure  $H_1$  depends on the water level in the suction reservoir  $z_s$ , and on the hydraulic losses in the suction pipeline  $H_{loss,s}$ . As can be seen from the equations and the related diagram, the  $NPSH_{av}$  is greatly dependent on the water level in the suction reservoir. The value  $NPSH_{av}$  falls slightly with an increase in flow rate, due to the effect of hydraulic losses in the suction pipeline.

In Fig.C.3.5. an example with a submersible pump is shown. The pump and motor are submerged and there is no suction pipeline, and  $H_{loss,s} = 0$ . From the related equations and diagram it can be seen that the  $NPSH_{av}$  is independent of the pump flow rate but depends greatly on the water level in the well.



$$H_i = -z_s \quad NPSH_{av} = H_i + \frac{P_b}{\rho \cdot g} - \frac{P_{vp}}{\rho \cdot g} \quad NPSH_{req} = \frac{P_b}{\rho \cdot g} - z_s - \frac{P_{vp}}{\rho \cdot g}$$

Fig.C.3.5. Pumping from well with submersible pump



water temperature:  
 ① T = 40°C  
 ② T = 70°C  
 ③ T = 100°C

$$H_i = -z_s - H_{loss,s} \quad H_{loss,s} = f(Q^2) \quad NPSH_{av} = H_i + \frac{P_b}{\rho \cdot g} - \frac{P_{vp}}{\rho \cdot g} \quad NPSH_{req} = \frac{P_b}{\rho \cdot g} - z_s - H_{loss,s} - \frac{P_{vp}}{\rho \cdot g}$$

Fig.C.3.6 Pumping of hot water

An example of pumping hot water from a suction reservoir located above the pump axis is shown in Fig.C.3.6. The values for  $NPSH_{av}$  are strongly dependent on the temperature of the water, as fluid vapour pressure is a function of fluid temperature:  $p_{vp} = f(T)$ . With increasing water temperature the  $NPSH_{av}$  decreases, as is shown in related equations and diagrams. In the case of pumping boiling water, vapour pressure and atmospheric pressure have the same values.

### C.4. Types of cavitation

Different types or forms of cavitation can develop in different parts of the pump, e.g. in the pump suction chamber, the diffuser, the exit of the axial thrust balancing system, etc. The most frequent appearance of cavitation is in the inlet part of the impeller. The most frequent types of cavitation, with their causes and consequences, are described below.

#### 1. Cavitation on the suction side of the blade

At reduced pump flow rates or at a large blade inlet angle  $\beta_{1i}$ , the flow approaches the blade with an angle of incidence  $\beta_{1i}$ . A cavitation cloud is formed on the blade suction side near the blade inlet edge (see also Fig.C.2.1). This type of cavitation is also called "sheet cavitation". Cavitation damage can be observed in the areas of bubble implosion.

#### 2. Cavitation on the pressure side of the blade

A similar cavitation behaviour to that described under item 1, but on the blade pressure side, develops at an increased pump flow rate or at a small blade angle. A negative angle of incidence ( $-\beta_{1i}$ ) occurs, and a cavitation cloud forms on the blade pressure side near the blade inlet edge. The cavitation intensity is much higher than that described under item 1.

#### 3. Cavitation due to impeller inlet recirculation

At part-load operation, impeller inlet recirculation takes place (see also section C.5.). In the outer part of the impeller channel (in the meridional cross-section) a recirculating flow pattern forms, while the inner part of the channel is still under "normal" flow conditions. Due to unfavourable flow conditions near the mixing zone between the "recirculation flow" and "normal flow", and to low pressure in the core of the recirculation vortex, cavitation damage takes place on the pressure side of the blade.

Type	Position in the meridional plane	Position on the blade	Local flow pattern
1		pressure side PS SS suction side $\omega$	$w_1$ $+\beta_{11}$
2		PS SS $\omega$	$-\beta_{11}$ $w_1$
3		PS SS $\omega$	
4			
5		$\omega$	$\omega$

Fig.C.4.1 Types of cavitation

#### 4. Cavitation in the corners between the impeller blade and hub/shroud

Due to unfavourable local flow conditions, vortexes form in the corners of the impeller channel (even at the optimal pump operating regime). This is due to the thicker blade profile in the transition zone between the blade and hub/shroud. In cases when, due to the action of centrifugal forces in the vortex core, static pressure drops to the value of the fluid vapour pressure, cavitation bubbles form. Cavitation damage can be increased because of hidden casting irregularities in the area of the impeller blade and hub/shroud connection.

#### 5. Gap cavitation between impeller blade and casing, with open impellers

Gap cavitation takes place in open impeller types in the gap between the impeller blade and the stationary casing wall. Due to the pressure difference between the blade pressure and the suction side, a fluid jet forms in the gap. The fluid jet exits the gap to the blade suction side and creates vortexes. As a consequence, especially in the area near the impeller entry, the local static pressure drops to the level of the vapour pressure. Cavitation damage often takes place on the blade tip (suction side) and on the impeller casing wall on the entire periphery.

### C.5. Recirculation at the pump inlet

When a pump is operating at part-load, a "forced" flow pattern builds up at the impeller inlet. At the outer part of the impeller eye the flow exits from the impeller channels back into the suction pipe, and at the inner part of the impeller eye the flow re-enters the impeller channel (see Fig.C.5.1). The recirculation zone chokes the outer part of the impeller eye, while the inner part still operates "normally". The flow exiting from the impeller to the suction pipe has an essential peripheral velocity component due to impeller rotation. This rotational motion is transferred to the entire fluid quantity in the suction pipe, and it rotates in the same direction as the impeller itself. In cases where there are no stationary ribs in the suction pipe, the fluid rotation can be observed a long way from the impeller.

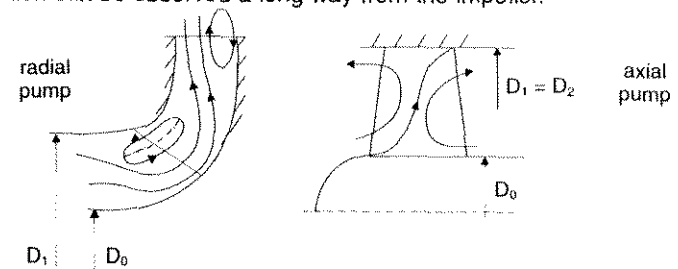


Fig.C.5.1 Typical recirculation flow patterns

The flow conditions described above have been confirmed by many different experiments on radial, mixed-flow and axial-flow impellers. Certainly, a clear qualitative difference exists between different impellers regarding the start of recirculation and recirculation intensity. Although there has been a lot of work in this field in the past, until now no general method has been developed for determining the start of recirculation.

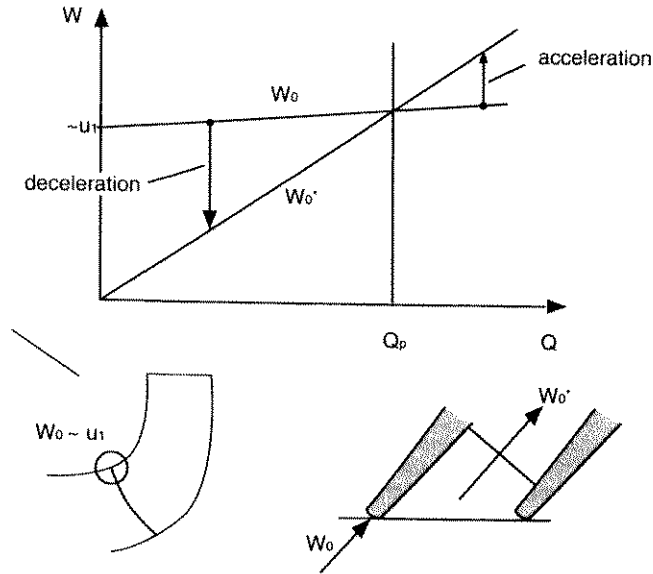


Fig.C.5.2 Velocity conditions at impeller inlet

The onset of impeller inlet recirculation can be explained with the help of the velocity conditions at the impeller inlet, as shown in Fig.C.5.2. This diagram defines the relative velocity  $w_0$  at the impeller leading edge, and the impeller throat velocity  $w_0^*$  (velocity at the smallest cross-section between the blades at the impeller inlet). Without taking into consideration flow recirculation, the relative velocity equals the impeller eye velocity  $u_1$  at  $Q=0$ . When the flow approaches the blade without rotation,  $w_0$  increases slightly with an increasing flow rate. The impeller throat velocity  $w_0^*$ , as defined in Fig.C.5.2., increases proportionally to the flow rate. Above a particular flow rate  $Q_p$  the flow accelerates from the leading edge to the throat, and below  $Q_p$  the flow decelerates. When the deceleration becomes excessive, for example below a ratio of  $w_0^*/w_0$ , flow separation and subsequent recirculation must be expected

Basically three physical mechanisms are thought to contribute to triggering flow recirculation at the impeller inlet during part-load:

- Deceleration of the relative velocity upstream of the impeller  $w_0$  to the velocity in the impeller throat  $w_0^*$
- Pressure gradients perpendicular to the direction of main through-flow
- Excessive angle of incidence  $\beta_{1i}$  at the impeller vane leading edge

Any flow recirculation leads to zones with a high shear flow creating strong vortices, which entail the following consequences:

- In the vortex core the pressure falls with respect to the surrounding bulk flow, due to centrifugal forces. If the local pressure in the centre of the vortex falls below the vapour pressure, a steam cavity is formed which implodes violently when the vortex is swept into zones of higher pressure. Cavitation erosion at the impeller or even at the diffuser vanes, or volute cut-water can be the consequence.
- Vortexes create large-scale turbulence and fluctuating lift forces on either impeller or diffuser vanes, and are thus a source of unsteady forces which can cause structural vibration in the pump rotor, bearing housings, bedplate or parts of the piping.
- The wake flowing off the impeller vane trailing edge becomes broader and more unsteady, which leads to increased pressure pulsation when the wake impinges on the volute cut-waters or on the diffuser vane leading edges.

It must be stated that recirculation develops in all pumps at part-load operating conditions. Only measurement of the excitation forces, pressure pulsation or cavitation noise, or operational experience can give the final answer as to whether the above-mentioned effects of part-load recirculation will reach damaging levels, or can be sustained without damage by the particular design of the pump in question. It should be clearly noted that the limit of damaging recirculation is by no means a universal quantity, but depends to a large extent on the particular pump design.

## C.6. Suction specific speed

To describe the suction ability of a pump or the quality of the suction impellers, a non-dimensional parameter named "Suction Specific Speed –  $n_{ss}$ " is used. The parameter is defined for best efficiency point BEP and can also be used to compare the suction characteristics of different pumps:

$$n_{ss} = n \cdot Q^{0.5} / NPSH_{3\%}^{0.75}$$

To calculate the  $n_{ss}$  in double entry pumps, the flow of one impeller side has to be considered (or half of the pump flow rate). The suction specific speed  $n_{ss}$  is calculated in an analogous way to pump specific speed  $n_q$ .

	nss
1 normal impeller with axial inlet	160 – 220
2 suction impeller with axial inlet	220 – 280
3 suction impeller for double suction pumps and multi-stage pumps	180 – 240
4 inducer for process pumps	400 - 700

Table C.6.1. Typical values of suction specific speed

In Table C.6.1. the values of suction specific speeds for different pump basic designs and impeller types are shown. The values given are valid for impeller executions into which an extensive knowledge of cavitation behaviour has been introduced.

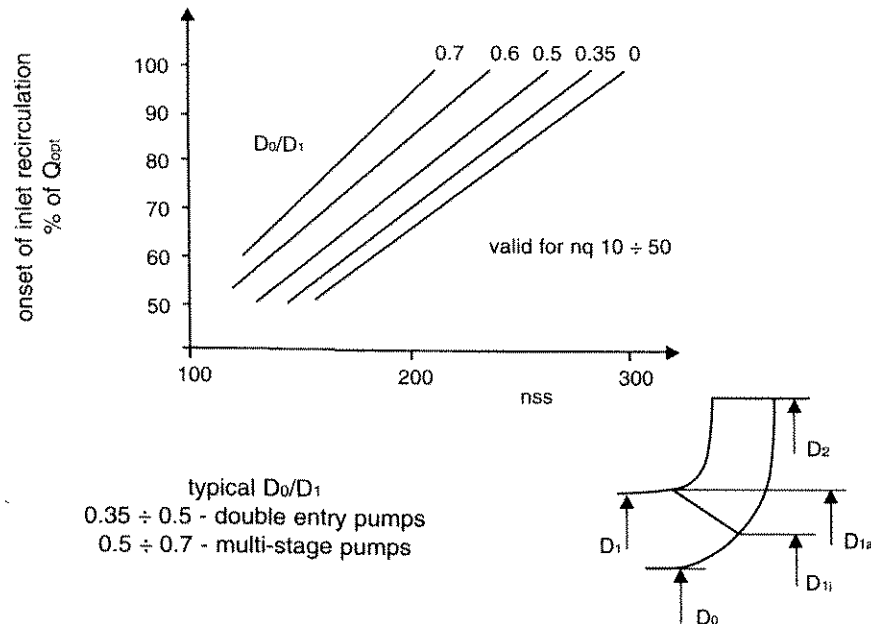


Fig.C.6.1 Relationship between nss and inlet recirculation

**Relationship between nss and inlet recirculation:** The main geometrical parameters which have an impact on impeller inlet recirculation are:

- Impeller throat area
- Angle of approaching flow
- Impeller inlet vane angles
- Ratio of impeller eye diameter to hub diameter -  $D_1/D_0$
- Ratio of diameters at vane tip and hub -  $D_{1a}/D_{1i}$
- Impeller shroud curvature - R
- Position of impeller vane leading edge (in plane view and meridional section)

Practically all the above-stated parameters also affect the  $NPSH_{3\%}$  and thus the pump suction specific speed. It is obvious that a clear relationship exists between nss and impeller inlet recirculation. The diagram shown in Fig.C.6.1. is well known, and represents the onset of suction recirculation versus suction specific speed, and for different diameter ratios  $D_0/D_1$ . For a better understanding of the consequences when increasing nss, the following explanations can be helpful:

**Increase in impeller eye diameter:** With an increased impeller eye diameter  $D_1$  higher values of nss can be reached. Due to the larger ratio of blade tip/hub diameter  $D_{1a}/D_{1i}$ , the recirculation phenomenon increases (higher pressure gradients along the impeller channel at inlet).

**Increase in inlet blade angle:** The flow rate, which adapts to the impeller inlet angle of incidence  $\beta_{1i}=0$ , shifts to higher flow rates. At BEP the cavitation characteristic is normally improved due to an "increased capability of vapour bubble transport through the impeller channels". On the other hand the recirculation intensity increases due to the increased impeller throat area, and thus flow deceleration  $w_0^*/w_0$  increases.

**Limitation of suction specific speed:** As a result of past experience, different recommendations for limiting suction specific speed have been proposed. These are based on statistical data which show that much more damage was detected in pumps with suction specific speeds higher than 220. The explanation for this fact is the following: to reach higher nss values, an impeller with a larger inlet eye diameter and greater inlet blade angles has to be designed. Such changes are on the other hand connected with higher recirculation intensity, which can cause increased cavitation erosion (depending on the material of the impeller), vibration and pressure pulsation. This conclusion is only partly correct because other parameters beside impeller eye diameter and inlet blade angle are also of great importance for the intensity and dangerous consequences of recirculation. A lot of pumps have already been installed in different types of application, and which have run for a long time trouble-free and without material damage, despite having an nss higher than 220.

## C.7. Cavitation erosion

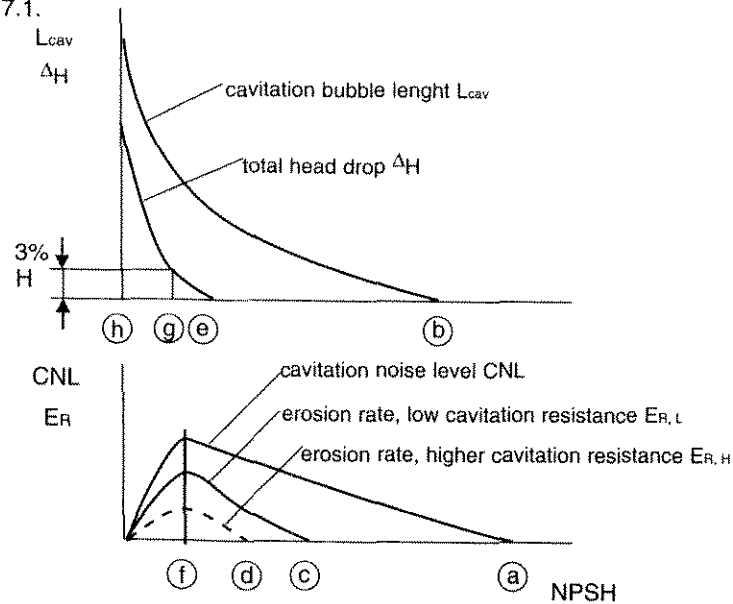
**Description of cavitation damage mechanisms:** A simplified analysis of bubble implosion leads to the conclusion that extremely high local pressures are created by an imploding bubble (see Table C.1.1.). If these pressure pulses exceed the strength of the material on which the implosions occur, material erosion is likely to result.

The details of the erosion process have been the subject of a great number of fundamental investigations carried to a high degree of sophistication. It now appears that the most probable damage mechanism is the formation of a microjet of very



high velocity, caused by the bubble implosion. This microjet is thought to be created by asymmetries of the flow around the imploding bubble, caused by its proximity to a solid wall (see Fig.C.1.3.). The pressure pulses are damaging if the pressure created exceeds the strength of the material.

Microscopically, the erosion rate depends on and increases with the ratio of cavitation intensity to cavitation resistance. At low cavitation intensity, the failure mechanism may be fatigue. At higher intensities it may be plastic deformation and finally rupture, if the tensile strength is exceeded. This statement coincides with the relationship between the different cavitation parameters, shown in diagram Fig.C.7.1.



- (a) onset of cavitation noise
- (b) onset of visual cavitation
- (c) beginning cavitation erosion, low resistance material
- (d) beginning cavitation erosion, higher resistance material
- (e) 0% head drop
- (f) maximal erosion rate
- (g) 3% head drop
- (h) full cavitation

Fig.C.7.1 Typical pump cavitation parameters

When pump inlet pressure decreases, at a certain NPSH level a moderate cavitation noise can be detected, and then the first cavitation bubbles are observed. With further decreasing, the cavitation cloud grows and the cavitation intensity, represented by cavitation noise level (CNL), also increases. Only after a certain level of cavitation intensity is reached, can material damage be observed. Material damage can take place even before the pump head starts to drop, depending on material cavitation resistance. At very low NPSH values in fully developed cavitation, the material damage decreases again due mainly to the compressibility effect of the fluid under those conditions (see chapter C.1.).

**Material properties:** The material of the pump elements has a strong effect on cavitation erosion via the following parameters:

- Tensile strength, hardness, ultimate resilience, heat treatment
- Good corrosion resistance in the liquid being pumped is a prerequisite for good cavitation resistance.
- Metallographic structure, in particular near the surface.

Despite many attempts, there is no general correlation to quantify the influence of these parameters on resistance to cavitation erosion. There are many comparative data available, showing the cavitation resistance ratio of the different materials which are commonly used in pump applications. One of them is shown in Fig.C.7.2. This example is valid for cold water and for a defined NSPH value and cavity length. Although the ratios shown should only be used for information purposes, they could be very helpful in choosing the correct impeller material.

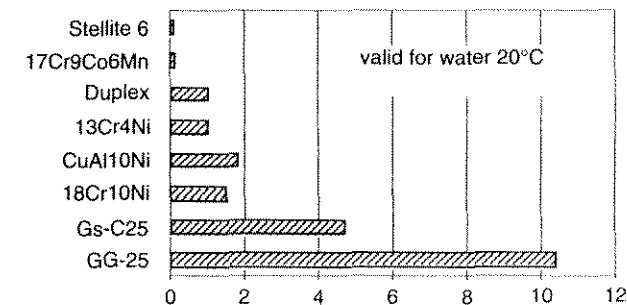


Fig.C.7.2 Comparison of cavitation erosion for different materials

There is no unique material property appropriate for correlating and fully describing the cavitation resistance of different materials. Another reason is that it is difficult to simulate and understand the reaction of a material to a highly localised, non-stationary impact loading. The metallographic structure of the material must play an important role in this reaction. When analysing the materials with regard to cavitation resistance, the influence of the parameters shown in Fig.C.7.3. has to be taken into account.

A very compressed recommendation for material with an optimal cavitation resistance might be: a combination of hardness with good toughness and corrosion resistance (especially when corrosive fluid is pumped).

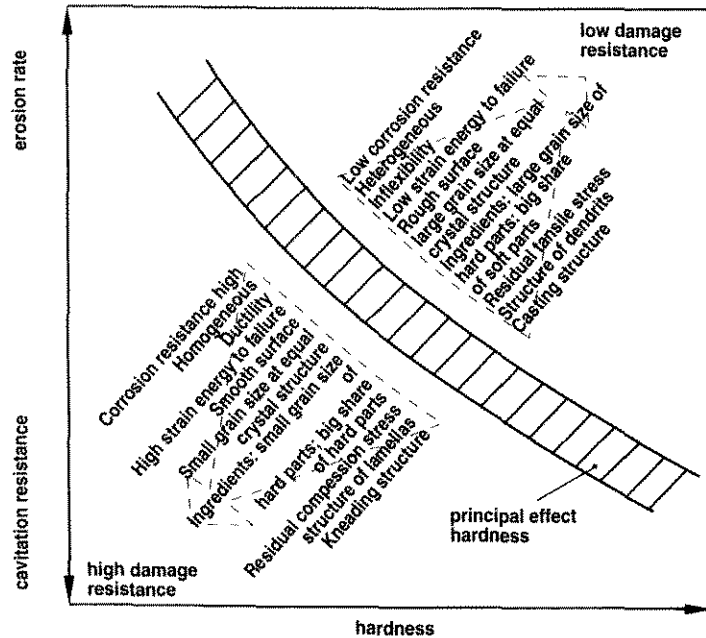


Fig.C.7.3 Effects of different parameters on the cavitation behaviour of metallic materials

### C.8. Cavitation safety values

As shown in diagram Fig.C.7.1., enlarged fields of cavitation clouds are formed long before the pump total head drops by 3%. In order to avoid the dangerous effects of noise, vibration and cavitation erosion, the pump inlet pressure (defined by  $NPSH_{av}$ ) should be reasonably higher than  $NPSH_{3\%}$  (NPSH at 3% head drop). The following relationship has to be fulfilled across the whole pump operating range:

$$NPSH_{av} \geq NPSH_{req}$$

The most important parameters influencing the level of  $NPSH_{req}$ , which will allow long-term trouble-free operation, are the following:

- circumferential velocity at impeller inlet
- material properties of the impeller
- properties of the fluid being pumped
- required operating range (min. and max. flow rates)
- the quality of pump hydraulic design, especially suction chamber and first stage impeller

In order to determine the acceptable level of  $NPSH_{av}$  on the basis of  $NPSH_{3\%}$ , a safety margin or safety factor has been introduced, which is dependent on the parameters described above. These safety margins or factors express how much higher  $NPSH_{av}$  has to be in comparison to  $NPSH_{3\%}$ , so that no dangerous consequences of cavitation can be noticed during permanent pump operation. The safety margins and factors most commonly used are given below:

definition	limitation	area of application
(a) $NPSH_{av} \geq NPSH_{3\%} + 0,5 \text{ m}$	$u_1 < 10 \text{ m/s}$	small size pumps
(b) $NPSH_{av} \geq SA \cdot NPSH_{3\%}$ $SA = 1,25$	$u_1 < 20 \text{ m/s}$	medium size pumps
(c) $NPSH_{av} \geq SA \cdot NPSH_{3\%}$ $SA$ (see Fig.C.8.1.)	$u_1 < 60 \text{ m/s}$	general criteria for industrial pump application
(d) $NPSH_{av}$ determined on the basis of equations from Table C.8.2.	$u_1 > 60 \text{ m/s}$ $H$ (stage) $> 600 \text{ m}$	pumps of high power concentration

Table C.8.1 Criteria and cavitation safety values

- When the criteria under (a) and (b) are applied, no deterioration in the pump characteristic (head, flow rate) can be expected during pump operation. The parameters for the impeller material are not included in the criteria, so their application is limited to pumps with a low cavitation intensity (low  $u_1$ ).
- The criteria under (c) are much improved. They take into account the material properties of the impeller (the borderlines in Fig.C.8.1. represent two classical materials for impellers). On the other hand  $SA$  is dependent on  $NPSH_{3\%}(atBEP)$ , which is in close correlation with implosion pressure (see section C.1.).
- When the criteria under (d) are applied, it is necessary to know the cavitation bubble length. This can be observed visually during model testing through plexi windows, or determined by paint erosion procedures (for details see Ref. EPRI).

The criteria under (d) take into account impeller material properties, pumped fluid properties, static pressure at impeller suction side and cavitation bubble length. These are parameters which are in correlation with the cavitation intensity as well as cavitation resistance. When applying the criteria under (d), an acceptable erosion rate has to be defined. Very often the following prescription is used: after 40 000 hours of operation the cavitation erosion (depth of cavitation damage) should not be deeper than 1/3 of the impeller blade thickness.

- It is common practice that most of the criteria described above are checked when defining  $NPSH_{av}$  and the highest value is taken as final.

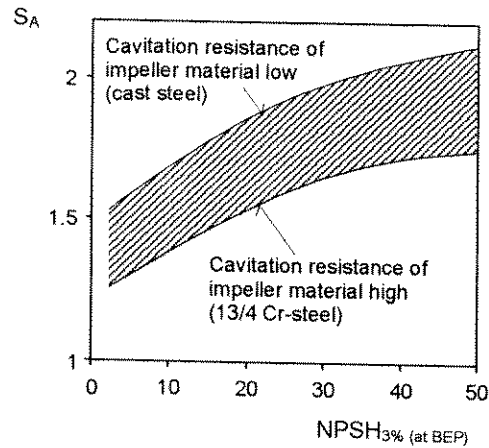


Fig.C.8.1 Cavitation safety values  $SA$  as a function of  $NPSH_{3\%}$  (at BEP)

<ul style="list-style-type: none"> <li>• Blade suction side erosion rate</li> </ul> $E_R = 2.3 \cdot 10^{-12} \cdot \left( \frac{L_{cav}}{L_{cav,R}} \right)^{2.83} \cdot \frac{(p_0 - p_{vp})^3 \cdot F_{cor}}{R_m^2 \cdot F_{mat}} \cdot \left( \frac{\alpha_R}{\alpha} \right)^{0.36} \cdot \left( \frac{a}{a_R} \right) \cdot \left( \frac{\rho_R'''}{\rho'} \right)^{0.44} \left[ \frac{m}{s} \right]$
<ul style="list-style-type: none"> <li>• Blade pressure side erosion rate</li> </ul> $E_R = 1.1 \cdot 10^{-10} \cdot \left( \frac{L_{cav}}{L_{cav,R}} \right)^{2.6} \cdot \frac{(p_0 - p_{vp})^3 \cdot F_{cor}}{R_m^2 \cdot F_{mat}} \cdot \left( \frac{\alpha_R}{\alpha} \right)^{0.36} \cdot \left( \frac{a}{a_R} \right) \cdot \left( \frac{\rho_R'''}{\rho'} \right)^{0.44} \left[ \frac{m}{s} \right]$

Table C.8.2 (continuation on pages 69-70)

- Erosion in mm  
 $E = 3.6 \cdot 10^6 \cdot E_R \cdot T$  [mm]  
 T – operation time in hours

- Meridional velocity at impeller inlet  

$$c_{om} = \frac{4 \cdot Q \text{ (per impeller eye)}}{\pi \cdot (D_1^2 - D_0^2)} \left[ \frac{m}{s} \right]$$

Q – flow rate [m<sup>3</sup>/s]  
 D<sub>1</sub> – eye diameter [m]  
 D<sub>0</sub> – hub diameter [m]

- Impeller inlet pressure, NPSH available  

$$(p_0 - p_{vp}) = \rho' \cdot \left( g \cdot NPSH_{av} - \frac{c_{om}^2}{2} \right) \left[ \frac{N}{m^2} \right]$$

p<sub>0</sub> – static pressure at impeller inlet [N/m<sup>2</sup>]  
 p<sub>vp</sub> – fluid vapour pressure [N/m<sup>2</sup>]  
 ρ' – density of pumping fluid [kg/m<sup>3</sup>]  
 g – acceleration due to gravity [m/s<sup>2</sup>]  
 NPSH<sub>av</sub> – NPSH available [m]

- Fluid properties  

$$\left( \frac{\alpha_R}{\alpha} \right)^{0.36} \cdot \left( \frac{a}{a_R} \right) \cdot \left( \frac{\rho_R'''}{\rho'} \right)^{0.44} \equiv 1 \text{ for cold water}$$

- Reference values  
 Length of cavitation cloud:  $L_{cav,R} = 10 \text{ mm}$   
 Gas content:  $\alpha_R = 24 \text{ ppm}$   
 Sound velocity:  $a_R = 1490 \text{ m/s}$   
 Density of saturated steam:  $\rho_R''' = 0.0173 \text{ kg/m}^3$

Table C.8.2 (continuation on page 70)

## • Material properties

Material factor  $F_{mat}$  and corrosion factor  $F_{cor}$ 

material	$F_{mat}$	$F_{cor}$	
		feedwater, fresh water	sea water
ferritic steels	1.0	1.0	1.5
austenitic steels	1.7	1.0	1.3

material DIN	ASTM	composition (%)				$10^6 R_m$ (N/m <sup>2</sup> )	
		Cr	Ni	Mo	other	range	average
GS-C25	A216GrWCA	-	-	-	-	440-590	515
G-X10CrNi131	A743GrCA-15M	13	1	0.4	-	640-740	690
G-X5CrNi134	A743GrCA-6NM	13	4	0.7	-	760-960	860
G-X7CrNiMoNb15 5	A747CB7Cu-1	17	7	1	Nb0.34	840-1140	990
G-X15CrCoMo13 10		13	-	-	-	-	975

Table C.8.2 Estimation of cavitation erosion rate from cavity length

## C.9. Methods for improving the pump system cavitation performance

When cavitation damage, unacceptable noise or vibration, or deterioration of the pump characteristic are observed during pump operation, improvements in the pump system cavitation performance are necessary. After checking and analysing the consequences of unsatisfactory cavitation conditions, and when based on these consequences the causes for the problems can be defined, possible remedial measures should be focused on the following items:

**Increasing NPSH<sub>av</sub>:** By increasing the NPSH available, the pump inlet pressure is increased, and with this the pump cavitation conditions are improved. The NPSH<sub>av</sub> can be increased by the following measures:

- in "wet installations" (see Fig.C.3.5.), by deeper submergence of the pump,
- in "dry installations" (see Fig.C.3.4. and Fig.C.3.6.), by increasing the water level in the suction basin, by increasing the pressure in the suction tank, and by decreasing the hydraulic losses in the suction pipe,
- by installing a "booster pump" in front of the main pump.

**Decreasing NPSH<sub>req</sub>:** When the pump cavitation characteristic is improved, then with an unchanged NPSH<sub>av</sub> the negative effects of cavitation are eliminated or reduced. The NPSH<sub>req</sub> can be decreased by the following measures:

- by reducing the pump rotation speed (the changed Q-H operating point has to be taken into account, or a possible correction applied to the outlet section of the impeller blades),
- when a pump is running permanently at part-load or at overload, correction of the impeller inlet geometry is needed in order to adapt the impeller inlet geometry to the actual pump flow rate data,
- in cases when the pump suction specific speed  $n_{ss}$  is considerably lower than that shown in Table C.6.1., an improvement in the impeller suction geometry is necessary by changing one or more parameters: blade angle, impeller eye diameter, number of blades, inlet blade profile,
- improvement in the impeller inlet conditions, in order to reach as far as possible a uniform velocity distribution around the entire impeller inlet periphery (especially in pump designs with a radial inflow).

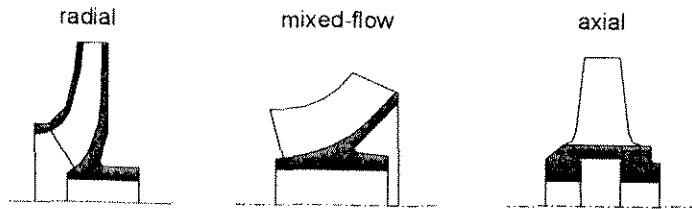
**Improved cavitation resistance:** The impeller has to be replaced with another one made of material with a higher cavitation resistance (see Fig.C.7.2. and Fig.C.7.3.). The lengthening of the impeller lifetime can be estimated by the method shown in Table C.8.2. It has to be stated that with improved impeller cavitation resistance, all other initial negative effects of cavitation, such as noise, vibration, and deterioration in the pump characteristic, remain unchanged.

In many cases the application of one of the above-mentioned improvements does not lead to a satisfactory improvement in the pump system cavitation conditions and a combination of two or more improvements has to be applied.

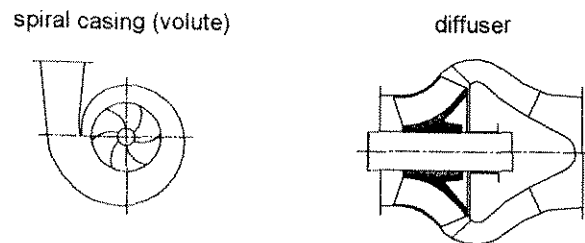
## D. BASIC PUMP DESIGN

### D.1. Designs of hydraulic elements

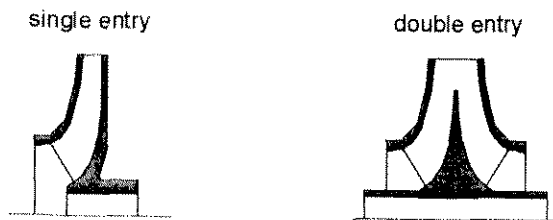
Impeller:



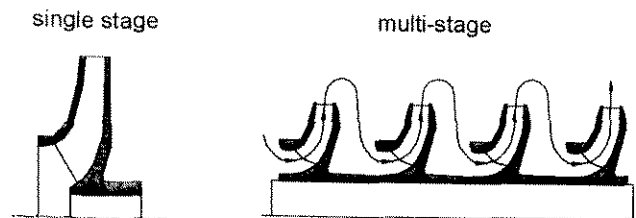
Casing/ diffuser:



Inflow:

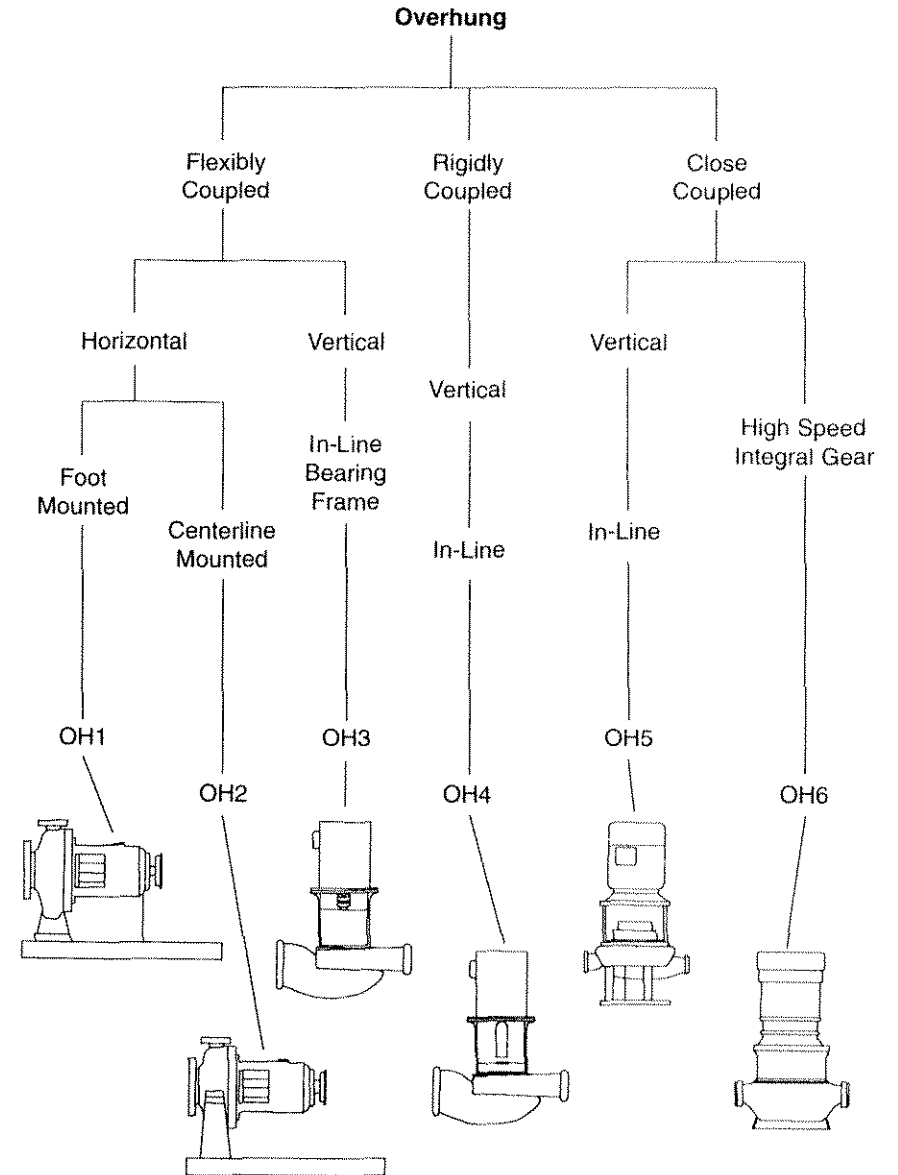


Stages:

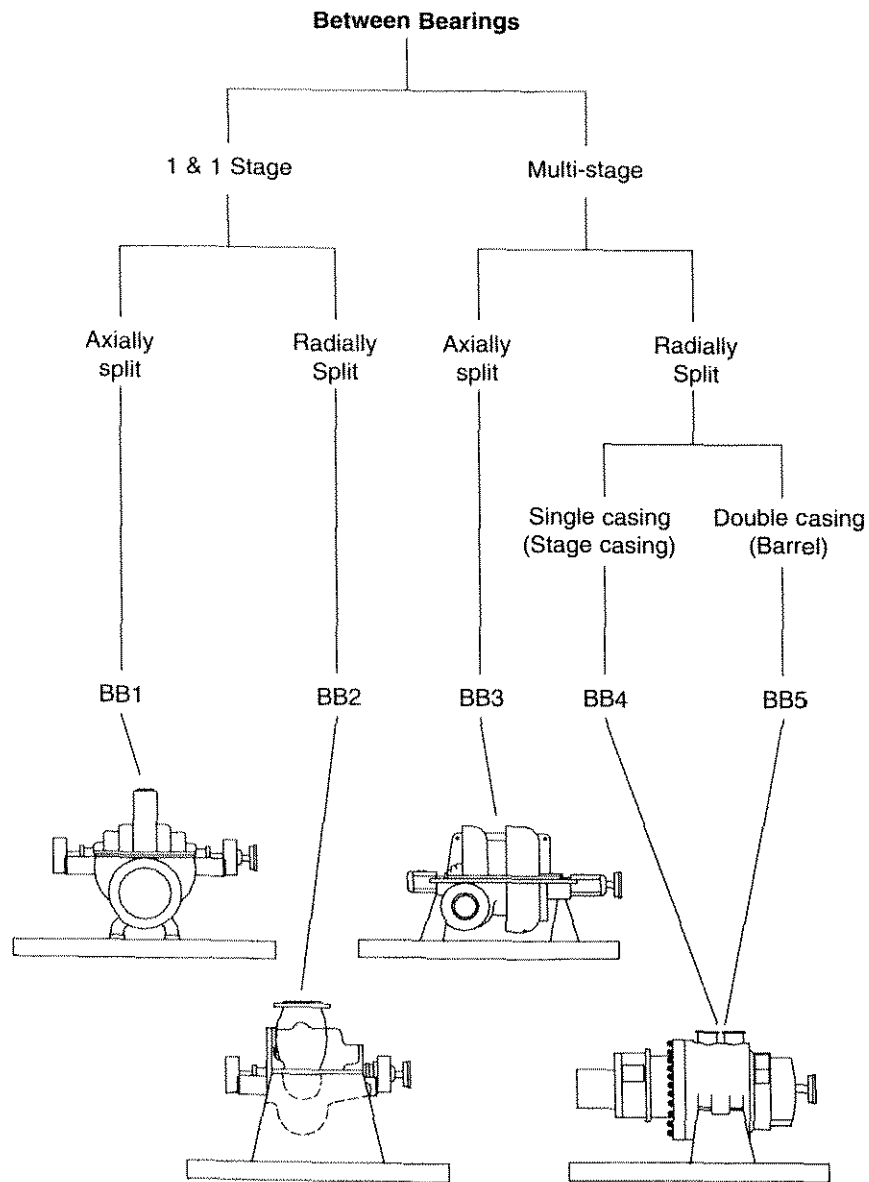


## D.2. Mechanical design (pump types according to API 610/8)

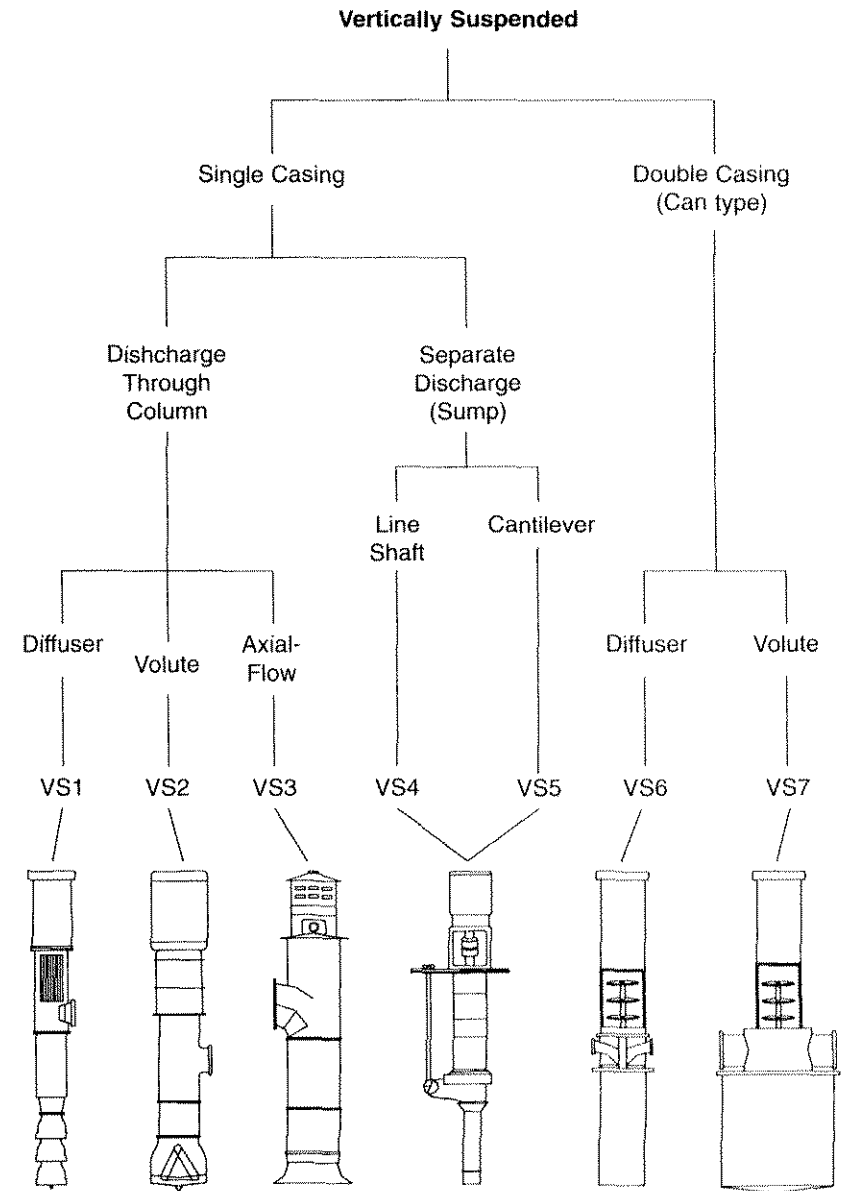
### D.2.1. Centrifugal pump types – Overhung



### D.2.2. Centrifugal pump types – Between Bearings



### D.2.3. Centrifugal pump types – Vertically Suspended



### D.3. Main application areas

#### D.3.1. Water

Sub-area	Basic design types			
Water transport	OH1	OH3		
	BB1	BB3	BB4	BB5
	VS1	VS3		
Irrigation, Drainage	OH1	OH3		
	BB1			
	VS1	VS3		
Sewage	OH1	OH3	OH5	
	VS1	VS3	VS4	
Desalination	BB1	BB4	BB5	
	VS2	VS3	VS6	VS7

#### D.3.2. Power generation

Sub-area	Basic design types		
Boiler-feed	BB2	BB4	BB5
Condensate	VS1	VS2	VS6
Cooling water	BB1		
	VS1	VS3	
Auxiliary	OH1	OH2	OH3
	BB1	BB4	
	VS1	VS4	VS5

#### D.3.3. Oil and gas

Sub-area	Basic design types		
Oil and Gas transport	BB1	BB2	BB3
Water injection	BB5		
Refinery	OH2		
	BB2	BB5	
	VS6	VS7	
Auxiliary	OH1	OH2	OH3
	BB1	BB3	BB4
	VS1	VS3	VS4

#### D.3.4. Industry

Sub-area	Basic design types		
Mining	BB3	BB4	
	VS1		
Flue gas desulphurisation	OH1		
	VS1	VS4	VS5
Paper	OH1	OH3	OH4
	BB1	BB4	
	VS1	VS3	VS4
Sugar	OH1	OH2	OH3
	BB1		
	VS1		

## E. MECHANICAL COMPONENTS OF A CENTRIFUGAL PUMP

### E.1. Bearings

The bearings in a centrifugal pump have the function of positioning the shaft correctly against the stationary pump parts, according to the static and dynamic radial and axial forces, which can have different origins (see section F). The selection of the bearing type is based on a combination of load, rotational speed, and economic factors. Many types of bearing have been used in centrifugal pumps. Today roller contact and hydrodynamic bearings are used in most pumps for supporting radial as well as axial forces.

A basic classification regarding speed and loading is shown in table E.1.1. More detailed bearing characteristics are given in sections E.1.1. and E.1.2..

Type	Load	Lubrication system	Speed*	Loading*
Rolling contact bearings	Radial	grease-sealed bearings	moderate	light to moderate
		oil-bath or mist	moderate to high	moderate
	Axial	grease-sealed bearings	moderate	moderate
		oil-bath or mist	moderate to high	moderate
hydrodynamic bearings	Radial	grease-shaft driven grease pump	moderate	moderate
		oil-forced lubrication	high	high
	Axial	water or product pumped	moderate	light
		self lubrication	moderate	light
Axial	oil-forced lubrication	moderate	high	

\* limits acc. to Standard API 610/8 are given below

Table E.1.1 Basic classification of bearings

Generally hydrodynamic bearings are used where loads exceed the capacity of roller contact bearings. The limits are sometimes prescribed, for example in Standard API 610/8, where it is stated that rolling contact bearings can be used, if:

- the rolling element speed factor defined as  $n \cdot d_m$  does not exceed 500.000 ( $n$  (rpm) – speed of rotation,  $d_m$  (mm) – mean bearing diameter)

- the rolling element bearing life, defined as  $L_{10h}$  (ISO 281) is at least 25.000 h at rated conditions and 16.000 h at maximum radial and axial loads and rated speed (usually at shut-off)
- the energy density, defined as  $P \cdot n$ , is lower than 4 million (P (kW) – power, n (rpm) - rated speed).

In all other cases oil-lubricated hydrodynamic bearings should be used.

### E.1.1. Rolling contact bearings

Rolling contact bearings are the most convenient for the majority of standard pumps. Their major advantages over hydrodynamic bearings are: lower price, lower friction losses, and the capability of operating in both directions of rotation. They are also called anti-friction bearings.

Some types of rolling contact bearings which are used most often in pumps, are shown in Fig.E.1.1. The most popular are deep groove ball bearings, which carry radial and axial thrusts.

The bearing size is selected based on its required lifetime, which should be higher than the rated bearing lifetime. For bearings operating at a constant speed, the basic rated lifetime equation (acc. to ISO 281) is:



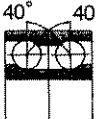



$$L_{10h} = \frac{10^6}{60 \cdot n} \left( \frac{C}{P} \right)^p$$

- where:
- $L_{10h}$  rated bearing lifetime (millions of hours)
  - $n$  speed of rotation (rpm)
  - $C$  rated dynamic load for selected bearing (from bearing supplier catalogue, N)
  - $P$  equivalent dynamic bearing load (N)
  - $p$  exponent of the life equation, dependent on type of bearing (from bearing supplier catalogue)

Fig.E.1.2 gives the method of determining the equivalent dynamic bearing load, a combination of axial and radial forces, for a bearing arrangement for a single-stage end suction centrifugal pump. In addition to the hydraulic loads, the forces resulting from couplings or belt drives should also be taken into account.

The rated dynamic bearing load  $C$  is strongly affected by bearing temperature and decreases considerably with temperature rise. For calculating the bearing lifetime, the dynamic bearing load has to be multiplied by the temperature factor from Table E.1.2.

### Approximate relative load, speed and misalignment capabilities

	Radial load	Axial load	Speed	Misalignment
 Single row deep groove ball bearing	+	+	++++	++
 Double row angular contact ball bearing	++	++	+++	+
 Single row angular contact ball bearing pair	++	++++	+++	+
 Cylindrical roller bearing	+++	-	++++	+
 Spherical roller bearing	++++	++	++	++++
 Taper roller bearing set	++++	++++	++	+

- no capacity
- + low
- ++ moderate
- +++ high
- ++++ very high

Fig.E.1.1 Rolling contact bearings for centrifugal pumps – design and characteristics



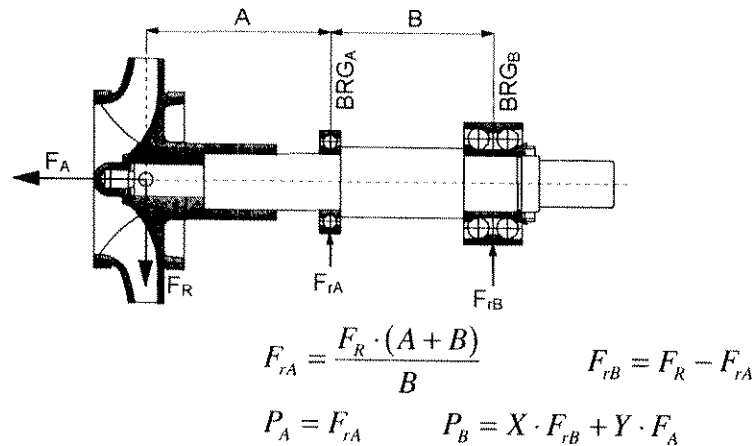


Fig.E.1.2 Determination of bearing reactions  $F_{rA}$  and  $F_{rB}$  and equivalent dynamic bearing loads  $P_A$  and  $P_B$  for a single-stage end suction centrifugal pump ( $F_A$  and  $F_R$  calculated or measured,  $X, Y$  from bearing catalogue)

Bearing operating temperature	50°C	200°C	250°C	300°C
Temperature factor	1	0.9	0.75	0.6

Table E.1.2 Temperature factor for calculation of bearing lifetime

For satisfactory operation, the roller bearing should be loaded with a certain minimum radial or axial load, depending on bearing type. A minimum axial load for angular contact ball bearings is defined by the following equation (SKF catalogue):

$$F_{amin} = A \cdot \left( \frac{n}{1000} \right)^2$$

where:  $F_{a \min}$  minimum required axial load (N)  
 $A$  minimum load factor (see SKF catalogue, Kg.m)  
 $n$  rotational speed (rpm)

At increased speeds, unloaded balls could begin to slide instead of rolling. Sliding damages the raceways, balls and cage, and increases friction. The temperature increases very rapidly, the effectiveness of the lubricant is reduced and as a result of this the lifetime drops, or the bearing is even destroyed.

In addition to lubrication, the lubricant (oil or grease) also provides cooling of the bearing and corrosion protection. Rolling contact bearings can be grease-lubrica-

ted at the normal speeds of the majority of pumps, which means simple and cheap maintenance. Special attention should be given to bearings with shields or seals on both sides (Fig.E.1.3.); these are lubricated for life and are maintenance-free. If the pump is not in operation for a long period, the shaft should be turned occasionally, so as to maintain the lubricant film coating of the balls.

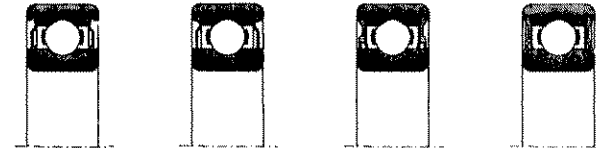


Fig.E.1.3 Deep groove ball bearings with shields and seals on both sides

For higher rotational speeds and bearing dimensions, as well as for more severe applications, oil lubrication should be used. The most common methods are oil baths, oil rings and oil mist. To maintain a constant oil level, a vessel which replenishes oil lost is sometimes mounted on the bearing casing. The generally recommended lubricating oil viscosity grades for bearings used in centrifugal pumps, if they operate between 50 and 100% of rated speed (from catalogue), are shown in Table E.1.3.

Bearing operating temperature	Ball and cylindrical roller bearings	Other roller bearings
70°C	ISO VG 46	ISO VG 68
80°C	ISO VG 68	ISO VG 100
90°C	ISO VG 100	ISO VG 150

Table E.1.3 Oil viscosity grades

At lower speeds, oils with higher viscosity grades should be considered, and at higher speeds oils with lower viscosity grades.

An oil bath can be used in horizontal and vertical pump arrangements, for low to moderate peripheral velocities. In horizontal applications the oil bath level is set at the centre of the bearing's lowest rolling element (Fig.E.1.4.a). The housing must have a bypass beneath the bearings, to allow the oil to flow into both sides of the bearing. The cross-sectional area should be big enough.

For vertical applications, the oil level is set slightly above the centre of the upper surface of the bearing (Fig.E.1.4.b). Vertical oil bath lubrication produces high ventilation losses if bearings are fully submerged. In order to reduce high ventilation losses and to avoid creating an oil/air mixture, oil mist lubrication can be used in more severe applications.

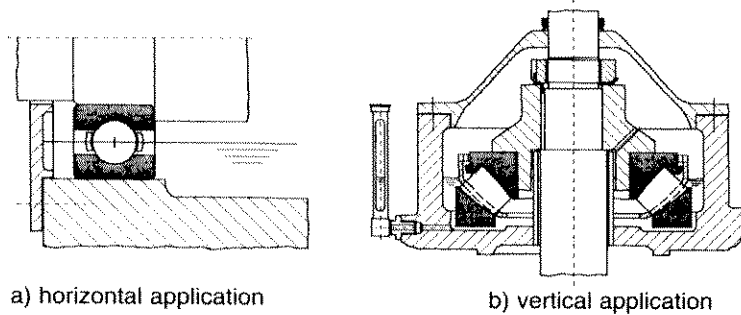


Fig. E.1.4 Oil bath lubrication of roller bearings

Oil ring lubrication is used for horizontal arrangements only. It is shown schematically in Fig.E.1.5.a. The rotation of the shaft and oil ring throws oil from the bath into the bearings and housing channels. An oil ring is made of brass or steel. Its inner diameter is generally 1,6 to 2,0 times the diameter of the shaft, and its submergence should be 3 to 5 mm above the lower edge of the bore of the oil ring. Oil ring lubrication reduces the oil volume brought to the bearing and therefore the bearing friction. Because of the lower friction and better cooling, higher shaft speeds and lower viscosity oils are possible with oil ring lubrication. According to experience, shaft peripheral speed is limited to about 20 m/s. Oil mist lubrication provides droplets of clean and cool oil to the bearings (Fig. E.1.5.b). The mist, produced by a mist generator, is conveyed to the bearing house by compressed air.

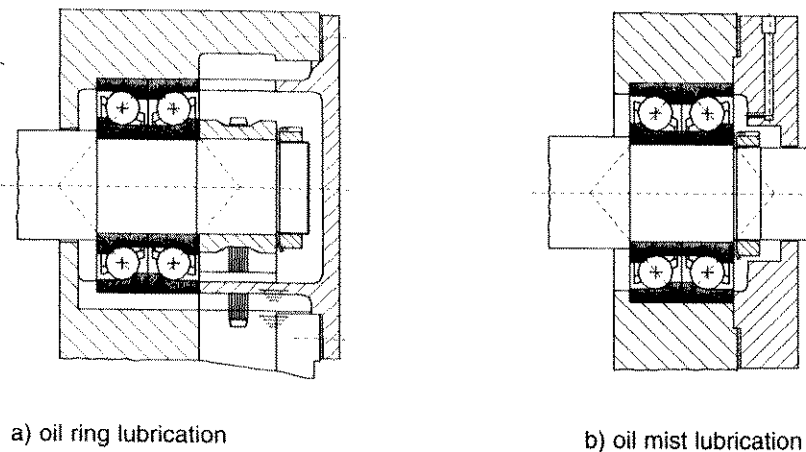


Fig. E.1.5 Oil ring and oil mist lubrication of roller bearings

### E.1.2. Hydrodynamic radial bearings

The function of a hydrodynamic radial bearing is to take over the radial loads at the allowed temperature of the bearing material. The surfaces of the rotating shaft (journal) and the stationary parts of the bearing are separated by an oil film. The rotating shaft pumps the oil into the bearing gap and causes the development of an oil film with a well-defined pressure distribution. An example for a cylindrical bearing with oil pressure distribution around the shaft in radial and axial directions is in Fig.E.1.6. Due to the radial loading of the shaft, the latter moves into an eccentric position by eccentricity  $e$ . The position of the shaft is given by the equilibrium between the radial force and the reaction force created by the integral of the oil pressure distribution around the shaft. Oil is used most frequently as the lubricating and also cooling fluid.

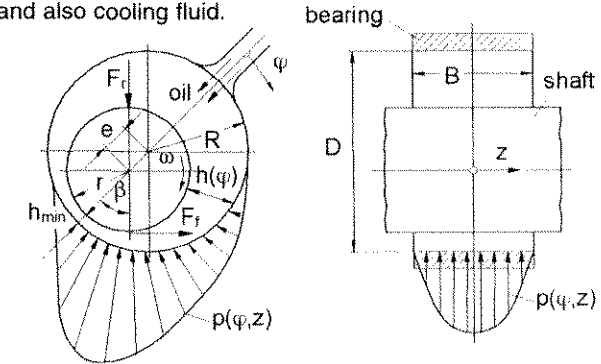


Fig.E.1.6 Schematic drawing of a radial cylindrical hydrodynamic bearing

During pump starting, operating and stopping, three different types of friction occur in hydrodynamic bearings: dry, mixed and fluid friction. They are shown in a Stribeck curve in Fig.E.1.7. When the pump is at standstill ( $\omega = 0$ ) there is no gap between the shaft and the bearing shell. At this point, the dry friction of solid bodies is valid, and depends on the characteristics of the materials of the shaft and bearing shell which are in contact. At start-up, dry friction is immediately (after a few turns of the shaft) converted into mixed friction. As the sliding speed increases, the amount of dry friction decreases and that of fluid friction increases. Finally at a speed of  $\omega_{tr}$ , the transition point is reached where the sliding surfaces separate from each other, and pure fluid friction prevails, with a minimum of friction losses. As the sliding speed increases further, the thickness of the lubricating film increases, but also the friction losses increase slowly again. Curve (a) represents the friction at a constant bearing temperature, i.e. at constant oil viscosity. In practice the temperature in a bearing rises from the start-up and causes a decrease in oil viscosity and a more constant shape in the friction curve, curve (b). The bearing operating point should always be in the region of fluid friction, otherwise mixed friction occurs, producing a rise in temperature and excessive wear.

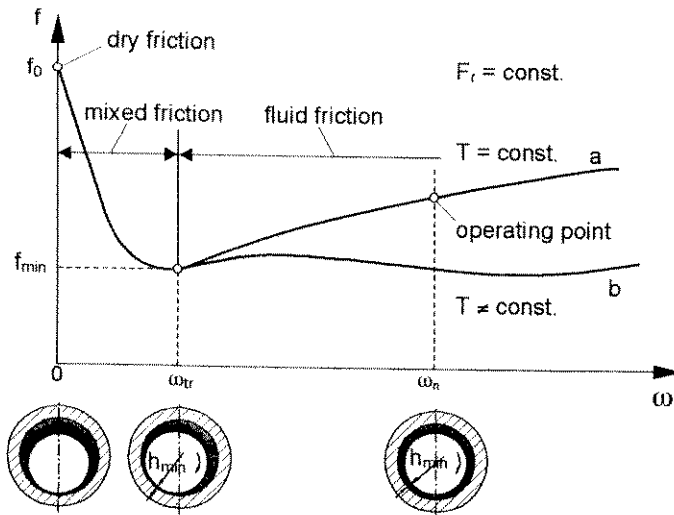


Fig.E.1.7 Schematic representation of a Stribeck curve,  $T$  – oil temperature,  $f$  – friction coefficient,  $\omega$  – angular velocity

The most important parameter for the lay-out of a radial bearing is the Sommerfeld number, a dimensionless representation of the carrying capacity, according to the definition (see also Fig.E.1.6.):

$$So = \frac{\bar{p} \cdot \psi^2}{\eta \cdot \omega}$$

$$\bar{p} = \frac{F_r}{B \cdot D}$$

$$\psi = \frac{2 \cdot (R - r)}{D} \quad (\text{based on experience } \psi \approx 1.2 \text{ to } 1.4 \text{ ‰})$$

- $\bar{p}$  mean pressure on bearing surface
- $\psi$  relative gap
- $\eta$  oil dynamic viscosity (at operating conditions)
- $\omega$  angular velocity

For each radial bearing type and each bearing size  $D/B$ , there is a well-defined relationship between relative eccentricity  $\epsilon$  and the Sommerfeld number  $So$ . Relative eccentricity is defined as:

$$\epsilon = \frac{e}{R - r}$$

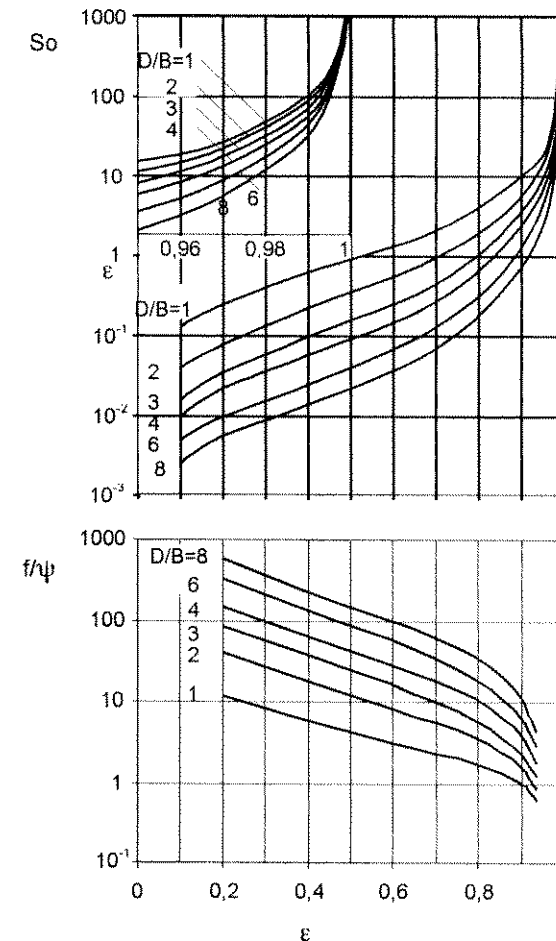


Fig.E.1.8 Sommerfeld number  $So$  and friction coefficient  $f/\psi$  for radial hydrodynamic bearings as a function of geometry  $D/B$  and relative eccentricity  $\epsilon$

Different types of stationary parts are possible in radial bearings, and each one has its advantages and disadvantages. Two types which are most often used in centrifugal pumps are shown in Fig.E.1.9.

When tangential movement of the shaft occurs under certain loadings, a potential danger of self-excitation and bearing instability exists. Different geometries of radial bearing behave differently, and especially if the specific loading is low (low  $So$  number) the consequence can be an unstable behaviour with a danger of oil whip. Good stability against oil whip is particularly important in low-load radial bearings.

Four-lobe radial bearings have the best stability against oil whip, because they ensure the smallest possible tangential movement.

The bearing material, together with the material of the shaft and the lubricant, should create good sliding conditions. The bearing material should bind the lubricant effectively to the sliding surfaces, and this is especially important during start-up and slowdown, when mixed friction occurs and contact exists between the materials. With a shaft made of steel the following materials are used for the bearing shell:

- white metal on lead basis,
- white metal on tin basis,
- lead bronzes,
- tin bronzes,
- special brasses.

An important characteristic of the bearing material is also that it should allow the pump to operate for a short time during a failure of the lubrication system, without excessive damage. This is especially important with thrust bearings in vertical pumps. When a pump remains at standstill for a long time, the lubricating property of the remaining oil film is reduced. This fact can lead to damage to the bearing, if the specific loading is too high.

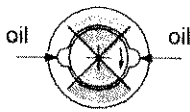
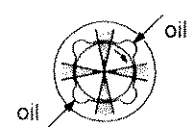
bearing type	stability against oil whip	carrying capacity	stiffness	damping	acceptance of rotating load
cylindrical with plain bore and two axial grooves 	+	+++++	++	++	++
four lobe 	+++	++	+++	+++	+++
	+ ++	low moderate	+++ +++++	high excellent	

Fig.E.1.9 Advantages and disadvantages of two types of radial hydrodynamic oil bearings

### E.1.3. Hydrodynamic thrust bearings

Thrust bearings take over the hydraulic axial forces of centrifugal pumps. For a vertical shaft position the weight of the pump rotor should be taken additionally by an axial thrust bearing. In the designing of a bearing, special attention should be paid to the starting of vertical pumps. Reverse rotation of the pump during full load rejection, resulting in run-away, must also be considered in the designing.

Tilting pad bearings are usually used as thrust bearings. There are two basic designs of tilting pad thrust bearings (Fig.E.1.10.):

- for a single direction of rotation, the pads are eccentrically supported. If the bearing operates in the reverse direction, the temperature increases considerably.
- for both directions of rotation, the pads are centrally supported; however, the bearing carrying capacity is lower

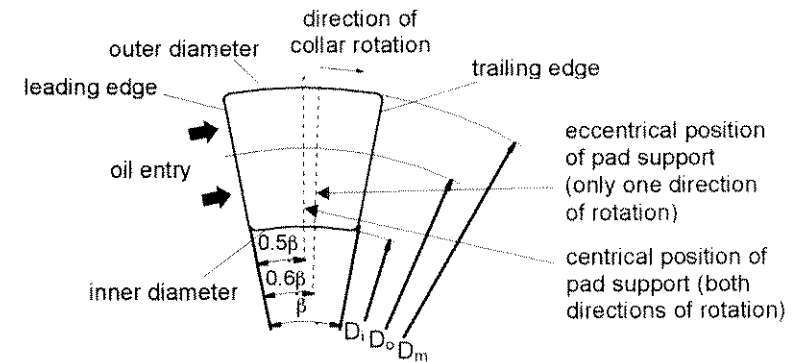


Fig.E.1.10 Schematic drawing of a segment of an axial tilting pad bearing

The basic pressure and velocity distributions in a bearing are in Fig.E.1.11. The size of the thrust bearing depends on the pump shaft size, permitted pressure loading of the pads, permitted temperature rise in the bearing (the recommended temperature rise is between 30 and 40°C), peripheral velocity and method of cooling.

The conventional method of lubricating tilting pad thrust bearings is fully flooded lubrication (Fig.E.1.12.a). A housing over-pressure of 0.7 to 1.0 bar is usual, and seal rings are required. Flooded lubrication is simple, but at higher peripheral collar speeds the losses are relatively high. Where speed exceeds 50 m/s directed lubrication is introduced (Fig.E.1.12.b). Oil is injected directly between the pads. It reduces ca. 50% of the power losses due to ventilation, and it also reduces bearing temperature, and therefore the amount of oil required. The preferred oil supply over-pressure in directed lubrication is ca. 1.4 bar.

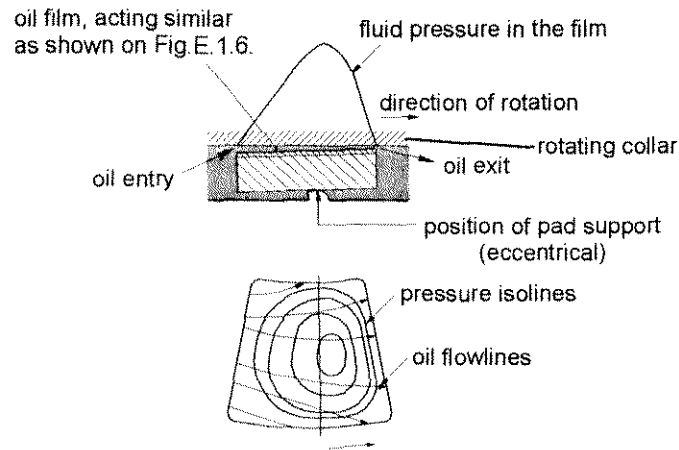


Fig.E.1.11 Pressure distribution in an eccentrically supported pad of a thrust bearing

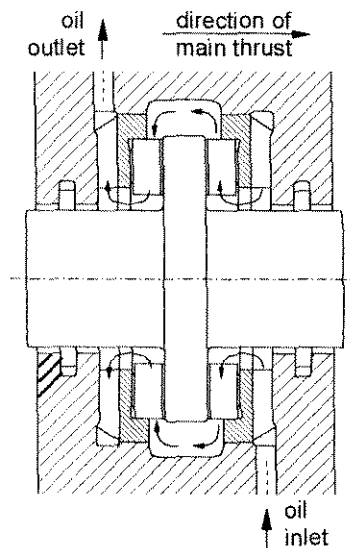


Fig.E.1.12.a Tilting pad thrust bearing - flooded lubrication

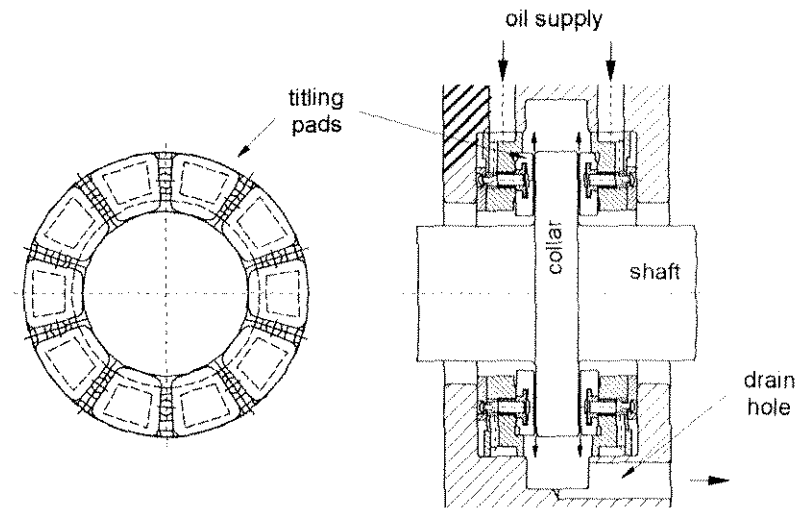


Fig.E.1.12.b Tilting pad thrust bearing - directed lubrication

The supply of lubricating oil is executed by an external pressurised lubricating oil system. Usually the system includes a shaft-driven oil pump, oil reservoir, heat exchanger, filter, flow-, pressure- and temperature indicators, safety low-pressure switches, and various valves and piping. In order to improve the redundancy of this important auxiliary system and consequently also the availability of the pump system, a motor-driven auxiliary oil pump is added to the system. One central system is often used for several pumps.

For horizontal pumps with a moderate power concentration ( $PC < 5 \text{ MW/m}^2$ ) one option with a safe auxiliary oil system is a self-contained bearing system. A schematic drawing showing such a system according to Glacier Co. is in Fig.E.1.13. It contains two main parts:

- a central unit is positioned on one side of a pump shaft, and includes thrust and radial bearings, and produces the necessary oil flow for all the pump bearings
- a remote unit with a radial bearing is mounted on the other side.

Forced lubrication is autonomous, being provided by a pumping system driven directly by the shaft. No priming is necessary because the pump inlets are always submerged. The pump and bearings are designed for both directions of rotation. This pump generates sufficient pressure and flow to ensure an oil supply to separate remote radial bearings as well. The system eliminates the need for an external lubrication system. Self-contained bearing systems accommodate thrust loads up to ca. 200 kN, shaft sizes up to ca. 200 mm and speeds up to ca. 10000 rpm.

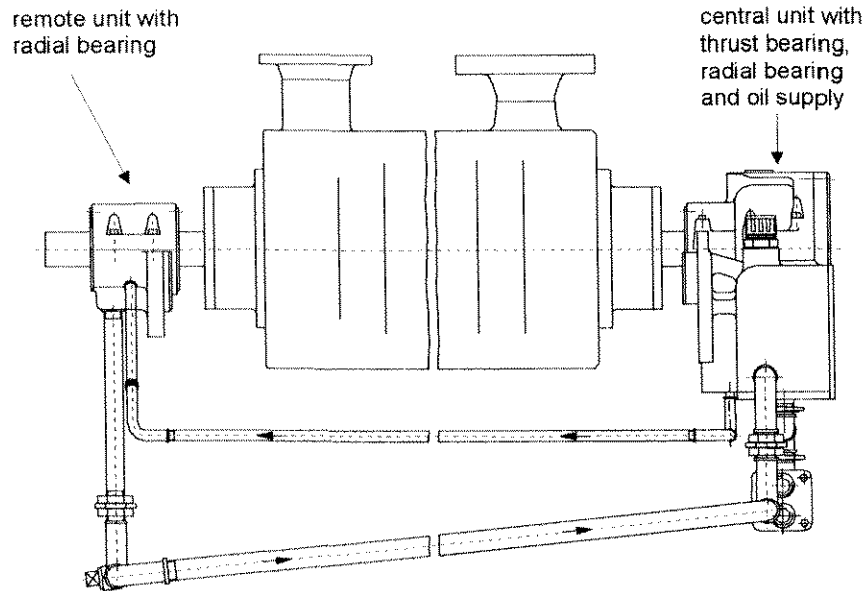
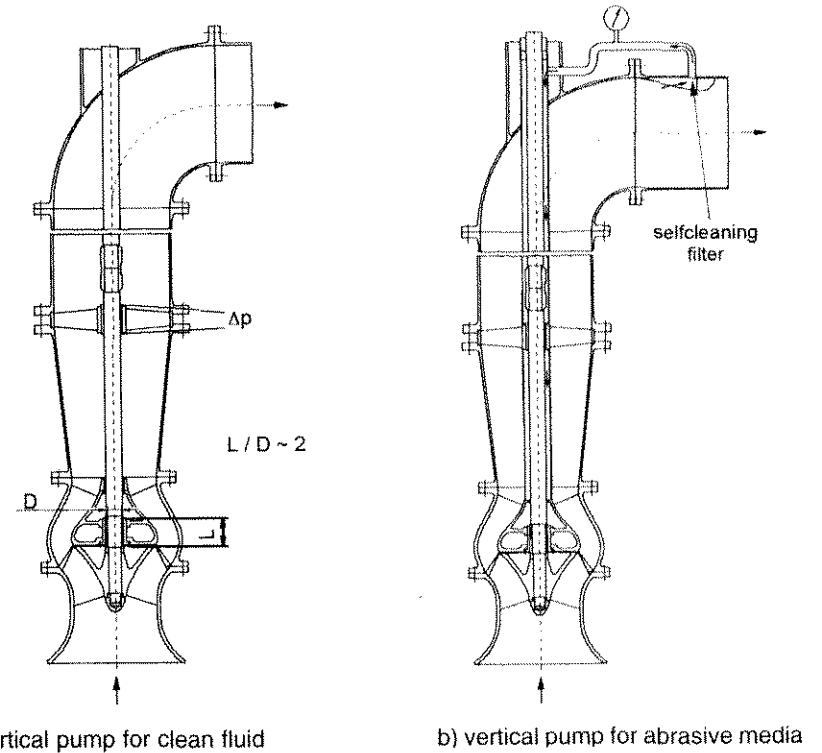


Fig.E.1.13 Self-contained bearing system

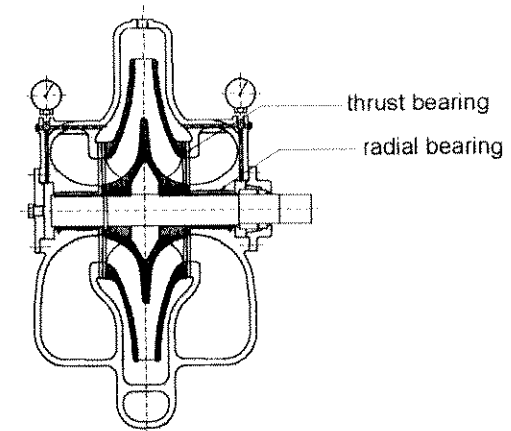
**E.1.4. Product-lubricated hydrodynamic bearings**

Hydrodynamic bearings are usually lubricated with oil, but in some arrangements hydrodynamic bearings lubricated with the pumped fluid are also used. The most common applications are radial bearings in boreholes and well pumps at water works, where no oil or grease contamination of the water is allowed. Another field where product-lubricated radial and axial bearings have already been introduced is single- and multi-stage hermetic pumps, which pump toxic or flammable fluids. Product-lubricated bearings often operate, unlike oil-lubricated bearings, in a region of mixed friction, and therefore contact between both surfaces is frequent. Especially during the start-up of very long single- or multi-stage pumps (Fig.E.1.14.), which also have multi-radial bearing support to the shaft, it can happen that the product-lubricated bearings have to run for a short time in a dry condition. Product-lubricated bearings are very much dependent on the pump execution: single- or multi-stage pump, vertical or horizontal arrangement. The right choice of combination of materials and the quality of machined surfaces are decisive for the high availability and long life expectation of product-lubricated hydrodynamic bearings.



a) vertical pump for clean fluid

b) vertical pump for abrasive media



c) double suction horizontal pump

Fig.E.1.14 Pump arrangements with product-lubricated bearings

The most frequent executions of pumps with product-lubricated radial bearings are vertical single- or multi-stage pumps. The following materials are used for the product-lubricated bearings of such pumps:

- pumped fluid is abrasive:
  - shaft – with protective steel sleeve
  - bearing – SiC
  - shaft – with protective steel sleeve with SiC coating
  - bearing – hard rubber
- pumped fluid is clean:
  - shaft – steel
  - bearing – hard rubber, tin bronze, different combinations of graphite, PTFE, SiC

When an abrasive fluid (a fluid loaded with solids) is being pumped, the hardness of the solid particles should be known, if possible. In addition, the corrosion and abrasion resistance as well as the swelling properties of the material used for the product-lubricated bearing should be known. For an execution with a shaft sleeve of steel and a rubber bearing, special attention should be given to the difference in hardness between both elements. If the product-lubricated bearing is made from SiC, the surface should have the highest possible surface finish. Pumps for pumping abrasive media are often equipped with a filtering system. The filtering of larger particles can be arranged by a simple self-cleaning filter, shown schematically in Fig.E.1.14.b.

The lubrication of a product-lubricated bearing is different from the classical oil-lubricated bearing. It is caused by the axial pressure difference between the inlet and outlet of the bearing  $\Delta p$  (Fig.E.1.14.a). The temperature rise in a bearing with longitudinal grooves is about 1 to 3°C, and the radial clearance  $\_$  should be between 1 and 3%.

The loading of radial bearings in vertical pumps is low. The exception is the first stage of a multi-stage pump, where in addition to the mechanical and hydraulic unbalances, there are also static and dynamic radial thrusts caused by asymmetrical inlet conditions acting on the bearings, especially in higher specific speed pumps. In the case of plain bearings without any lubrication grooves (similar to cylindrical bearings), the total radial loading must be determined. Usually it is low, and with a low Sommerfeld number. Thus unstable behaviour can be expected in the bearing. Because of the low load of the radial bearings, the calculation of rotordynamics is also difficult. To reduce instability in the case of rubber radial bearings, longitudinal grooves are introduced. The different types of rubber bearing executions are shown in Fig.E.1.15. A tangential-type bearing with a well-defined geometry in the transition region between the groove and the cylindrical part of the bearing guarantees safe operation.

The span between the bearings depends on the maximum operating speed and shaft diameter. It has to be chosen under the assumption that it is a rigid bearing, and the first critical speed should be above the design speed. Suggestions for between-bearing spans are given in Standard API 610/8. In order to avoid unacceptable vibration in vertical pumps, in addition to the shaft vibration, the vibration in the couplings and rising pipe should also be considered in detail.

Dry running of the bearings is quite common during pump start-up. To reduce problems, non-metallic elastomeric bearings can be used in water, and also in mild acid or caustic solutions. They have a relatively low friction coefficient. Their limitation is their temperature range: the operating temperature should be less than 60°C. Dry running is limited to ca. 10 to 15 seconds. Some types of elastomeric radial bearings allow dry start-up operation for up to 1 to 2 minutes. For detailed information, the bearing manufacturer's instructions should be obeyed.

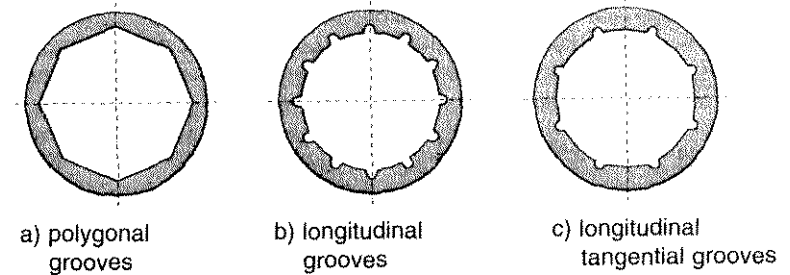


Fig. E.1.15 Three types of rubber bearing

### E.1.5. Hydrostatic and combined bearings

Hydrostatic bearings represent a different type of bearing. The oil pressure is generated outside the bearing and then brought into the separate pressure chambers of the bearing surface. The advantage of the hydrostatic over the hydrodynamic bearing is that pure fluid friction is present all the time and at all operating conditions, including start-up and stopping, and therefore no danger of wear exists. For the same carrying capacity they have smaller dimensions and lower frictional losses than hydrodynamic bearings. However, they are more expensive, because a special pump for generating the hydrostatic pressure of the lubricant is required, meaning higher investment and operating costs.

In some cases, both types of bearing are combined. If the pump has to be started against a high static thrust, the hydrostatic pressure device is used only during start-up and stopping. During steady-state operation, the bearings operate hydrodynamically, and the auxiliary lubricant feed is shut off. This execution is usually used in the thrust bearings of vertical pumps, but also in radial bearings in cases of extremely heavy rotors (high Sommerfeld number).

## E.2. Seals

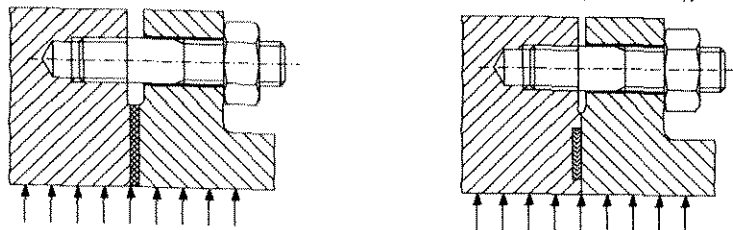
The function of the seals used in pumps is to separate two spaces with different pressures and temperatures at all stationary and non-stationary operating conditions. Static seals separate two spaces without any leakage, and in dynamic seals a certain minimal controlled leakage occurs. Depending on the application, seals should be thermally, chemically and pressure resistant, and they should seal toxic, flammable or explosive fluids at high or very low temperatures against the surroundings or against other fluids. Pump availability depends strongly on the seals. Seals must be selected carefully in order to ensure the highest possible pump availability.

### E.2.1. Static seals

A static seal is built between two surfaces with a minimal relative movement against each other (e.g. flanges). It must be capable of compensating geometric and volumetric changes arising from an alternating pressure and/or temperature loading. A static seal should have a certain degree of deformability in order to compensate for the roughness of the contact surfaces, but it should also have enough strength to seal the fluid pressure and to bear the forces of any required prestressing.

#### E.2.1.1. Flat gaskets

Flat gaskets are discs, rings or frames that adapt to the sealing surface across their entire width. They consist either of a uniform material or are made of several materials. Examples of the installation of a gasket made from a uniform material and of one made of several materials, a spiral-wound gasket, are in Fig.E.2.1.



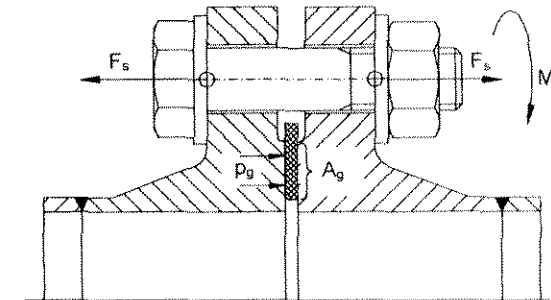
a) Flat gasket of uniform material

b) Spiral-wound flat gasket

Fig.E.2.1 Flat gaskets

Flat gaskets are mainly used in flange joints. For the successful functioning of a flat gasket it is important to treat carefully the whole flange joint consisting of the two flanges, the gasket and the screws (Fig.E.2.2.). The parameters shown in Fig.E.2.2. are needed for correct dimensioning. Safe operation is only ensured in

the case of the optimal interaction of all elements. There are several standards and recommendations for determining flange joints, e.g. DIN 2505, DIN 2509, ASME section VIII, VDI 2230.



$F_s$	force in screw	$p_g$	surface pressure on the gasket
$M_t$	tightening torque	$A_g$	sealing surface

Fig.E.2.2 Flange joint with a flat gasket

There are several possibilities for mounting flat gaskets (Fig.E.2.3.). In types A and B the gasket has to support all the forces between the two flanges and to ensure sealing. In type C, the functions of supporting the forces between the flanges and of sealing are separated, and the gasket takes over only the function of sealing. Sealing surfaces do not move after plastic deformation of the gasket, and this represents an advantage, especially when the pump is often working under transient conditions (cold/hot start conditions). Spiral-wound gaskets are usually installed for type C. Spiral-wound gaskets can be of different types, according to the application; however, special attention must be paid to the dimensioning of the flanges and screws.

The minimum thickness of a flat gasket depends on:

- roughness of the flange surface,
- compressibility of the gasket material,
- surface pressure on the gasket.

Gaskets with a thickness smaller than 0.5 mm are applied in joints with ground surfaces, and pressures over 16 bar. For reasons of strength, the width of the gasket should be at least 5 times greater than its thickness.

The material for flat gaskets depends on the application. For flat gaskets of uniform material, the following basic materials and their combinations are used: aramid, synthetic, mineral and carbon fibres, PTFE, with or without metal reinforcement. As blend and cover materials, NBR and SBR elastomers, graphite coatings and resins are used. The limits of their normal operating range are about 150 bar and 500°C. The maximum permitted pressure is also limited by the execution of the flange joint.



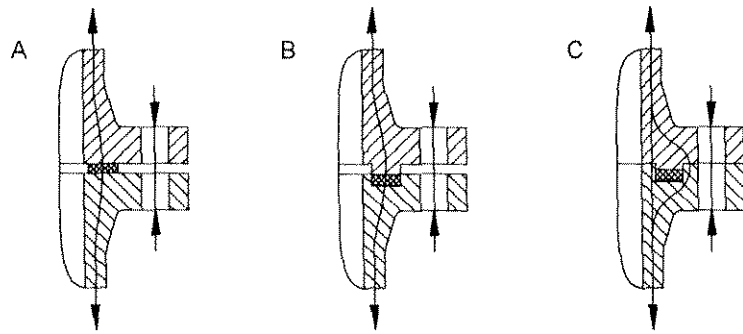


Fig.E.2.3 Possibilities of flat gasket installation – distribution of the sealing forces

In spiral-wound gaskets, different types of stainless steel are used for the metal strip, while the filler strip can be PTFE, ceramic or graphite. Their normal operating range limits are about 550°C and 400 bar. For special applications they can be enlarged via special designs for a pressure up to about 1000 bar, and, depending on the environment (reducing or inert atmosphere), they can operate at temperatures up to about 3000°C.

#### E.2.1.2. O-rings and C-rings

O-rings and C-rings are static seals that require relatively low prestressing. The sealing force is generated automatically by inner pressure, which is why they are also called self-energising gaskets. The small tightening forces needed have a positive influence on the dimensions of the flanges and screws. Joints with O-rings are of a simple design, and O-rings dimensions are standardised and need little space. The danger of sudden failure is very small. Rubber, elastomer and metal rings are possible (Fig.E.2.4.). Almost all rubber and elastomer O-rings can be reused after disassembly. This is not the case with plastically deformed metal O- and C- rings and flat gaskets. The disadvantage of rubber and elastomer O-rings is that applications are limited by a temperature of about 200°C. The limits are caused by the material used as well as by extrusion, which is dependent on pressure, material hardness and the clearance between the two flanges under operating conditions.

Metallic O-rings and C-rings are capable of sealing extreme pressures (from high vacuum up to a few 1000 bar) and extreme temperatures (-260°C to 1100°C). They can be used only once, because at the first compression metal rings are plastically deformed.

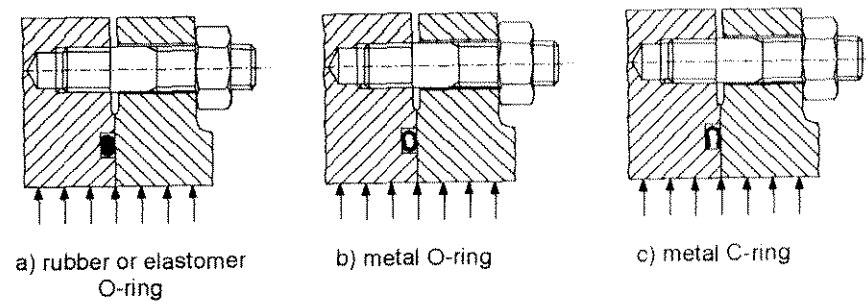


Fig.E.2.4 Different installations of O- and C-rings

#### E.2.2. Dynamic seals – shaft seals

The point where the pump shaft passes through the casing wall from the inner, liquid-filled part of the pump, to the atmosphere, represents one of the most critical pump zones, and therefore determines the total availability of the pump system. The function of the shaft seal is the separation, with a certain minimal leakage, of these two spaces with different pressures and temperatures. It is installed between one static part, the casing, and one rotating surface, the shaft. Different types of shaft seal are available, according to the operating conditions (stationary, transient, breakdown; pressure, temperature), fluid characteristics, required degree of leakage losses, as well as safe operation. The two most commonly used types are stuffing box packings and mechanical seals.

##### E.2.2.1 Stuffing box packings

Stuffing box packings are contact shaft seals that are widely used in the pump industry, because they are of a simple design. Basically the stuffing box packing is a pressure reduction device. The packing rings, which must have a certain elasticity, are axially compressed by the gland in order to give the desired radial fit to the shaft. The leakage around the shaft is controlled by tightening or loosening the gland studs (Fig.E.2.5.). The leakage has the function of lubricating and cooling. The packing must absorb the energy generated by friction. When high temperature fluid is being pumped, additional cooling has to be introduced (Fig.E.2.5.b.). When a liquid is pumped near its vaporising temperature, the cooling must be sufficient to prevent any vaporisation at the outlet of the stuffing box.

Packing rings are easy to fit, they can be changed without disassembling the pump, and maintenance is simple. The likelihood of a sudden failure is very small. Their major weakness is that the operating range is relatively limited regarding shaft circumferential velocity, sealing pressure, and temperature, and in some

cases when pumping certain hydrocarbons, due to relatively low lubrication characteristics. Simple stuffing box arrangements are limited to shaft circumferential velocities of about 18 m/s and pressures of about 25 bar. Arrangements with cooling can operate up to circumferential velocities of about 25 m/s and pressures of about 30 bar.

Stuffing box packing is shown schematically in Fig.E.2.5. When pumping abrasive media, it is important that the entrance of abrasive particles under the sliding surface is prevented. To prevent this, clean fluid with an overpressure of between 1 and 2 bars should be injected into the lantern ring (Fig.E.2.5.b.).

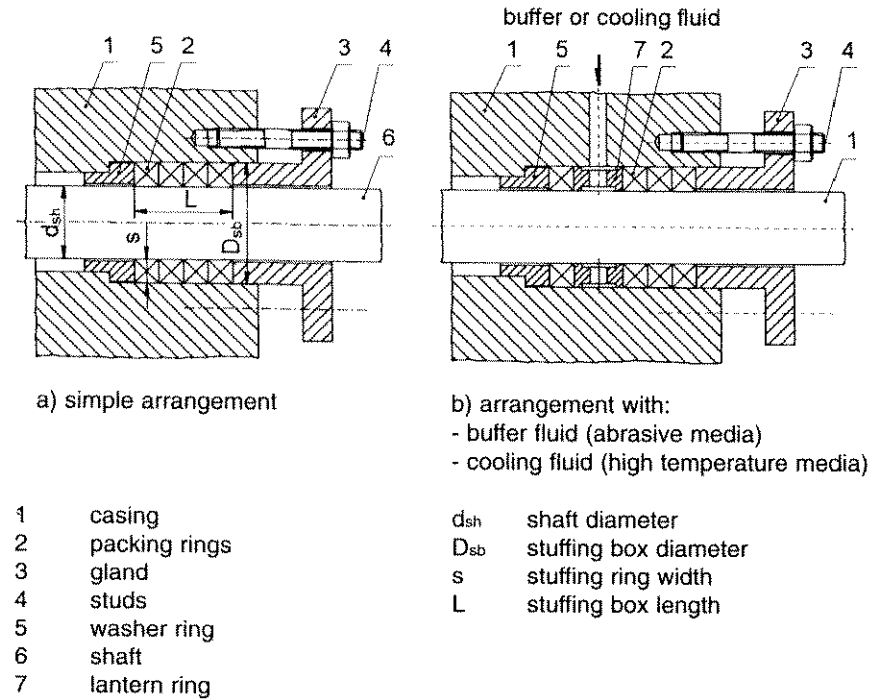


Fig.E.2.5 Schematic drawing of a stuffing box

To determine the thickness of the packing and the number of packing rings, the manufacturer's recommendations should be followed. The largest amount of pressure reduction in the stuffing box is taken by the last ring. The number of rings should be limited to about 6 in order to reduce friction losses.

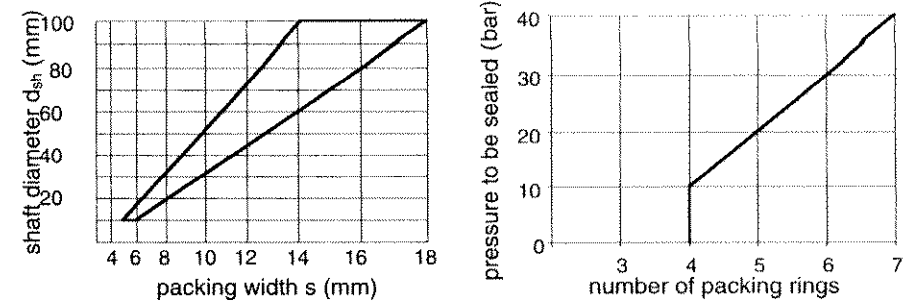


Fig.E.2.6 Guidelines for selecting the packing width and number of rings (acc. Burgmann Co.)

A wide range of packing materials makes them convenient for sealing the majority of fluids. The base materials are chiefly chosen from the viewpoint of chemical resistance and the temperature of the pumped fluid, and can be the following: cotton, glass, PTFE, graphite, etc. Other criteria are circumferential speed, friction coefficient against the shaft material and mechanical loads. Impregnations improve chemical stability, cross-sectional density and sliding properties. At the same time they act as a lubricant to prevent the seizure of the packing in dry running at pump start-up. Commonly used impregnation materials are greases, oils, graphite, rubber, PTFE and their combinations. For a long lifetime, it is preferable that shaft sliding surfaces are hardened; the recommended hardness is 40 to 60 HRC, and with low roughness values ( $R_a < 1.6 \mu m$ ) in order to reduce friction losses. However, for seals for a specific pumped fluid, the optimal material selection has to follow the recommendations of the packing ring manufacturers.

#### E.2.2.2. Mechanical seals

A mechanical seal is a contact shaft seal, where two faces slide on each other. In principle it is similar to a stuffing box, but the sealing surfaces are perpendicular to the axis of rotation. The sealing surfaces are highly polished and much smaller in comparison with the surfaces of a stuffing box, permitting higher circumferential speeds. They are pressed together with different axial forces. Between the sliding surfaces there is a liquid lubricating film which also ensures the necessary cooling. The direction of the leakage flow is from the outside diameter of the mechanical seal, towards the inner diameter. Leakage losses depend on the quality of the sliding surfaces, the flatness of the faces, distortion caused by pressure and temperature loading, vibration of the shaft, mode of operation and fluid properties. The basic elements of a mechanical seal are in Fig.E.2.7.

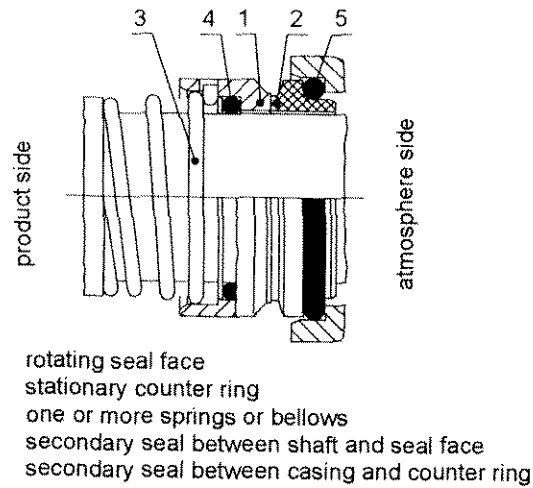


Fig.E.2.7 Basic elements of a mechanical seal

The axial sealing force  $F_{asf}$  is a result of all the forces acting on a mechanical seal (Fig.E.2.8.).

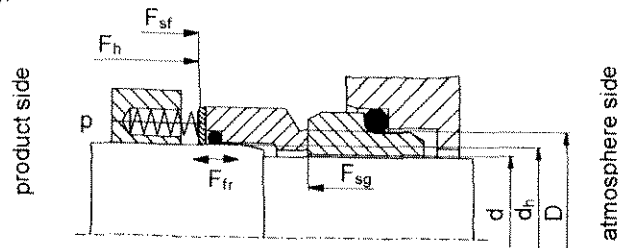


Fig.E.2.8 Forces acting on a mechanical seal

$$F_{asf} = F_h + F_{sf} - F_{sg} \pm F_{fr}$$

$$F_h = A_h \cdot p = \frac{\pi}{4} (D^2 - d_h^2) \cdot p$$

- $F_h$  hydraulic loading force
- $F_{sf}$  spring force
- $F_{sg}$  hydraulic force of the sealing gap, caused by pressure distribution in the gap
- $F_{fr}$  frictional force of the secondary seal (can be ignored)
- $A_h$  hydraulic loaded area
- $A$  sliding surface
- $d$  internal sliding surface diameter
- $D$  external sliding surface diameter
- $d_h$  hydraulic diameter
- $p$  pressure acting on the hydraulic loaded area  $A_h$

The ratio of the hydraulic loaded area  $A_h$  to the sliding surface  $A$  is defined as the hydraulic load factor  $k$  (balance ratio of the seal).

$$k = \frac{A_h}{A} = \frac{D^2 - d_h^2}{D^2 - d^2}$$

With  $k > 1$ , a mechanical seal is said to be loaded (unbalanced), and with  $k < 1$  it is said to be balanced. Fig.E.2.9. shows the hydraulically loaded area. Load factors usually lie in the range between 0,6 and 2. As the value for  $k$  increases, the sealing face load rises, the sealing gap becomes narrower, leakage decreases and wear increases. As the value for  $k$  decreases, the sealing face load decreases. This is why balanced mechanical seals are used for applications in the high pressure and high speed range, high power concentration pumps. A decreasing value for  $k$  improves the formation of a lubricating film, but it also produces greater leakage. Too low a value for  $k$  can cause the opening of the sliding faces and endangers the safe operation of the pump. In order to obtain a high availability of the mechanical seal, strict requirements in the seal face material (low wear, corrosion resistance, low friction, good heat transfer as well as high stiffness) are of vital importance.

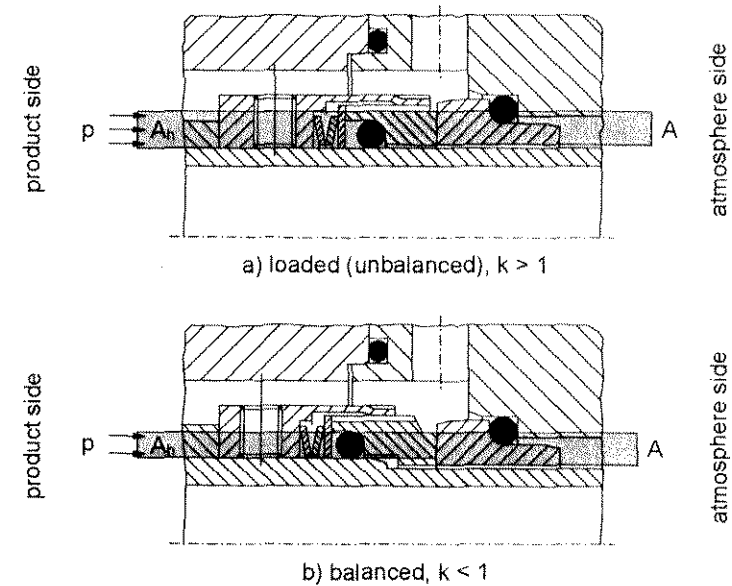


Fig.E.2.9 Loaded and balanced mechanical seals

### Mechanical seal arrangement

More than 90% of all mechanical seals are used as single mechanical seals (Fig.E.2.10.). The lubricating film between the sliding faces is formed by the medium to be sealed. Their approximate operational limits are:

- sliding velocities up to 70 m/s (balanced seals) and 20 m/s (loaded seals)
- differential pressures up to 150 bar
- temperatures up to 300°C (cooling of a mechanical seal is obligatory)

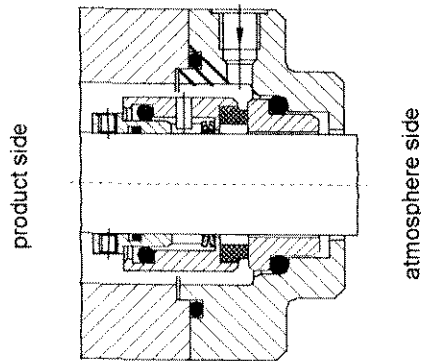


Fig.E.2.10 Single-acting mechanical seal

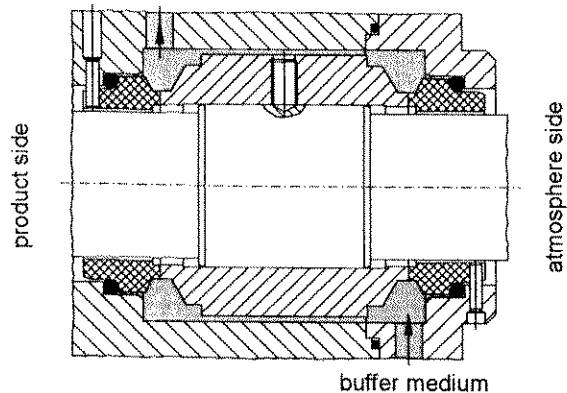


Fig.E.2.11 Double-acting mechanical seal in a back-to-back arrangement

Double mechanical seals in a back-to-back arrangement (Fig.E.2.11.) are used where no leakage of the pumped media can be allowed to emerge from a pump handling explosive, toxic, aggressive or highly inflammable media that cannot be allowed to escape into the atmosphere. In addition, mechanical seals in a back-to-back arrangement are installed where media with poor lubricating properties are pumped. An external buffer fluid serves to separate the product from the atmosphere. Buffer fluid pressure lies at around 2 to 3 bar or 10% above the pressure of the product. One part of the buffer fluid is mixed with the product, and the mixture must be compatible with the pumping system.

A double mechanical seal in a tandem arrangement is another term for two single mechanical seals installed in series and acting in the same direction (Fig.E.2.12.). This kind of seal is installed where the mixing of product and buffer fluids is prohibited. The purpose of the mechanical seal on the atmosphere side of a tandem arrangement is either to enable two-stage pressure reduction or else to seal in the quenching medium and to monitor the primary mechanical seal on the product side. It ensures that no product leakage escapes, and should be applied for corrosion aggressive media or for mixtures consisting of fluid and solids.

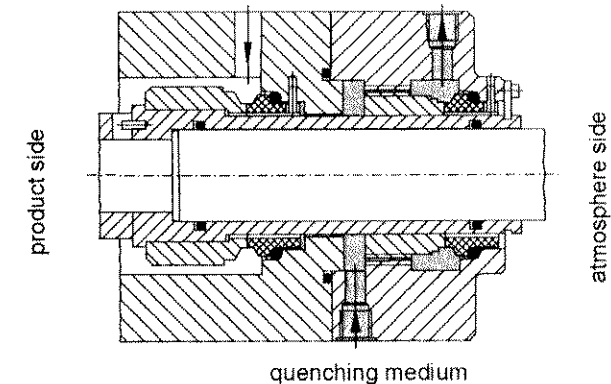


Fig.E.2.12 Double-acting mechanical seal in a tandem arrangement

Depending on the application, the following materials are used for seal faces and stationary rings:

- synthetic carbons (carbon graphite or electrographite with different impregnations)
- metals (CrMo steel, CrNiMo steel, Hastelloy B or C)
- metal carbides (tungsten or silicon carbide with different binders or sintered)
- metal oxides (aluminium oxides)
- plastics (PTFE, fibre or carbon reinforced)

The limits of the application of the material combinations are widely influenced by the fluid viscosity and content of solids.

The right choice of mechanical seals in pumps in thermal power plants and in petrochemical plants is decisive to the availability of the whole plant, and is often problematical. The fluid must be cooled before it enters the sealing gap, in order to prevent evaporation due to heating caused by friction. From experience, the temperature of the fluid entering the gap should be about 15°C lower than its evaporation temperature. If this condition is fulfilled for all operational cases, evaporation does not occur and therefore there is no danger of cavitation at the outlet of the seal faces. Cavitation would cause the erosion of the sealing surfaces and would damage the mechanical seal in a very short time.

Standards API 610/8 and API 682 suggest different plans for auxiliary piping systems to maintain the appropriate operating conditions for mechanical seals, in respect of cooling of the seal chamber, keeping the seal chamber clean without harmful deposits, evacuation of vapours or gases that may collect in the seal chamber, using quenching to prevent solids from building up on the atmosphere side of the seal, and installations for buffer fluids in double-acting mechanical seals.

### E.2.2.3. Hydrodynamic seals

This type of contact-free seal is used mainly for pumps that pump fluids loaded with solids (e.g. paper industry) and whose operating point is constant. The pump operates without any leakage and seal wear, and there is no need for additional cooling, quenching or buffer fluids, and therefore the pump availability is high. The working principles of one possible execution of a hydrodynamic seal can be seen in Fig.E.2.13. The sealing is executed by the liquid ring. The sealing fluid is pumped from the sealing chamber by an auxiliary impeller, and it prevents the escape of the product fluid. When the pump is at standstill, the sealing fluid compresses the elastic disc which produces the seal. Immediately after start-up a certain pressure is generated in the sealing chamber, and deforms the disc in such a way that no contact occurs. The fluid temperature should be lower than the evaporation temperature.

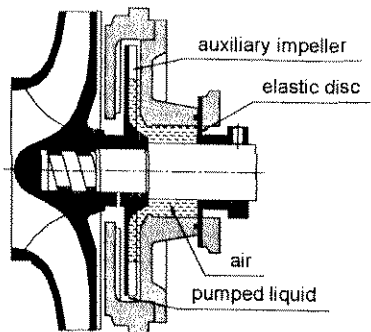


Fig.E.2.13 Hydrodynamic seal

### E.2.3. Canned motor pumps

The chemical industry, medicine, reactor engineering and space technology on the one hand, and on the other hand a growing awareness of the need for environmental protection, demand fully leak-free pumps. Only canned motor pumps and magnetic coupled pumps allow the realisation of the demand for leak-free pumps, as stuffing box packings and mechanical seals require an unavoidable minimum leakage flow needed for cooling and lubricating the seal. Magnetic couplings are discussed in section E.3.4.

Single- and multi-stage canned motor pumps are mainly installed in the process industry, in chemical and petrochemical plants. A schematic drawing of a canned motor pump is in Fig.E.2.14. The decisive part of the machine is the can, a thin tubular casing of non-magnetic and product-resistant high-grade stainless steel or nickel alloy. A magnetic drive torque is transmitted from the motor stator windings, through the can to the rotor. The can should take over the whole pressure difference between the product pressure and the atmosphere. As in magnetic couplings, the radial and axial bearings in canned motor pumps are product-lubricated and must be designed to withstand the conditions imposed by the fluid, mainly viscosity and temperature. The bearings are normally designed as plain bearings, although in a few cases they consist of roller bearings. A partial flow taken from the pump pressure side provides a cooling flow through the rotor-stator can gap and is then returned to the main flow.

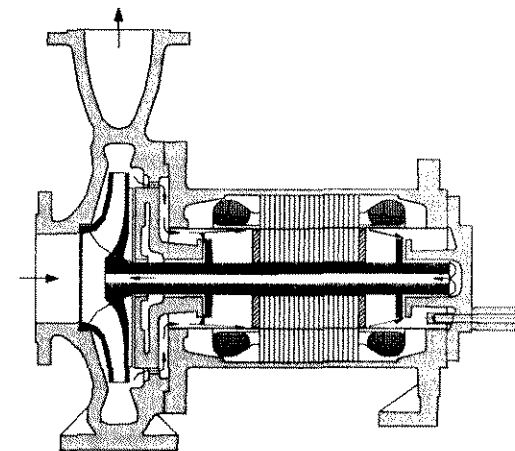


Fig.E.2.14 Canned motor pump

### E.3. Couplings

A coupling is used whenever it is necessary to connect two shafts and to transfer torque from one shaft (drive) to another shaft (pump). The drive can be an electric motor, diesel engine, or steam or gas turbine.

The method of operation is decisive for the correct choice of the type of coupling.

The following parameters have to be considered:

- load factor (continuous or intermittent operation)
- relative axial displacement of the shaft ends (transients, axial loading)
- relative radial displacement of the shaft centre
- changes in the shaft centre angles
- probable magnitude of the pump shaft vibration
- transient conditions
- weight and length of the coupling
- possibility to be dynamically balanced

The required torque transmission is decisive for the correct choice of coupling size.

The couplings used in the centrifugal pump industry can be classified in the following way:

- rigid couplings
  - flange-rigid couplings
    - split rigid couplings
- flexible couplings
  - permanent elastic couplings
    - elastomer couplings
    - all-metal couplings
  - torsional stiff self-aligning couplings
    - gear couplings
    - membrane (diaphragm) couplings

Besides these, hydrodynamic couplings are used for some applications, and nowadays magnetic couplings are also used in the process industry.

#### E.3.1. Rigid couplings

Rigid couplings are used where two shafts have to be maintained in precise alignment. The precise alignment of the pump and drive bearings is of extreme importance because rigid couplings do not accommodate misalignments between two shafts. In addition, an extreme accuracy in the manufacturing of the flanges is very important. Two types are commonly used (Fig.E.3.1.): flange couplings and split couplings.

Flange couplings are used in vertical pumps which do not have their own thrust bearing. The common axial thrust bearing is generally located in the electric motor. The coupling flange bolts have to transmit the total hydraulic axial thrust together with the weight of pump rotating parts. A ring can be built between two flanges, (adjustable flanged rigid coupling). The ring allows the positioning of the pump shaft axially with respect to the drive, or to adjust the gap between the impeller and the casing wall when an open impeller is used.

Split couplings are used in vertical pumps with long shafts, which are assembled from many parts.

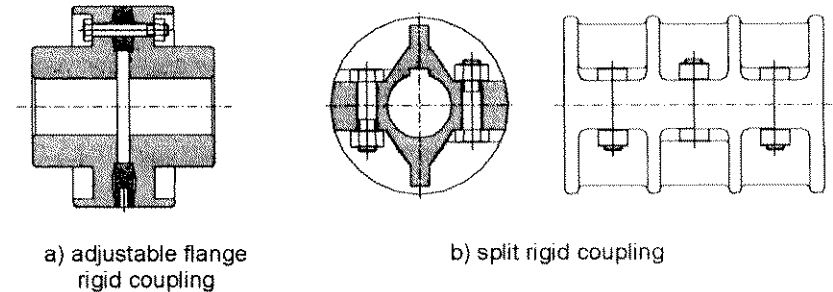


Fig.E.3.1 Flange and split rigid couplings

#### E.3.2. Flexible couplings

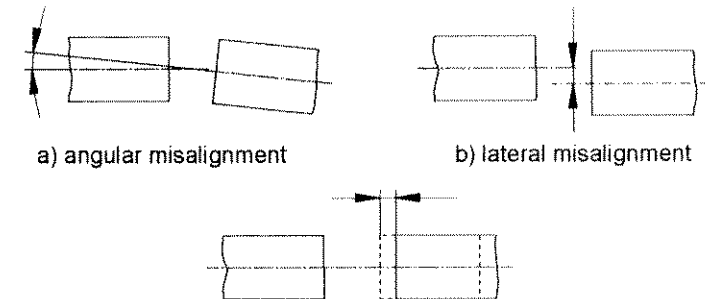


Fig.E.3.2 Angular, lateral and axial shaft misalignment

Besides their primary purpose, to transmit torque from drive to pump, flexible couplings are capable of compensating for certain unavoidable shaft misalignments – angular, lateral and axial (Fig.E.3.2.) – in order to minimise their influence on the vibration and rotordynamic behaviour of the pump. For a good dynamic behaviour of the pump, it is important that the misalignments are as small as possible; however, the instructions of the coupling manufacturer should be respected.

There are two main types of flexible couplings: permanent elastic couplings and torsional stiff self-aligning couplings. Both types can be installed as spacer couplings (see section E.3.2.2.2.).

### E.3.2.1 Permanent elastic couplings

Elastic couplings are the most common and widely used couplings in the pump industry. They are used for standard pumps with a low or medium power consumption (up to about 300 kW) and operating speeds up to 3600 rpm. Some additional advantages of elastic couplings are that they can reduce and damp torsional shock loads caused by the drive (for example a diesel engine), and they also allow small axial, radial and angular bearing deflections. There are many types of elastic couplings. Some of them are shown in Fig.E.3.3. (elastomer couplings) and E.3.4. (all-metal coupling).

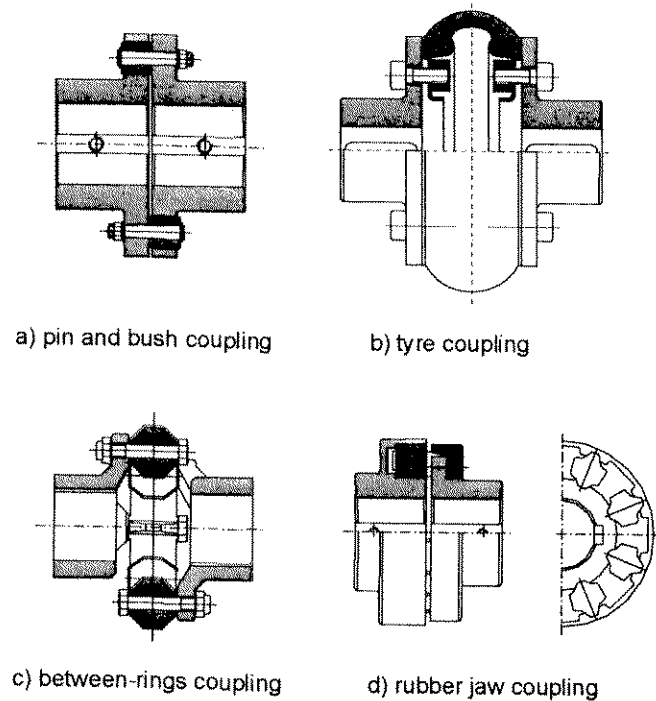
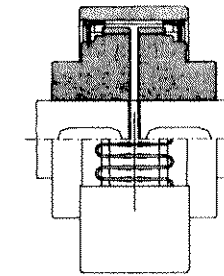


Fig.E.3.3 Elastic couplings – elastomer couplings



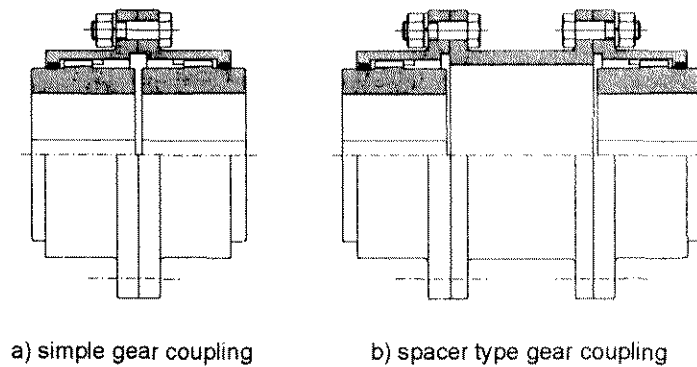
spring-grid coupling

Fig.E.3.4 Elastic couplings – all-metal coupling

### E.3.2.2 Torsional-stiff flexible couplings

For more severe applications, torsional-stiff self-aligning flexible couplings are used. Gear and membrane couplings belong to this group. Both are metal couplings and can be used in pumps according to Standard API 610/8.

#### E.3.2.2.1 Gear couplings



a) simple gear coupling

b) spacer type gear coupling

Fig.E.3.5 Gear couplings

Sometimes these are also called mechanical flexible couplings. Gear couplings (Fig.E.3.5.) are used for high-speed pumps up to 5000 rpm with torque transmission up to 7000 kNm. They have some disadvantages. There is a metal contact and relative sliding movement between two teeth due to the possible thermal expansion of both shafts, which means that gear couplings are exposed to wear and must be lubricated. They can be filled with lubricant, and grease is used for

speeds up to 3000 rpm. Another option for higher speeds is continuously supplying the coupling with oil. A critical point is the sealing at the shaft, where certain volumetric losses occur. The balancing of a gear coupling set is very difficult, as only the hub part can be dynamically balanced. The advantages of gear couplings are that their natural frequency is independent of axial shaft movements, and their torsional stiffness can be altered with the thickness of the sleeve. Due to frictional forces in the teeth, an axial thrust is generated, which has to be considered when dimensioning the pump axial thrust bearing.

#### E.3.2.2.2 Membrane (diaphragm) couplings

This type of coupling relies on the flexing of the coupling elements in order to compensate for misalignment. They are also called flexible material couplings. The elements must have a sufficient material resistance to fatigue failure. A high degree of manufacturing tolerances is required.

They do not need any lubrication, which represents a great advantage compared to gear couplings. In addition they are not exposed to any material wear. However, the alignment of the coupling must be maintained within the required limits given by manufacturer, and they are defined by the fatigue limits of the membranes (discs). High-speed multi-stage pumps require a minimum coupling weight and minimum length between coupling flanges. These two parameters are important, because they influence the shaft deflection at the driving end, and therefore the general critical speed and rotordynamics of the whole system. They can be fitted to high-speed pumps up to 10000 rpm and torque transmission up to 3000 kNm. The axial thrust generated by a membrane coupling is between 10 and 20% that of a gear coupling, and it has to be taken into account when dimensioning the pump axial thrust bearing. The disadvantages of membrane couplings are that they require high quality assembly and disassembly, as mechanical damage to the membranes can cause dangerous cracks. Their natural frequency depends on the compression of the membranes, and a certain axial prestressing is required. Several executions of membrane couplings are possible: couplings with one or more membranes (Fig.E.3.6.), and couplings with membranes of constant or variable thickness. In a disc coupling a single element is fitted instead of a number of membranes. It has a hyperbolic contour in order to produce a uniform stress distribution in the membrane.

Spacer couplings (Fig.E.3.6., Fig.E.3.7.) are commonly used with end-suction process pumps. Their advantage is that when they are dismantled, the pump bearing bracket with the impeller and seal can be removed while the pump casing and drive remain in place. Another application of spacer couplings is when angular or lateral shaft misalignments are high and exceed the limits of the usual coupling. Gear or membrane couplings should be used especially when the drive temperature during start-up is different to the pump shaft temperature (different thermal gradients).

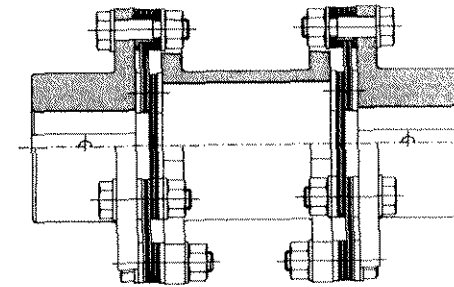


Fig.E.3.6 Membrane-type flexible coupling with a spacer

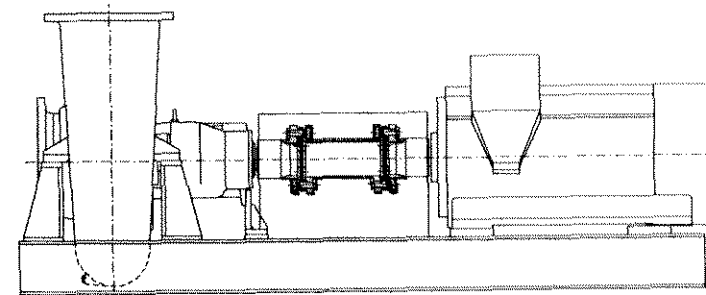


Fig.E.3.7 Single-stage end-suction pump with a membrane spacer coupling

#### E.3.2.2.3 Flexible drive shafts

Flexible drive shafts are a form of spacer coupling (Fig.E.3.8.), usually used in vertical, but also horizontal arrangements. The flexible couplings on both ends are replaced by universal joints. Such a coupling arrangement is suitable for the following cases:

- large angular and lateral misalignments of the pump and drive centrelines, eliminating the need for perfect alignment
- large distances between drive and pump (only in the case of vertical pumps).

A flexible drive shaft cannot take over any axial or radial forces, and this must be taken into account in the design of the radial and axial bearings on the drive and pump sides; sometimes additional bearings must be planned. Special attention should be paid to vibration in a flexible drive shaft, and the natural frequency must be a long way from the operating speed. They are not suitable for high-speed pumps.



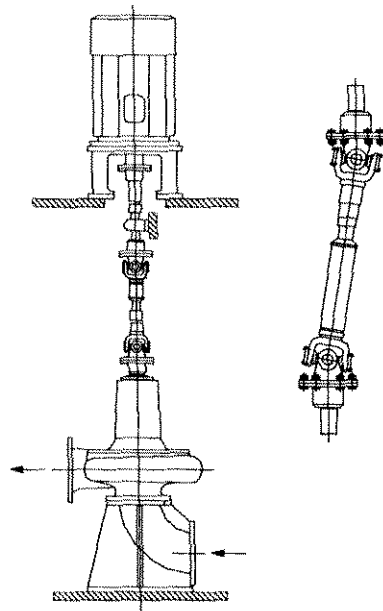


Fig.E.3.8 Flexible drive shaft arrangement

### E.3.3. Hydrodynamic couplings

A hydrodynamic coupling is a converter that transfers energy directly through a working fluid, from the driving machine (e.g. electric motor) to the working machine (e.g. pump). Hydrodynamic couplings are used where high energy has to be transferred in a limited space (high energy concentration), with possible additional requirements for working machine speed control (example: boiler feed pumps). The main parts of a hydrodynamic coupling are two rotating cascades (Fig.E.3.9.): the pump wheel (primary) and turbine wheel (secondary). The working fluid is accelerated by the pump wheel and decelerates in the turbine wheel. As a result of the power transfer process, the oil temperature rises because of energy losses, and therefore a cooling system is necessary. The turbine wheel has a 1.5 – 3% slip against the pump wheel, which represents energy losses in the coupling. Speed control in the turbine wheel is achieved by a variable fluid filling in the coupling, as shown schematically in Fig.E.3.9.b. Hydrodynamic couplings enable:

- smooth acceleration of heavy loads with optimally designed drives,
- no drive overload when the working machine is overloaded,
- no need for oversized drives,
- separation of vibration sources and damping of vibration,
- speed control of the turbine wheel (variable fluid filling coupling).

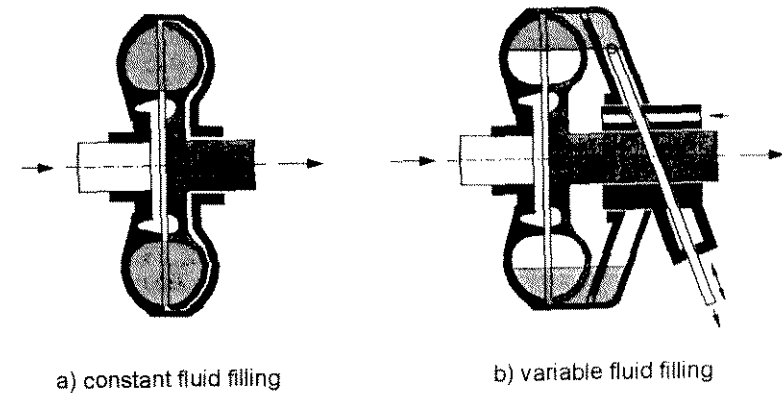


Fig.E.3.9 Hydrodynamic couplings

### E.3.4. Magnetic couplings

Environmental protection requirements are higher every day. A pump arrangement with a magnetic coupling in combination with a standard electric motor (Fig E.3.10) eliminates leakage losses to the atmosphere, and this is important when pumping toxic, flammable or other harmful media. They are applied more and more frequently, due to the improvements in magnetic materials and product-lubricated axial and radial hydrodynamic bearings. The designing of high-reliability axial and radial bearings requires a full knowledge of the radial and axial forces acting on the pump impeller. The influence of the product viscosity must be carefully considered. Together with canned motor pumps (section E.2.3.), magnetic couplings belong to the group of leak-free pumps.

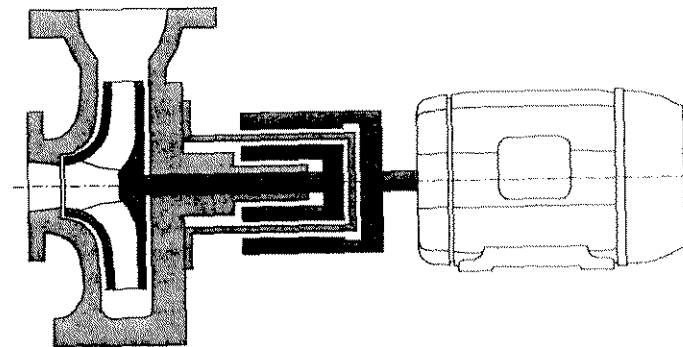


Fig.E.3.10 Magnetic coupled pump

## F. HYDRAULIC THRUSTS

### F.1. Axial thrust

#### F.1.1. Origins of axial thrust

The static pressure at the impeller exit also represents the initial static pressure at the outer periphery of both impeller side chambers. Due to the effect of fluid rotation in the side chambers, static pressure is reduced in the radial direction towards the impeller axis. The basic static pressure distribution and the components of the hydraulic axial thrust are shown in Fig.F.1.1. The main part of the axial thrust represents the thrust components acting on the impeller front  $F_{fs}$  and back shrouds  $F_{bs}$ , resulting from the pressure distribution on the related shroud area. The lesser part represents the impulse thrust  $F_i$  resulting from the inlet axial velocity component, and the resultant force due to the difference in static pressure distribution on the hub and shroud streamlines  $F_{ch}$ . Force  $F_{ch}$  can reach higher values in impellers with higher specific speeds and in operating conditions a long way from BEP.

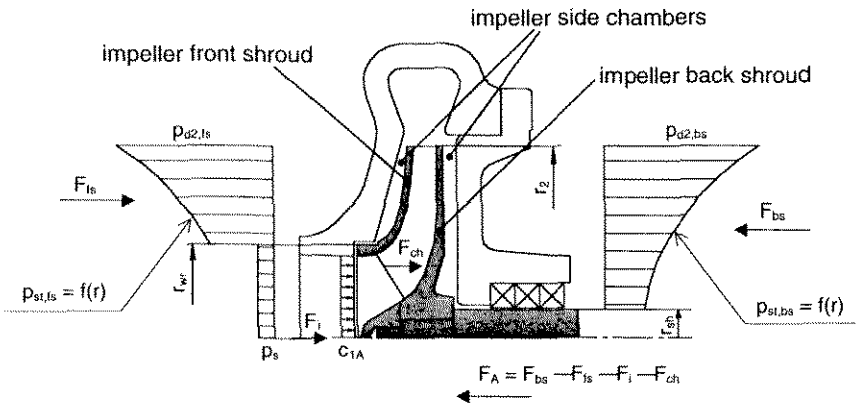


Fig.F.1.1 Simplified static pressure distribution for a single-stage pump

The parameters that influence the hydraulic axial thrust are: initial pressures at the impeller outlet, fluid rotation in the impeller side chambers, axial velocity component at the impeller inlet, and static pressure distribution on the hub and shroud streamlines. On the other hand, the fluid rotation in the impeller side chambers is influenced by the leakage flow rate (wear ring clearance), geometry of the side chamber, impeller axial position towards the diffuser or spiral casing, and the effectiveness of separation of the side chamber flow from the main impeller flow.

#### F.1.2. Calculation of the hydraulic axial thrust

A schematic representation of the pressure distribution on the impeller front and back shrouds and the position of the axial thrust components is shown in Fig. F.1.1. The hydraulic axial thrust  $F_A$  is defined as follows:

$$F_A = F_{bs} - F_{fs} - F_i - F_{ch}$$

The axial thrust components can be calculated as shown below.

Thrust on the impeller back shroud:

$$F_{bs} = \pi \cdot (r_2^2 - r_{sh}^2) \cdot \left( p_{d2,bs} - 0,5 \cdot \rho \cdot \omega^2 \cdot k_{bs} \cdot \left( r_2^2 - 0,5 \cdot (r_2^2 + r_{sh}^2) \right) \right)$$

Thrust on the impeller front shroud:

$$F_{fs} = \pi \cdot (r_2^2 - r_{wr}^2) \cdot \left( p_{d2,fs} - 0,5 \cdot \rho \cdot \omega^2 \cdot k_{fs} \cdot \left( r_2^2 - 0,5 \cdot (r_2^2 + r_{wr}^2) \right) \right) + p_s \cdot \pi \cdot r_{wr}^2$$

Impulse thrust:

$$F_i = Q \cdot \rho \cdot c_{1A}$$

Resultant force due to the difference in static pressure distribution on the front and back shroud streamlines:

$F_{ch}$  – defined through numerical flow analysis (NFA); in radial pumps it is small and can be ignored.

The first main parameter for calculating the axial thrust is the initial pressures at the impeller outer periphery  $p_{d2,bs}$  and  $p_{d2,fs}$ . The correct way to define these pressures is to use results measured from a pump of the same or very similar hydraulic geometry. When such data are not available, the following expression can be used for rough estimation (valid near BEP):

$$p_{d2,bs} = p_{d2,fs} = p_d - 0,25 \cdot \Delta p_{tot}$$

$\Delta p_{tot}$  – pump total pressure difference

$p_d$  – discharge pressure

In the procedure shown above for calculating the axial thrust components, the values for the pressures  $p_s$ ,  $p_d$ ,  $p_{d2,fs}$  and  $p_{d2,bs}$  should be taken as over-pressures (pressures above the atmospheric pressure). In the case of under-pressure at the pump suction side, the suction pressure  $p_s$  is negative.

The second main parameter for calculating the axial thrust is the coefficients of fluid rotation  $k_{fs}$  and  $k_{bs}$  in both impeller side chambers ( $fs$  – at front shroud,  $bs$  – at back shroud).

$$k_{fs} = \beta_{fs} / \omega$$

$$k_{bs} = \beta_{bs} / \omega$$

$\beta$  - fluid angular speed  
 $\omega$  - impeller shroud angular speed

The coefficient of fluid rotation is very much dependent on the type of hydraulic element at the impeller exit (spiral casing or diffuser) and on the leakage flow direction and amount in the impeller side chambers. When no experimental values for the same hydraulic geometry are available, the values from Fig. F.1.2 can be used for estimating the fluid rotation coefficients.

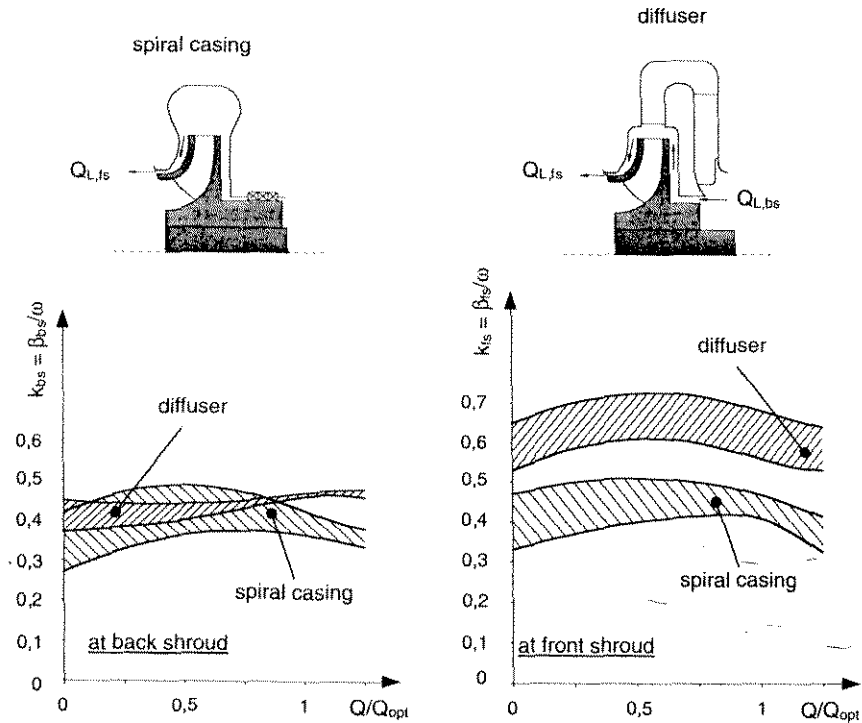
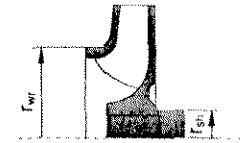


Fig. F.1.2 Coefficients of fluid rotation in impeller side chambers

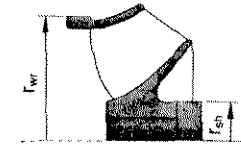
As shown above, for an accurate calculation of the axial thrust components experimental data are needed, and these are not always available. In such cases the relationships from table F.1.1 can be used for a rough estimation of the hydraulic axial thrust of different pump types.

Radial-flow pumps



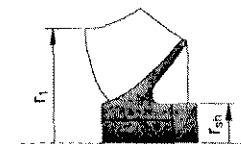
$$F_A = (0,7 - 0,9) \cdot \Delta p_{tot} \cdot \pi \cdot (r_{wr}^2 - r_{sh}^2)$$

Mixed-flow pumps (closed impeller)



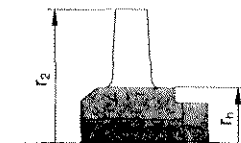
$$F_A = (nq / 220)^{0,17} \cdot \Delta p_{tot} \cdot \pi \cdot (r_{wr}^2 - r_{sh}^2)$$

Mixed-flow pumps (open impeller),  $nq < 200$



$$F_A = (200 / nq)^{0,28} \cdot \Delta p_{tot} \cdot \pi \cdot (r_1^2 - r_{sh}^2)$$

Axial-flow pumps



$$F_A = (1 - 1,1) \cdot \Delta p_{tot} \cdot \pi \cdot (r_2^2 - r_h^2)$$

Table F.1.1 Rough estimation of hydraulic axial thrusts for different pump types

F.1.3. Design possibilities for reducing axial thrust

**Single-stage pumps:** The simplest solution for smaller pump sizes with low rotational speeds, is that the total axial thrust is transferred from the rotor to the pump casing through an axial thrust bearing. When the size of the bearing becomes uneconomically large, or the expected bearing lifetime too short, the thrust component acting on the back shroud  $F_{bs}$  has to be reduced. When pumping clean fluid without solid particles, a solution with an additional wear ring and bores in the impeller back shroud is applied (see Fig.F.1.3.). The pressure in the chamber between the back shroud wear ring and the impeller hub is reduced practically to the level of the impeller inlet pressure, and thus hydraulic axial thrust is largely balanced. It is recommended to execute one bore per impeller channel, and the area of all the bores should be 4–5 times bigger than the total flow area in the wear ring gap. The negative aspects of this solution are additional leakage losses and flow

disturbance at the impeller inlet due to flow jets at the bore exit, thus worsening the pump cavitation characteristic.

When the pumping fluid is also loaded with solid particles, a solution with additional ribs on the impeller back shroud is usually applied (see Fig.F.1.4.). In the side chamber area where the ribs are installed, the pressure is reduced due to an "auxiliary simplified impeller", which reduces the axial thrust on the back shroud  $F_{bs}$ . This execution is simpler and cheaper than the solution using additional wear rings, but the negative side is the additional power losses due to the mixing effect of the ribs.

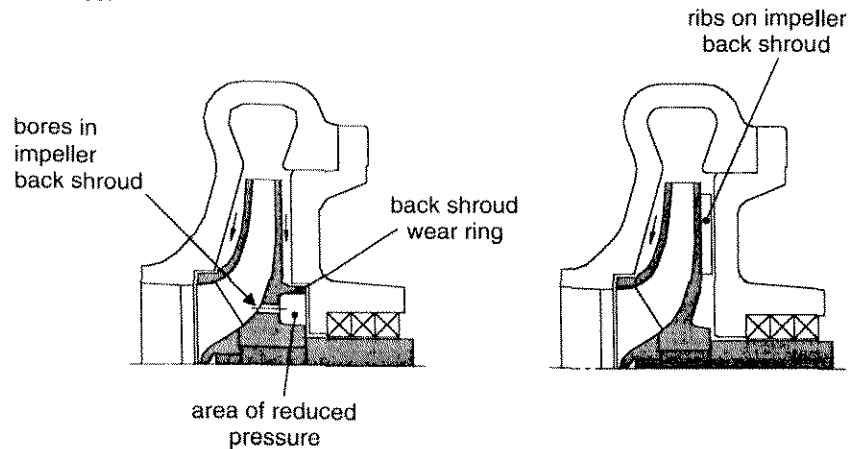


Fig. F.1.3 Solution with wear ring on the impeller back

Fig. F.1.4 Solution with ribs on the impeller back shroud

Double entry impellers (see Fig.F.1.5.), have axial thrust balancing established through a symmetrical impeller design ( $F_{ts,l} = F_{ts,r}$ ). Nevertheless, the unbalanced thrust can be essential when a non-symmetrical inflow takes place to both impeller sides, when the impeller position is not in the casing centreline, when the impeller side chamber geometry and wear ring diameter on both sides are not equal, and when a difference exists in the leakage flows on both impeller sides.

**Two-stage pumps:** Two-stage process pumps (see Fig.F.1.6.), have the main part of the axial thrust balanced through a "back-to-back" impeller arrangement. The residual axial thrust resulting from the differing pressure distribution in both impeller back side chambers (due to the opposite leakage flow direction), has to be taken by relatively small axial thrust bearings. Impellers are inserted axially into the casing. The fabrication of the casing is complicated from the moulding and casting point of view.

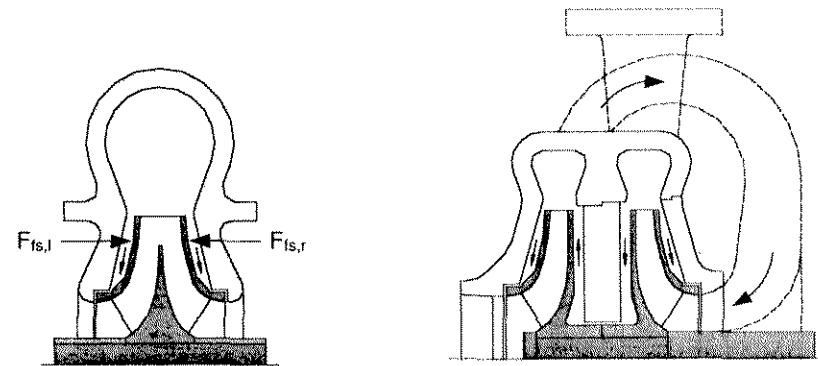


Fig. F.1.5 Double entry impeller

Fig. F.1.6 Two-stage pump in a "back-to-back" impeller arrangement

**Multi-stage pumps:** Due to the higher pump total head, produced by more impellers within the same casing, the axial thrust balancing in multi-stage pumps is more demanding and sensitive than in single-stage pumps. An extensive knowledge of the origins of hydraulic axial thrust and of the influences of different geometrical parameters on axial thrust is needed in order to design an axial thrust balancing device correctly, and to size the axial thrust bearing economically. Due to the relatively complex calculation of axial thrust from the pressure distribution on the impellers shrouds, frequently in practice the measured values of thrust from the testing of the model pump serve as a basis for sizing the axial thrust balancing device and thrust bearing.

In multi-stage pumps with a "back-to-back" arrangement (see Fig.F.1.7.), the casing is axially split. The connecting channel between the first and second package of impellers is executed inside the casing parts, which are complicated from the fabrication point of view. The piston which is placed between both impeller packages has an additional positive effect on the pump rotordynamic behaviour. Nevertheless, some residual axial thrust remains that must be taken by a relatively small axial thrust bearing.

A simpler casing design is in multi-stage pumps with all the impellers in series (see Fig.F.1.8.). The consequence is a high axial thrust, which has to be compensated by one of the following axial thrust balancing devices: disc, piston or combination disc/piston. In all the above-mentioned executions, a pipe connection is necessary from the exit of the balancing device to the suction side of the pump.

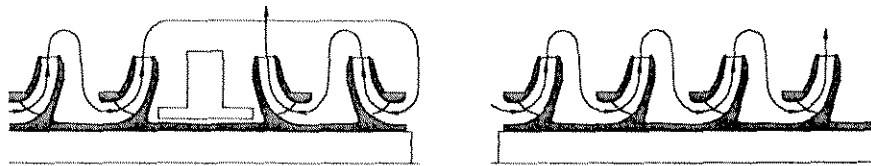


Fig. F.1.7 Multi-stage pump in back-to-back impeller arrangement

Fig. F.1.8 Multi-stage pump with all impellers in series

An execution with a balancing disc (see Fig.F.1.9.), normally has no need for an axial thrust bearing. The axial thrust on the disc  $F_{A,d}$  acts in the opposite direction to the axial thrust on the impellers  $F_{A,imp}$ , and is self-adjusting by changing the axial clearance between the disc and the stationary counter piece. An execution with a disc has relatively low leakage losses  $Q_{L,d}$ . The disadvantage of this solution is a possible evaporation of the fluid in the disc gap during start/stop regimes, which can lead to contact between the metals of the rotating and stationary parts of the disc. In the case of daily start-up/shut-down operations, metal contact can cause premature wear of the disk. In order to avoid this inconvenience, a lift-off device can be provided, located in the bearing casing.

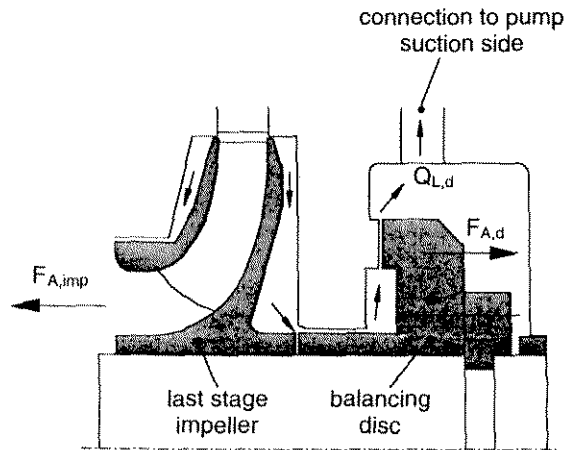


Fig.F.1.9 Execution with a balancing disc

In an execution with a balancing piston (Fig.F.1.10.), the pump rotor is fixed in the axial direction by an axial thrust bearing. The major part of the impeller hydraulic axial thrust  $F_{A,imp}$  is balanced by the axial thrust of the piston  $F_{A,p}$ , which is produced by a high pressure difference between both sides of the piston, and acts in the opposite direction. With a non-compensated thrust the axial bearing is loaded. The

advantage of a pump design with a piston is robust execution with high pump reliability, but the disadvantages are relatively high piston leakage losses  $Q_{L,p}$  and friction losses of the piston.

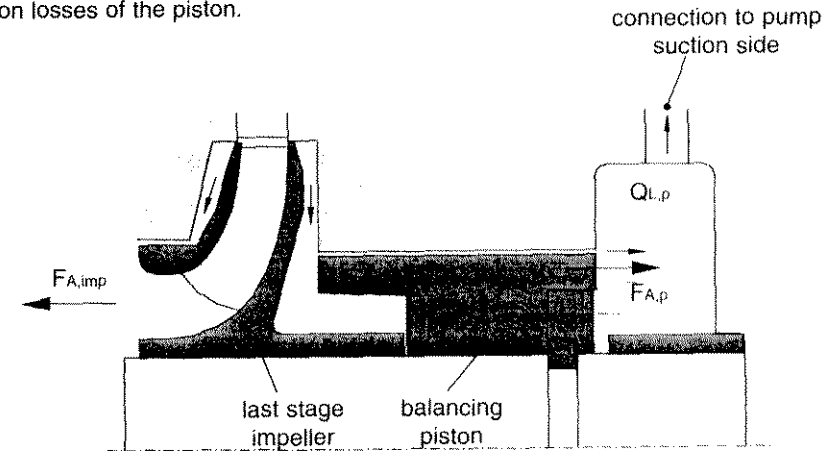


Fig.F.1.10 Execution with a balancing piston

An execution with a combination disc/piston (Fig.F.1.11.) is intended to combine the advantages and reduce the disadvantages of both separate designs.

It has to be pointed out that the axial thrust balancing principles shown in Fig.F.1.3, and normally used in single-stage pumps, can also be implemented in multi-stage pumps.

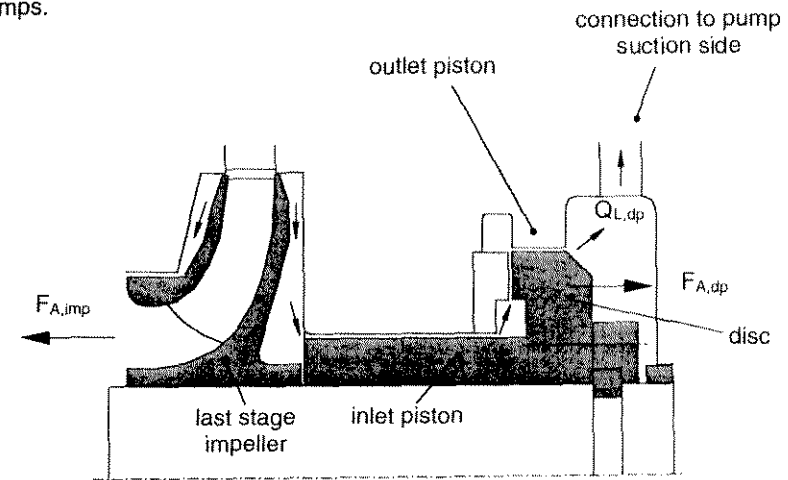


Fig.F.1.11 Execution with a combination disc/piston

### F.1.4. Axial thrust in pump start regimes

During pump start regimes, an axial thrust can result which is much higher or even in the opposite direction to that in steady-state operation. It has to be considered that it takes several seconds before the fluid rotation in the impeller side chambers reaches steady-state conditions. Due to this, during the starting period, the pressure distributions on both impeller shrouds, and consequently the axial thrust, are changing. Additionally, during pump start regimes with an open discharge valve, the impulse force on the impeller is higher than at the duty point. All the facts described above can lead to the result that during the starting procedure of vertical pumps, the resultant axial thrust can act in the opposite direction and lift the rotor temporarily. The design of an axial thrust bearing has to withstand such transient conditions.

Additional care regarding the problem of axial thrust has to be taken in multi-stage pumps when pumping fluids with a higher temperature. The consequences of thermal transients in "hot/cold" starting procedures are temporary changes in the radial clearances in the impeller wear rings and shifting of the impellers in an axial direction due to shaft thermal deformation. These temporary changes affect considerably the pressure distribution in the impeller side chambers and with this, the hydraulic axial thrust.

## F.2. Radial thrust

### F.2.1. Origins of radial thrust

Radial thrust on the impeller results from a non-symmetrical pressure distribution on the impeller outer periphery. Non-symmetrical pressure distribution can result from the geometrical form of the pump casing (spiral casing, concentric casing, vaneless or vaned diffuser), from a non-symmetrical impeller inflow or from the pump operating regime. This physical mechanism is the main cause of a non-symmetrical pressure distribution at the impeller outer periphery, and can be explained by the example of the single spiral casing in Fig.F.2.1.

At the design flow rate of the casing ( $Q \approx Q_{des,c}$ ), the flow pattern is settled, and the flow angle  $\alpha_2$  at the impeller exit matches the angle of the spiral casing tongue. The static pressure distribution  $p_{st} = f(\varphi)$  is practically uniform along the whole impeller periphery.

At reduced flow rates ( $Q \ll Q_{des,c}$ ), the spiral casing cross-section is too big, and the flow in the spiral casing decelerates ( $c_{c1} < c_2$ ). The inflow to the tongue is at too small an angle  $\alpha_2$ , and an area of reduced pressure builds up at the inner part of the casing tongue (see area of flow separation, Fig.F.2.1.b.).

At increased flow rates ( $Q > Q_{des,c}$ ), the spiral casing cross-section is too small and the flow in the spiral casing accelerates ( $c_{c1} > c_2$ ). The flow approaches the tongue at too big an angle  $\alpha_2$ , and an area of reduced pressure builds at the outer part of the casing tongue (see area of flow separation, Fig.F.2.1.c.).

From the flow field and static pressure distribution at the impeller outlet described above, it can be concluded that the radial thrust  $F_R$  has its minimum at the flow rates for which the spiral casing was designed -  $Q_{des,c}$ . The direction of the radial thrust  $F_R$  changes with the pump flow rate, and can be explained by a changed static pressure distribution around the impeller periphery (see Fig.F.2.1.). On the other hand the magnitude and direction of  $F_R$  also depend on the shape of the spiral casing and the pump specific speed, as well as on the flow conditions at the impeller inlet.

### F.2.2. Reduction of radial thrust

Radial thrust is an important parameter when designing a pump's mechanical elements, especially shafts and bearings. The requirements for radial thrust limitation are mainly connected with the following problems:

- excessive bending of the shaft at the impeller wear rings, and consequently possible metal contact between rotating and stationary elements,
- stresses too high in the shaft, danger of cracks,
- overloading of the radial bearings,
- danger of damage to the mechanical seals, due to the shaft bending at the seals: the limit of shaft bending according to API 610/8 is 50  $\mu\text{m}$ .

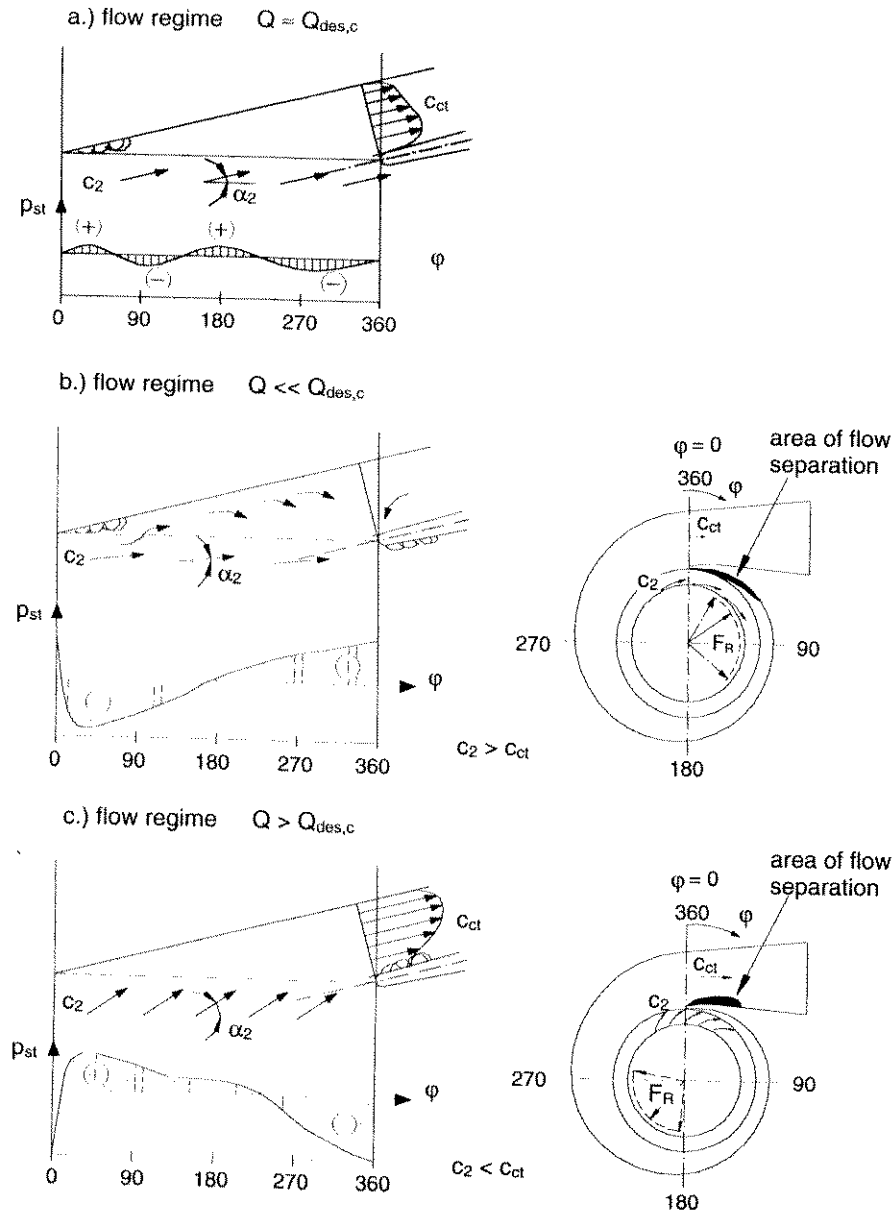


Fig.F.2.1 Schematic flow and pressure distributions at the impeller exit for a single spiral casing and different flow regimes

The most frequently applied designs for radial thrust reduction are double spiral casings (double volutes) in single-stage pumps, or vaned diffusers in multi-stage pumps. Sometimes a concentric casing can be an acceptable and simple solution in pumps with a low specific speed, to be operated only in the range  $Q < Q_{des,c}$ . To obtain a radial thrust characteristic without any major irregularities or instabilities in the whole pump operating regime, it is important to separate efficiently the main flow at the impeller exit from the flow in the impeller side chambers. The same recommendation is also valid for axial thrust (see chapter F.1.).

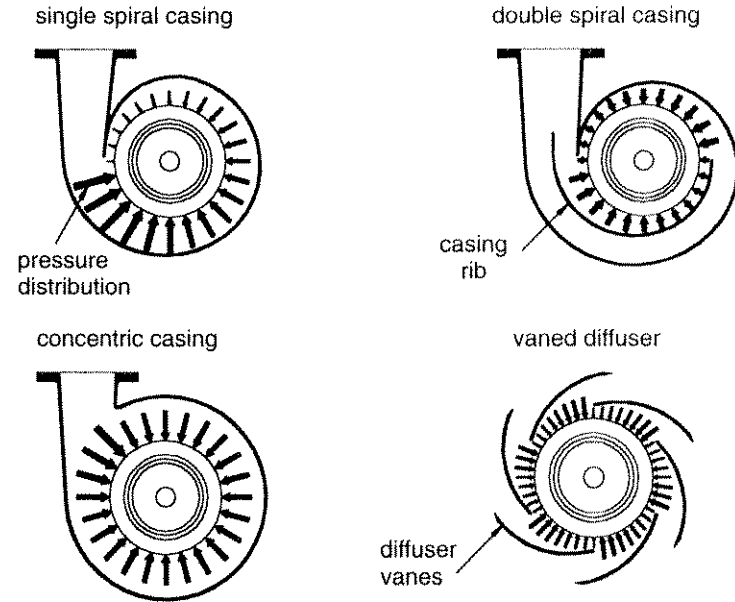


Fig.F.2.2 Schematic static pressure distribution at the impeller outlet for different casing geometries and flow regimes  $Q \ll Q_{des,c}$

Double spiral casing: With the introduction of double spiral casings, the pressure distribution on the impeller periphery becomes practically symmetrical; partial forces act against each other, and both casing halves compensate each other. A schematic comparison of the pressure distribution at the impeller outlet is shown in Fig.F.2.2. for different casing geometries and flow regimes  $Q \ll Q_{des,c}$ .

Vaned diffuser: The effect of a vaned diffuser on pressure distribution at the impeller exit is similar to a double volute, but in a vaned diffuser the number of channels is higher and the gap between the impeller and diffuser blades is smaller. For this reason the geometrical tolerances on the diffuser have an important impact on the symmetry of the pressure distribution.

Concentric casing: At the flow regimes  $Q < Q_{des,c}$ , the flow in a concentric casing can circulate without any obstacle (such as the tongue in a spiral casing), and due to this effect the pressure distribution at the impeller outlet is practically symmetrical, and the radial thrust is low. At flow rates  $Q > Q_{des,c}$ , the velocity and pressure distribution are disturbed and the radial thrust increases.

A comparison of radial thrust in a dimensionless form for one radial pump with a specific speed  $nq19$ , and tested with different casing variants, is shown in Fig.F.2.3. The results match logically the above-stated explanations of flow and pressure distribution in different casing geometries.

A complete elimination of radial thrust should be avoided because the consequence for an unloaded radial bearing can be unstable operation.

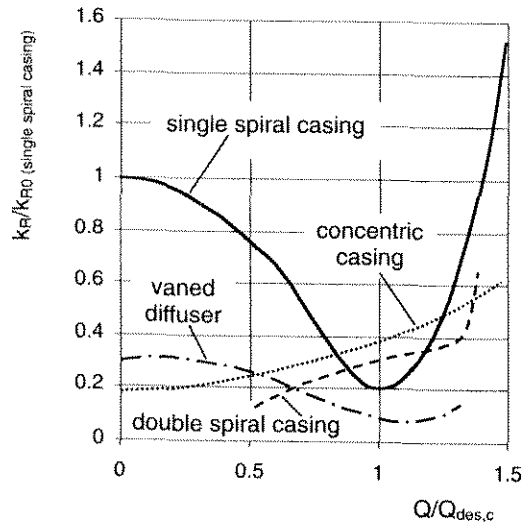


Fig.F.2.3 Radial thrust in a dimensionless form for different casing variants, pump specific speed  $nq19$

**F.2.3. Determination of radial thrust**

The flow at the impeller exit is non-stationary, mainly due to the effect of a non-uniform pressure distribution between two blades at the exit of the impeller channel. This pressure field rotates with the frequency ( $f = n \cdot z_2$ ), and the consequence is that radial thrust is also time-dependent. The time average value gives the so-called static radial thrust, which is dominant. The dynamic component is called the dynamic radial thrust, and is smaller and time-dependent.

The radial thrust in pumps can be experimentally defined by the following methods:

- integration of the static pressures on the impeller periphery,
- measurement of the reaction forces on the bearings,
- measurement of the shaft deflection,
- measurement of the stresses in the shaft.

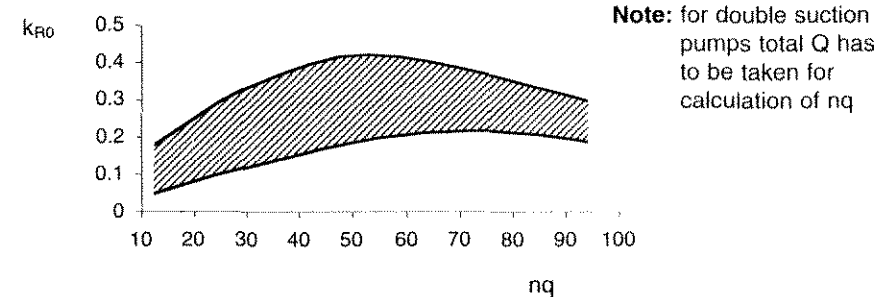
In the technical practice of pump design, the method for estimating the radial thrust from the pump geometrical parameters and characteristics is also well known. This determining of thrust is based on the statistics of much experimental data and is valid with a high degree of certainty for flow regimes near  $Q_{des,c}$  and for regimes  $Q = 0 \div Q_{des,c}$ . At flow rates  $Q \gg Q_{des,c}$ , the radial thrust determination is more delicate and can change drastically. The method shown for determining radial thrust is helpful when no radial thrust measurements are available.

The static radial thrust  $F_R$  is in a linear relationship with the pump total head  $H$  and the projection of the impeller outlet area ( $d_2 \cdot B_2$ ). The dimensionless radial thrust coefficient  $k_R$  is defined according to the relationships in F.2.1.

$$F_R = k_R \cdot \rho \cdot g \cdot H \cdot d_2 \cdot B_2$$

casing type	radial thrust coefficient $k_R$
single spiral casing	$k_R = (k_{R0} - 0.05) \cdot (1 - Q_{des,c}^2) + 0.05$ <i><math>k_{R0}</math> - see Fig.F.2.4.</i>
double spiral casing	$k_R = 0.03 \cdot k_{R0}$ (single spiral casing)
vaned diffuser	$k_R = 0.05 - 0.10$

Table F.2.1 Radial thrust coefficient  $k_R$  for different casing geometries



**Note:** for double suction pumps total  $Q$  has to be taken for calculation of  $nq$

Fig.F.2.4 Radial thrust coefficient for a single spiral casing as a function of specific speed, flow conditions  $Q=0$



## G. NOISE EMISSION FROM CENTRIFUGAL PUMPS

### G.1. Basic acoustic terminology

**Sound:** cyclical variations of ambient pressure (sound waves) at frequencies which are detectable to the human ear (normally between 30 Hz and 17 kHz)

**Noise:** the general term for undesirable and unwanted sound

**Sound power:** power emitted, transferred or received as sound waves,  $P$  (W).

It can be measured either by sound pressure or by sound intensity.

**Sound intensity:** sound power through a surface normal to the direction of propagation, divided by the area of the surface,  $I$  (W/m<sup>2</sup>)

**Sound pressure:** the difference  $p$  (Pa) between the total pressure measured during noise emission and the static pressure which would exist in the absence of sound waves

The relationship between sound intensity and sound pressure (rms) is:

$$I = p^2 / (\rho \cdot c)$$

$\rho$  - air density (kg-/m<sup>3</sup>)

$c$  - sound velocity in air (m/s)

The human ear does not have a linear acoustic response, but its perceptions are logarithmically proportional to the actual sound pressure. Logarithms are used in expressing the magnitude (level) of sound.

**Sound pressure level (SPL):**

$$L_p = 20 \cdot \lg(p / p_0) \dots [\text{dB}], \text{ where } p_0 = 20 \cdot 10^{-6} \text{ Pa} - \text{reference sound pressure}$$

**Sound power level:**

$$L_w = 10 \cdot \lg(P / P_0) \dots [\text{dB}], \text{ where } P_0 = 10^{-12} \text{ W} - \text{reference sound power}$$

**Sound intensity level:**

$$L_I = 10 \cdot \lg(I / I_0) \dots [\text{dB}], \text{ where } I_0 = 10^{-12} \text{ W/m}^2 - \text{reference sound intensity}$$

**Frequency spectrum:**

A visual representation of sound level as a function of frequency

**Octave band:**

A term used to express ranges of frequencies of sound. One octave is the range of sounds from a frequency  $f_1$  (Hz) up to a frequency  $2 \cdot f_1$  (Hz). Octaves are units

which are used for dividing sound frequencies into frequency bands. In noise treatment, octave bands are normally used with centre frequencies of 63, 125, 250, 500 Hz, 1, 2, 4 and 8 kHz. Sometimes a 1/3-octave band spectrum is used, where each octave is divided into three parts (three third-octaves per octave).

**A-weighted sound pressure level**

The perception of the human ear is maximal at a frequency of about 4 kHz and decreases rapidly at lower frequencies. In order to adapt sound pressure levels measured by a sound level meter to the perception characteristics of the human ear, different weighting filters (A, B or C) have been used. Most often an A-weighted sound pressure level is used as a measure of the perceptual magnitude of sound. It takes into account the sensitivity of the human ear.

### G.2. Origin of noise in pumps

Pump noise is generated by liquid motion in pumps and systems, and by mechanical motion of the pump components. Pressure fluctuations caused by the interaction between impeller and diffuser (or volute tongue) make the flow in a centrifugal pump non-stationary. The result is hydraulic forces, which cause shaft vibration and non-stationary loading on the pump parts. The vibrations which are transferred to the baseplate propagate to the building walls, and produce structure- (solid) borne sound. The pressure fluctuations also propagate in piping systems as fluid-borne sound. Pressure fluctuations can cause pump casing vibration and propagate as airborne sound. A simplified sketch of sound propagation routes is in Fig.G.2.1.

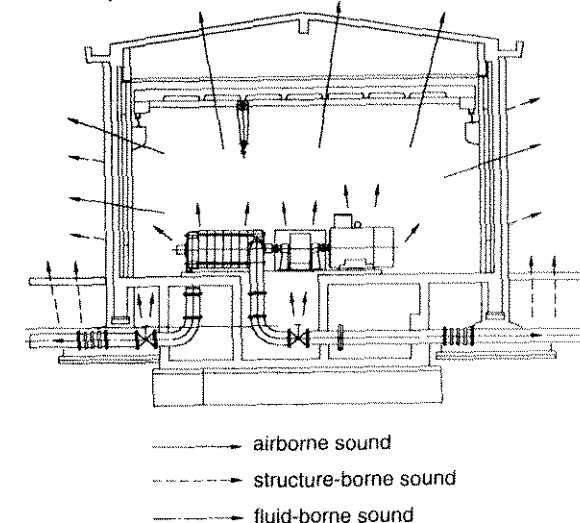


Fig.G.2.1 Schematic representation of the sound propagation routes in a pumping plant

The pump noise level increases with pump head, impeller circumferential speed (impeller diameter  $D_2$  and rotational speed  $n$ ), and with pump shaft power. The A-weighted sound pressure level for different types of centrifugal pumps working at best efficiency point for "pump alone" can be estimated according to the following equation:

$$L_p = a + b \cdot \lg(P/P_r) + 3 \cdot \lg(n/n_r) \dots [\text{dB A}]$$

where  $P_r = 1 \text{ kW}$  – reference shaft power  
 $n_r = 1 \text{ rpm}$  – reference rotational speed

Pump type	coefficient a	coefficient b
Single-stage with volute	43	12.5
Multi-stage with diffuser	55	7.5
Double entry with volute	40	12.5
Axial flow	52	9.0

Table G.2.1 Table of coefficients for estimating SPL

### G.2.1. Liquid (hydraulic) noise sources

The following sources are responsible for hydraulic noise:

- interaction between the impeller blades and diffuser vanes (or volute tongue),
- turbulent flow in the pump passages,
- pump operation at part-load (recirculation) or in the region of cavitation.

Interaction between the impeller blades and diffuser vanes (or volute tongue) creates periodic excitation and induces so-called rotary noise. The velocity distribution at the impeller outlet is highly non-uniform (Fig.G.2.2.) and the velocity decreases in the wake of each impeller blade, where Karman vortexes occur. The rotating non-uniform flow pattern creates pressure fluctuations at the diffuser vanes. The diffuser vanes themselves influence flow in the impeller, making it non-stationary. These phenomena cause periodic pressure fluctuations, impeller vibration and noise. They are minimal at the point of maximum hydraulic efficiency, where the velocity distribution at the impeller outlet is the most uniform. Excitation frequencies are multiples of blade passage frequencies ( $n \cdot z_2$ ,  $n \cdot z_3$ ,  $n \cdot z_2 \cdot z_3$ ) and are as follows:

$$f_D = n \cdot z_2 \cdot k \quad (\text{impeller-excited frequencies})$$

$$f_D = n \cdot z_3 \cdot k \quad (\text{diffuser-excited frequencies})$$

$$f_D = n \cdot z_2 \cdot z_3 \cdot k \quad (\text{interference frequencies of impeller and diffuser})$$

where:  $f_D$  excitation frequency  
 $n$  rotational speed  
 $z_2$  number of impeller blades  
 $z_3$  number of diffuser vanes or volutes  
 $k = 1, 2, 3, \dots$  1st, 2nd, 3rd, ... harmonic

Every disturbance in the axi-symmetrical flow at the pump inlet causes a non-stationary flow around the impeller and diffuser blades, resulting in pressure fluctuations, rotor vibration and noise. Such disturbances are bends, ribs and inlet suction vortexes in vertical pumps with free water surfaces. Changes in flow direction, secondary flows, flow separations and vortexes create a highly non-uniform flow distribution in the impeller, as is also the case in the diffuser (or volute). The spectrum of this noise shows a wide range of frequencies – a broadband frequency spectrum.

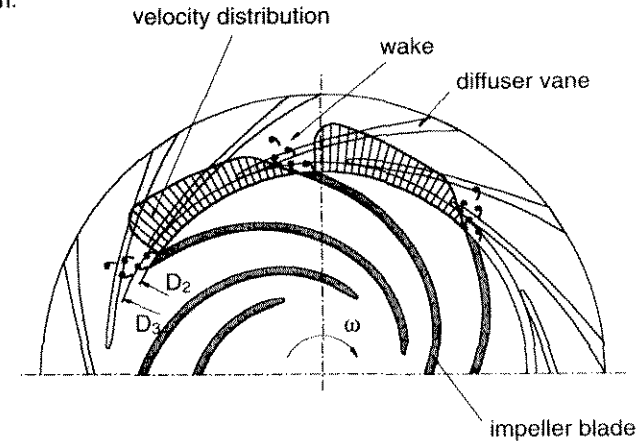


Fig.G.2.2 Non-uniform flow at an impeller outlet

When a pump operates at part-flow or at overflow, it generates more noise, because the geometrical vane angles (guide vanes, impeller and diffuser or volute) are incorrect for the actual flow angles. Another major source connected with part flow is recirculation (see section C.4). The magnitude and frequency of this hydraulic noise depends on the specific pump design and varies from pump to pump.

If a pump cavitates, it generates cavitation noise at high frequencies due to the implosion of the vapour bubbles. Apart from the noise, cavitation can cause severe material damage. For details see section C.8.

### G.2.2. Mechanical noise sources

Mechanical noise has two components. One results from vibration caused by an unbalance of impellers (mechanical and hydraulic), shaft and coupling. The second is generated by the rotation of the bearings and shaft seals. Rolling contact bearings with grease lubrication generate higher noise levels than bearings with oil lubrication; however, the lowest noise level is achieved by hydrodynamic bearings.

High quality in the manufacturing of rotating parts, and in their assembly and maintenance is also important from the point of view of noise, because rubbing in the bearings, seals or impellers induces noise, as can too great a coupling misalignment.

Pump drivers, hydraulic couplings and mechanical gears are also important noise sources. Their noise level is many times higher than that generated by the pump itself. Reference limiting values of the sound pressure level (SPL) for air-cooled electric motors, according to VDE 0530, are in Fig.G.2.3. Usually the SPL of standard AC electric motors lies under the limiting curves.

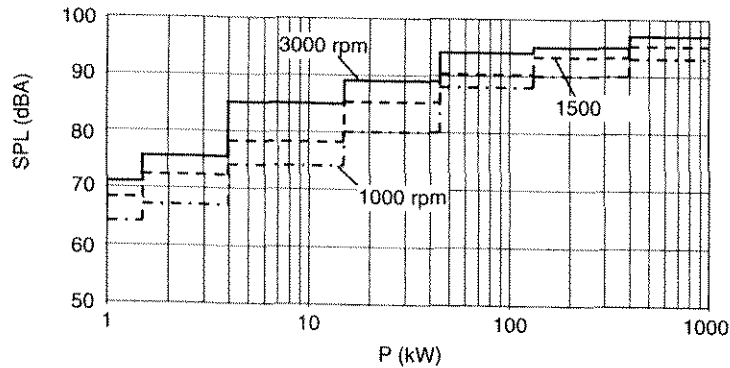


Fig.G.2.3 Reference values of SPL for AC electric motors

### G.3. Measuring noise

Pump noise is measured basically for two purposes:

- to verify if the pump noise (together with the baseplate, suction and delivery parts of the piping) meets applicable environmental criteria;
- to diagnose possible faulty operation of the pump or pump parts.

Various standards and recommendations have been developed to specify airborne noise emission measurement methods and procedures that must be used for the test. At each specified location the noise emission characteristics include both the sound pressure level and the sound power level.

The following standards are often used for measuring the airborne noise emission of liquid pumps and pump units:

- EN 12639 (2000) Liquid pumps and pump units – Noise test code – Grade 2 and Grade 3 of accuracy
- ANSI/ISO 9.1-9.5-1994 Pumps – General Guidelines for Types, Definitions, Application and Sound Measurement

### G.3.1. Standard EN 12693

According to this standard, Grade 2 means engineering method (higher grade) and Grade 3 means survey method (lower grade). The standard provides two possibilities for measurement: either pump alone or pump unit. In these two cases the pumps can be installed:

- on site
- on a shop test stand
- in a specific facility intended for acoustic measurement

Usually the end-user is interested in the overall noise level of the pump unit. To select the basic standard for determining the sound power level of a pump unit, Table G.3.1. should be used. The preferred method is written without brackets, and should be used where practical. If it is not practical, one of the other basic standards (in brackets) should be used. A table for "pump alone" is also available in EN 12693.

Test arrangement	Grade	Driver rated power, P (kW)			
		0.5 < P ≤ 15	15 < P ≤ 75	75 < P ≤ 300	P > 300
On site	2	9614 (3744)			9614
	3	3746 (9614)		9614 (3746)	
Shop test stand	2	3744 (3746-1, 9614)	3744 (9614)	9614 (3744)	9614
	3	3746 (9614)		9614 (3746)	
Specific Facility	2	3744 (3746-1, 9614)		3744 (9614)	9614 (3744)

Table G.3.1 Selection of standards for determining sound power level for a pump unit – all standards in the table are EN ISO (3744 means EN ISO 3744)

Fig.G.3.1 Shows the typical microphone positions for Grade 2 sound pressure level measurement of a pump unit. For details, Standard EN 12639 and other related standards should be used.

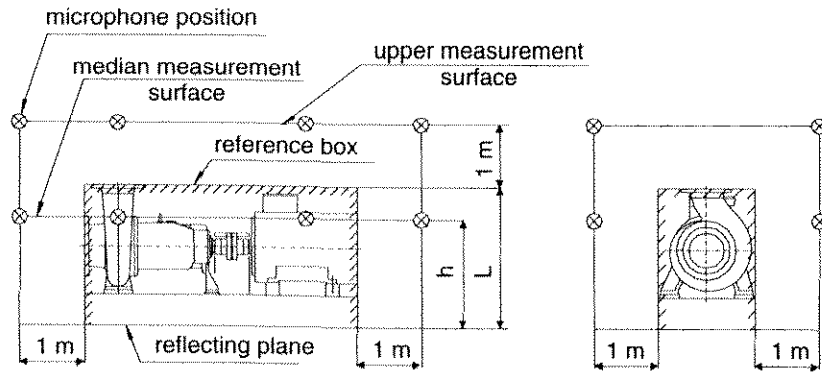


Fig.G.3.1 Typical measurement surfaces and planes for sound pressure level measurement for a pump unit – Grade 2

**G.3.2. Examples of SPL measurement results**

Two examples of the results of sound pressure level measurement are presented in Fig.G.3.2. and Fig.G.3.3. Fig.G.3.2. shows the 1/3-octave band frequency spectrum of the sound pressure level measurements on a vertical volute mixed-flow pump and its driving electric motor, operating near to best efficiency point. The pump itself is underground, while the motor is on the floor above. The only noise on the upper floor is from the motor. A comparison of the noise spectra shows clear differences between noise near the motor and noise near the pump.

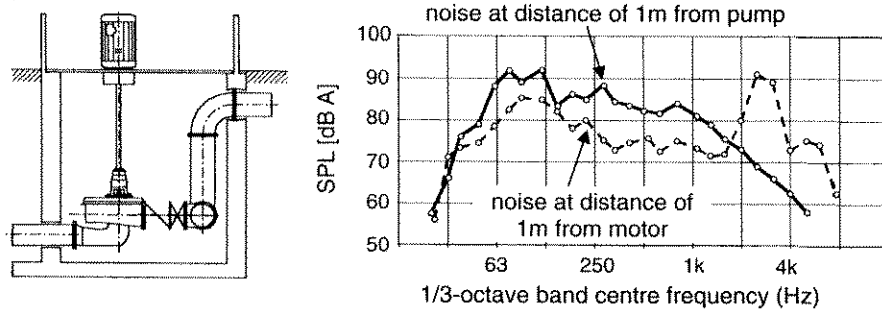


Fig.G.3.2 Frequency spectrum of sound pressure level measured on a vertical volute mixed-flow pump

Fig.G.3.3. shows how the sound pressure level (dB A) of a radial pump depends on its operating point. The shape of the diagram is also similar for shaft vibration. The lowest noise values are in the near vicinity of the best efficiency point.

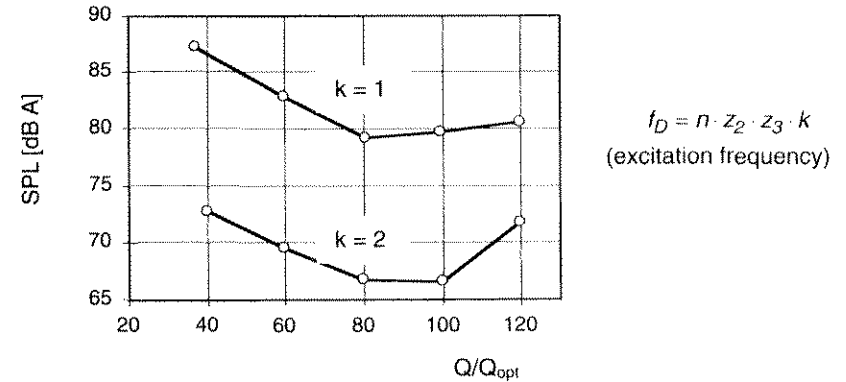


Fig. G.3.3 Sound pressure level as a function of the operating point of a radial pump

**G.4. Ways of abating noise**

Several ways exist for abating noise and some of them are always helpful, while others can be helpful in one case, but not in another. The guidelines are arranged in two groups:

- primary approaches – noise reduction at source (see G.4.1)
- secondary approaches – interruption of noise transmission (see G.4.2)

**G.4.1. Noise reduction at source**

Reduction of pressure pulsations

- increase of the clearance between impeller and diffuser vanes (or volute casing tongue),  $D_3/D_2$

The following recommendations should be followed:

diffuser:  $nq < 40$ ,  $D_3 / D_2 \geq 1.01 + 0.75 \cdot 10^{-2} \cdot (H_{st} / 100 - 1)$   
 $(D_3 / D_2 \geq 1.04 \text{ for } H_{st} \geq 500 \text{ m})$

$nq < 40$ ,  $D_3 / D_2 \geq 1.04 + 1.01 \cdot (nq - 40)$

volute:  $D_3 / D_2 \geq 1.03 + 0.1 \cdot (nq / 40) + 0.07 \cdot (H_{st} / 1000)$

- selection of the correct number of impeller and diffuser vanes  
The selection should be done according to the following recommendation:

$$m = V_3 \cdot z_3 - V_2 \cdot z_2$$

- m number of diametrical nodes defining pressure pattern
- $z_2, z_3$  number of impeller ( $z_2$ ) and diffuser ( $z_3$ ) vanes
- $v_2, v_3 = 1, 2, 3, \dots$  order numbers of impeller and diffuser periodicities

The number of impeller and diffuser vanes should be selected in such a way that number  $m$  is not equal to 0 or 1 for  $v_2, v_3 = 1, 2$  and 3 (it can be equal to 0 or 1 at  $v_2$ , and  $v_3$  as big as possible).

For pumps with a head per stage higher than 100 m, it is recommended that:  $z_2 \geq 5$ .

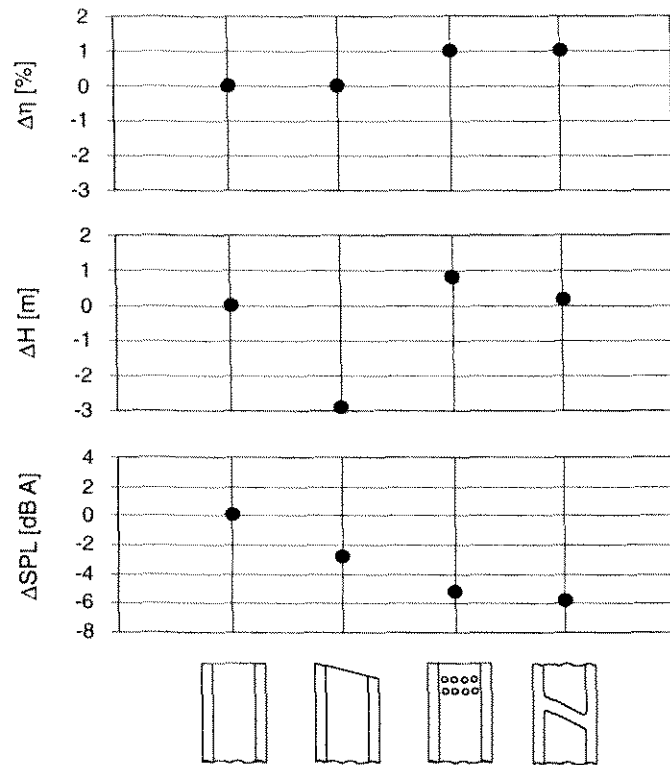


Fig.G.4.1 Reduction of noise with various impeller blade outlet geometry modifications for single-stage volute pump

- modification of impeller blade geometry at outlet acc. Fig.G.4.1.
- modification of volute casing tongue by slanting acc. Fig.G.4.2.
- impeller of double suction pump with blades not in phase acc. Fig.G.4.3.
- profilation of trailing edge of ribs mounted in suction ducts and of diffuser vanes acc. Fig.G.4.4.

Reduction of mechanical noise

- increase in the quality of balancing of the rotating elements
- minimal misalignment of coupling
- selection of drive (motor, gears, coupling) with a lower noise level; for example, water-cooled electric motors are less noisy than air-cooled
- use of lubricating oil with higher viscosity

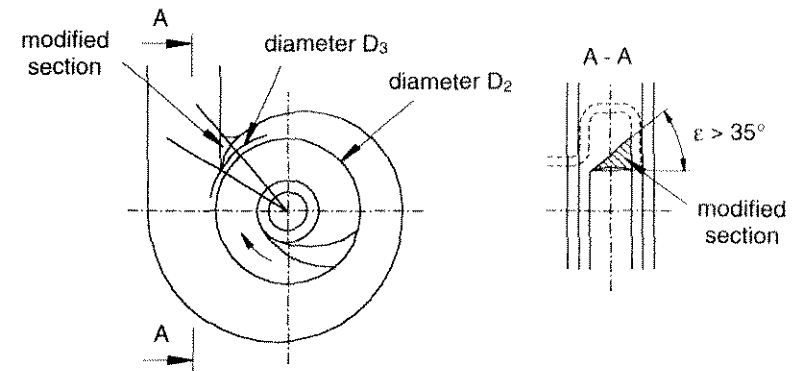


Fig.G.4.2 Reduction of pressure pulsations with volute casing tongue modification

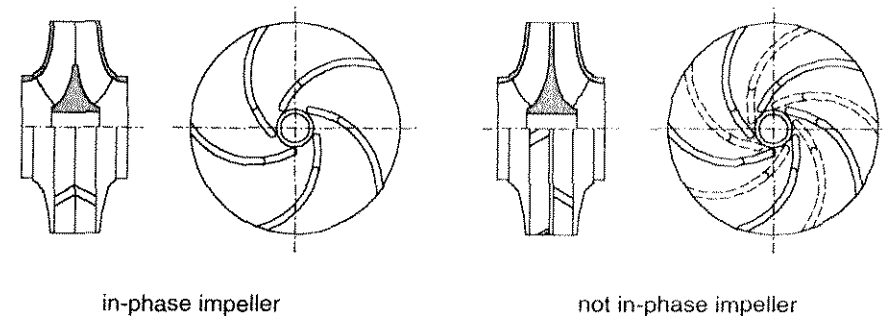


Fig.G.4.3 Designs for impellers of double suction pumps in relation to pressure pulsations



Fig.G.4.4 Recommendations for profilation of trailing edge of ribs and outlet of diffuser vanes

#### Improvement in pump – system interaction

- increase NPSH<sub>av</sub> to avoid cavitation
- inject small quantity of air into the suction part of the pump to reduce cavitation noise
- selection of pump which operates near the best efficiency point in order to minimise recirculation, cavitation and vibration problems
- selection of pump with different rotational speed to avoid system resonances

#### Improvement in piping system

- selection of low velocities in pipelines
- use of low-noise control valves
- avoidance of instantaneous changes of cross-sectional areas
- use of large-radius elbows
- avoidance of acoustic resonance

#### **G.4.2. Interruption of noise transmission**

- use of vibration isolators between pump baseplate and foundation
- use of compensators between pump flanges and pipelines
- use of vibration-isolating supports for pipelines
- use of acoustic filters (silencers) or other control equipment on the pipelines upstream and downstream of the pump
- use of noise-damping walls around the pump
- use of noise-isolated pipelines
- ensure that the structure-borne noise created by the pump unit is radiated as little as possible by adjacent elements

## H. VIBRATION IN CENTRIFUGAL PUMPS

### H.1 Introduction

Different kinds of vibration are usually the principal cause of operational difficulties observed during pump operation. In order to solve such operational disturbances, the interaction between mechanical vibration and excitation forces has to be understood. The following are three major types of vibration:

**Natural (free) vibration:** Each mechanical system combined of mass, stiffness and damping possesses natural (free) vibration which occurs at natural frequencies.

**Forced vibration:** Such vibration occurs if a system, combined of mass, spring and damping, is excited by a periodic force. If the natural frequency coincides with the forced vibration frequency, the result is the resonance of the whole system: when the rotating speed of a pump coincides with the natural frequency of the rotor, that speed is referred to as the critical speed of the rotor. The amplitude of vibration is strongly dependent on the damping value of the rotor.

**Self-exciting vibration:** This type of vibration occurs when a mutual effect exists between the vibration of a mechanical system and the exciting phenomenon. In such cases, the vibration is self-exciting. If the damping of the rotor is not sufficient, the vibration amplitude can be extremely high and can lead to the destruction of the pump in a very short space of time.

Based on the types of vibration described above, the following typical pump or pump element vibrations can be categorised:

**Lateral shaft vibration:** This vibration is perpendicular to the pump shaft centre line and always appears as forced vibration at a certain magnitude, due to unavoidable residual hydraulic and mechanical unbalances. Excessive shaft vibration can lead to wear of the impeller labyrinths, shaft seal failures and other structural damage.

**Bearing housing vibration:** As a result of reaction to lateral shaft vibration, bearing housing vibration occurs. This vibration can be easily monitored by accelerometers fitted on the bearing housing.

**Vibration in the system pump-baseplate:** This vibration is caused by shaft vibration and pressure pulsation originating in the pump. As the baseplate has six vibra-

tion modes, the system pump-baseplate has to be investigated in detail in conjunction with the possible dangers of the resonance.

**Vibration in vertical pumps:** In this case not only the shaft vibration, but also the vibration of the rising pipe, as well as the shaft coupling, have to be analysed. In addition, the vibration of the system electromotor support has to be carefully observed.

In order to find the real cause of the vibration, a separation of the problems must be made, as originating either from the system or from the pump itself.

System-related problems:

- excitation from the drive,
- excitation from the coupling,
- excitation from the components of the piping system,
- unfavourable pump inlet conditions (NPSH, inlet vortices),
- unfavourable dynamic behaviour of the foundations, or pump pedestal resonance,
- torsional natural frequency excited by the pump drive,
- excessive piping loads acting on the pump casing.

Problems related to the pump:

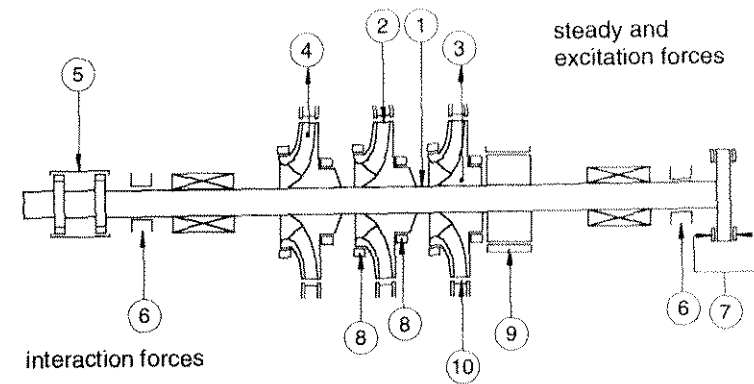
- mechanical unbalance of all rotating parts,
- hydraulic unbalance due to imperfection or fault in the impeller casting,
- hydraulic excitation when the pump is working outside the admissible operating range,
- inadequate NPSH producing cavitation in the impeller,
- acoustic resonance,
- increased radial clearance in the annular seals or in the journal bearings.

## H.2 Forces acting on the pump rotor

In every pump, static and dynamic forces are present; therefore a certain amount of vibration of the pump and the pump system has to be accepted. A schematic representation of the forces acting on a pump impeller is shown in Fig. H.2.1.

### H.2.1 Steady forces

Steady (stationary or static) forces, such as the weight of the rotor and the static radial thrust on the impellers, produce reaction forces in the bearings, and with this they influence the stiffness and damping effects of the bearings. An example of measured static radial forces on a pump impeller is shown in Fig. H.2.2 in the form of a polar plot. The direction and the magnitude of the force change with the pump operating regime.



Steady forces: {  
1 – rotor weight  
2 – static radial thrust

Excitation forces:  
3 – mechanical unbalance  
4 – hydraulic unbalance  
5 – coupling force

Interaction forces in:  
6 – journal bearings  
7 – thrust bearing  
8 – annular seals (sealing rings)  
9 – balancing piston  
10 – impeller/diffuser interaction

Fig. H.2.1 Forces acting on a pump rotor

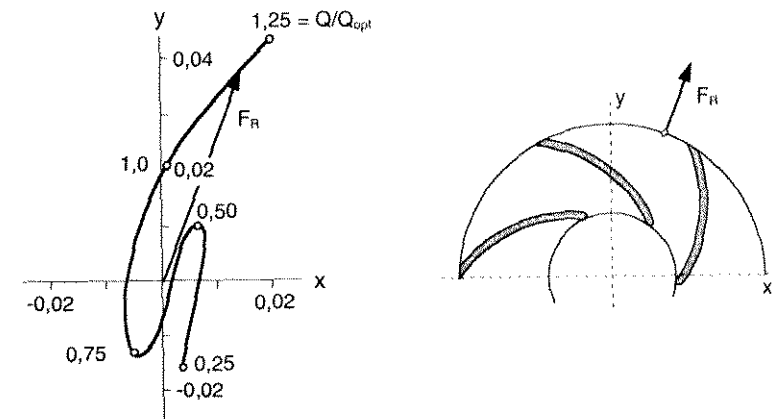


Fig. H.2.2 Measured static radial force for a radial pump with diffuser

## H.2.2 Excitation forces

These forces are always present if the rotor is turning, independently of whether the shaft is deflected or not. The rotordynamic behaviour (especially for multi-stage pumps with a high power concentration and high head per stage) is determined mainly by unbalanced forces. The unbalanced forces with well-defined frequencies are:

**Hydraulic unbalance of the pump impeller:** This excitation is caused by impeller imperfections and is dependent on:

- outlet width variation (casting imperfection),
- outlet vane angle, deviating from blade to blade of the impeller,
- blade pitch variation,
- eccentricity between the centre of the hydraulic channels and the impeller bore.

All these parameters lead to a variation of the blade forces resulting in a net hydraulic force which rotates with the impeller speed. The hydraulic unbalance force  $F_{hu}$  can be expressed as follows:

$$F_{hu} = k_{hu} \cdot \rho \cdot g \cdot H \cdot d_2 \cdot B_2$$

$\rho$  – fluid density

$g$  – acceleration due to gravity

$H$  – head per stage

$d_2$  – impeller outer diameter

$B_2$  – outlet width of the impeller (including shrouds)

$k_{hu}$  – dimensionless hydraulic unbalance coefficient:

$$k_{hu} = 0.01 - 0.03 \text{ (for precision cast impeller)}$$

$$k_{hu} = 0.04 - 0.06 \text{ (for sand casting)}$$

**Mechanical unbalance:** This excitation force is due to the residual mechanical unbalance of all rotating parts of the rotor and is defined as follows:

$$F_{mu} = Q \cdot m \cdot \omega \cdot 10^{-3}$$

$F_{mu}$  – mechanical unbalance force (N)

$Q$  – ISO balance grade (mm/s)

$m$  – mass of rotating part (kg)

$\omega$  – angular velocity of rotor (s<sup>-1</sup>)

From the vibration point of view, the hydraulic unbalance force  $F_{hu}$  is far more important than the mechanical unbalance force  $F_{mu}$ . Even for a precision cast impeller the hydraulic unbalance is approximately one order of magnitude higher than the mechanical unbalance when the impeller is balanced according to ISO Grade 2.5. According to Standard API 610/8 this balancing grade is required for pumps with a rotational speed below 3800 min<sup>-1</sup>.

When an impeller has already been cast, only the mechanical unbalance can be further reduced. However, with an improvement in balancing grade no substantial changes in rotor vibration usually result. In contrast, a hydraulic unbalance cannot be reduced or altered once the impeller is cast. A hydraulic unbalance can really be improved only by better quality casting.

**Vane passing forces:** The origin of these forces is the sudden change in the pressure distribution (wake) at the impeller outlet when an impeller blade passes a diffuser blade or spiral casing tongue. The frequency of vane passing forces is the number of impeller blades times the rotating frequency of the shaft.

**Rotating stall forces:** These are periodic excitation forces observed especially at pump part-load operation. The frequency of rotating stall forces is low, normally near 0,2 times the rotating frequency of the shaft.

All the excitation forces described above are dynamic forces with different excitation frequencies. An example of a frequency spectrum of excitation forces is shown in Fig. H.2.3, together with self-excitation forces in annular seals (frequency near 0,8 times shaft rotational frequency).

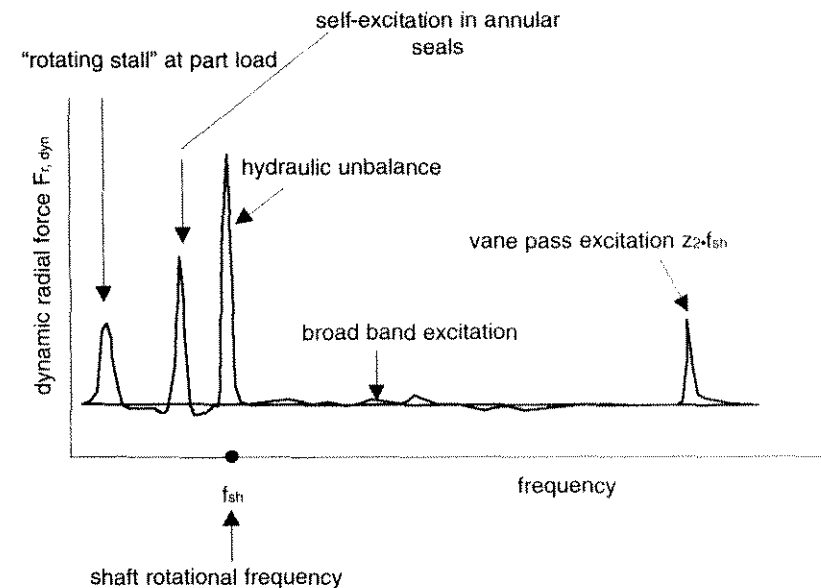


Fig. H.2.3 Frequency spectrum of dynamic radial forces



### H.2.3 Interaction forces

Interaction forces (hydraulic reaction forces) are response forces due to rotor deflection, and occur in the following pump elements (see Fig. H.2.1):

- annular seals of the impeller and balancing piston,
- thrust bearings,
- journal bearings,
- gap between impeller and diffuser.

The main and the most important difference between a radial journal bearing and an annular seal is that an axial pressure differential ( $p_1 - p_2$ ) acts on a seal. This leads to an axial flow through the seal gap. The basic flow patterns and pressure distributions in an annular seal are shown in Fig. H.2.4. When the rotor is displaced from the central position, the axial flow through the clearance of the annular seal produces an uneven pressure distribution around the annular seal. The result is a restoring force  $F_{r,as}$ , which pushes the rotor towards a central position. This effect is called the "Lomakin effect". As a rough approximation, force  $F_{r,as}$  is proportional to displacement  $e$  and is also proportional to the stiffness coefficient, which has a great influence on the value for critical speed.

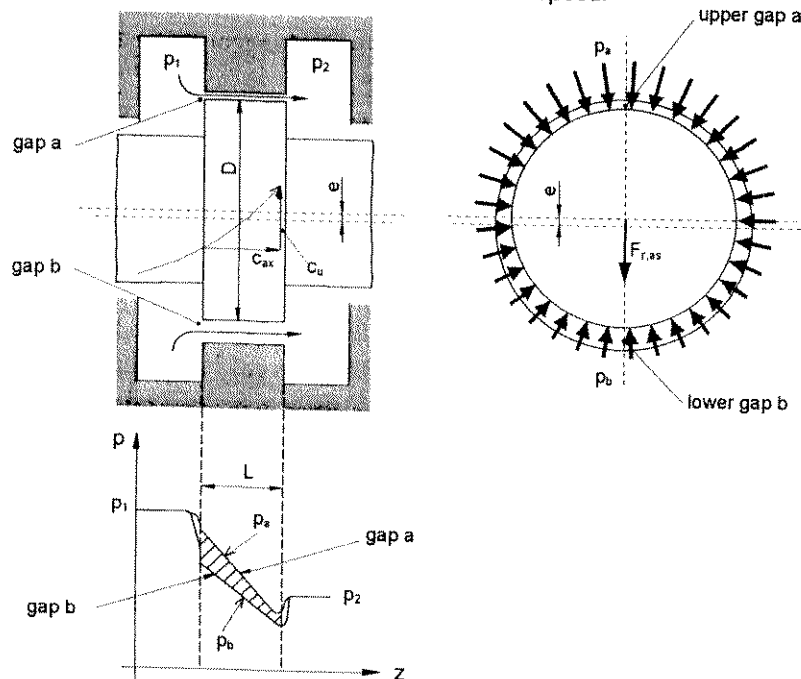


Fig. H.2.4 Schematic representation of the Lomakin effect

The effect of forces acting in the annular seals of a multi-stage pump is shown in Fig. H.2.5. In the region of the first critical speed, the rotor vibration amplitude is greatly reduced due to the Lomakin effect in annular seals (impeller wear rings) described above. As a consequence, the pump can even operate in the range of natural frequency, as the annular seals and piston greatly affect the pump rotordynamic behaviour, due to their stiffness and damping effects.

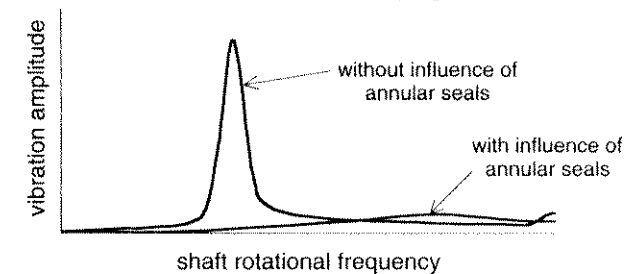


Fig. H.2.5 Predicted shaft vibration amplitude of a three-stage centrifugal pump showing the effect of annular seals

The flow in the gap also has a tangential component. This is due to the rotation of the shaft, and possible pre-rotation of the flow in the gap inlet. The result is an asymmetrical pressure distribution in a circumferential direction, generating a tangential force. This force is the cause of self-exciting vibration in the pump rotor. The magnitude of this force influences the damping very much and therefore determines the threshold of safe operation of the pump.

## H.3 Rotordynamic behaviour of pumps

### H.3.1 Rotordynamic analysis

Due to the rise in the power concentration, especially in multi-stage pumps, rotordynamic analysis is essential at the design stage, in order to determine the natural frequencies, critical speeds, separation margin and damping ratio necessary to ensure safe pump operation. Rotordynamic analysis is carried out by computer programs. The following parameters are the most important for pump rotordynamic behaviour:

- geometry of the rotor (shaft span between the bearings, shaft diameter) and overhang masses on the shaft,
- type of journal bearing and properties of the oil used,
- type, weight and overhang of the coupling,
- geometry of the annular seals and pre-rotation of the fluid at the gaps,
- hydraulic interaction between the impeller and diffuser.

Typical results of rotordynamic analysis are natural frequencies, damping ratio and shaft displacement as a function of pump speed. The shafts of horizontal multi-stage pumps are supported by two journal bearings and multiple annular seals and, due to gravitational load, produce shaft sag at standstill (see Fig. H.3.1). Each annular seal has lateral stiffness and acts like a product-lubricated bearing when the rotor rotates, and lifts the shaft towards the central position, as shown in Fig. H.3.1. With time, due to wear in the elements, the radial clearances in the impeller wear rings (annular seals) and balancing piston increase and with this the damping and stiffness characteristics of these elements change. It is obvious that a rotordynamic calculation has to be performed for new and worn wear ring conditions.

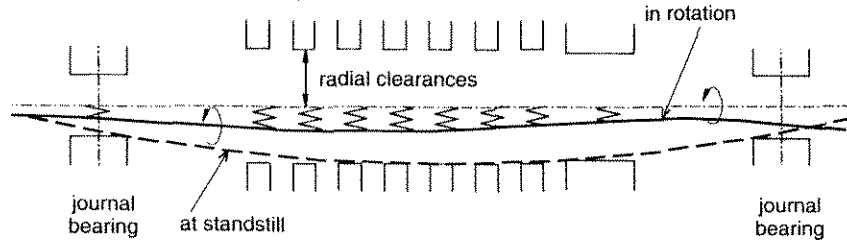


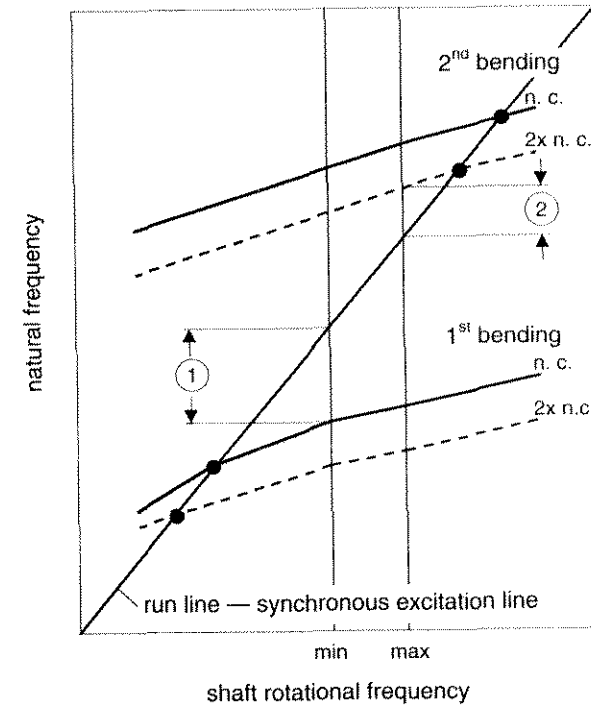
Fig. H.3.1 Multi-stage pump shaft displacement at standstill and in rotation

Standard API 610/8 prescribes the procedure for rotordynamic analysis when pump rotors are not classically stiff. In the first step, damped natural frequencies are calculated for new and worn (twice the new radial clearance) annular seals. Separation margins (the difference between natural and rotating frequencies) are defined as shown in a typical Campbell diagram in Fig. H.3.2. In the second step, the calculated damping factors of the rotor are compared with the values from Fig. H.3.3. When the separation margin is small (the natural and rotating frequencies are close to each other), then the minimal required damping factor should be higher than 0,15. When the separation margin is greater (the essential difference between natural and rotating frequencies), then the minimum required damping factor is decreased. From the above-stated, it can be concluded that a pump can operate trouble-free, even at a critical speed, if the damping value of the rotor is of the required level.

Some important concluding remarks on rotordynamic analysis, mainly related to multi-stage pumps:

- a critical speed below the operating speed exists even for pumps with very stiff shafts,
- new annular seals have high damping, and with the increased radial clearance of the seals during pump operation, damping drops heavily,
- it is possible to increase the rotor damping properties by simple design changes to the annular seals as well as to the balancing piston,
- calculation results of the critical speed depend heavily on the coefficients used for interaction forces,

- the precondition that the critical speed has to be outside the range of rotation speed is not necessary for high reliability if the damping properties of the rotor system are sufficiently high.



- ① and ② - separation margins
- n. c. - natural frequency for annular seals with new clearances
- 2x n. c. - natural frequency for annular seals with double new clearances

Fig. H.3.2 Typical Campbell diagram

### H.3.2 Possibilities for improved rotordynamic behaviour in centrifugal pumps

In order to move the rotor natural frequencies towards higher values, as well to improve the pump rotordynamic behaviour, the following measures should be taken:

- thicker shaft diameter, shorter span between journal bearings, change of shaft material, design change in the bearing housing,
- reduction of impeller and coupling masses and coupling overhang,
- change of impeller material,
- increase of stiffness and damping effect of the annular seals and of the piston by introducing special groove geometry,
- improvement in the stiffness of the journal bearings (multi-lobe journal bearings),
- change in the viscosity of the lub oil,
- modification of the support stiffness for the casing and foundation.

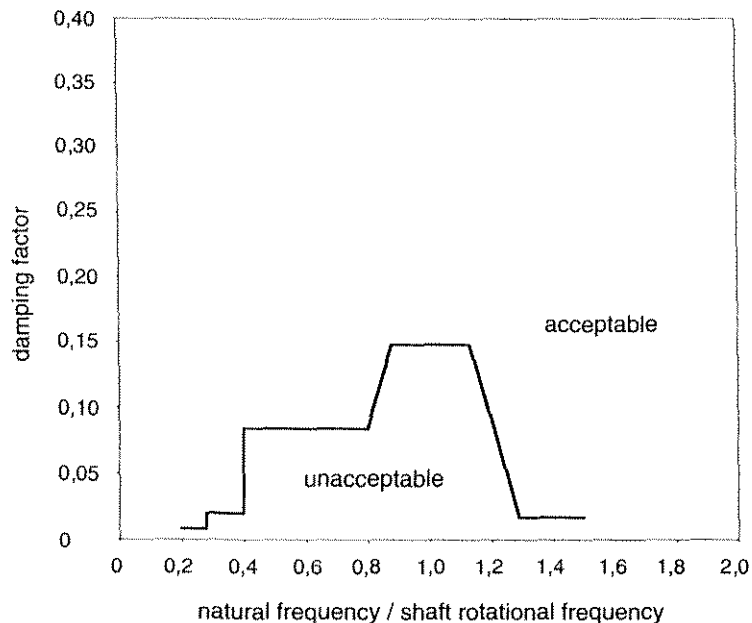


Fig. H.3.3 Damping factor versus frequency ratio –API 610/B

It must be pointed out that the impeller labyrinth and also the piston of a multi-stage pump have a dominant influence on the rotor natural frequencies, damping ratio, stability threshold, and leakage losses, with consequences for pump efficiency and axial thrust. Great attention should be given to the clearance dimen-

sions in the annular seals, in order to obtain the maximum required availability of the pump. The following are measures for improving damping properties and increasing rotor stability:

- introduction of swirl brakes at the entrance to the annular seals and piston (see Fig. H.3.4),

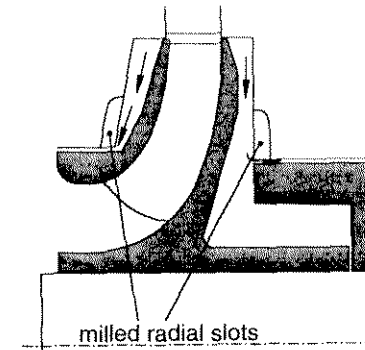


Fig. H.3.4 Swirl brakes at the entrance to an annular seal and piston

- execution of smaller radial clearances in the annular seals combined with longer seals,
- introduction of cellular-form annular seal and piston casing surfaces (see Fig. H.3.5),

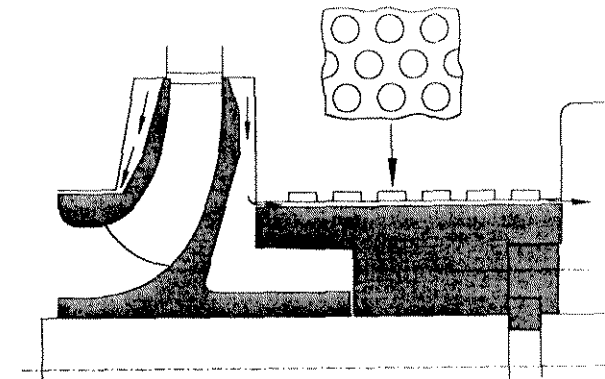


Fig. H.3.5 Cellular-form piston casing

- introduction of very tight casting tolerances for the impellers, in order to reduce the hydraulic unbalance (for head per stage over 500 m),
- carrying-out of a pump rotordynamic analysis at the design stage, taking into consideration all the dynamic influences of the journal bearings and the interaction between the impeller and diffuser, as well as the influences of the annular seals.

## H.4 Measuring bearing and shaft vibration

### H.4.1 General

In order to ensure the safe operation of pumps and their auxiliary components, the vibration in the shaft and bearing supports has to be within the range of the required limits. If the vibration increases with operating time, this is an indication of possible mechanical and/or hydraulic problems in the pump. Measurement of the shaft vibration in multi-stage pumps with a high power concentration gives a clear indication of the wear in the annular seals as well as in the piston.

Vibration problems are in most cases the source of operational difficulties in centrifugal pumps, and therefore the diagnostic of the vibration has great practical significance. The following vibration measurements are the most significant for a diagnostic:

- Vibration measurement with the help of acceleration transducers fitted directly to the bearing casing. This method can be considered only as an indirect indication of the shaft vibration,
- Direct measurement of the shaft vibration with the help of two non-contacting transducers, installed on both ends of a multistage pump,
- Impact test in order to determine the structural natural frequencies. This measurement is necessary when the danger exists of resonance in different pump station elements (piping, baseplate, etc.).

To ensure the safe and reliable operation of the pump and adjacent plant components, the vibration in the shaft or bearing casing must be kept within certain limits. Usually these limiting values are obtained without difficulty by ensuring the good mechanical condition of the pump and drivers, good inlet flow conditions to the pump, and an acceptable pump operating mode. If the vibration increases, especially with operating time, this can indicate some mechanical or hydraulic problems within the pump itself, and is a very valuable indication of the state of wear in the rotating parts.

### H.4.2 Measurement of vibration

**Measurement on non-rotating pump parts:** For all pumps built with anti-friction bearings, and also pumps with hydrodynamic bearings with a smaller power input, the vibration in the bearing support is measured in order to judge the running behaviour. The vibration consists of many vibration velocities at different frequencies. To evaluate the pump vibration behaviour, a frequency analysis of the vibration spectrum is very helpful.

In order to define pump vibration behaviour, the measuring instruments (accelero-

meters) have to be fitted to the bearing housing in three perpendicular directions (see Fig. H.4.1). Particular attention should be given to ensuring that the vibration transducer is correctly mounted. Vibration can be expressed as vibration displacement, vibration velocity or vibration acceleration. Detailed recommendations about measuring instruments, measuring positions and evaluation of results can be found in the relevant standards, listed in item H.4.3.

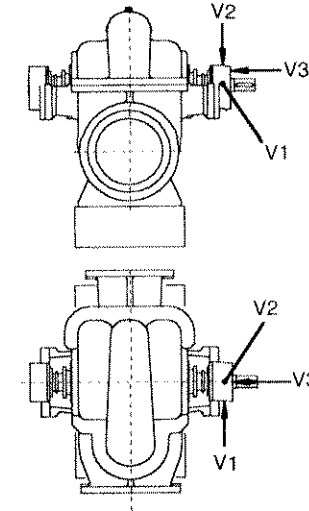


Fig. H.4.1 Position of accelerometers on the bearing housing of a double entry pump

**Measurement on rotating shafts:** In centrifugal pumps with a larger input and higher power concentration, equipped with hydrodynamic bearings, it is nowadays common practice to determine the shaft vibration. Such measurement shows the relative movement between the shaft and the bearing housing. The position of the two transducers, usually fitted at 90° to each other (see Fig. H.4.2), has to be as near as possible to the journal bearings. Such a position makes it possible to detect the orbit of the shaft movement.

Vibration measurement makes it possible to judge directly the dynamic behaviour of the rotor. The result of the measurement is shaft orbit, as shown schematically in Fig. H.4.3. The severity of the vibration is usually expressed as shaft vibratory peak-to-peak displacement  $S_{(p-p) \max}$ . For assessment purposes a distinction must be drawn between the measured values of individual transducer displacement ( $S_{A(p-p)}$ ,  $S_{B(p-p)}$ ) and of shaft orbit ( $S_{(p-p) \max}$ ). The magnitude of the  $S_{(p-p) \max}$  cannot be calculated from the values  $S_{A(p-p)}$  and  $S_{B(p-p)}$ . Detailed recommendations about measuring instruments, signal processing and the evaluation of results can be found in the relevant standards, listed in item H.4.3.

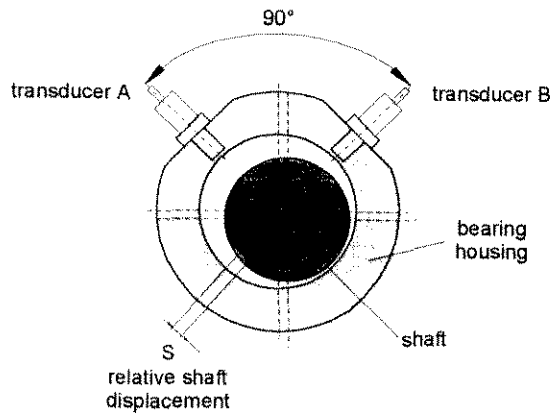
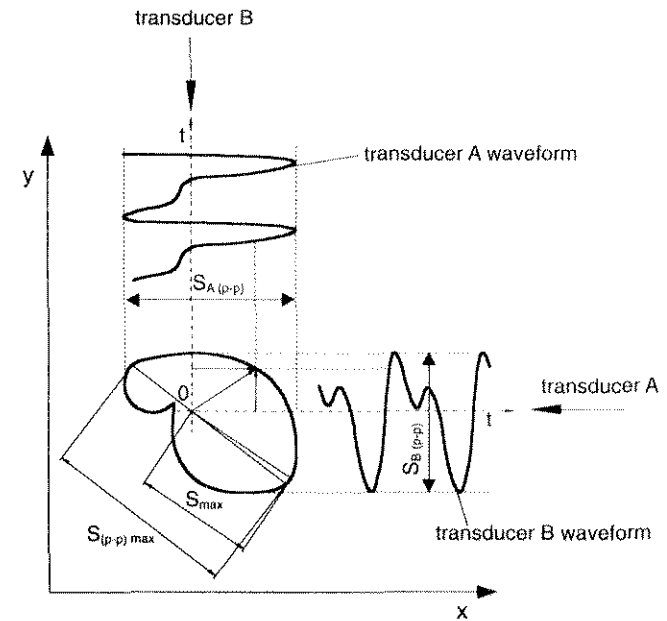


Fig. H.4.2 Positioning of transducers for shaft vibration measurements

#### H.4.3. Standards related to vibration

The following is a list of standards relating to mechanical vibration in rotating machinery and particularly in centrifugal pumps.

- ISO 10816 – Mechanical vibration; evaluation of machine vibration by measurements on non-rotating parts
- ISO 7919 – Mechanical vibration of non-reciprocating machines; measurements on rotating shafts and evaluation criteria
- ISO 9905 – Technical specifications for centrifugal pumps, Class I
- ISO 5199 – Technical specifications for centrifugal pumps, Class II
- ISO 9908 – Technical specifications for centrifugal pumps, Class III
- API 610/8 – Centrifugal Pumps for Petroleum, Heavy-duty Chemical and Gas Industry Services
- ANSI/HI 1.1-1.5 – Centrifugal pumps



- $S_{A(p-p)}, S_{B(p-p)}$  peak-to-peak displacement on transducer A and B
- $S_{max}$  maximum value of shaft displacement from time-integrated mean position 0
- $S_{(p-p) max}$  maximum value of peak-to-peak displacement

Fig. H.4.3 Schematic representation of shaft displacement measuring results

#### H.4.4. Vibration limits

For the vibration limits of centrifugal pumps, several different recommendations exist which are given and explained in the standards listed under item H.4.3. The values presented below are not the only ones valid for pumps, but they are the most frequently used.

**Bearing housing vibration:** Standard ISO 10816 defines the vibration limits usual for rotating machines, but these values are also frequently applied to pumps. In Table H.4.1 the limiting values of vibration velocity are shown for different machine groups (classes) and for typical evaluation zones.

Evaluation zones *	vibration velocity limits r.m.s. (mm/s) **	Class I	Class II	Class III	Class IV
		A	good	0.7	1.1
B	usable	1.8	2.8	4.5	7.1
C	still admissible	4.5	7.1	11.2	18
D	inadmissible	> 4.5	> 7.1	> 11.2	> 18

\*) detailed description of evaluation zones is in ISO 10816-1

\*\*) r.m.s. means "root-mean-square" value, more details in ISO 10816-1

- Class I – small machine sets with power input up to 15 kW
- Class II – medium size units with power input up to 300 kW
- Class III – large units on rigid foundations
- Class IV – large units on flexible supported foundations

Table H.4.1 Limiting values of bearing housing vibration velocity – ISO 10816-1

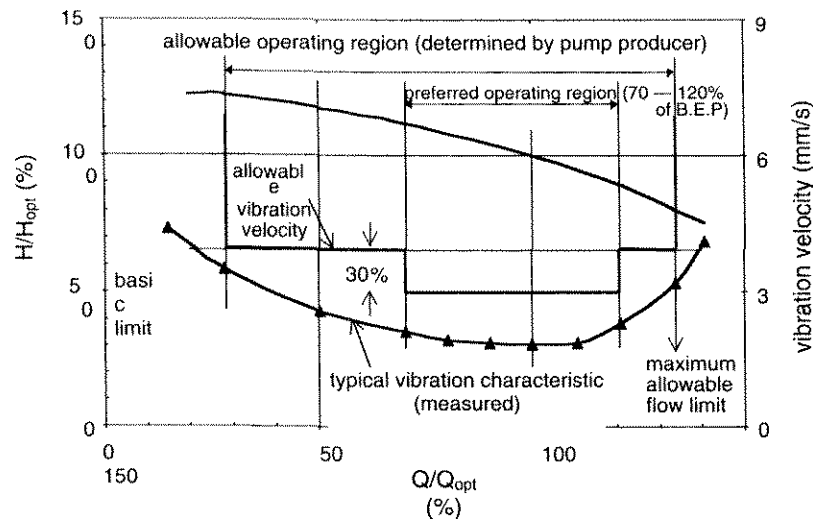


Fig. H.4.4 Pump operating ranges and vibration velocity limits for overhung and between-bearing pumps – API 610/8

Standard API 610/8 defines different limiting values for horizontal shaft as well as for vertical suspended pumps, and two limiting values for vibration velocity with regard to the pump flow operating regime. The lower limiting value of vibration

velocity is valid for the preferred operating region (0,7 – 1,2 Q/Q<sub>opt</sub>). For the allowable operating regime, which is defined by the pump manufacturer, the higher limiting value for vibration velocity is valid (see Fig. H.4.4 and Table H.4.2).

vibration velocity limits r.m.s. (mm/s)	preferred operating regione	allowable operating region
overhung and between-bearing pumps	3.0	3.9
vertically suspended pumps	5.0	6.5

Table H.4.2 Limiting values for bearing housing vibration velocity - API 610/8

**Shaft vibration:** Standard ISO 7919 defines the limits of vibratory shaft displacement for different machine groups. The values for coupled industrial machines (including centrifugal pumps) are shown in Fig. H.4.5. The limiting values of maximum relative shaft displacement are for typical quality zones given as a function of the pump running speed.

Standard API 610/8 defines the different limiting values for horizontal shaft as well as for vertical shaft pumps. Beside this, two different limits are defined with regard to pump flow operating regimes. Within the preferred operating region (0,7 – 1,2 Q/Q<sub>opt</sub>) the limiting values are lower than in the allowable operating region (see Table H.4.3).

limiting values of relative shaft displacement peak-to-peak	preferred operating region	allowable operating region
overhung and between bearing pumps	$\left(\frac{5.2 \cdot 10^6}{N}\right)^{0.5}$	$1.3 \cdot \left(\frac{5.2 \cdot 10^6}{N}\right)^{0.5}$
vertically suspended pumps	$\left(\frac{6.5 \cdot 10^6}{N}\right)^{0.5}$	$1.3 \cdot \left(\frac{6.5 \cdot 10^6}{N}\right)^{0.5}$

N – pump rotational speed (1/min)

Table H.4.3 Limiting values for relative shaft displacement - API 610/8

The limiting values for vibration according to Standard API 610/8 (pumps for petroleum, heavy-duty chemical and gas industry services) are more severe than in Standard ISO 7919-3. According to practical experience in operating centrifugal pumps, the limiting values from Standard ISO 7919-3 are satisfactory for general pump applications.

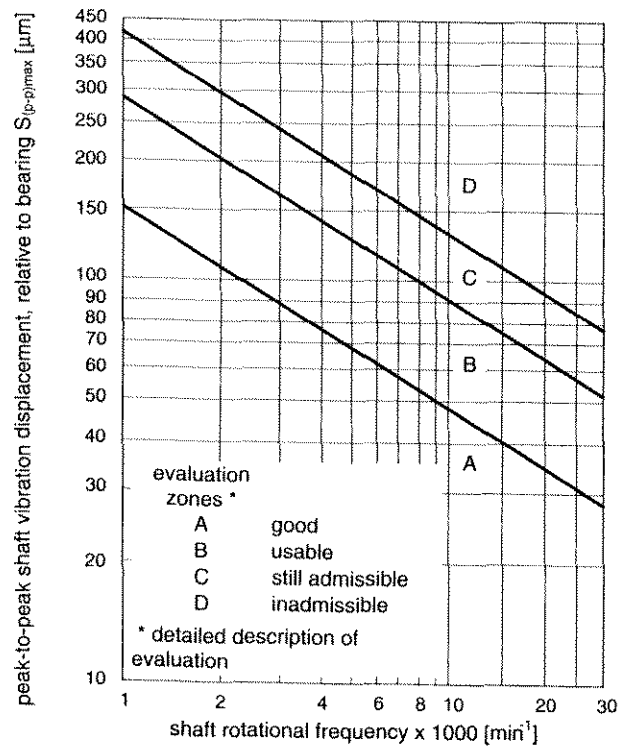


Fig. H.4.5 Limiting values of relative shaft displacement in centrifugal pumps – ISO 7919-3

For centrifugal pumps with hydrodynamic bearings the recommendations of shaft displacement relative to bearing gap, shown in Table H.4.4, are simple and helpful. The limiting values given are generally valid for centrifugal pumps running in steady-state conditions, within the allowable operating region. The values given are not applicable for varying operating regimes.

$S_{(p-p)max} / (D - d)$	assessment
$\leq 0.35$	limiting value for "good" behaviour in allowable pump operating region
0.7	value for alarm setting
0.9	value for shut-down setting

- $S_{(p-p)max}$  - maximum value of peak-to-peak shaft displacement
- D - inside diameter of hydrodynamic bearing
- d - diameter of the shaft or shaft sleeve

Table H.4.4 Recommended values for the assessment of shaft vibration in centrifugal pumps with hydrodynamic bearings

# I. MONITORING, DIAGNOSTIC AND EARLY FAILURE DETECTION

## I.1 General

The requirements for high reliability in pumps can only be reached when the status and condition of the pump and its vital elements are continuously monitored. This is especially important for pumps operating in power generation systems, and the oil, chemical and process industries. When a pump is monitored, maintenance can be planned and the risk of unplanned stops with high downtime costs (loss of production) can be very much reduced. A comparison of approaches with or without pump monitoring, and its effect on maintenance planning, different cost parameters and pump availability is shown schematically in Fig. I.1.1.

	maintenance philosophy	monitoring costs	maintenance costs	risk of unplanned breakdown	availability
without monitoring	operate until failure	none	medium	high	low
	calendar-driven	none	high	medium	medium
with monitoring	maintenance condition-maintenance	high	low	low	very high

Fig. I.1.1 Monitoring possibilities and their influence on pump cost parameters and availability

By using actual measured values and their deviation from the predicted operational data, the pump operator is in a position to avoid abnormal pump operation and consequently unexpected breakdowns during operation. When using more sophisticated monitoring methods, the measuring signals are fed into a computer diagnostic system, which is supported by statistical data and past experience (the chronological development of the measured values prior to breakdown). An integrated monitoring and diagnostic system can be used as a system for the early detection of failure, in conjunction with a control system for alarms and emergency pump shutdown.

The additional costs for a monitoring and diagnostic system are in most cases covered in a short time due to the reduced downtime costs (see also chapter O).

## I.2 Monitoring of large and high-speed pumps

In large pump installations like boiler feed pumps, water transport pumps, and injection pumps, where the efficiency and availability demands are very high, a permanently installed monitoring system is normally used. A typical disposition of sensors is shown in Fig. I.2.1.

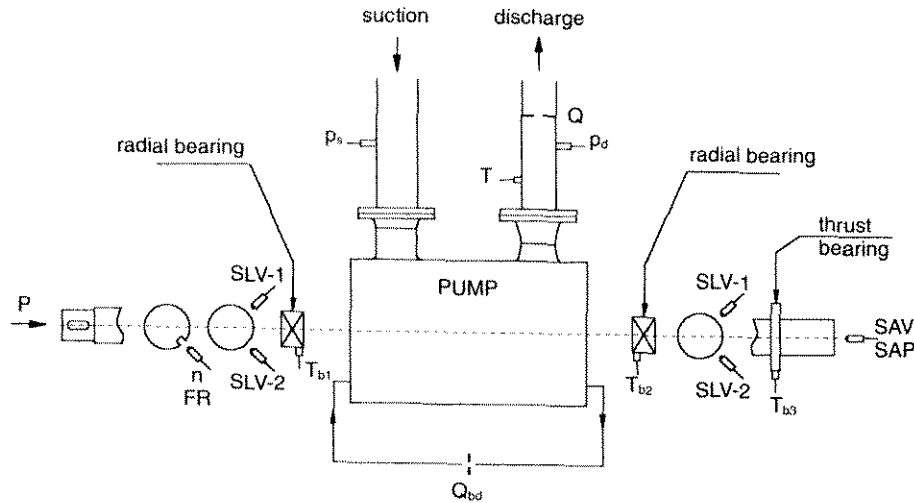


Fig. I.2.1 Typical disposition of sensors for large and high-speed pumps

Monitoring sensors are divided into two groups:

Sensors which define the operating parameters of the system as well as the pump operating point (performance monitoring):

- suction and discharge pressures:  $p_s$ ,  $p_d$
- pump flow rate:  $Q$
- fluid temperature:  $T$
- speed of rotation:  $n$
- power input:  $P$
- flow rate in balancing device (piston leakage):  $Q_{bd}$

Sensors which detect pump shaft vibration and bearing conditions (condition monitoring):

- shaft lateral vibration: SLV
- phase reference: FR
- shaft axial vibration and shaft axial position: SAV, SAP
- bearing temperatures:  $T_{b1}$ ,  $T_{b2}$ ,  $T_{b3}$

The analysis of the measuring values is important in order to detect changes in the system parameters, and consequently the position of the pump operating point, possible dangers of cavitation, reduced pump efficiency, and the condition of internal pump elements (wear rings and piston radial clearances), etc. The lateral shaft vibration system consists of two sensors SLV, mounted radially (with an angle of  $90^\circ$  between them) close to the radial bearings, and a phase reference probe FR. With such a system it is possible to detect the lateral shaft vibration and also the shaft orbit. Actual data can be compared with values from different standards (see chapter H). The observed trends in the measured parameters are then used for planning maintenance.

## I.3 Monitoring of process pumps

In process systems different operating problems occur to those in power generation or oil/water transport systems. On the other hand process pumps are smaller and have a lower power input, and temporary abnormal operating conditions do not cause the destruction of pump elements; however, they can reduce considerably the pump lifetime, and have a negative influence on the process itself. Typical abnormal operating conditions (failures) in process pumps, and their possible detection, are shown in Table I.3.1.

Each process has its own specific conditions which can cause abnormal pump operation, and these have to be detected. A process pump is rarely equipped with all the sensors shown in Fig. I.3.1, but only with those which detect possible failures in the specific process. In combination with the appropriate diagnostic system, three or four sensors are sometimes enough to establish an effective failure detection system.

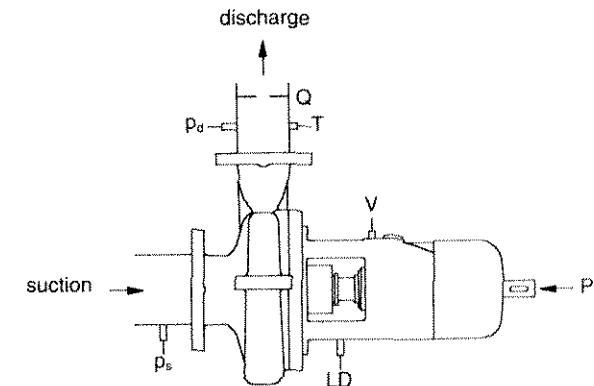


Fig. I.3.1 Typical disposition of sensors for process pumps



failures	possible detection, sensor designation (see Fig. I.3.1)
dry running	<ul style="list-style-type: none"> <li>• flow rate interruption: Q</li> <li>• discharge pressure collapse: <math>p_d</math></li> <li>• reduction of power consumption: P</li> <li>• increased fluid temperature: T</li> </ul>
impeller channel blockage	<ul style="list-style-type: none"> <li>• increased vibration: V</li> <li>• discharge pressure and/or flow rate reduction: <math>p_d</math>, Q</li> </ul>
increased gas content in pumping liquid	<ul style="list-style-type: none"> <li>• discharge pressure and/or flow rate reduction: <math>p_d</math>, Q</li> <li>• reduction of power consumption: P</li> </ul>
cavitation	<ul style="list-style-type: none"> <li>• suction pressure reduction: <math>p_s</math></li> <li>• increased vibration: V</li> <li>• discharge pressure and/or flow rate reduction: <math>p_d</math>, Q</li> </ul>
bearing damage	<ul style="list-style-type: none"> <li>• increased vibration: V</li> </ul>
impeller damage	<ul style="list-style-type: none"> <li>• increased vibration: V</li> </ul>
(abrasion, corrosion)	<ul style="list-style-type: none"> <li>• discharge pressure and/or flow rate reduction: <math>p_d</math>, Q</li> </ul>
shaft seal damage	<ul style="list-style-type: none"> <li>• leakage detection: LD</li> </ul>

Table I.3.1 Typical failures in process pumps and their possible detection

From the pump-operator point of view, as few monitoring sensors as possible should be installed. Lately extensive efforts have been directed towards the development of combined monitoring sensors, in order to simplify failure detection in a pump and to reduce the costs for installed sensors and monitoring systems. Pumps with integrated monitoring and failure detection systems are called intelligent pumps.

### I.4 Diagnostic based on vibration analysis

The measured values of pump casing or shaft vibration can be effectively used for a machine diagnostic. Based on the analysis of the measuring signals obtained by the vibration monitoring system, the causes for a changed pump operating behaviour can be identified. The vibration frequency spectrum is required for such an analysis (see example on Fig. I.4.1). An assessment of the most probable causes of changed pump vibration is shown in Table I.4.1.

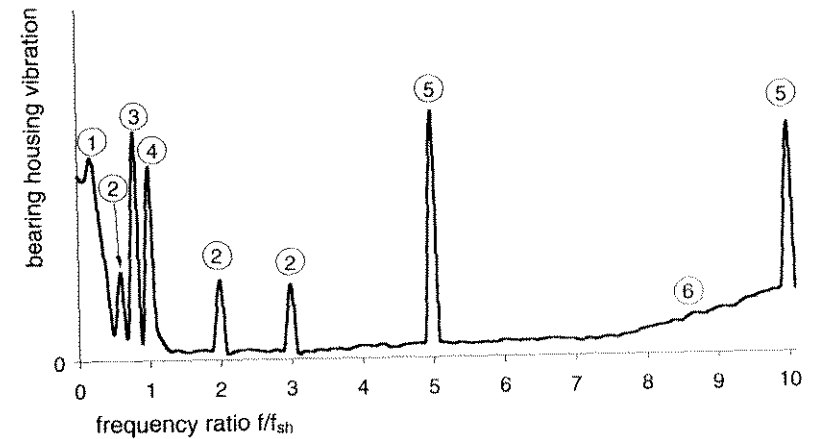


Fig. I.4.1 Example of a pump vibration frequency spectrum indicating various vibration phenomena

designat. from Fig. I.4.1	identification	most probable causes
1	peak at frequency $\sim 0,2 \cdot f_{sh}$	<ul style="list-style-type: none"> <li>• unsteady flow (recirculation) at part-load,</li> <li>• rotating stall phenomena</li> </ul>
2	peaks at frequencies $0,5 \cdot f_{sh}, 2 \cdot f_{sh}, (3 \cdot f_{sh})$	<ul style="list-style-type: none"> <li>• shaft misalignment,</li> <li>• loose coupling or bearing,</li> <li>• motor vibration transmitted to the pump</li> </ul>
3	peak at frequency $(0,5-0,9) \cdot f_{sh}$	<ul style="list-style-type: none"> <li>• rotor instability due to large clearances in the annular seals,</li> <li>• low loaded or worn journal bearing</li> </ul>
4	peak at shaft rotating frequency $f_{sh}$ (synchronous vibration)	<ul style="list-style-type: none"> <li>• residual unbalance (hydraulic or mechanical),</li> <li>• bent shaft,</li> <li>• lateral critical speed,</li> <li>• bearing housing or pump casing structural resonance</li> </ul>
5	peaks at blade passing frequencies $Z_2 \cdot f_{sh}, 2 \cdot Z_2 \cdot f_{sh}, \dots$ ( $Z_2 = 5$ )	<ul style="list-style-type: none"> <li>• unfavourable impeller/diffuser blade numbers,</li> <li>• insufficient radial gap between impeller and diffuser blades (spiral casing tongue)</li> </ul>
6	broadband vibration at high frequencies	<ul style="list-style-type: none"> <li>• cavitation in the pump elements</li> </ul>

Table I.4.1 Description of the most probable causes for vibration in pumps

## J. PUMP INTAKE AND SUCTION PIPING DESIGN

### J.1. Open sump intakes

Intake structures should be designed to ensure that pumps achieve their optimal hydraulic performance. The main objective when designing suction sumps is to generate a smooth water flow and to avoid as much as possible an uneven flow and stagnant water zones. A good sump design avoids adverse phenomena like swirling flows, submerged vortexes or air-entraining vortexes. Velocity distribution at the impeller entry must be as uniform as possible; if not, local flow separation may occur, resulting in a disturbed hydraulic and mechanical behaviour in the pump.

A swirling flow may produce the following effects:

- swirl rotation in the same direction as impeller rotation lowers the pump head,
- swirl rotation in the opposite direction to the impeller rotation increases the pump head, and a danger of overload exists,
- when the swirl intensity is not stable, a fluctuation in pump flow rate and head should be expected.

An air-entraining vortex can cause the following adverse effects:

- pump flow rate and head decrease,
- excitation of vibration and noise caused by hydraulically unbalanced impeller operation,
- increased radial force on the impeller,
- increased risk of cavitation erosion on the impeller blades,
- wear in submerged shaft bearings.

The negative impact of swirling flow and vortexes on pump performance depends on the pump specific speed and size, as well as other specific design features of the pump. In general, large pumps and axial-flow pumps (high specific speed) are more sensitive than small pumps or radial-flow pumps (low specific speed).

In this chapter several guidelines regarding minimum water level in the sump (or pump submergence) are stated. It has to be taken into account that these water levels are recommended based on trouble-free flow conditions in the pump sump, and have no connection with the minimum water level defined on the basis of pump cavitation requirements. The minimum water level based on  $NPSH_{av}$  must be defined separately (see chapter C.3). The higher water level of the two above-mentioned values has to be maintained during pump operation.

#### J.1.1. Individual installation

The basic recommended layout for rectangular intake and wet pit pumps is shown in Fig. J.1.1.a. The pump is positioned near the rear wall of the intake channel. Additionally a wall/floor splitter is installed to prevent swirling flow and vortex formation. Corner fillets are introduced in order to reduce flow separation and possible vortex development in corner areas. The recommended installation dimensions with pump submergence can be taken from diagram Fig. J.1.4.

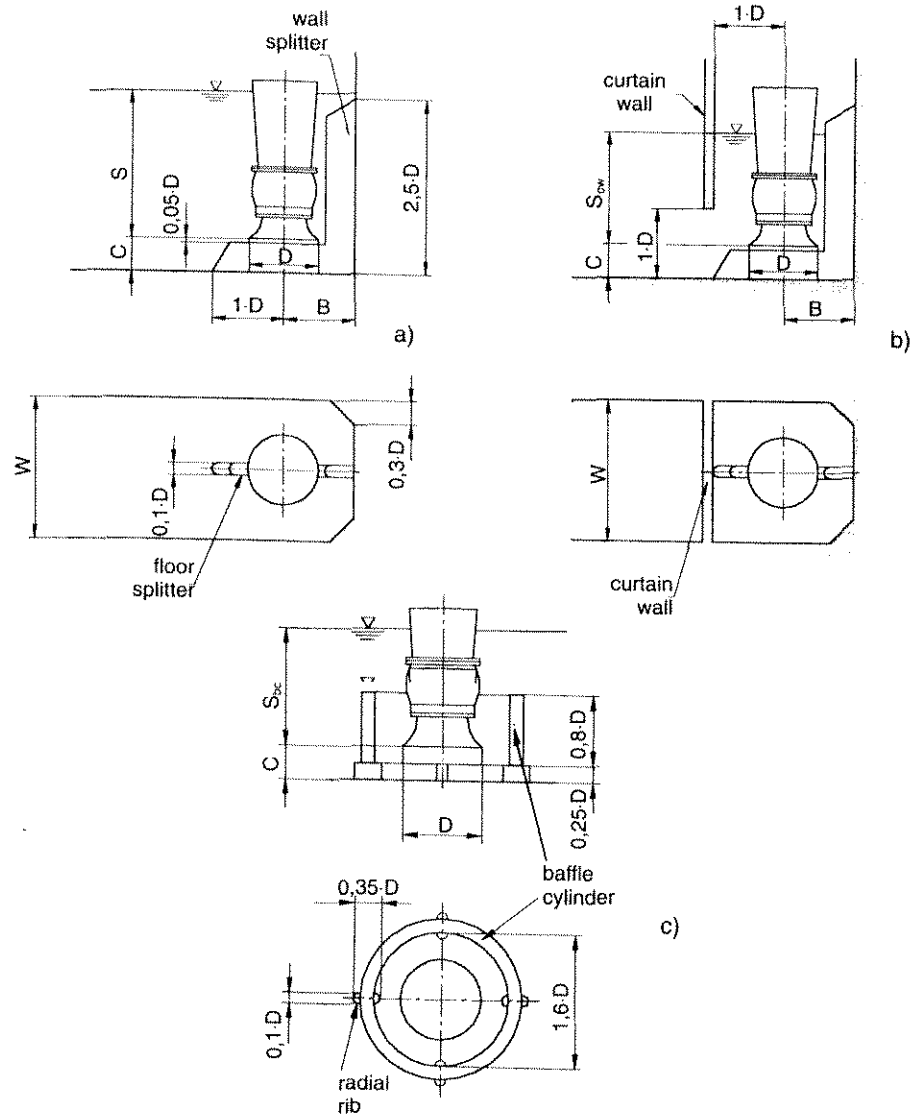
A solution with an additional curtain wall is recommended when pump submergence is not sufficient (Fig. J.1.1.b). Curtain walls control the flow near the water surface and prevent the formation of air-entraining vortexes. With this modification the required minimum pump submergence  $S_{cw}$  can be lower than with the solution shown in Fig. J.1.1.a.

For large intake sumps when the pump cannot be positioned near a rear wall, a solution with a baffle cylinder is often applied. A baffle cylinder with short radial ribs ensures symmetrical inflow conditions to the pump impeller, and avoids possible vortex formation (Fig. J.1.1.c). When applying this solution the required minimum submergence  $S_{bc}$  can be lower than with the solution shown in Fig. J.1.1.a., but a certain increase of inlet hydraulic losses can be expected.

#### J.1.2. Multiple parallel installation

If multiple pumps are installed in a single intake structure (see Fig. J.1.2), dividing walls placed between the pumps result in more favourable flow conditions. Dividing walls are obligatory when installing pumps with flow rates higher than  $0,3 \text{ m}^3/\text{s}$ . When installing a through-flow travelling screen or trash rack the minimum recommended distance to the pump has to be considered. Care must be taken to ensure that clogging of the screen does not generate a large non-uniformity in the pump approach flow. The approach flow conditions can be disturbed when the wall and floor inclination angles are not within the values recommended in Fig. J.1.2. The basic recommendations for calculating the dimensions of a rectangular intake in a multiple parallel pump installation are the same as for an individual pump installation, and are shown in Fig. J.1.4. Additionally, a general design recommendation for suction bell diameter  $D$  can be taken into consideration:  $D \approx 1,4 \cdot D_1$  when  $D_1$  is the impeller eye diameter.

The design of sump intakes for vertical wet pit pumps is in many cases a compromise between the structural constraints or possibilities, and the hydraulic requirements. To avoid any possible problem during the operation of the pumping station it is worthwhile, as early as at the design stage, following as much as possible the recommendations for sump intake design. A comparison of some recommended and non-recommended designs is shown in Fig. J.1.3.



- a) design with wall/floor splitter
- b) design with additional curtain wall
- c) design with baffle cylinder

Fig. J.1.1 Design possibilities for an individual pump installation

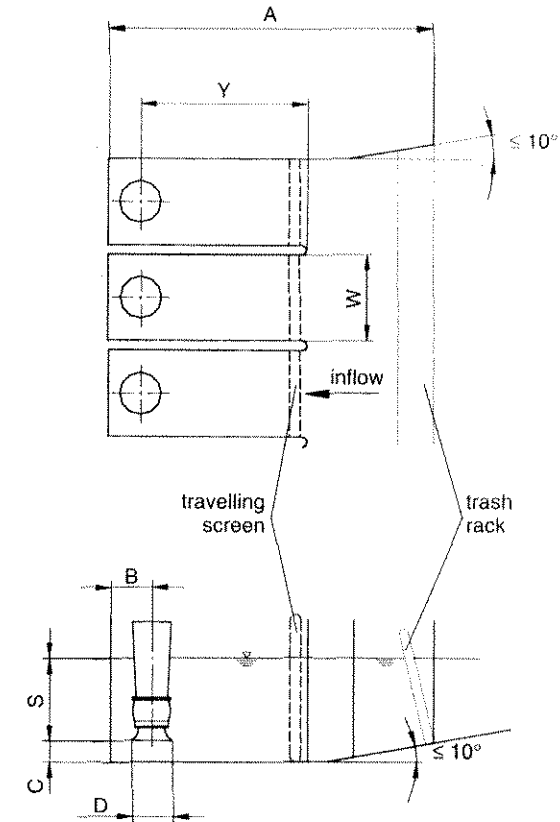
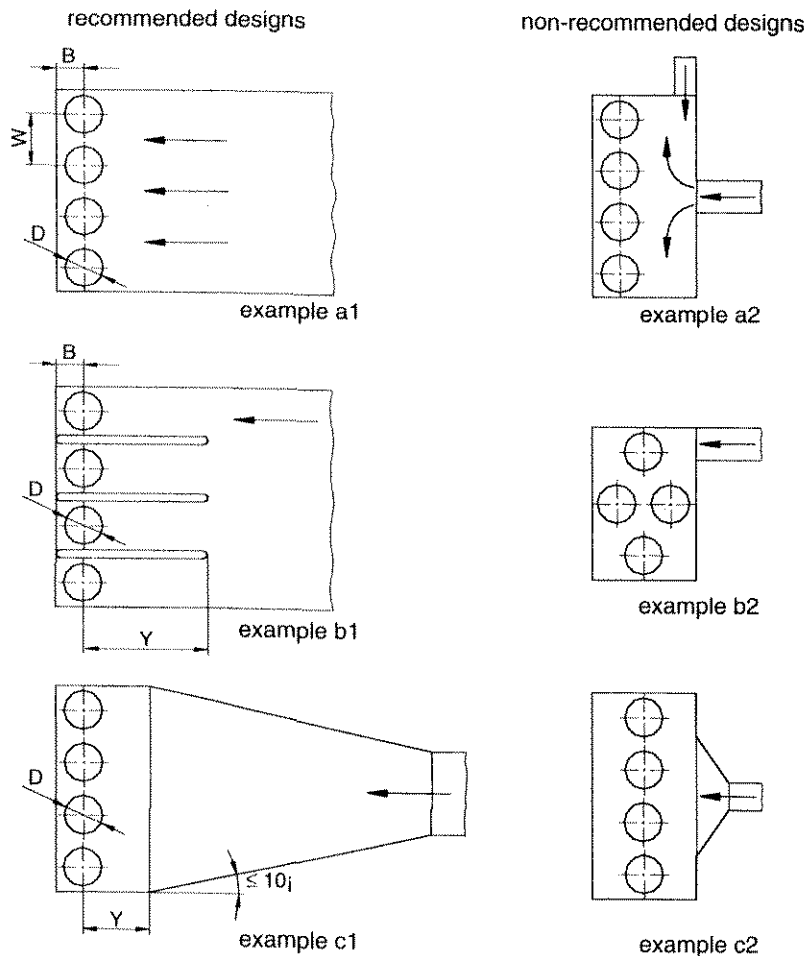


Fig. J.1.2 Parallel pump installation with a rectangular intake channel

An abrupt change in the size of the inlet pipe or the inflow to the sump from one side only is not recommended (Fig. J.1.3.a2). A recommended solution which ensures a straight in-line flow with low velocity to all pumps is shown in Fig. J.1.3.a1.

The placing of a number of pumps around the sides of a sump is not recommended (Fig. J.1.3.b2). Separation of the pumps by walls is obligatory when the pump flow rate is higher than 0,3 m<sup>3</sup>/s (Fig. J.1.3.b1).

Abrupt changes in flow channel size (width) are not desirable (Fig. J.1.3.c2). The wall inclination angle  $\alpha$  should be as small as possible, preferably not more than 10 degrees (Fig. J.1.3.c1).



**J.1.3 Multiple pump installation - recommended and non-recommended designs**

In diagram Fig. J.1.4 guidelines are given for the basic dimensions of rectangular intake sumps, and are valid both for individual pump and multiple parallel pump installations. The values in the diagram refer to an average of different pump types, and cover the entire range of specific speeds and are based on the rated pump flow rates. They are not absolute, but typical values, and are subject to variation.

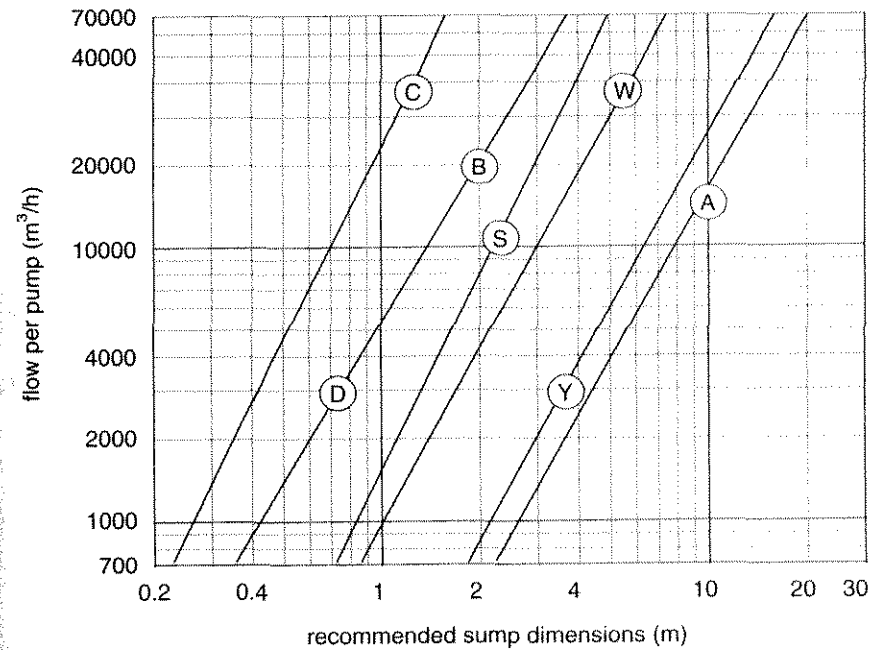


Fig. J.1.4 Recommended dimensions for rectangular intake

To Fig. J.1.4.:

- A – distance from the trash rack or intake structure entrance to the rear wall (minimum)
- B – distance from the rear wall to the pump axis (maximum)
- C – distance between the floor and the suction bell (average)
- D – suction bell diameter (average)
- S – submergence depth (minimum)
- W – pump bay channel width (minimum)
- Y – distance from the pump axis to the bay entry or screen (minimum)

**J.2. Can-type intakes**

Can-type intakes are normally provided for vertical turbine pumps. It is necessary to design the can intake so that the inflow velocity profile at the suction bell is uniform. An asymmetrical velocity profile may result in hydraulic disturbances, such as swirling, submerged vortexes and cavitation, which may result in performance degradation and accelerated pump wear. Care must be taken regarding the design of components that can affect the pump hydraulic performance. These include suction barrels, turning elbows and vortex suppressors.

### J.2.1. Open bottom can intakes

Recommended installation possibilities for open bottom can intakes are shown in Fig. J.2.1. These recommendations are to be applied when the pump flow rate is lower than 0,3 m<sup>3</sup>/s. In the case of higher flow rates a model test is required.

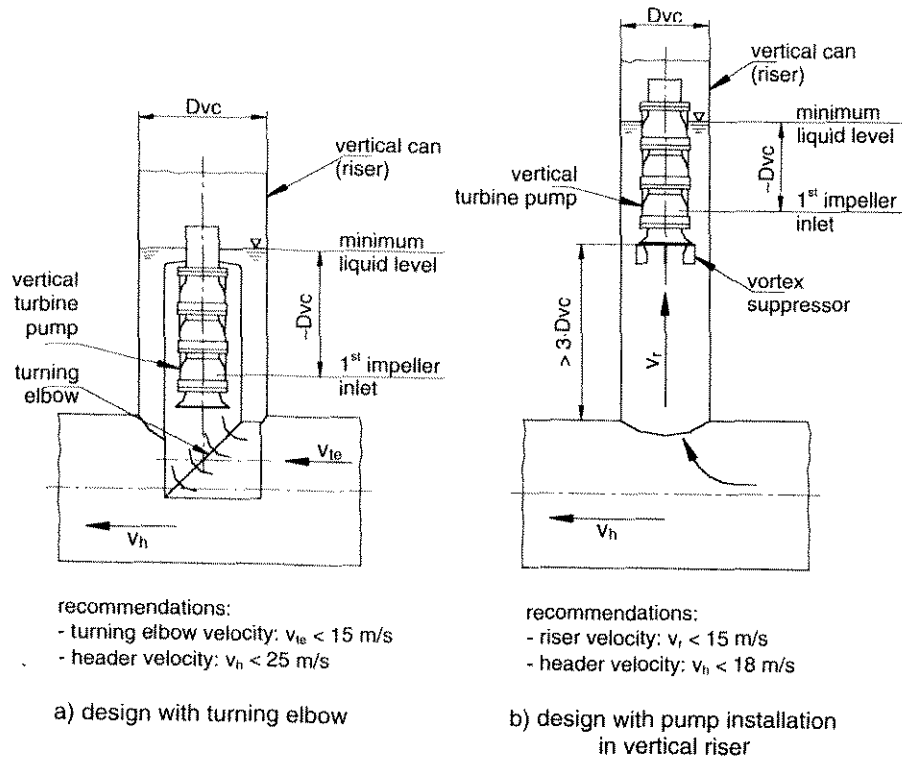


Fig. J.2.1 Open bottom can intakes

The configuration shown in Fig. J.2.1.a is particularly effective when liquid elevation (pump submergence) is limited. A flow through a horizontal header with a velocity  $v_h$  of up to 2,5 m/s can be effectively directed into a vertical turbine pump by the use of a turning elbow. To ensure a more uniform velocity distribution at the pump suction bell, the installation of turning vanes in the elbow is recommended. The inlet diameter of the turning elbow should be sized to limit the inflow velocity  $v_{te}$  to 1,5 m/s. Caution is necessary when using this intake configuration in liquids containing trash or incrustations (such as barnacles) that can stick to the turning vanes.

In cases with lower header velocities and higher liquid elevations, the simplified solution shown in Fig. J.2.1.b is effective as well. A vortex suppressor that is an integral part of the pump is necessary to break up abnormal flow patterns ahead of the pump suction bell. The installation must allow the pump to hang centred in the vertical riser pipe. For this installation the header velocity  $v_h$  is limited to 1,8 m/s and the velocity in the riser pipe  $v_r$  is limited to 1,5 m/s.

The minimum water level shown in the Fig. J.2.1 is considered as the minimum level in steady-state pump operating conditions. When the pump is started the minimum liquid level will reduce momentarily, until the steady-state condition is achieved. When sizing the pipes, it has to be taken into account that the draw-down of the liquid level below the recommended minimum level should be limited to a period of less than 3 seconds during pump start-up.

### J.2.2. Closed bottom can intakes

The most typical can pump configurations are closed bottom can intakes as shown in Fig. J.2.2. Care must be taken to ensure the centring of the pump to the can. This is important to avoid a rotational flow being generated with a non-uniform velocity distribution around the pump and in the suction bell. Flow-straightening vanes are required for pump flow rates higher than 0,2 m<sup>3</sup>/s. A pair of vanes should be centred in the inlet to the barrel, and extended on one side to above the normal liquid level and on the other side to the bottom of the barrel. A cross-rib should be provided under the pump suction bell.

Because of the limited volume of the can, surging of the liquid level within the can may be a problem when operating with a partially filled can. The intake piping must be large enough to limit draw-down below the recommended minimum liquid level to a period of less than 3 seconds during pump start-up.

### J.3. Wet pits for solid-bearing liquids

Special care must be taken when designing wet pits for solid-bearing liquids such as wastewater, industrial discharges, storm or canal drainage, combined wastewater, raw water supplies, etc. These liquids contain solids that may float or settle in the wet pit. When organic solids are accumulated in the pit and not removed, they may become septic, causing odours, increasing corrosion and releasing hazardous gases.

The main principle for wet pit design is to minimise the horizontal surfaces which are not under the influence of the pump suction. Thereby all solids are directed to a location where they may be removed by the pump. Vertical and steeply sloping walls should be provided for the transition from the upstream conduits or channels to the pump inlets.

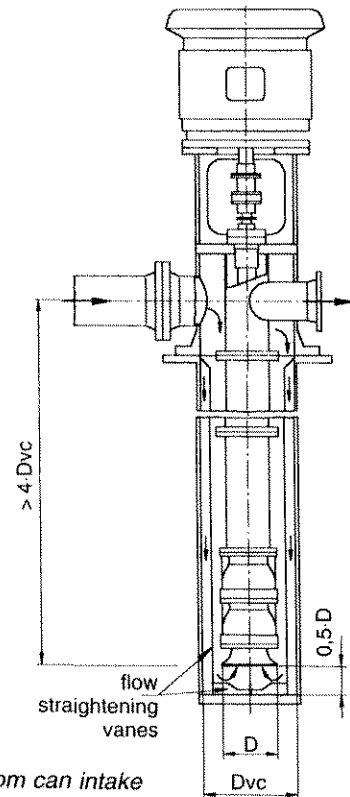


Fig. J.2.2 Closed bottom can intake

A recommended circular wet pit design with two submersible sewage pumps is shown in Fig. J.3.1. The bottom of the pit has sloping surfaces around the pumps, and the horizontal floor area is minimised as much as possible. Pumps are installed in the sump by means of a guide hoop. Sealing between the pump and the discharge bend is achieved by the pump weight. The use of accessories in the installation should be limited, due to the possibility of the collection or entrapment of solids. The minimum water level should be defined by the pump manufacturer, taking into consideration the formation of air-entraining vortices and the motor cooling requirements.

The installation of submersible sewage pumps in a confined wall wet pit is shown in Fig. J.3.2. These wet pit designs are frequently applied when pumps with axial inflow and outflow are used. Each pump is installed separately into a confined pocket to isolate it from possible flow disturbance. The horizontal surface area on the pit bottom, where solids can settle, is minimised. A cone under each suction bell and an anti-rotation wall splitter should be installed when the pump flow rate exceeds  $0,2 \text{ m}^3/\text{s}$ .

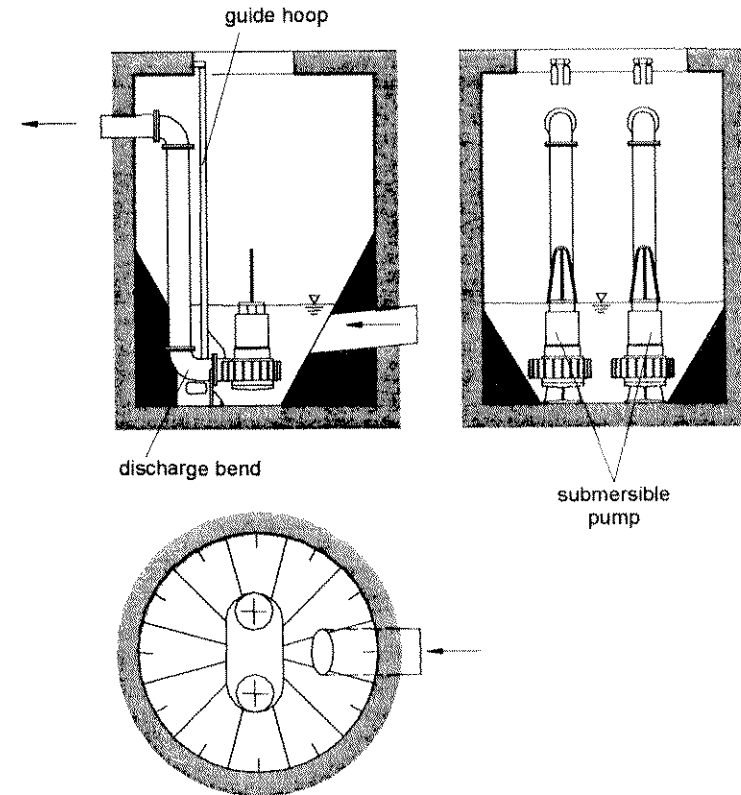


Fig. J.3.1 Circular wet pit with sloping walls

A regular cleaning procedure for removal of the solids from a wet pit is obligatory. This can be achieved by operating the pumps selectively, so as to lower the level in the wet pit until the pump loses priming. Both settled and floating solids are removed and pumped into the discharge pipe. Pumping under these severe conditions will cause noise, vibration and high loads on the impeller, and should be limited to brief periods. Pumps for such applications should be designed to withstand abrasion and corrosion, and also severe conditions during the pit cleaning procedure.

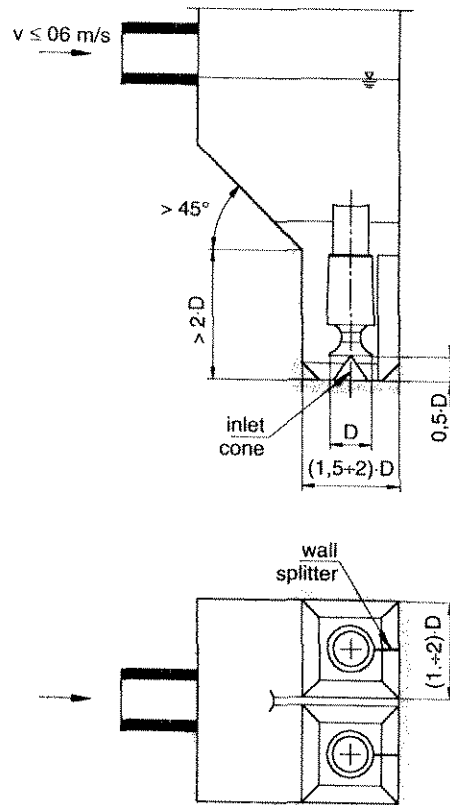


Fig. J.3.2 Wet pit with confined walls

### J.4. Pump suction piping

The proper design of suction piping is vital in order to ensure the uniformity of the flow delivered to the pump. A disturbed inflow causes deterioration in the pump performance and may shorten pump life because of vibration and cavitation. The suction piping should be designed so that it is simple, with gradual transitions if there is a change in pipe size. Transitions resulting in a flow deceleration near the pump entry should not be applied.

#### J.4.1. Common intakes for suction piping

The effects of disturbed flow conditions at the beginning of the suction piping (at the inlet bell) tend to diminish with distance. Short suction piping is less effective in reducing disturbances before the flow reaches the pump. Good flow conditions exist at the inlet bell if the velocity in the inlet bell  $v$  and submergence  $S$  are within recommended values. Common intake designs for suction piping with reference submergence data are shown in Fig. J.4.1. For dimensions  $B$ ,  $C$  and  $W$  the values from Fig. J.1.4 are recommended. The method of calculating the minimum recommended submergence  $S$  is:

$$S / D = 1,0 + 2,3 \cdot Fr_D$$

$$Fr_D = v / (g \cdot D)^{0,5}$$

$S$  – minimum recommended submergence

$D$  – inlet bell diameter

$Fr_D$  – Froude number at inlet bell

$v$  – fluid velocity in inlet bell

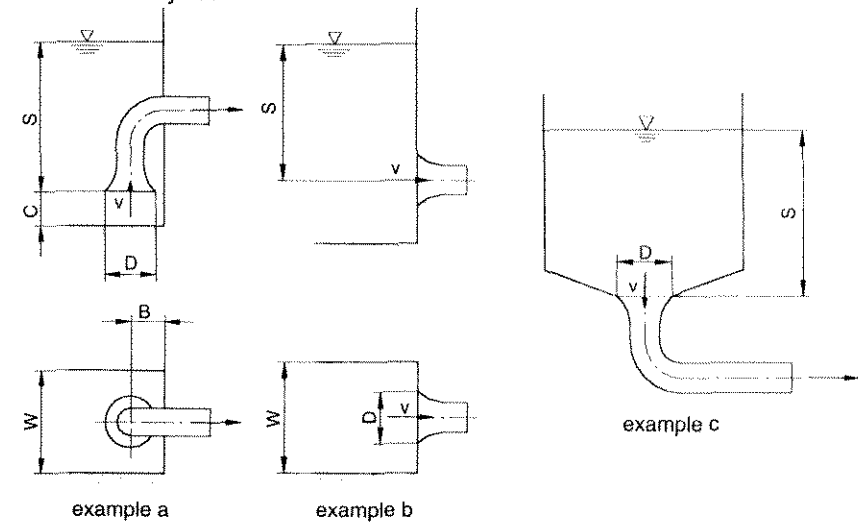


Fig. J.4.1 Common intakes for suction piping

pump flow range Q (l/s)	recommended inlet bell design velocity (m/s)	acceptable velocity range (m/s)
< 315	$v = 1,7$	$0,6 \leq v \leq 2,7$
$\geq 315$	$v = 1,7$	$0,9 \leq v \leq 2,4$
< 1260	$v = 1,7$	$1,2 \leq v \leq 2,1$
$\geq 1260$	$v = 1,7$	$1,2 \leq v \leq 2,1$

Table J.4.1 Recommended and acceptable velocities in the inlet bell

Recommended and acceptable velocities in the inlet bell for different flow rates are shown in Table J.4.1. The velocity in the suction piping should be constant, or increasing as the flow approaches the pump.

**J.4.2. Suction tank intakes with vortex breakers**

In the process installation, a suction pipe may be taken off the side or bottom of a process or suction tank. General rules, such as a symmetrical inflow without obstacles in the tank and rounded corners at the suction pipe entry, must be applied to produce a sound intake design. An adequate submergence, as recommended under item J.4.1, should be provided to avoid vortexing and possible air (or other tank gases) entering the suction pipe. The air or gases drawn in may collect in the piping and cause degradation in the pump performance. If the recommended submergence cannot be obtained, the installation of an anti-vortex device in the suction tank is required. Some common types of such devices are shown in Fig. J.4.2.

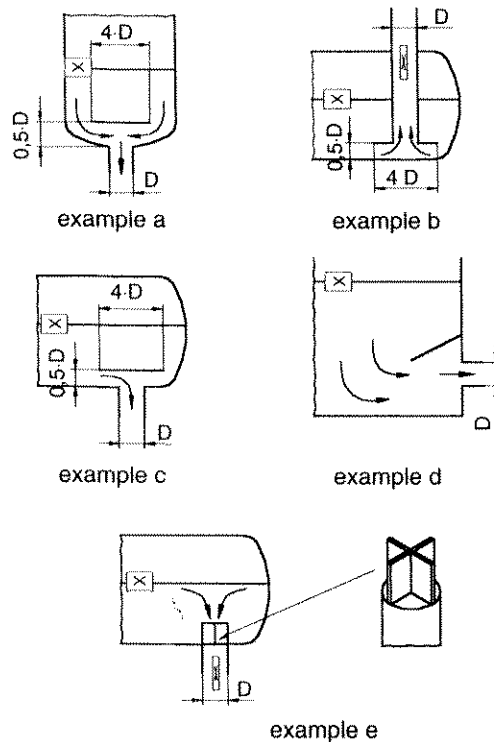


Fig. J.4.2 Anti-vortex devices for suction tanks

**J.4.3. Suction pipe configuration**

The general rule for suction pipe sizing is that the suction pipe velocity should not exceed the velocity in the suction nozzle. Pipe velocity may need to be reduced further to satisfy pump NPSH requirements, and to reduce suction pipe hydraulic losses. There should be no flow-disturbing fittings (such as partially open valves, tees, short radius elbows, etc.) closer than five suction pipe diameters from the pump (Fig. J.4.3.a).

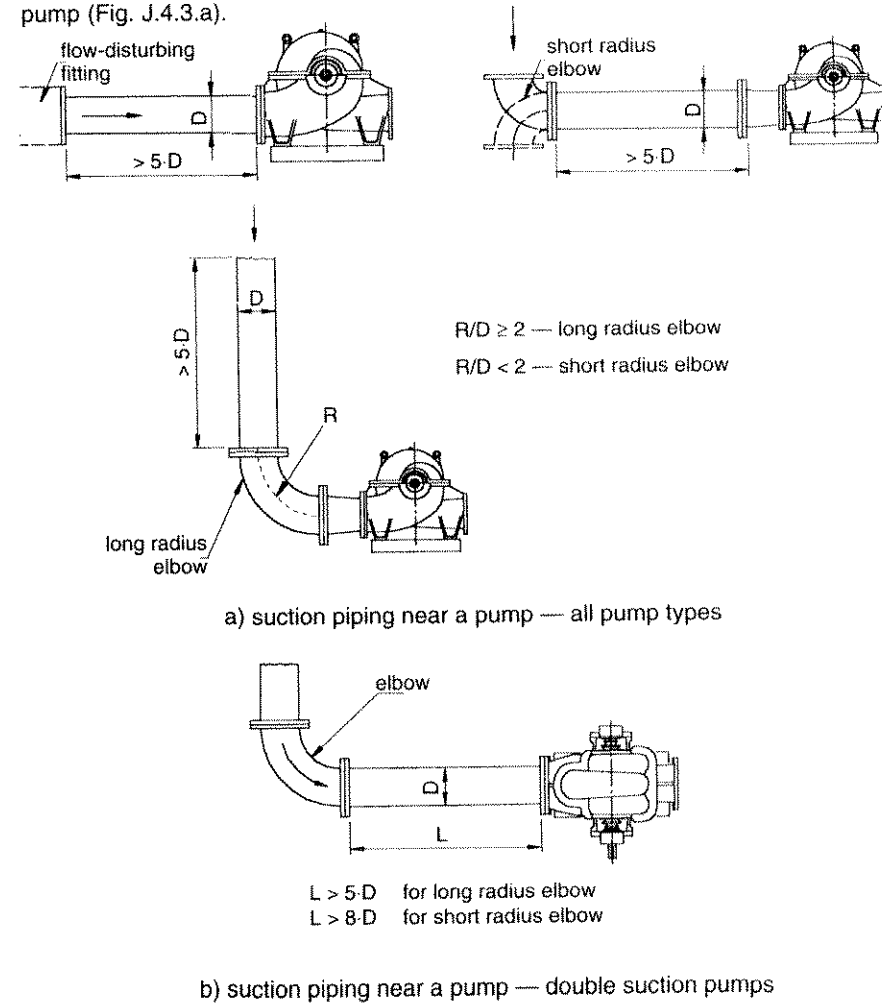


Fig. J.4.3 Recommended suction piping configurations



Long radius elbows and pipe reducers are not considered to be flow-disturbing fittings. For double suction pumps the elbow in the suction pipe should be positioned so that the elbow plane is perpendicular to the pump shaft axis (Fig. J.4.3.a). When this cannot be done, and the elbow plane is parallel to the pump axis, a sufficiently long straight pipe should be installed between the elbow and the pump suction flange (Fig. J.4.3.b). This is to improve or eliminate non-symmetrical and fluctuating flow patterns at the elbow exit, which could otherwise cause the inlet conditions on both impeller halves to be different.

## J.5. Model study of intake structures

### J.5.1 Need for model study

A properly conducted physical model study is a reliable method of identifying unacceptable flow patterns at the pump inlet for given sump or piping designs. Considering the costs of a model study, an evaluation is needed to determine if it is required. A model test of the intake structure should be conducted with one or more of the following features:

- sump or piping geometry that deviates from standard or already proven designs,
- non-uniform or non-symmetric approach flow to the pump suction,
- intakes with pump flow rate greater than 2,5 m<sup>3</sup>/s or total pump station flow rate greater than 6 m<sup>3</sup>/s,
- pumps with open bottom can intakes and flow rates greater than 0,3 m<sup>3</sup>/s per pump,
- when proper pump operation is critical, and when pump repairs, the reconstruction of a poor intake design and the impact of inadequate pump performance, all together would cost more than ten times the cost of a model study.

A model study of the intake structure should be conducted by a hydraulic laboratory using personnel that has experience in modelling pump intakes. During a model study the adverse hydraulic conditions that can affect pump performance should be detected. In the next phase, remedial measures to alleviate such adverse flow conditions should be identified. A typical hydraulic model study does not investigate the flow patterns induced by the pump itself. The objective of a model study is to ensure that the final sump or piping design generates favourable flow conditions at the pump entry.

### J.5.2. Hydraulic similarity

Models involving a free surface are operated using a Froude similarity, since the flow process is controlled by gravity and inertial forces. The Froude number, representing the ratio of inertial and gravitational forces, is defined as follows:

$$Fr = v / (g \cdot L)^{0,5}$$

Fr – Froude number

v – average axial velocity (such as in the suction bell)

g – acceleration due to gravity

L – characteristic length (such as bell diameter or submergence)

The same parameters for velocity and length must be used for both model and prototype when determining the Froude number. For a similarity of flow patterns, the Froude number should be equal for model and prototype (index m denoting model and index p denoting prototype):

$$Fr_m = Fr_p$$

Based on the similarity law stated above, the velocity and flow rate ratios are defined as follows:

$$v_m / v_p = (L_m / L_p)^{0,5}$$

$$Q_m / Q_p = (L_m / L_p)^{2,5}$$

When modelling a pump intake to study the potential formation of vortices, it is important to select a reasonably large geometric scale so as to minimise scale effects for viscous and surface tensions, and to allow visual observation of the flow patterns. No specific geometric scale ratio is recommended, but from the point of view of practicality and accurate measurement the minimum dimensions of the model should be as follows: pump bay width > 300 mm, minimum liquid depth > 150 mm, pump throat or suction diameter > 80 mm.

### J.5.3. Instrumentation and measuring techniques

The following instrumentation and measuring techniques are normally applied in model tests of intake structures:

Flow rate: Outflow from each simulated pump should be measured with a flowmeter.

Liquid level: Liquid surface elevation should be measured with any type of liquid level indicator.

Free surface vortices: Vortex type and intensity are identified in the model by visual observation with the help of dye and artificial debris. Photographic or video documentation of vortices is recommended.

Sub-surface vortices: Sub-surface vortices may be visible with the help of dye

injection near the vortex core. Photographic or video documentation is recommended.

Swirl in the suction pipe: The intensity of flow rotation should be measured using a swirl meter located downstream from the suction bell. The revolutions of the swirl meter propeller per unit time are used to calculate a swirl angle in the suction pipe.

Velocity profiles: Velocity traverses along at least two perpendicular axes, at the throat of the model suction bell or in the plane of the pump suction in a piping system, should be obtained for the final design using a pitot static tube or other suitable instrument.

The accuracy of each individual measuring instrument in an intake model study should be  $\pm 2\%$  or better.

#### J.5.4. Acceptance criteria

The acceptance criteria for the hydraulic model test of the final design should be the following:

- Only low-intensity clear surface vortexes may be acceptable. Any severe surface vortexes or vortexes pulling trash or air bubbles from the surface are not acceptable. Sub-surface vortexes are not acceptable, except for low-intensity sub-surface swirl.
- The average swirl angle indicated by the swirl meter rotation must be less than 5 degrees.
- The time-averaged velocities at the measuring points in the pump suction bell should not deviate more than 10% from the cross-sectional area average velocity.
- In the case of double suction pumps, the acceptable difference of flow at the pump suction flange, to each side of the pump impeller, is 3% of total flow.

## K. PUMPING SPECIAL LIQUIDS

### K.1. Pumping viscous liquids

#### K.1.1. Definition of viscosity

Real fluids are viscous fluids in which friction exists between the moving fluid particles. Fluid resistance against a tangential or angular deformation of the fluid is defined as fluid viscosity. The following are the most common definitions of viscosity:

##### Dynamic viscosity:

- symbol:  $\eta$
- units:  $\text{Pa}\cdot\text{s} = \text{N}\cdot\text{s} / \text{m}^2$ ,  
centipoise:  $1 \text{ cP} = 10^{-3} \text{ Pa}\cdot\text{s}$

##### Kinematic viscosity:

- symbol, definition:  $\nu = \eta / \rho$        $\rho$  - fluid density ( $\text{kg}/\text{m}^3$ )
- units:  $\text{m}^2 / \text{s}$ ,  
centistoke:  $1 \text{ cSt} = 10^{-6} \text{ m}^2 / \text{s}$

In the USA another definition of kinematic viscosity is often used: SSU (Saybold Seconds Universal). SSU is defined as the efflux time for a given quantity of liquid from the viscosity meter. The conversion is:

$$100 \text{ SSU} = 20,5 \cdot 10^{-6} \text{ m}^2/\text{s}$$

#### K.1.2. Description of a Newtonian fluid

When a plate moves against a stationary wall and the space in between is filled with viscous fluid, a certain force must be applied to produce plate movement (see Fig. K.1.1).

The following relationships are valid:

$$F = A \cdot \eta \cdot (dc/dy)$$

$$\tau = F/A = \eta \cdot (dc/dy)$$

- F – frictional force
- A – friction surface
- $\eta$  – dynamic viscosity
- $\tau$  – shear stress
- c – fluid velocity

$y$  – coordinate perpendicular to the wall  
 $dc/dy$  – shear rate

In cases where in the above-stated equation for shear stress  $t$ , the dynamic viscosity  $\eta$  is a constant value, such types of fluid are called Newtonian fluids ( $\eta = \text{const.}$ ). Other types of fluids (non-Newtonian fluids), have a dynamic viscosity which changes with the ratio  $dc/dy$  ( $\eta \neq \text{const.}$ ), as shown in Fig.K.1.2.

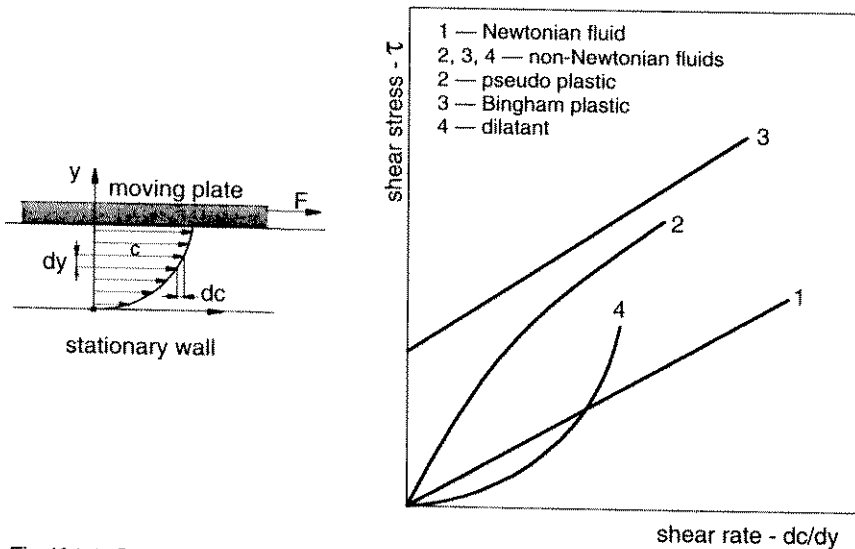


Fig. K.1.1 Schematic representation of the flow conditions between stationary wall and moving plate

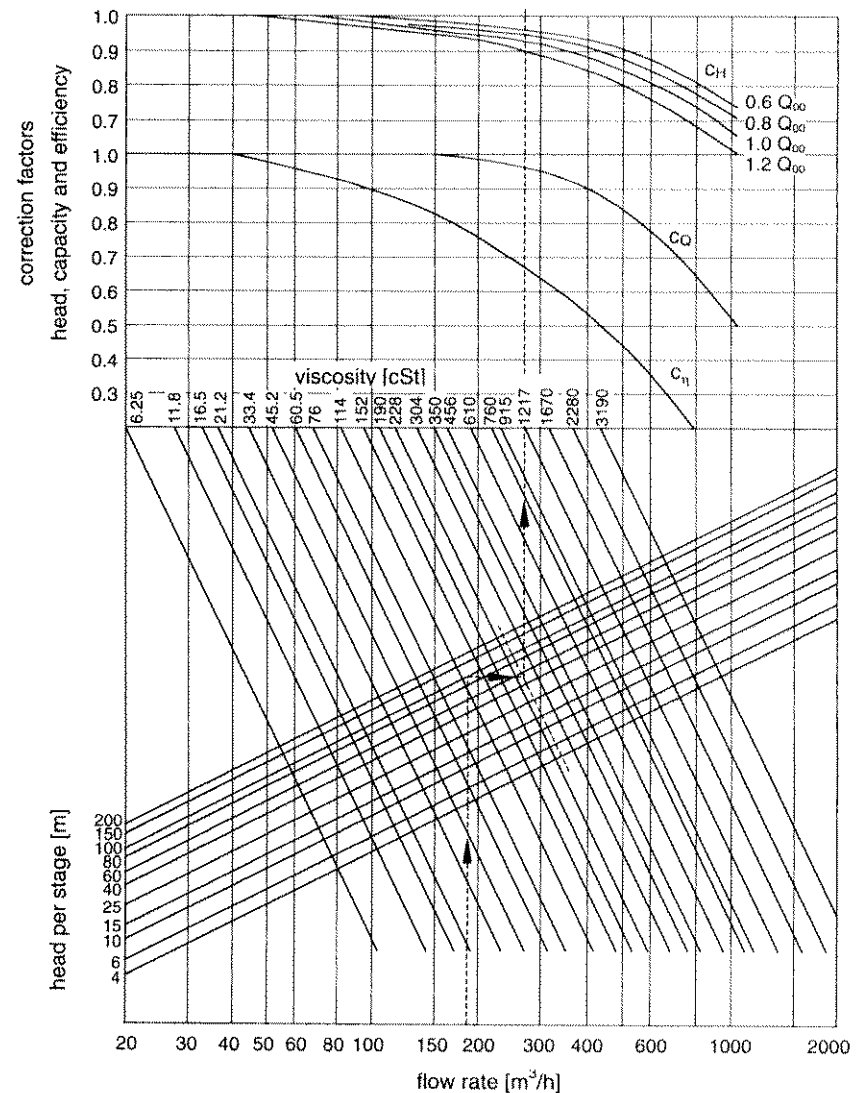
Fig.K.1.2 Shear stress versus shear rate for several fluids (qualitative)

### K.1.3. Effects of fluid viscosity on pump characteristics

When pumping viscous fluids which have a viscosity sufficiently above the value for cold water, additional losses take place which also affect the pump characteristics. The following are the most important factors which influence pump characteristics:

**Hydraulic losses:** With increased viscosity of the fluid, the hydraulic losses in all rotating and stationary pump flow channels also increase. This results in an additional head drop, which is more pronounced at increased pump flow rates (higher internal velocities). Pump designs with a higher percentage of hydraulic losses (low specific speed pumps, pumps with lower hydraulic efficiency), are more sensitive to an increased viscosity of the pumping fluid.

**Disc friction losses:** These losses also increase with increased fluid viscosity, and the consequence is higher pump power consumption.



Example: - nominal pump data (cold water):  $Q_{w,opt} = 180 \text{ m}^3/\text{h}$ ,  $H_{w,opt} = 100 \text{ m}$   
 - viscous fluid data:  $\nu_{vis} = 250 \text{ cSt} = 250 \cdot 10^{-6} \text{ m}^2/\text{s}$

Fig. K.1.3 Performance correction chart for viscous fluids according to Standard ANSI / HI 1.1-1.5

The influence on pump characteristics is higher in low specific speed pumps, where the ratio of disc friction losses with regard to the total pump internal losses is the highest.

**Boundary layer thickness:** Viscous fluids have thicker boundary layers, and due to this the "net channel width" is reduced. In the pump characteristics it is shown as a shift in optimum flow rate towards lower values.

**Fluid density:** Fluid density influences the pump power consumption, as shown in equation for  $P_{vis}$  in the continuation of this section.

Due to the influences described above, the pump characteristics will show the following general alterations when pumping viscous fluids: power consumption will increase, flow and head will decrease. A performance correction chart is given in Fig. K.1.3. This correction chart is based on average test results for single-stage pumps with discharge flange diameters of 50 – 200 mm. The tests were performed with petroleum oils having different viscosities.

Viscous fluid pump characteristics can be determined with the help of the correction factors from diagram Fig. K.1.3 and according to the following procedure:

$$\text{Flow rate: } Q_{vis} = c_Q \cdot Q_w$$

$$\text{Head: } H_{vis} = c_H \cdot H_w$$

$$\text{Efficiency: } \eta_{vis} = c_\eta \cdot \eta_w$$

$$\text{Power consumption: } P_{vis} = (Q_{vis} \cdot H_{vis} \cdot \rho_{vis} \cdot g) / \eta_{vis}$$

$c_Q$ ,  $c_H$ ,  $c_\eta$  – correction coefficients from Fig. K.1.3

$\rho_{vis}$  – density of viscous fluid

$g$  – acceleration due to gravity

index "vis" – related to viscous fluid

index "w" – related to cold water

The pump performance correction described above is limited to Newtonian fluids only, and is valid for open and closed radial pump impellers when running at a sufficiently high NPSH<sub>av</sub> (at cavitation-free conditions – no head/efficiency drop due to cavitation). When accurate details of the influence of a viscous fluid on pump characteristics are required, a pump performance test with the actual fluid should be conducted. This is possible in closed test loops and requires special arrangements.

#### K.1.4. Instructions for determining viscous fluid pump characteristics

Pump manufacturers normally give the pump characteristics for cold water. Viscous fluid pump characteristics are calculated as shown in the example below, using the procedure and correction factors from section K.1.4. Nominal pump data for cold water (for best efficiency point):

$$Q_{w,opt} = 180 \text{ m}^3/\text{h}$$

$$H_{w,opt} = 100 \text{ m}$$

$$\eta_{w,max} = 0,80$$

$$P_{w,opt} = 61,3 \text{ kW}$$

Viscous fluid data:

- viscosity:  $\nu_{vis} = 250 \text{ cSt} = 250 \cdot 10^{-6} \text{ m}^2/\text{s}$
- density:  $\rho_{vis} = 850 \text{ kg/m}^3$

water characteristics	$Q_w / Q_{w,opt}$	0,6	0,8	1,0	1,2
	$H_w / H_{w,opt}$	1,12	1,09	1,0	0,88
	$\eta_w / \eta_{w,max}$	0,925	0,975	1,0	0,975
	$P_w / P_{w,opt}$	0,726	0,894	1,0	1,083
correction factors	$c_Q$	0,96	0,96	0,96	0,96
	$c_H$	0,96	0,95	0,93	0,90
	$c_\eta$	0,67	0,67	0,67	0,67
viscous fluid characteristics	$Q_{vis} / Q_{w,opt}$	0,576	0,768	0,96	1,152
	$H_{vis} / H_{w,opt}$	1,075	1,036	0,93	0,792
	$\eta_{vis} / \eta_{w,max}$	0,62	0,653	0,67	0,653
	$P_{vis} / P_{w,opt}$	0,849	1,037	1,133	1,189

Table K.1.1 Examples of calculations of viscous fluid pump characteristics

Based on the calculation procedure described above, the nominal pump data for a viscous fluid (best efficiency point) are:

$$Q_{vis,opt} = 172,8 \text{ m}^3/\text{h}$$

$$H_{vis,opt} = 93 \text{ m}$$

$$\eta_{vis,max} = 0,536$$

$$P_{vis,opt} = 69,45 \text{ kW}$$

The comparison of pump characteristics for cold water and a viscous fluid (viscosity  $250 \cdot 10^{-6} \text{ m}^2/\text{s}$ , density  $850 \text{ kg/m}^3$ ) which serve as an example of a calculation, are in the dimensionless form shown in Fig. K.1.4.

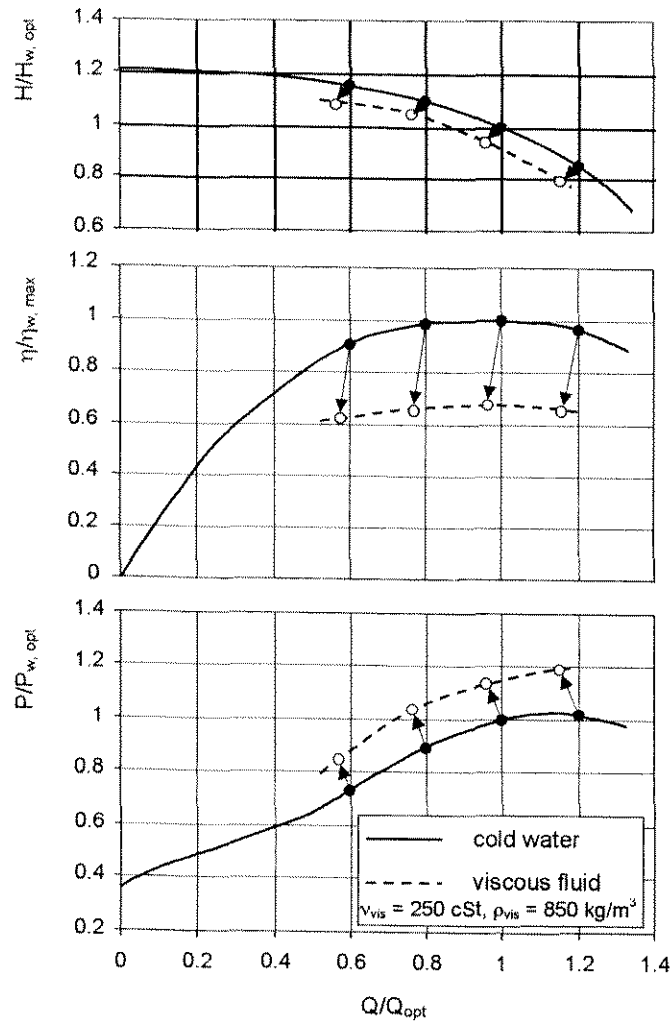


Fig. K.1.4 Example of pump characteristics for cold water and a viscous fluid

## K.2 Pumping gas-liquid mixtures

In the process industry especially, there are often cases where non-dissolved gases are also present in the liquid phase. When such a mixture is transported by a pump of standard design, the influence of the gas-liquid ratio on the pump characteristic and the limits of pumping capability have to be considered.

### K.2.1. Capabilities of standard pump designs

The most critical phenomenon when pumping gas-liquid mixtures is the separation of the gas phase from the liquid phase. Even if a homogenous gas-liquid mixture enters the pump, gas bubbles increase when passing regions of low local static pressure. These regions are at the impeller blade suction side near the impeller inlet. Due to the big difference in gas and liquid densities, the centrifugal force effect acts additionally towards the separation of the gas and liquid phases. The consequence is the formation of gas pockets at the impeller entry, near to the blade suction side and around the shaft. In cases of closed impeller designs, the gas phase also gathers in the inner portion of the impeller side chambers. With the increased percentage of gas in the pumped mixture, the impeller side chambers can be completely filled with gas, which can spread even into the spiral casing. Such gas pockets in the impeller, the impeller side chambers, and the spiral casing, represent a certain blockage of the flow channels, and results in a reduction of pump flow rate, head and efficiency. Under certain circumstances the flow may collapse.

In Fig. K.2.1 an example of pump characteristics with different gas/liquid ratios is shown. The example shows the characteristics of a single-stage standard pump design with closed impeller type, the pump specific speed being  $nq$  26.

Based on the diagram provided and also on other test results for standard pumps, the following conclusions can be derived:

- up to a gas content of  $\alpha = Q_{\text{gas}} / Q_{\text{liq,opt}} \approx 0,02$  the influence on the pump characteristic is relatively small and is still acceptable,
- the operating limit of a standard pump is at  $\alpha = 0,05 - 0,08$ ,
- even with a small percentage of non-dissolved gas in the liquid, a standard pump cannot operate near  $Q = 0$ ,
- the lowest effect of added gas in the liquid on the pump characteristics is at flow rates between 0,6 and 1,0 of  $Q_{\text{liq}}/Q_{\text{liq,opt}}$ ,
- the values given above improve slightly when the pump specific speed is rising.

In the case of multi-stage pumps the influence of the gas content on the characteristics is produced by the geometry of the first stage. In the next stages the volume of gas bubbles is already very much reduced due to increased static pressure

and with this, its influence on the characteristics. Therefore a multi-stage pump is, as a general tendency, less sensitive to the gas content.

It has to be taken into account that with an increased gas content in the liquid, the pump cavitation characteristic  $NPSH_{req}$  is also worsened.

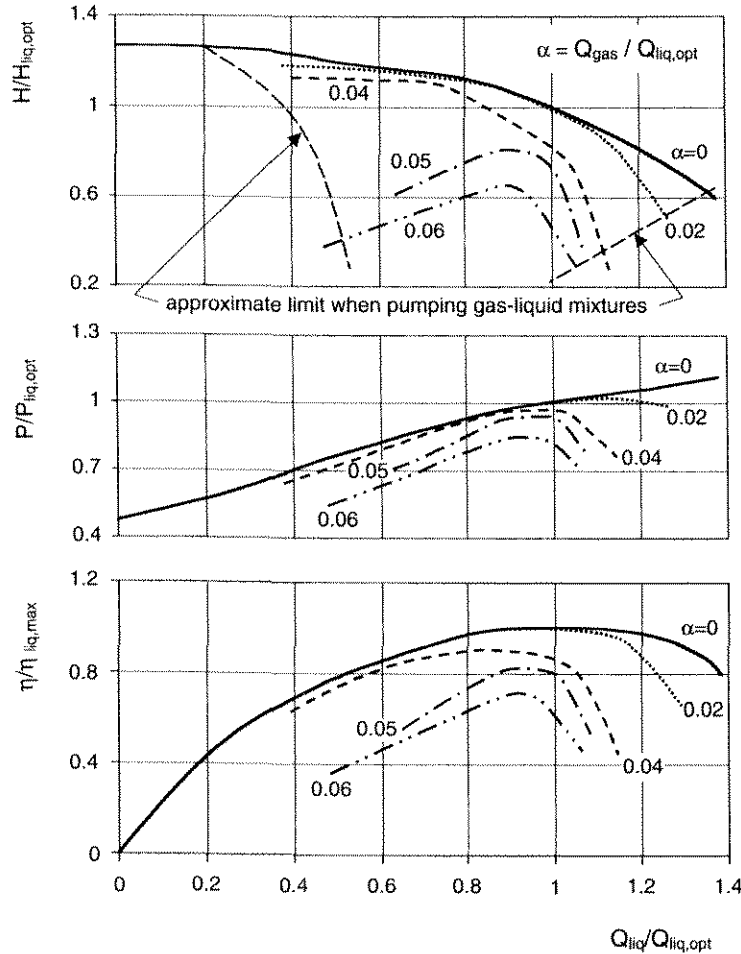


Fig. K.2.1 Effect of the gas content in a liquid on the pump characteristics

### K.2.2. Possible improvements and special designs

Improvements to standard pump designs with regard to gas content sensitivity are mainly connected with solutions which reduce or postpone the separation of the gas and liquid phases in the pump. The following are the most common measures:

**Open impeller type:** Additional internal circulation between the impeller blade pressure and suction sides postpones the formation of gas pockets on the blade suction side. With an open impeller type the negative effect of accumulated gas in the impeller side chamber is eliminated.

**Evacuation of impeller hub area:** Gas accumulates in this area of the pump, due to the centrifugal force effect. When the impeller hub area is connected to an external evacuation device, the accumulated gas is constantly removed, thus improving pumping capability.

**Impellers with higher specific speeds:** In impellers with higher specific speeds, the separation of the two phases is less pronounced, due to a reduced centrifugal force effect and more pronounced recirculation.

A special pump design (two-phase pump) for handling an extremely high gas content in a fluid is shown in Fig. K.2.2. This is a multi-stage pump provided with mixed-flow open impellers which have a low head per stage and low impeller blade loading (low pressure difference between pressure and suction sides of the blade and very gradual increase in pressure from leading to trailing edges). Between the two impellers, the diffuser vanes are placed so as to transform part of the kinetic energy into pressure, and to guide the mixture flow into the next impeller. Such a pump design allows a reduction in the separation of the two phases, and the pump can operate with a gas/liquid ratio  $\alpha$  up to 0,97.

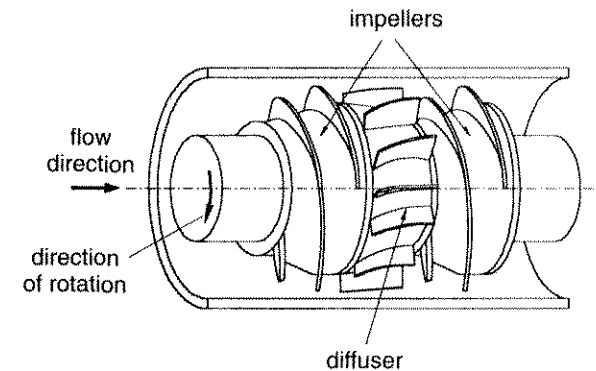


Fig. K.2.2 Schematic representation of a two-phase pump

### K.3 Pumping solid-bearing fluids (slurries)

#### K.3.1 General description of flow regimes

The pumping of solid-bearing fluids and the transportation of solids by slurry pipelines have a wide variety of industrial applications: agriculture; oil, food, paper and chemical industries; mining; industrial and municipal waste treatment; etc. Depending upon the properties of the solids and liquids, and the pipe size and flow velocity, different flow regimes can develop which are qualitatively represented in Fig. K.3.1.

The following are the main flow regimes which can develop when pumping solid-bearing fluids (slurries):

**Homogeneous flow (1):** In the homogeneous flow regime the solid particles are distributed homogeneously in the fluid. This type of flow develops when the solid particles are small and/or the flow velocity high enough.

**Heterogeneous flow (2):** A solid concentration gradient exists along the vertical axes of a horizontal pipe in the case of a heterogeneous flow regime. This type of flow occurs when solid particle size and density increase, and the mean flow velocity is not high enough to establish a homogeneous distribution of particles.

**Flow with moving bed (3):** When solids contain large particles like coarse coal or gravel, the particles will travel in the form of a moving bed near the pipe bottom. This type of flow normally occurs in the transportation of solids in slurry pipelines.

**Flow with stationary bed (4):** This type of flow occurs when the flow velocity is not sufficiently high to keep all the solids in motion. Some solids may be in a heterogeneous flow above the stationary bed of solids. This type of flow should be avoided in commercial practice.

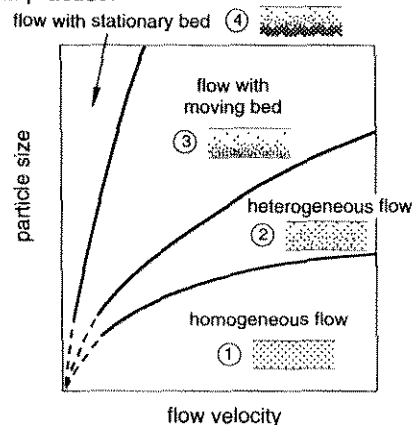


Fig. K.3.1 Qualitative representation of flow regimes for solid-bearing fluids (slurries)

When pumping solid-bearing fluids the pump performance characteristics, as well as the pipeline-system characteristics, differ from the performance characteristics for cold water. Generally the pump head and efficiency decrease and power consumption increases when pumping solid-bearing fluids. More information about the performance correction is given in sections K.3.2 and K.3.3.

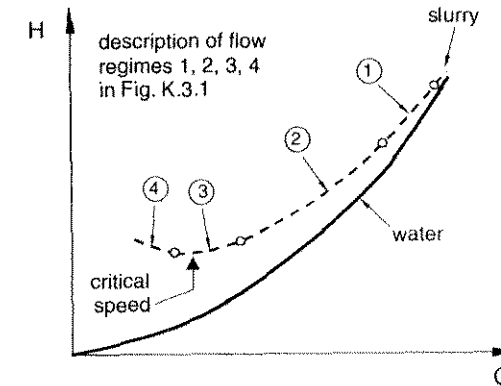


Fig. K.3.2 Typical example of solid-bearing fluid (slurry) and water pipeline characteristics

#### K.3.2. Non-settling solid-bearing fluids (slurries)

Non-settling solid-bearing fluids (slurries) have the properties of a homogeneous flow and behave as a Newtonian fluid (see section K.1.2). Due to this, performance corrections can be done in the same way as for viscous fluids.

**Pipeline characteristics:** When calculating the pipeline characteristics, the real values for fluid viscosity and density have to be taken into account. Friction losses in a pipeline when pumping slurries are higher than for pumping water.

**Pump performance characteristics:** The same procedure for pump performance correction should be used as that shown in sections K.1.3 and K.1.4 for viscous fluids. In order to get a realistic correction it is important to have reliable values for viscosity and density of the slurry.

#### K.3.3. Settling solid-bearing fluids (slurries)

When pumping settling slurries, all the flow regimes described under item K.3.1 can generally occur. Which type of flow will develop, depends mainly on the fluid velocity and particle size. According to pipeline and pump parameters, many precautions have to be considered in order to ensure the trouble-free pumping of settling slurries.

**Pipeline characteristics:** A typical pipeline characteristic for settling slurries is shown in Fig. K.3.2, and compared to the characteristic for water. In the slurry characteristic (for constant solid content), the margins between the different flow regimes are marked. Each flow regime has different coefficients of pressure loss: the lowest pressure loss coefficient is in a homogeneous flow (the slurry characteristic in Fig. K.3.2 closest to the water characteristic) and the highest pressure loss coefficient is in a flow regime with a stationary bed.

**Pump performance characteristics:** When slurry flows through a pump, the solid particles take different paths in the flow channels from the liquid particles. This effect is connected to some additional hydraulic losses which, together with the increased friction losses of the slurry in the pump flow channels, reduce the pump head and efficiency. Power consumption increases due to the increased density of the slurry in comparison with the water characteristic. Fig. K.3.3. shows a schematic representation of the differences in the pump performances for pumping water or slurry. Based on experimental results with pumps of different specific speeds, a formula is available to calculate the correction factors; these factors depend mainly on the size and density of the solid particles and on the concentration of solids in the liquid, but also on pump specific speed. The procedure for calculating is:

Head:

$$H_{sl} = f_H \cdot H_w$$

$$f_H = 1 - \frac{x}{26} \cdot \left( \frac{\rho_s}{\rho} - 1 \right) \cdot \left( 1 + 4 \frac{\rho}{\rho_s} \right) \cdot \ln \frac{d_s}{d_{ref}} \cdot \left( \frac{25}{n_q} \right)^{0.34}$$

$$x = (\rho_s / \rho_{sl}) \cdot c_v$$

$$c_v = (\rho_{sl} - \rho) / (\rho_s - \rho)$$

Efficiency:

$$\eta_{sl} = f_\eta \cdot \eta_w$$

$$f_\eta = f_H$$

Power consumption:

$$P_{sl} = (\rho_{sl} / \rho_w) \cdot P_w$$

- $c_v$  – volume concentration of slurry
- $d_s$  – particle size (diameter)
- $d_{ref} = 0,023$  mm – reference particle size
- $f_H, f_\eta$  – correction factors
- $n_q$  – pump specific speed
- $x$  – mass concentration of slurry
- $\rho$  – density of “carrier liquid”, normally water
- indices: “s” – solid, “sl” – slurry, “w” – water

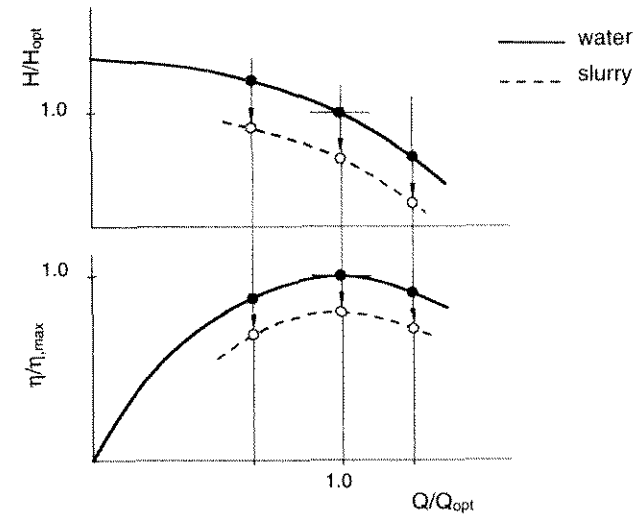


Fig. K.3.3 Schematic comparison between pump characteristics for water and slurry

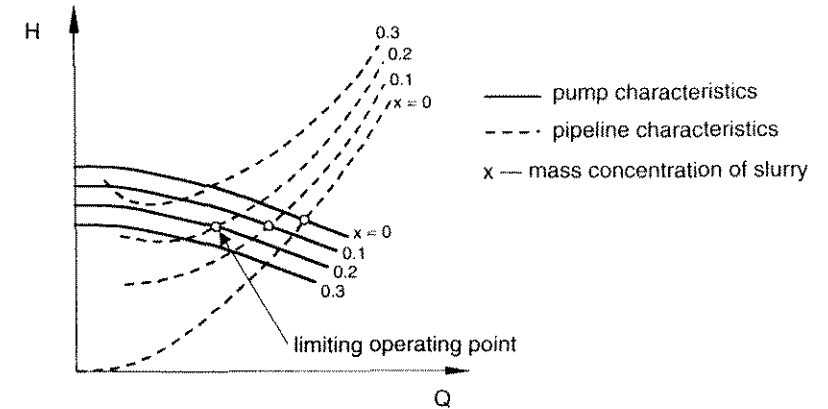


Fig. K.3.4 Pump and pipeline characteristics for different concentrations of slurry

When pumping slurries, the concentration of solid particles may vary during the operation, and consequently the pipeline and pump characteristics as well. An example of characteristics with different mass concentrations of slurry is shown in Fig. K.3.4. With the increased concentration, the pump operating point moves from homogeneous or heterogeneous flow regimes towards moving bed flow regimes or stationary bed flow regimes. There is also a limiting concentration when pumping is no longer possible because the pump characteristic has become lower than the pipeline characteristic.



### K.3.4. Design guidelines and speed limitation

There are many different slurry pump designs which can cover various industrial applications. Pumps have to resist abrasion (often also corrosion) and are therefore made from hard abrasion-resistant metals, from elastomers or ceramic. In order to minimise wear the following guidelines for pump design may be helpful:

- use metals which are harder than the hardest slurry particles,
- utilise pump elements which combine soft and hard materials in such a way as to reduce abrasion and provide resilience,
- increase the wall thickness of pump parts in areas of high wear,
- use hydraulic designs with specific speeds  $nq \leq 30$  (wastewater  $\leq 50$ ),
- limit pump operating region to  $(0,8-1,2) \cdot Q_{opt}$ .

Velocity is one of the most important parameters influencing wear in the pump elements. The wear rate when handling abrasive solids is generally proportional to the relative velocity between the slurry and the pump elements, to the power 2–3. From practical experience some guidelines for impeller tip speed limitation have been established, and are shown in Table K.3.1.

type of slurry	Impeller peripheral tip speed limitation [m/s]
dirty water, waste water	40 (50)
slurries up to mass concentration of 25% and particle size lower than 200 mm	35
slurries with higher mass concentration and larger particle size as stated above	30

Table K.3.1 Guidelines for speed limitation of slurry pumps

## K.4 Pumping hydrocarbons

Operating experience on site has shown that pumps handling hydrocarbons can operate satisfactory at a lower  $NPSH_{av}$  than is required for cold water. These practical results have also been confirmed by laboratory tests. The main cause of the differences between cold water and hydrocarbon  $NPSH$  values is linked to the differences in vapour pressure and density of both fluid types.

When performing pump cavitation testing with different fluids, the following can be observed: at the same value of  $NPSH_{av}$ , the volume of vapour bubbles at the impeller entry is greater with cold water than with the hydrocarbons. The size (volume) of vapour bubbles is directly related to the degree of flow obstruction at

the impeller entry, and causes a drop in head. With hydrocarbons the volume of the vapour bubbles is reduced and results in the delaying of the head drop, as shown schematically in Fig. K.4.1 (see also chapter C).

The diagram in Fig. K.4.2 is a composite chart of the  $NPSH_{req}$  reductions which may be expected for hydrocarbon liquids and high-temperature water. The diagram is based on available laboratory data from tests conducted on the fluids shown, and plotted as a function of the fluid temperature and true vapour pressure at that temperature.

When using diagram Fig. K.4.2, the following limitations have to be taken into account:

- the  $NPSH_{req}$  reduction should be limited to 50% of the  $NPSH_{req}$  of the pump for cold water,
- the diagram is valid for hydrocarbons free of gas and air,
- when it is applied to hydrocarbon mixtures, vapour pressure should be determined for the actual pumping temperature,
- values from the diagram should not be applied for temperature and/or absolute pressure transient conditions.

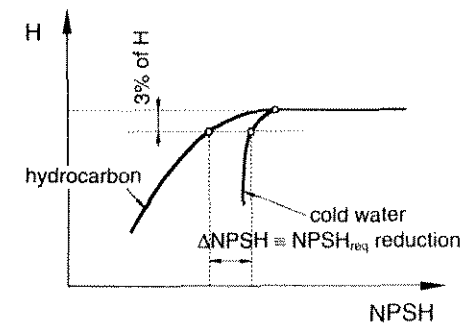
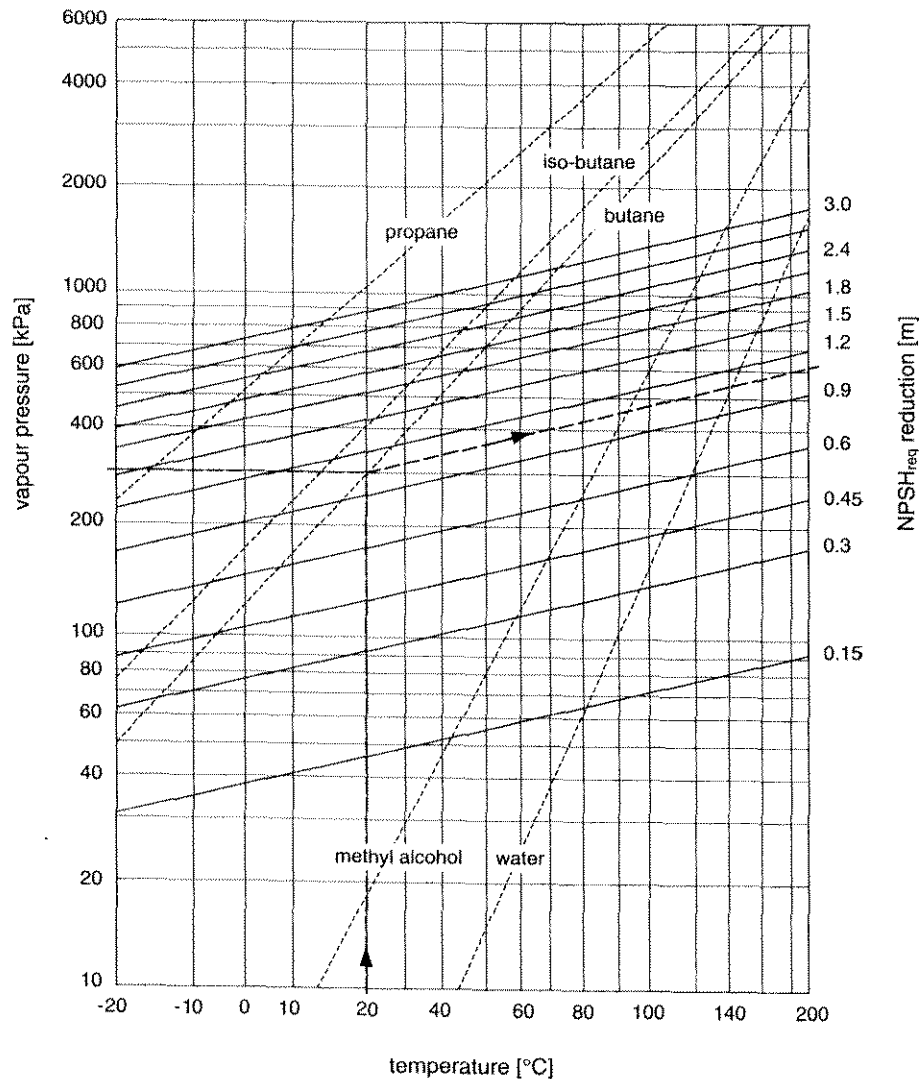


Fig. K.4.1 Schematic representation of head drop curves for cold water and hydrocarbons



Example: - pumping fluid: butane - temperature = 20°C  
 - vapour pressure = 300 kPa (absolute) - NPSH<sub>req</sub> reduction = 1,05 m

Fig. K.4.2 NPSH<sub>req</sub> reduction for pumps handling hydrocarbon liquids and high-temperature water, according to Standard ANSI / HI 1.1-1.5

## L. CORROSION AND MATERIAL SELECTION

### L.1. General

Corrosion is described as the reaction of a material with its environment, causing measurable changes in the material used, and possibly leading to corrosion damage. This so-called "impairment" of the function of the pump elements can therefore reduce not only the life, but also the performance of the pump. For an economical pump installation, the most important requirements are the life expectancy and the required performance. The operational life gives the expected total number of running hours for all the pump elements, before they have to be replaced. The life is related primarily to the design of the pump and the resistance of the material used, with regard to cavitation, corrosion and erosion, or a combination of all three, under operating conditions. It is therefore essential to select the most economical material that is adequately resistant to the fluid characteristics and the velocity effect in the different parts of the pump, as the latter also influences the life cycle costs (LCC).

The following factors ensure a long operational life for the pump:

- neutrality of the pumped fluid at ambient temperature,
- necessary safety margin over the NPSH<sub>3%</sub>,
- continuous operation of the pump, in the vicinity of the best efficiency point,
- absence of abrasive particles in the fluid.

If the properties of the fluid differ from neutral, the pump designer has to choose the best possible material with the help of an expert in metallurgical corrosion in order to obtain the expected life.

Different standards define the chemical properties of the materials used for pump elements, and give recommendations for the choice of materials for different fluids and velocities.

### L.2. Factors influencing corrosion

The most important parameters influencing the corrosion resistance of the materials used are as follows:

- chemical properties of the fluid,
- temperature of the fluid,

- static mechanical stresses including the influence of flow rate variation,
- cavitation phenomena due to bubble implosion on the surface of the material,
- metallurgical composition of the material, including heat treatment as well as welding influences,
- influence of the erosive and corrosive matter in the fluid.

Different aspects of corrosion must be distinguished:

- Uniform corrosion, where the rate of corrosion is concentrated on all the metal surfaces of the pump (the so-called rusting process). Usually this kind of corrosion is not very critical because it can be properly considered during the design phase (for example by increasing the thickness of the pump components) and it can be monitored during the life of the pump, so that overhauling and replacement of damaged parts can be planned. Local corrosion on lightly stressed parts, such as pitting, crevice corrosion, and galvanic and intergranular forms of corrosion (see section L.4).
- Local corrosion on parts with an evident mechanical stress concentration, such as erosion corrosion and cavitation corrosion (surface phenomena) or stress corrosion cracking and corrosion fatigue (subsurface phenomena). This form of corrosion acts either on the material surface, when it has a great influence on the values of corrosion fatigue strength (see Table L.2.1), or produces local destruction of the material due to cavitation or erosion attacks.

The last two types of corrosion are often undetectable, and destruction of the attacked pump elements can occur suddenly. In table L.2.1 the decrease in the fatigue strength, resulting from corrosion attack, is shown for a specific material.

relative alternating fatigue strength for $10^7 - 10^8$ load cycles	description of test conditions	comments
1	in air	constant fatigue strength for higher load cycles
~ 0,9	with covering layer formation	constant fatigue strength for higher load cycles
~ 0,4	fatigue cracking due to corrosion attack	falling fatigue strength for increased load cycles

Material: forged material for pump shafts, Ni - Cu alloy

Table L.2.1 Alternating fatigue strengths of smooth forged material

The corrosive properties of a pumped fluid can vary during operation, when the process requires changes in the temperature, concentration of entrained solids or amounts of gas. Such variations can produce different forms of corrosion, depending on the very specific fluid properties and the type of material used for the pump parts.

### L.3. Corrosive properties of the liquid being pumped

#### Non-water-based fluids:

This group includes all typical organic substances like oil, petrol etc. These fluids usually have no corrosive effect at all on metals. A corrosion attack can be expected only when these fluids contain some water.

#### Water-based fluids:

These liquids usually contain some salts and also gases. Depending on the source, distinction must be made between the following three types:

- natural water (groundwater, surface water, sea water),
- treated water (demineralised, degassed water),
- special chemical and salt solutions (cooling brines, fluids from industrial sectors).

Depending on the source, natural water contains different substances in the form of salts, free acids, and also gases, and depending on their quantity, corrosion attacks take place on the materials. As the solubility level of these substances in water also depends on the temperature, this factor has an important influence on material loss due to corrosion. Natural water contains additionally a varying quantity of calcium carbonate. The concentration of this substance, responsible for water hardness, is defined in degrees of carbonate hardness by internationally used concentration units.

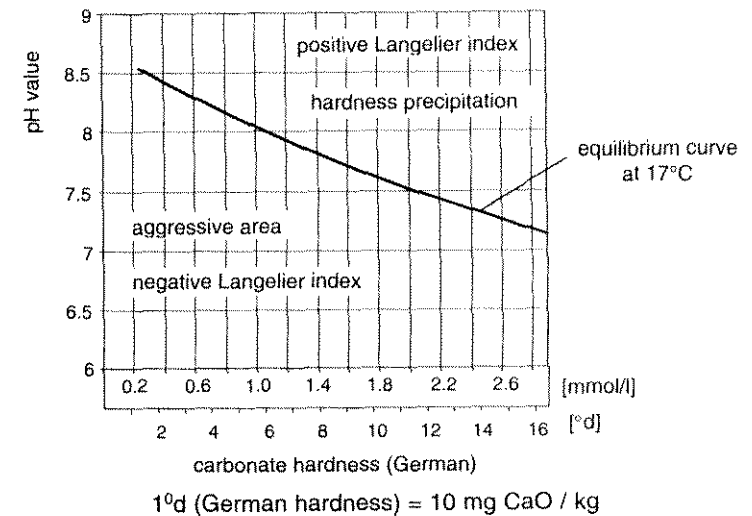


Fig.L.3.1. Simplified illustration of calcium-carbon dioxide equilibrium

Diagram Fig. L.3.1. defines the water quality, according to German hardness. The carbonate hardness is an important criterion for the selection of materials. As the

formation of a protective layer is heavily dependent on the pH value of the natural water, the decision when to use unalloyed or low-alloyed steel (Cr content below 13%) is taken on the basis of the degree of hardness. Fig. L.3.1. shows the aggressive and also non-aggressive areas for a water temperature of 17°C and for different hardnesses as a function of pH values.

The corrosion behaviour of most metals is determined to a great extent by the pH value of the pumped fluid. If the fluids contain salts and/or gases, the pH value falls below the neutral value of 7,5, into the acid region. Corrosion attacks become very intensive and can be dangerous for all pump elements. The corrosion danger increases additionally with the rising velocity of the fluid in the pump. Special attention must be given when pumping sea water, as this fluid contains about 3% of dissolved salts. The corrosion aggressivity depends also on the water temperature.

For fluids with unknown chemical properties it is recommended to carry out a chemical analysis, in order to prevent unacceptable corrosion attacks. This is especially important for injection water, used for crude oil production. This water is a product of the oil wells and is obtained after the separation of gases and crude oil from the mixture. This water can be very aggressive, especially when containing a high amount of hydrogen sulphide  $H_2S$  (few hundred ppm) and also a high amount of chlorides.

## L.4. Types of corrosion

For the right choice of pump material for a given fluid, the corrosion properties have to be evaluated, as in many cases they are unknown. In order to choose the optimum material, it is advisable to test the material under most static conditions, in different fluids. The results of these tests only give information about local corrosion, whereas its effects in conjunction with the fluid velocity are unknown. However, for acid fluids especially, the influence of water velocity is very important for the optimum choice of material.

### L.4.1. Inhomogeneities in a material: galvanic corrosion

This type of corrosion is defined as electro-chemical corrosion, when metals with different nobilities are in electrical contact through the fluid, which acts as an electrolyte. The galvanic corrosion results in the rapid destruction of one of the materials, creating a corrosion protection of the other material. Therefore special attention must be given to the nobilities of the materials under consideration. The ratio of areas of the materials also has a large effect on the galvanic corrosion. The degradation is even more pronounced when the less noble material has a large contact area with the noble material.

In order to minimise galvanic corrosion, the following recommendations should be considered:

- the elimination of combinations of materials, when the area of the less noble material is small,
- the insulation of materials with different nobilities,
- the selection of combinations for materials which are in contact, with as close as possible a nobility in the galvanic corrosion series.

An approximate series of materials and alloys, beginning with the lowest nobility are: aluminium, cast iron, chromium steel, austenitic nickel and nickel-copper-cast iron alloys, chromium-nickel stainless steel, nickel-based alloys, bronzes.

Detailed recommendations on combinations of metals which should be avoided in different contact areas are given in Standard ANSI/HI 9.1-9.5.

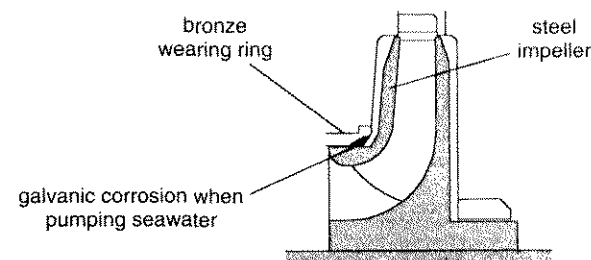


Fig.L.4.1 Schematic representation of galvanic corrosion in a pump

### L.4.2. Pitting corrosion

Small cavities, randomly distributed over a surface, are typical for this type of corrosion attack. The result of the attack is local perforation of the surface of the metal used, and it can have very dangerous consequences. With the formation of a small corrosion anode, the passive layer is eliminated. In the cavity the fluid reaches a very low pH value, activated additionally by chlorides. If the fluid is in a stagnant condition (pump at standstill), the danger of pitting corrosion is additionally increased, as no fresh oxygen is transported to the surfaces by the fluid. An additional increase in the corrosion attack can be caused by a rise in temperature of the fluid. Austenitic steels are especially sensitive to this type of corrosion. By adding a percentage of Mo to the material, corrosion resistance can be improved considerably.

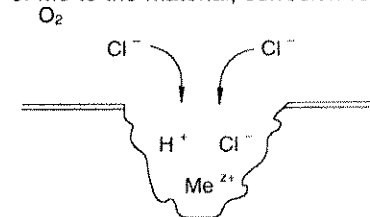


Fig.L.4.2 Schematic representation of pitting corrosion

### L.4.3. Crevice corrosion

The formation of this type of corrosion is similar to pitting corrosion. Crevice corrosion can be explained as a local destruction of the corrosion-resistant protective layer in the crevices, resulting from a scarcity of oxygen and a reduction in the pH value.

A pronounced danger exists when a pump is out of operation and the delivery of oxygen is cut off, thus preventing the formation of a protective layer. The danger of the formation of crevice corrosion can be greatly reduced by an improved design, eliminating as far as possible all unnecessary crevices, for instance between the shaft and the protecting shaft bush. Regularly starting the pump, which supplies fresh water and therefore also oxygen to the crevices, helps to reduce the danger of a corrosion attack. Intense crevice corrosion attacks are observed in stainless steels which have a relatively low content of Cr and Mo, when the pumped fluid includes a high content of chlorides, combined with a high temperature.

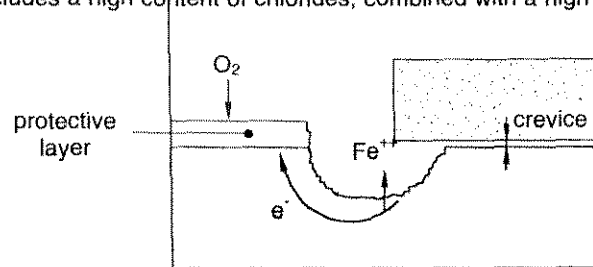


Fig.L.4.3 Schematic representation of crevice corrosion

### L.4.4. Intergranular corrosion

Intergranular corrosion is a special form of local corrosive attack. The reason is the precipitation of Cr carbides, which produces a shortage of Cr in the grain boundaries of the material. Based on this, the sensitivity to corrosion rises. The reason lies in the difference in the potentials between the boundary and the inside of the crystal. Even if the loss of material is small, this form of corrosion leads to disintegration. High-alloyed austenitic Cr-Ni steels are very susceptible to this type of corrosion and the mechanical properties of such materials can be greatly reduced. Cast material of the same composition is less sensitive to this type of corrosion than forged material. Heat treatment (including local heating during welding processes), can affect the formation of intergranular corrosion. The susceptibility of austenitic stainless steels can be very much influenced by their carbon content. Steels with a carbon content of  $C < 0,03\%$  are resistant to stress corrosion. An increased Ni content and optimised heat treatment avoid the cracking of such materials. Modern stainless steels containing Ni, Cr, Mo with additions of Cu and N, have shown an excellent corrosion resistance and high strength.

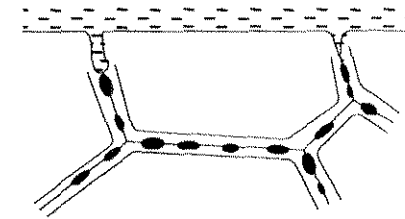


Fig.L.4.4 Schematic representation of stress corrosion

### L.4.5. Corrosion caused by interaction with cavitation

If high local stress is produced on the surface of the material, due to vapour bubble collapse resulting from cavitation in a corrosive fluid, the rate of metal destruction is accelerated. The corrosion protection layer is destroyed by the cavitation, and therefore the corrosion process proceeds very rapidly. In Table L.4.1 a comparison of combined corrosion-cavitation material loss is shown for different types of water. It is obvious that, due to the increase in  $H_2S$  content, the rate of damage rises very fast. Only by using higher-alloyed materials, with a Cr content higher than 12%, can the damage rate be reduced. The loss of material due to the interaction is additionally influenced by rising flow velocities. This is especially important for impellers, if the NPSH available cannot be increased.

water characteristic	relative material loss per unit time
distilled water	1
sea water according to DIN	1,2
sea water with 0,1 ppm $H_2S$	2,3
sea water with 10 ppm $H_2S$	3,1
sea water with 50 ppm $H_2S$	3,8

Material: G-CuAl10Ni (2.0975.01)

Table L.4.1 Comparison of material loss due to cavitation corrosion interaction for different water characteristics

### L.4.6. Uniform corrosion and the influence of flow velocity

Practically all the wetted surfaces of pump elements are subject to relatively high fluid velocities. The corrosion deposits, which act as a protective layer, are influenced by the chemical composition and velocity of the fluid. The selection of materials should therefore be based on the velocity-corrosion resistance of the material used. Laboratory tests which determine the different types of local corrosion for corrosive fluids, are static. When a pump is working outside the BEP, the angles of fluid flow become larger than the geometrical ones. Separation occurs, including the creation of vortices in this zone. The erosion-corrosion attack intensifies.

The erosion-corrosion process of material loss can be divided into three phases:

**Phase 1:** Every corrosion-resistant material with a Cr content larger than 12% creates a protective covering layer in a corrosive fluid, according to Fig. L.4.5 (a and b). This phase is controlled by diffusion and loss of material, caused by transporting oxygen to the material.

**Phase 2:** This phase is chemically controlled. In this phase a passivation layer is built up as a result of a chemical reaction with the material. In this phase the layer protects the original material, and the “wash away” of the protective layer is compensated by building up again with a “fresh” layer.

**Phase 3:** With the increased velocity of the fluid, the covering layer is locally destroyed and creates unevenness. The latter produces local higher velocities and separations with a rising “wash away” effect of the material. When the “wash away” is greater than the newly built up “fresh” layer, passivation no longer takes place and it cannot protect the original bare material. A full attack on the unprotected base material occurs: Fig. L.4.5 (c and d).

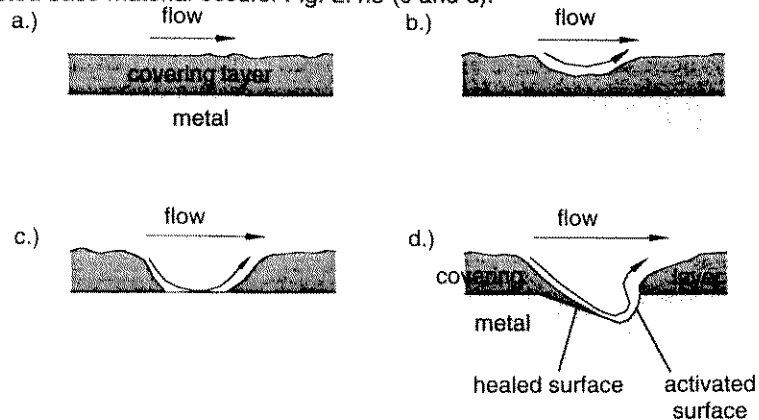


Fig. L.4.5 Flow-influenced uniform corrosion (chronological representation of the destruction of the passivation layer)

In the case of high fluid velocities, meaning a high manometric head per stage, erosion–corrosion plays a very important role. For each material there is a limiting velocity, which should not be exceeded. This limit is clearly influenced by the chemical properties of the pumped fluid, as well as by the composition of the materials used. This limit can only be determined experimentally on the basis of samples running under the same conditions (velocities and fluids) as in the pump plant. Fig. L.4.6 shows test results for the losses of different materials, as a function of the velocity for given fluid properties. The resistance to erosion–corrosion rises with a higher Cr content in the stainless steel. Based on these, the most economical choice of material can be made by the designer, with the help of experimentally obtained corrosion rates.

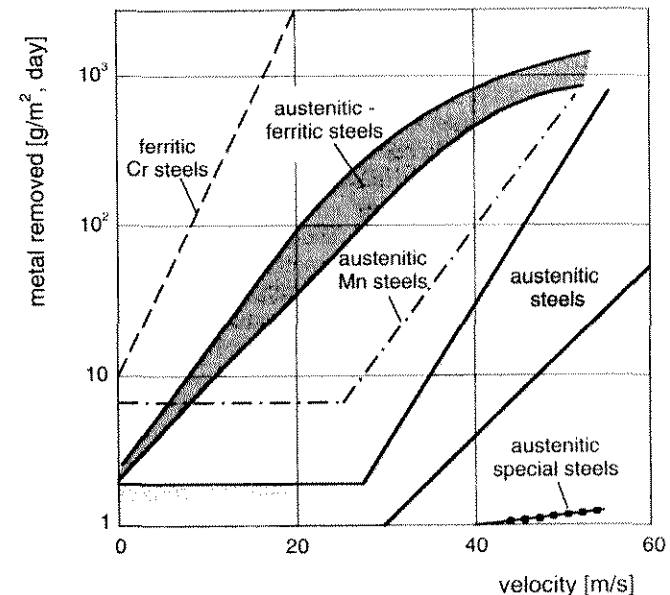


Fig. L.4.6 Erosion–corrosion rates of different steels as a function of velocity. Medium: injection water, 60°C, 270 000 mg/l dissolved salts, pH 4,5

## L.5. Selection of materials for a pump

The physical and chemical characteristics of the materials selected for the pump parts must be carefully considered in order to choose the optimum solution. If reliable performance data for the materials are not known, test samples of the same materials should be exposed to the pumped fluid, and selection based on the corrosion attack.

### L.5.1 Optimising the life cycle costs

The cost of a pump by itself is a compromise between the initial and maintenance costs. The right choice of material has an important influence on the life cycle costs (LCC), as the latter greatly influence the operating, service and repair costs. In many cases, due to a change in operational requirements, the material of the pump parts must be upgraded in order to obtain the desired life expectation. This is especially true when the chemical properties of the pumped fluid or the operational requirements (temperature, range of operation) have to be changed.

### L.5.2. Influence of the fluid properties on corrosion fatigue.

When pumping fluids with corrosive properties, the durability of the pump parts that are subjected to cyclic stresses, such as shaft or impeller, has to be considered very carefully. This is especially true when the alternating fatigue strength, based on experimental results, is constantly falling as a function of the number of cycles. For pump shafts, materials must be used whose experimentally defined endurance values on "wetted samples" are sufficiently high. This is especially important when pumping sea water or formation water. The relative alternating fatigue strength on smooth samples of shaft material in different media is shown in Table L.2.1. The negative effect of notches (caused by threads, keyways, shoulders on the shafts), which further reduce the alternating fatigue strength, must be pointed out.

### L.5.3. Influence of material properties on pitting resistance equivalent (PRE)

Pitting resistance equivalent (PRE) is an empirical relationship which describes the expected susceptibility to, or resistance against, pitting and crevice corrosion (see sections L.4.2 and L.4.3). This relationship is only applicable to stainless steels with a Cr content larger than 12%. By using stainless steels, the ability to create a stable passivation corrosion layer is ensured, and resistance to pitting and crevice corrosion rises. The PRE relationship is valid only for stainless materials such as:

- martensitic Cr- steels,
- ferritic Cr-steels,
- austenitic Cr – steels,
- duplex steels with ferritic-austenitic structure.

The relationship is as follows:

$$PRE = 1 * \% Cr + 3.3 * \% Mo + 16 * \% N$$

It can be seen from the above relationship, that the corrosion resistance (PRE) is dictated primarily by raising the content of Cr, Mo and N. The PRE should be at least 25 for low-aggressivity fluids (i.e. sea water at ~ 20°C) and at least 33 for high-aggressivity fluids (i.e. sea water at higher temperatures, formation water, fluids for desulphurisation plants with a relatively high content of chlorides). In Table L.5.2, the values for different duplex stainless steels are given, with their compositions and PRE values. These duplex steels are especially resistant to pitting and crevice corrosion type.

## L.5.4. Choice of materials for important pump elements

### L.5.4.1. Pump shaft

Pump shafts are subjected to cyclic stresses, and therefore the endurance strength must be considered when selecting the material. The following criteria must be taken in account:

- endurance limit in conjunction with the characteristics of the fluid,
- notch sensitivity of the material,
- corrosion resistance, especially PRE.

The endurance strength in a high load cycle is vital in the case of pumping sea water, formation water or similar highly corrosive fluids. Only by considering all the existing loads on the shaft, can life expectation, combined with high availability, be achieved. Recommendations for the selection of shaft materials for different fluids are given in Tables L.5.2 and L.5.3.

### L.5.4.2. Impellers

The pump impeller in particular is susceptible to all types of corrosion. The following criteria for pump impellers and diffusers should be considered:

- alternating fatigue strength for high load cycles, due to the static and dynamic forces acting on the impeller,
- corrosion resistance to all forms of corrosion,
- cavitation resistance,
- abrasive wear resistance, because of solids in the fluid,
- machining properties of the casting,
- costs.

When pumping fluids with higher temperatures (>120°C), attention must be paid to the material combination of the shaft and impeller. In multi-stage pumps especially, attention must be given to the different rates of thermal expansion of the materials. By neglecting this influence, unacceptable stresses in the shoulders of the impellers are possible, and clearances can occur between the shaft and the impeller, with the consequence of mechanical unbalance. Fluids with a certain content of solids, and pumping under cavitation conditions, cause damage to the impeller, the diffuser tips and the surfaces. The casting of these elements must be performed so as to enable the end-user to repair these parts by welding during the operational life of the pump. In such cases, the limit to the carbon content (C < 3%) in the castings must be strictly followed in order to avoid intergranular corrosion (see section L.4.5).

### L.5.4.3. Casing

The velocities in the volute, as well as in the side walls of the spiral casing, are lower than those in the impeller or diffuser passages. Due to different pump operating regimes, the approach flow angle to the casing tongue varies very much, resulting in flow separation. This effect can produce corrosion damage. The form of the tongue must be executed very carefully. The right distance between the tongue and the impeller outlet must be chosen correctly.

In selecting the material for the casing, the following points should be considered:

- Strength of the material: The spiral of a pump is a "pressure tank" that is subjected to different loads, such as transient thermal conditions during the warm up of the pump, and hydraulic shocks (water hammer).
- Corrosion and abrasive wear resistance: Standards prescribe during the design stage a well-defined additional wall thickness in order to ensure safe operation during the lifetime.
- Casting and machining properties: Special attention must be given to the casing walls if the pumped liquid also contains abrasive particles. Relatively high velocities exist in the side chambers, combined with local flow separation. The casing walls should therefore be reinforced by separate walls with a higher corrosion-erosion resistance. If necessary the original spiral walls can also be clad with hard surface coatings in order to prevent unacceptable material losses.
- Costs.

### L.5.4.4. Wearing rings

Wearing rings are a combination of a stationary ring fixed in the casing, and a rotating ring on the impeller. The primary function of these elements is to minimise the leakage losses and to ensure a good rotordynamic behaviour. The design should ensure the smallest possible gap clearances between both rings during the operational life of the pump. The resulting velocities in the gaps are high and depend on the stage head of the pump. The following must be considered when selecting the material for the wearing rings:

- galling properties,
- corrosion and abrasion resistance,
- casting and machining properties,
- costs.

In the wearing ring design and execution, the following should be considered:

- proper dimensioning of the gap in order to eliminate the touching of both rings during transient conditions,
- choice of material in order to prevent any galvanic corrosion,
- attention to the fixing of both rings if the expansion coefficients of both materials differ and transient conditions exist during pump operation,

- easy replacement of both rings,
- the entrance shape to the gap must be carefully executed in order to prevent separation at the entrance (especially important when the fluid contains solids),
- the surfaces of the stationary parts should have a serrated or honeycomb form in order to optimise the pressure losses in the gap. These executions have advantages in comparison with plain surfaces, with regard to galling. The influence of honeycomb wearing ring forms on rotordynamics is described in chapter H.3.2.

Special attention must be given to the galling resistance of both materials. As the resistance of different material combinations is often not known, the choice of materials should be based on experimental data or on experience. Generally the following can be stated:

- galling resistance is very dependent on the material combination,
- the higher the hardness of material, the better the galling property,
- the hardness difference between both materials should be larger than 50 HB,
- the galling resistance of the ring material combination is influenced by the touching velocity of the rotating ring against the stationary ring,
- hard surface coatings, executed by thermo spray or plasma flame spray process (ceramics or carbides) have a good galling resistance. But it must be ensured that the coated surface is very well bonded to the base material. This requirement is important in order to resist thermal shocks. Surface coating can only be executed on plain surfaces.

The ranking of materials from the galling danger point of view, is based on experience (starting with the highest galling resistance):

- bronzes,
- austenitic grey iron,
- hardened steels with hardness higher than ~ 300 HB,
- steels with hardness below ~ 240 HB.

### L.5.5. Materials frequently used for the wetted parts of pumps

The choice of material depends heavily on the cost implications, with two possible extremes:

- low-cost pumps, like standard pumps, having a relatively short life and often resulting in high running costs,
- high-cost pumps with special materials, in order to obtain a long life combined with relatively low running costs.

A compromise must be reached between the two extremes, depending very much on the requirements and guarantees proposed by the client, in conjunction with the life cycle costs (LCC). An overview of the possible materials to be used for the wetted parts of the pump elements is shown in Tables L.5.1 and L.5.2. No limitations due to uniform corrosion or velocity influence on the corrosion rate are given in the



above-mentioned tables. When special operating conditions and guarantees have to be fulfilled (e.g. cavitation erosion rates) in conjunction with the requirement for optimal LCC, a special pump design in combination with higher quality materials must be chosen.

Table L.5.3. shows the recommendations for the most economical choice of materials for some well-defined fluids, and for the most important elements of a centrifugal pump. Standard pump designs have clearly-defined pressure and temperature ranges, speed limits and fluid characteristics, and are frequently made of the materials shown in Tables L.5.1. and L.5.2.

Some remarks on the selection of materials for different types of water, with regard to corrosion:

**Clean non-aggressive water:** In most cases the whole pump is executed in cast iron or with an iron casing combined with bronze internals.

**Sea water (corrosive medium without H<sub>2</sub>S):** Sea water has about 75% salt content in the form of sodium chloride, consequently the pH value is usually between 7,5 and 8,5. Cast iron is only to be used for the casing at very low flow velocities. Unalloyed steels should not be used. Ni-resist can be used for the pump parts, but only up to flow velocities of about 20 m/s. Sn-bronze or Al-bronze with a high resistance to pitting corrosion can be used up to about 30 m/s.

**Sea water with H<sub>2</sub>S content:** Cast Cr steels with a higher Cr content should not be used, as they are susceptible to local corrosion attacks, and the PRE is lower than 20. For sea water with elevated temperatures, materials with a higher PRE should be used, such as austenitic Cr-Ni steels with a PRE  $\geq 25$ . For sea water with a high content of chlorides and H<sub>2</sub>S, and with low pH values, austenitic-ferritic duplex steels with a PRE  $\geq 33$  should be used (see also Table L.5.2). Recommendations for other fluids are given in Table L.5.3.

	designation DIN 17006 (EN 10027-1)	material nr. DIN 17007 EN 10027-2	specification ASTM	designation ASTM
cast iron	GG 25	0.6025	A 48	Class 40
cast iron	GGG 40	0.7040	A 536	Grade 60-40-18
cast iron	GGG 50	0.7050	A 536	Grade 60-45-12
austen. cast iron, Ni-resist	GGL-NiCr 20 2	0.6660	A 436	Type 2
cast steel	GS-C 25	1.0619	A 216	Grade WCB
cast steel	GS-17 CrMoV 5 11	1.7706	A 356	Grade 9
steel-non cast	CK 45	1.1191	A 108	Grade 1045 A 576
Cr steel-non cast	X 20 Cr 13	1.4021	A 276	Type 420
cast Cr steel	G-X 5 CrNi 13 4	1.4313	A 743	Grade CA-6NM A 757
cast Cr steel	G-X 5 CrNiMo 16 5	1.4405	A 743	Grade CA-6NM
CrNi steel-non cast	X 2 CrNi 18 9	1.4306	A 276	Type 304 L
cast CrNi steel	G-X 6 CrNi 18 9	1.4308	A 351	Grade CF8 A 741
CrNi steel-non cast	X 2 CrNiMoN 18 12	1.4406	A 276	Type 316 LN
cast CrNi steel	G-X 6 CrNiMo 18 10	1.4408	A 351 A 743	Grade CF8M
cast CrNi steel	G-X 7 CrNiMoNb 18 10	1.4581	A 351	Grade CF-10MC
duplex steel-non cast	X 8 CrNiMo 27 5	1.4460		
duplex steel-non cast	X 2 CrNiMoN 22 5	1.4462	A 276	Grade XM-26
cast duplex steel	G-X 3 CrNiMoN 26 6 3	1.4468	A 743	Grade CD-4M
cast NiCrMo steel	G-X 7NiCrMoCuNb 25 20	1.4500	A 351 A 743	Grade CN-7M
cast Sn bronze	G-CuSn 10	2.1050.01	B 427	C 90700
cast Al bronze	G-CuAl 10 Ni	2.0975.01	B 148	C 95800

Table L.5.1 Designations of frequently used materials for pump parts

material nr. DIN 17007 EN 10027-2	pitting resistance equivalent PRE	0,2 yield limit (N/mm <sup>2</sup> )	application for pump parts
0.6025		230	impeller, wear ring, cover
0.7040		250	casing, impeller
0.7050		320	casing, impeller
0.6660		210	casing, impeller
1.0619		245	casing
1.7706		440	casing
1.1191		310	shaft, wear ring
1.4021	12 – 14	450	shaft, wear ring
1.4313	12 – 14	540	casing, impeller, diffuser
1.4405	17 – 23	540	casing
1.4306	17 – 20	205	shaft
1.4308	17 – 20	175	casing, impeller
1.4406	23 – 33	280	shaft
1.4408	24 – 28	175	casing, impeller, wear ring
1.4581	24 – 27	185	casing, impeller, wear ring
1.4460	30 – 34	450	shaft, wear ring
1.4462	30 – 35	450	shaft
1.4468	32 – 36	450	casing, impeller, diffuser
1.4500	27 - 33	185	casing, impeller, wear ring
2.1050.01		130	casing, impeller, diffuser
2.0975.01		270	impeller, diffuser

Table L.5.2 Recommendations for materials for different pump parts

material nr. DIN 17007 EN 10027-2	wear ring	casing	impeller diffuser	shaft
clean water	0.6025 0.7040	0.6025 0.6025	0.6025 2.1050.01	1.1191
sea water without H <sub>2</sub> S	2.1050.01 0.7040	0.6025 0.7040	2.1050.01	1.4306
salt water (small amount of Cl) pH ~ 7,5 ÷ 8,5	2.1050.01	0.6025	2.1050.01	1.4306
water from underground, formation water for injection pH ≥ 5,0	1.4460	1.4500	1.4500	1.4460
boiler feed (O <sub>2</sub> free) T ≤ 180°C	1.4313	1.4313	1.4313	1.4306
condensate water, softened and demineralised	2.1050.01	0.6025	2.1050.01	1.1191
sewage water	2.1050.01 0.6025	0.7040 1.0619	0.6025 2.1050.01	1.1191
hydrocarbons, fuel, lubricant, paraffin, propane (cold)	1.1191 0.6025	0.7040 1.0619	0.6025 2.1050.01	1.1191
crude oil (hot)	1.0619	1.0619	1.0619	1.1191

Table L.5.3 Material selection table for the most economical execution of centrifugal pumps (single-stage with spiral casing; multi-stage with diffuser)

## M. QUALITY ASSURANCE

### M.1 General

The Quality Assurance Policy of the whole Termomeccanica Group is underlined in the following Management Commitment:

"The Quality Assurance System of the Termomeccanica Group has been established with the aim of directing all the Companies of the Group to implement specific QA programs in compliance with the present Management Commitment. In order to maintain the highest competitiveness on the market, the Management of the Termomeccanica Group is fully aware of the necessity to continuously improve the performance of the products as well as of the services and the organisational structure.

Following on from this commitment, the Quality Assurance programs of the Companies shall adhere to the following basic guidelines:

- The Companies shall recognise QUALITY to be the main target of their activities.
- Efforts to assure total Customer satisfaction in terms of performance and reliability shall be a permanent key factor in all the Companies' processes.
- The fundamentals for continuous improvement shall be strictly applied by all employees; each of them is responsible for acting in agreement with such fundamentals.
- The Company shall promote a culture change in people towards the criteria of "Certified Quality Programs".

The Quality Assurance Programs of Termomeccanica Group as well as the ones of the Companies shall comply with ISO 9001 or ISO 9002."

### M.2. Quality Assurance of TM.P S.p.A. - Termomeccanica Pompe

The Quality Assurance Program of TM.P. S.p.A has been designed in compliance with the requirements of Standard UNI EN ISO 9001, 1994 edition, and was certified by Lloyd's Register at the beginning of 1996. Through yearly audits the same organisation confirms the validity of the system. The rules of the Quality Assurance System are described in the following documents:

- Company Quality Manual,
- Procedures,
- Operating Instructions.

All the activities and processes of the company are governed by the above documents which also define the relevant responsibilities.

Major topics in the Quality Assurance Program:

#### Design and Engineering

For each specific job the design and engineering process are defined and planned in a suitable document, issued by the Project Engineer appointed for the work; this document is reviewed by the Quality Engineer and the Project Manager. From this document the Project Engineer identifies the various stages of the design process, and makes sure that all input data and technical requirements are fully identified and available, including quality and safety requirements. In addition, the persons responsible for the different processes are assigned, the internal and external interface organisations are specified, warning points are highlighted and design verifications or validations planned where necessary. For very large and/or critical projects the company management can require the job to be governed by a specific Quality Plan.

#### Quality Plan

The Quality Plan is a document prepared by the Project Manager in cooperation with the QA Manager with the aim of defining the working team, responsibilities, and procedures to be applied in a particular project, in order to conform the standards of the Quality Assurance Program to the special requirements of the contract.

#### Quality Control Plan

The Quality Control Plan is the document listing the destructive and non-destructive examinations to be carried out during manufacturing on the main parts of the pump as well as on sub-assemblies (rotor, pressure boundaries, etc.) and the fully assembled unit, with reference to the applicable technical specifications and acceptance criteria. Hold points, witnessed tests and quality certificate issues are specified on this document.

Three different quality levels can be applied, depending on the severity of the operating conditions, on critical matters of the design, and on contractual requirements.

A sample of a Quality Control Plan is shown in Fig.M.2.1.

#### Procurement and Logistics

Procurement and logistics are governed by procedures and working instructions which ensure a proper supply management system (suppliers' qualification records, vendor rating, etc.), including handling, storage, traceability, packing and transportation of materials.

#### Manufacturing, Assembling and Performance Tests

In compliance with the applicable Quality Control Plans, manufacturing, assembling and testing are carried out in the workshop through detailed work-sheets, which specify methods and machining tools to be used, measurements and instrumentation, and records and certificates to be made available.

The calibration of instruments is carried out according to specific instructions, and certified by adequate documents issued, at regular intervals, by the Quality Control Department.

Pump type: Material status: a - C : Casting F : Forged R : Rolled B : Bar b - G : Raw P : Premachined M : Machined	TM.P. quality Class:			
	Component	Mat.	Assembled pump	
	1	C	H	T
	2	A	T	T
	3	T	T	T
	4	I	H	D
	5	H	V	E
	6	V	D	E
	7	D	E	C
	8	R	C	C
	9	D	P	P
	10	M	T	T
	11	U	E	E
	12	R	E	E
	13	H	Y	Y
	14	D	B	B
	15	R		
	16	P		

○ without certification  
● with certification

□ customer approval not required  
■ customer approval required  
♦ witnessed test

Remarks:

1 - inspection on the machined surfaces only  
2 - run-out check

Fig. M.2.1 Example of a Quality Control Plan

## N. TESTING

### N.1. Hydrostatic tests

The aim of a hydrostatic test is to check that a pump will not leak or fail structurally when subjected to hydrostatic pressure. Each part of the pump which contains fluid should be able to withstand the test pressure. Several standards exist which define test parameters and procedure.

According to API 610/8 and ANSI/HI 1.6/94 the test should be conducted on either the assembled pump or on the pressure-containing parts. This means that double-casing pumps, horizontal multi-stage pumps, and other designs of pumps may be segmentally tested with different pressures. The gaskets used during the hydrostatic testing of an assembled pressure casing must be of the same design as those to be supplied with the pump. Provision should be made to vent all the air in the tops of the items.

The test pressure prescribed by API is 150% of the maximum allowable pressure for which the part is designed, when operating at the maximum allowable temperature. According to ANSI/HI 1.6/94 the greater of the two pressures should be taken for hydrostatic tests: 150% of the maximum allowed working pressure (same as API) or 125% of the pressure which would occur with a closed discharge valve. In all cases suction pressure must be taken into account. If the part tested has to operate at a temperature at which the strength of the material is below its strength at room temperature, the hydrostatic test pressure must be multiplied by a factor obtained by dividing the allowable working stress for the material at room temperature by that at operating temperature.

The test pressure should be maintained for a sufficient period of time to permit complete examination of the parts under pressure. The hydrostatic test will be considered satisfactory when no leaks or structural failures are observed for a minimum of:

- 30 min - API
- 3 min (pumps under 75 kW) or 10 min (pumps over 75 kW) - ANSI/HI

### N.2. Performance and NPSH tests

#### N.2.1. General

Performance and NPSH tests deal with the pump only, and not with the complete pump unit. Normally they are performed for one of the following purposes:

- research and development,
- acceptance tests - checking of contractual guarantees.

They can be divided in the following way:

#### Model tests

Test rigs for model testing usually have a high measuring accuracy. Models are tested for the following purposes:

- development of new designs; a comparison of the performances of several models is possible,
- with model acceptance tests the pump purchaser gets an assurance that guarantees are being met; they can replace shop and field tests

Model acceptance tests are practical, because they precede the final design of the prototype; they provide an advance assurance of performance and make alterations possible in time for incorporation in the prototype unit. The model should have a complete geometric similarity to the prototype in all wetted parts between the intake and discharge sections of the pump. Model tests are performed with clean cold water. If the real fluid pumped by the prototype (actual) pump is different, correction of the characteristics is needed (see sections N.2.5 and section K). To get satisfactory results, the minimum model impeller outlet diameter is  $D_2 = 300$  mm, minimum Re number related to  $D_2$   $Re = 3 \cdot 10^6$ , and the ratio between the prototype and model Re numbers should be less than 15. In high head pumps ( $H_{st} \geq 600$  m), cavitation bubble patterns for the suction stage can also be determined in model tests. From the cavitation bubble length obtained by visual observation an impeller lifetime guarantee can be given (see section C).

#### Shop tests

These are performed in the pump manufacturer's laboratory under controlled conditions and are usually assumed to be the most accurate tests. They are also called laboratory or factory acceptance tests. According to different standards, the pump may be tested at a lower or higher speed if the test cannot be run at the rated speed, due to power limitations, electrical frequency or other reasons. Regarding guarantees for vibration (bearings or shaft), a shop test can give only indicative results, as the latter are influenced by the rigidity of the fixing of the pump to the elastic foundation of the test bed. See also section H.

#### Field tests

Field tests are performed on site during normal operation. The accuracy and reliability of field-testing depend on the instrumentation used and the installation. During the design phase of the installation it is important to consider also the possibilities for pump testing. The suction and delivery pipelines should be of sufficient length to create adequate conditions for static pressure measurements. Nowadays many pumping stations are already equipped with flowmeters. If mutually agreed, field tests can be used as acceptance tests.

Field tests are often performed periodically to assess the pump's condition as a

function of operating time in order to discover the effects of wear or of a change in the system characteristic. It is important that tests are always carried out by the same instruments and according to the same procedure.

In order to simplify understanding between the pump manufacturer and the purchaser, and to reduce the extent of the part of the agreement concerning testing, the test procedures are written down in different Standards. Requirements or recommendations about the following topics are contained in various Standards:

- terminology and definitions
- test arrangements (closed and open test rigs for performance and NPSH tests etc.)
- test conditions (fluid and temperature – usually clean cold water, rotational speed, stability of operation – permissible fluctuations in readings etc.)
- instruments and permissible measuring uncertainties,
- calculation of test results to the guarantee conditions
- verification of guarantees
- test report

Standards usually define three quality classes regarding acceptance criteria and measuring accuracy:

- Precision Class – high level: mainly used for research, development and scientific work in laboratories, usually not used as an acceptance test code; exceptions are very big pumps (over 10 MW), where Engineering Grade 1 is too inaccurate
- Engineering Grade 1 – middle level: acceptance tests for pumps between 0,5 and 10 MW
- Engineering Grade 2 – low level: standard pumps manufactured in series; type testing

The Standards for centrifugal pump acceptance tests of Grades 1 and 2 are, for example:

- ISO 9906
- ANSI/HI 1.6 and 2.6 (Vertical pump tests)
- DIN 1944

Model acceptance tests are usually carried out according to special Standards, where tolerances regarding the geometric similarity between model and prototype are also defined (for example JIS B 8327 or IEC 497). Model pump performance and NPSH characteristics are often accepted according to one Standard (for example ISO 9906), while geometry control is carried out according to another (for example IEC 497).

#### **N.2.2. Testing arrangements**

Testing arrangements can be basically divided into closed and open systems. A typical closed system test rig for performance and NPSH tests is in Fig. N.2.1. The pump being tested sucks water from a suction tank, which should be volumetrically large enough, through a suction pipe of a minimum length of 7 D. In order to obtain a swirl-free flow into the pump, and symmetrical velocity and uniform static pressure distribution, one or more flow straighteners should be installed. The instru-

ment for measuring the suction pressure should be suitable for measuring the complete range of suction pressures, whether positive or negative. On the discharge side an instrument is installed for measuring the discharge pressure. A flowmeter is installed in the discharge pipe. The required length of straight pipe in front of the flowmeter depends on the flowmeter, and should be long enough, and usually a flow straightener is required additionally. A control valve or similar device should be installed to change the tested pump operating point. NPSH testing is provided by lowering or raising the suction pressure. Connections from the suction tank to the vacuum pump, or to compressed air (or gas, usually nitrogen) are fitted for changing the suction pressure. The NPSH range for closed systems is unlimited. During the testing of an NPSH below 4 m there is a danger that air coming out of the water could influence the results. It is advisable to run the test rig at a low NPSH for about one hour before beginning the test. Any dissolved air has to be sucked out by means of a vacuum pump.

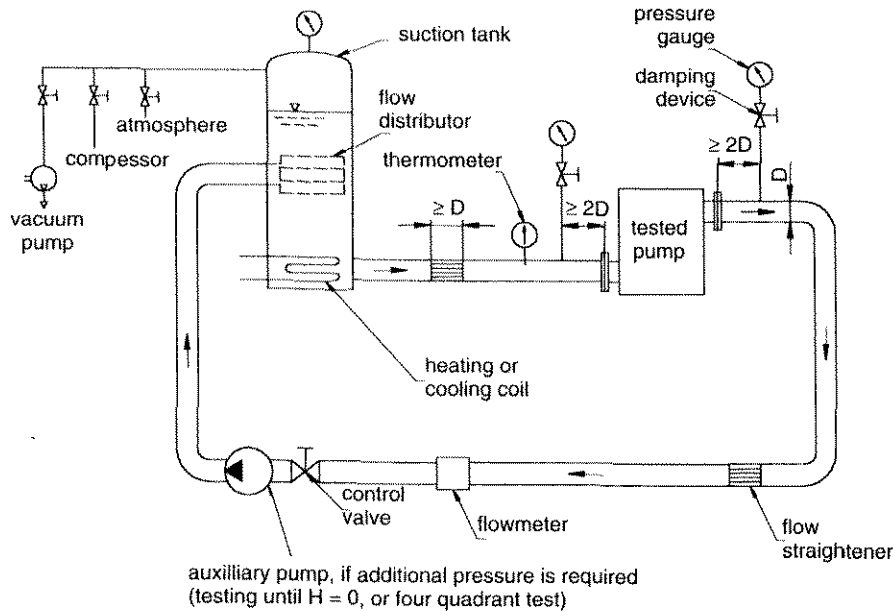
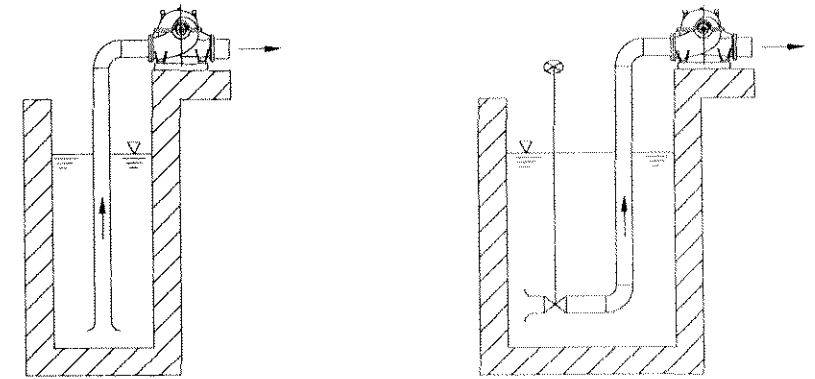


Figure N.2.1 Closed system test rig

If the test rig is an open system, the pump suction pressure is decreased either by lowering the water level in the suction sump or by throttling on the suction side (Fig. N.2.2). The highest NPSH level is limited to about 8 m and the lowest to about 2 m. In the case of throttling by a valve on the suction side, the valve should be executed without pressure recuperation in order to prevent cavitation. Otherwise the danger would exist of the air in the valve dissolving due to under-pressure, which could influence the NPSH values measured.

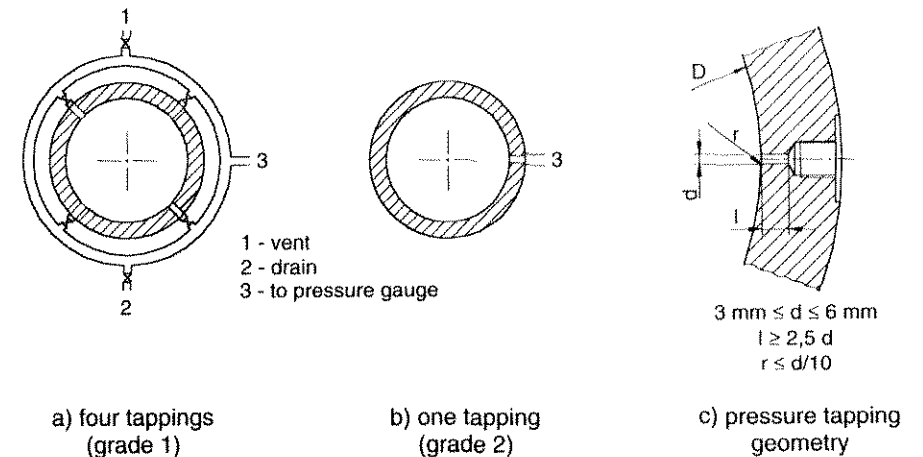
An ISO Standard prescribes the distance between pump suction and discharge flanges and pressure tapplings: it should be 2 pipe diameters for Grade 1; for Grade 2, pressure tapplings may be located on the flanges themselves, if the kinetic part of the total head is not too high. To minimise the influence of asymmetrical flow conditions, instruments for pressure measurement should be connected to the pipe through four tapplings for Grade 1, while for Grade 2 one pressure tapping is enough (Fig. N.2.3).



a) varying of water level

b) throttling

Figure N.2.2 Open system test rig - varying of suction pressure



a) four tapplings (grade 1)

b) one tapping (grade 2)

c) pressure tapping geometry

Figure N.2.3 Pressure tapplings

$3 \text{ mm} \leq d \leq 6 \text{ mm}$   
 $l \geq 2,5 d$   
 $r \leq d/10$

Standard ANSI/HI 2.6 describes the testing of vertical centrifugal pumps. Prototype pumps are usually tested in an open system test rig (Fig. N.2.4). Industrial practice is to permit the testing of the bowl assembly for hydraulic performance, since test pit depth limitations, discharge head, physical constraints like elbows, etc. make the testing of complete pumps impractical. It is important, especially for pumps operating at high flow rates and low heads, that the test inlet conditions are as similar to actual operating conditions as possible. In order to prevent disturbances due to a return flow to the sump, the recommendations from section J.1. (pump intakes) should be followed. It is important that the outlet of the discharge pipe is always under the water level. When test facility limitations do not permit full stage testing, it is permissible to perform reduced stage tests. The closed loop test rigs are used when model rather than prototype testing is performed.

If acceptance tests are being performed according to a particular Standard, the selection of measuring instruments is given in it. If mutually agreed by both parties, it is also possible to introduce other measuring instruments and procedures.

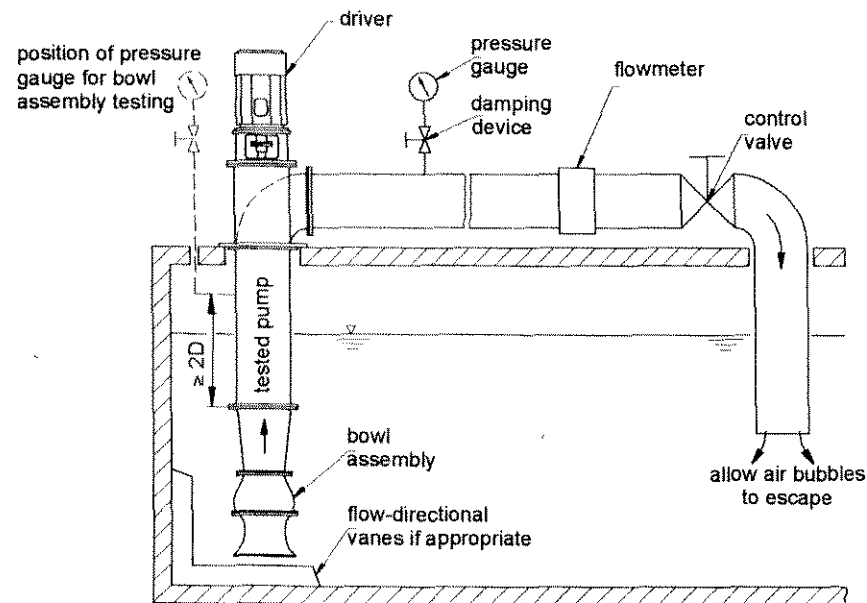


Figure N.2.4 Vertical pump testing

**N.2.3. Measuring accuracy, permissible reading fluctuations and performance tolerances**

EN ISO Standard Accuracy grade	9906 (1999) Grade 2	Grade 1	5198 (1987) Precision class
Permissible amplitude of fluctuations as a percentage of mean value:			
• flow rate, total head, torque, power	± 6%	± 3%	± 3%
• speed of rotation	± 2%	± 1%	± 1%
Permissible values of overall measurement uncertainties:			
• flow rate Q	± 3.5%	± 2.0%	± 1.5%
• speed of rotation n	± 2.0%	± 0.5%	± 0.2%
• torque M	± 3.0%	± 1.4%	-
• pump total head H	± 5.5%	± 1.5%	± 1%
• driver power input $P_{gr}$	± 5.5%	± 1.5%	-
• pump power input P (computed from torque M and speed of rotation n)	± 5.5%	± 1.5%	± 1%
• pump power input P (computed from driver power $P_{gr}$ and motor efficiency $\eta_{mot}$ )	± 4.0%	± 2.0%	± 1.3%
• pump efficiency $\eta$ (computed from Q, H, M and n)	± 6.1%	± 2.9%	± 2.25%
• pump efficiency h (computed from Q, H, $P_{gr}$ and $\eta_{mot}$ )	± 6.4%	± 3.2%	± 2.25%
Tolerance factors*:			
• flow rate - $t_Q$	± 8%	± 4.5%	-
• pump total head - $t_H$	± 5%	± 3%	-
• pump efficiency - $t_\eta$	- 5%	- 3%	-
• $NPSH_{req} - t_{NPSH_{req}}$ : greater between	+ 6% or + 0.30 m	+ 3% or + 0.15 m	-

\* To simplify the verification of guaranteed values, tolerance factors are introduced. In tolerance factors the overall measuring and manufacturing uncertainties are incorporated (see section N.2.4).

Table N.2.1 Measuring accuracy, permissible reading fluctuations and performance tolerances according to EN ISO Standards

ANSI/HI Standard Accuracy grade	1.6 and 2.6 (1994)	
	Grade A	Grade B
Permissible amplitude of fluctuations as a percentage of mean value:		
• flow rate, differential head, suction head, discharge head, pump power input	± 2%	
• speed of rotation	± 0.3%	
Permissible values of overall measurement uncertainties:		
• flow rate Q	± 1.5% (1% for vertical pumps)	
• speed of rotation n	± 0.3%	
• differential head H	± 1.0%	
• discharge head HT	± 0.5%	
• suction head HS	± 0.5%	
• pump power input P	± 1.5% (0.75% for vertical pumps)	
Head tolerances at rated capacity:		
• H < 60 m, Q < 680 m <sup>3</sup> /h	+ 8%, - 0	+ 5%, - 3%
• H < 60 m, Q > 680 m <sup>3</sup> /h	+ 5%, - 0	+ 5%, - 3%
• 60 m < H < 115 m, any Q	+ 5%, - 0	+ 5%, - 3%
• H > 115 m, any Q	+ 3%, - 0	+ 5%, - 0
• minimum efficiency	$\eta_P^*$	$\frac{100}{120/\eta_P^* - 0.2}$
Flow rate tolerances at rated head:		
• flow rate	+10%, - 0	+ 5%, -5%
• minimum efficiency	$\eta_P^*$	$\frac{100}{120/\eta_P^* - 0.2}$

\*  $\eta_P$  is the contract pump or unit efficiency for Grade A, and the published nominal efficiency for Grade B

For vertical pumps only Grade A performance tolerances (head or flow rate and efficiency) are valid.

Table N.2.2 Measuring accuracy, permissible reading fluctuations and performance tolerances according to ANSI/HI Standards

API	610/8	Shut-off
Performance tolerances:	Rated point	
• H < 150 m	+ 5%, -2%	+10%, -10%
• 150 m < H < 300 m	+ 3%, -2%	+8%, -8%
• H > 300 m	+ 2%, -2%	+5%, -3%
Rated power	+ 4%	-
Rated NPSH <sub>req</sub>	+ 0%	-
Efficiency is not a rating value and is for information only		

According to Standard API 610/8, performance and NPSH tests should be conducted in accordance with the Hydraulic Institute (HI) Standards.

Table N.2.3 Performance tolerances according to Standard API 610/8

#### N.2.4. Fulfilment of guarantee

According to Standard EN ISO 9906, the test results should be converted to the specified speed (see section N.2.5.).

A tolerance cross with the horizontal line  $\pm t_Q \cdot Q_G$  and the vertical line  $\pm t_H \cdot H_G$  is drawn through the guarantee point  $Q_G, H_G$  (Figure N.2.5.). The guarantees of the head and flow rate are met if the Q-H curve cuts, or at least touches, the vertical and/or horizontal line.

The efficiency should be derived from the measured Q-H curve where it is intersected by a straight line passing through the specified duty point  $Q_G, H_G$  and the zero of the Q and H axes, and from where a vertical line intersects the Q- $\eta$  curve. The guarantee condition on efficiency is within tolerances if the efficiency value at this point of intersection is higher or at least equal to  $\eta_G \cdot (1 - t_\eta)$ .

The NPSH guarantee is met if one of the following formulas is valid:

$$\bullet (NPSH_{req})_G + t_{NPSH_{req}} \cdot (NPSH_{req})_G \geq (NPSH_{req})_{measured}$$

$$\bullet (NPSH_{req})_G + (0.15 \text{ m, respectively } 0.3 \text{ m}) \geq (NPSH_{req})_{measured}$$

For performance tolerances see section N.2.3.



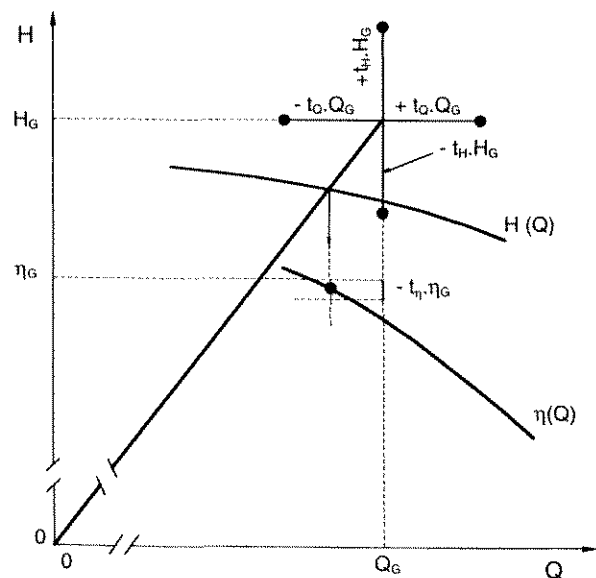


Figure N.2.5 Verification of guarantee on flow rate, head and efficiency according to Standard EN ISO 9906

According to Standards ANSI/HI and API, guarantees are fulfilled if at rated capacity the pump head, power and efficiency are within prescribed tolerances, or at rated flow rate the head, power and efficiency are within tolerances (see section N.2.3).

**N.2.5. Conversion of test results**

Pump characteristics are generally measured under conditions more or less different from those on which the guarantee is based. In order to determine whether the guarantee would have been fulfilled if the tests had been conducted under the guarantee conditions, it is necessary to convert the values measured under different conditions to those measured under guarantee conditions.

EN ISO 9906 states that, unless specified in the contract, tests may be carried out at a speed of rotation within the range of 50% to 120% of the specified speed, in order to establish the flow rate, pump total head and power input. However, it should be noted that when departing by more than 20% from the specified speed of rotation, the efficiency may be affected. For NPSH tests, the speed of rotation should lie within the range of 80% to 120% of the specified speed of rotation. The measured data (index 1) can be converted to specified speed of rotation (index 2) and density by means of the following equations:

Prototype pump acceptance test	Model pump acceptance test
$Q_2 = Q_1 * \left(\frac{n_2}{n_1}\right)$	$Q_2 = Q_1 * \left(\frac{n_2}{n_1}\right) * \left(\frac{D_2}{D_1}\right)^3$
$H_2 = H_1 * \left(\frac{n_2}{n_1}\right)^2$	$H_2 = H_1 * \left(\frac{n_2}{n_1}\right)^2 * \left(\frac{D_2}{D_1}\right)^2$
$P_2 = P_1 * \left(\frac{n_2}{n_1}\right)^3 * \left(\frac{\rho_2}{\rho_1}\right)$	$P_2 = P_1 * \left(\frac{n_2}{n_1}\right)^3 * \left(\frac{D_2}{D_1}\right)^5 * \left(\frac{\rho_2}{\rho_1}\right)$
$NPSH_2 = NPSH_1 * \left(\frac{n_2}{n_1}\right)^x$	$NPSH_2 = NPSH_1 * \left(\frac{n_2}{n_1}\right)^2 * \left(\frac{D_2}{D_1}\right)^2$
$\eta_2 = \eta_1$ or acc. to efficiency correction formula	$\eta_2$ or acc. to efficiency correction formula

Exponent x =2 may be used, if the speed of rotation is within acceptable limits and the physical state of the liquid at the impeller inlet is such that no gas separation can affect the operation of the pump. If the pump operates near its cavitation limits, or the deviation of the test speed from the specified speed is too high, values for exponent x of between 1,3 and 2 have been observed, and an agreement between the two parties is needed to establish the conversion formula (EN ISO 9906).

Efficiency correction formulas

Because of differing percentages of hydraulic, volumetric and mechanical losses in the total pump efficiency, due to different conditions in the test and during operation, it may be agreed in the contract that the efficiency can be converted according to one of the correction formulas for hydrodynamic machines, for the following reasons:

- the deviations in speed of rotation during the test are greater than allowed in the standards
- the viscosities of the liquids pumped in the test and in operation are different because of different fluid temperatures or different fluids
- the acceptance tests are performed on model pumps, so pump and prototype diameters are different. The efficiency of the model will not be exactly equal to that of the prototype. For example, the relative surface roughness is different (different hydraulic efficiency), the running clearances and bearing sizes are usually not modelled (different volumetric and mechanical losses).

All the efficiency correction formulas are applied solely for the best efficiency point. The following are used most often:

ANSI/HI:  $\eta_2 = 1 - (1 - \eta_1) * \left(\frac{v_2}{v_1}\right)^y * \left(\frac{D_1}{D_2}\right)^w$  y = 0,05 to 0,1; w = 0 to 0,26

The formula considers variations in temperature of the liquid pumped during tests and in operation, causing changes in viscosity (coefficient  $y$ ), and the different diameters for the model and prototype pumps (coefficient  $w$ ). The selection of coefficients  $y$  and  $w$  should be mutually agreed between the pump manufacturer and the purchaser, and should be based on all available test data of a similar nature, usually according to the pump manufacturer's experience.

$$\text{Karassik: } \eta_2 = \eta_1 * \left( \eta_1 + \left( (1 - \eta_1) * \left( \frac{n_1}{n_2} \right)^{0.17} * \left( \frac{v_2}{v_1} \right)^{0.07} \right) \right)^{-1}$$

This formula is not convenient for model tests. It is often used when guarantees for the prototype pump cannot be tested at full speed and operating temperature, due to test rig limitations. The increased efficiency is calculated on the basis of the measured total efficiency obtained at different speeds and temperatures, and also includes improvements for different losses which are not influenced by the Re number.

$$\text{Hutton: } \eta_2 = 1 - (1 - \eta_1) * \left( 0.3 + 0.7 * \left( \frac{D_1}{D_2} \right)^{0.4} * \left( \frac{n_1}{n_2} \right)^{0.2} * \left( \frac{v_2}{v_1} \right)^{0.2} \right)$$

The Hutton formula deals with internal efficiency (see section A), because it is based on the reduction of the losses related to the Re number only – hydraulic and volumetric losses. The efficiency improvement does not include changes in mechanical losses, which should be evaluated separately, and total efficiency should be corrected accordingly.

### N.3. Optional tests

If specified, additional tests can be carried out during model, shop or field tests. The details must be mutually agreed by the pump manufacturer and the purchaser.

- **Complete unit test:** the pump and driver train, complete with all auxiliaries that make up the unit, should be tested together.
- **Three quadrant characteristics:** these are needed for water hammer calculation, and are usually performed during model testing.
- **Dry-running and thermal shock test:** to verify transient conditions on boiler feed water pumps.
- **Sound level test** (see section G)
- **Axial thrust** (see section F): the axial thrust should be measured on all model pumps which are the basis for prototype pumps. It is also recommended to measure the axial thrust in prototype pumps during shop tests. A guarantee is often given for special versions of bigger pumps for the direction and maximal amount of the axial thrust. The measurement must demonstrate the fulfilling of the guarantees. It is usually performed on a test stand at the same time as the performance test, but field-testing is also possible.
- **Radial thrust** (see section F)
- **Vibration** in bearing housing or shaft (see section H) and bearing temperature.

## O. LIFE CYCLE COSTS

### O.1 Introduction

In most pumping systems, although the pump represents one of the installed components which has relatively low investment costs, it influences decisively the availability and economy of the whole system. It is therefore understandable that in the future the end-user will pay greater attention to the machine, although a pump is characterised as a technically mature product.

More attention will be given in future to reducing the life cycle costs (LCC), which represent the total cost in the whole lifetime of the pump. The question of the relevant cost elements of the LCC of the pumping system must therefore be clarified, and the main influencing factors must be stated, as considerations of the LCC have a great influence on the total business process. This influences not only the philosophy on the user side, but also on the side of the pump manufacturer, as well as decisions in the procurement process. Today procurement decisions are mostly based on the initial investment costs, which often represents only about 10-20% of the total LCC. In future, in order to obtain the optimal pumping system, initial investment costs will no longer be decisive. Life cycle costs (LCC) will become the deciding factor.

This guide, produced by the Hydraulic Institute and Europump, gives a complete model for estimating the total costs for the life cycle of a pumping system (LCC), including all the important pump parameters, as well as those for the associated auxiliary equipment.

It is to be expected that users will pay more attention to the guidelines for determining the LCC. However, the application of LCC requires a very radical rethinking by all the participants who influence the planning of pumping systems. Not only engineers and purchasers, but also end-user managers are responsible for production, maintenance and repair. The optimisation of the pumping system from the LCC point of view means not only minimising the pressure losses in the piping system, and maximising the efficiency in order to save energy costs, but also making the best choice of pump design, which would require a minimum need for spare parts service, and also require the shortest repair times.

During the procurement phase, the LCC can be optimised by comparing the individual cost elements for different alternatives with well-defined operating data for the pumping system. Based on these results, it is possible to decide on the optimum type of centrifugal pump and associated equipment to be purchased. As

direct relationships do not exist between the different elements of the LCC that influence the economy of the pumping system, the contribution of each element to the reduction in the total cost has to be considered.

## O.2 Elements of LCC and their definitions

### O.2.1 Calculation of life cycle costs

Based on the study by Europump and the Hydraulic Institute, the following cost elements determine the life cycle costs - LCC:

$$LCC = C_{ic} + C_{in} + C_e + C_o + C_m + C_s + C_{env} + C_d$$

LCC elements are also shown graphically in Fig. O.2.1.

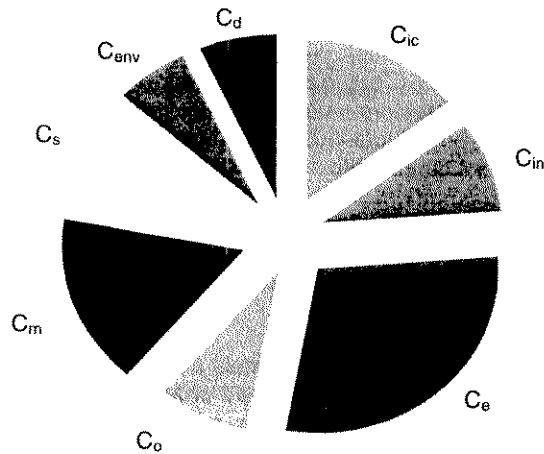


Figure O.2.1 Elements of LCC

### O.2.2 Description of LCC elements

**$C_{ic}$  - Initial investment costs of the pump, pumping system, piping and auxiliary services**

The layout of the pumping system is one of the most important factors of the initial investment costs  $C_{ic}$ . For installations with a long pipe length especially, the pipe, valve and fitting diameters are of decisive importance, since they have a big influence on the material costs. The smaller the pipe diameter, the higher the pump power input must be, due to higher pressure losses. This results in higher energy consumption, and therefore leads to higher energy costs  $C_e$ . An example of the distribution of the energy costs  $C_e$  and the initial investments costs  $C_{ic}$  for different pipeline diameters  $D$  is shown schematically in Fig. O.2.2.

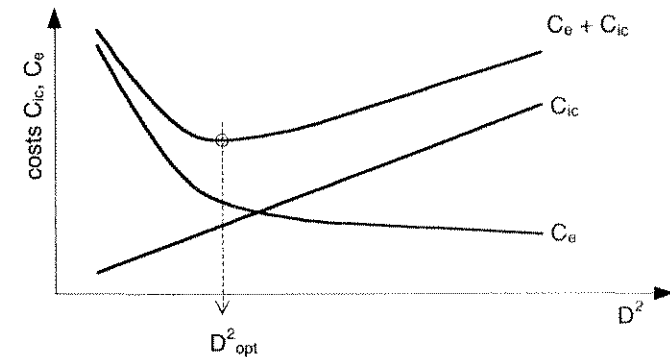


Fig. O.2.2 Comparison of initial investment costs  $C_{ic}$  and energy costs  $C_e$  for different pipeline diameters  $D$

An additional important factor is the correct choice of material for all the equipment, depending on the properties of the pumped fluid. This can be of decisive importance for the wear rates of the pump elements, due to possible corrosive or abrasive attacks by the fluid.

The initial investment costs  $C_{ic}$  must also involve all the auxiliary services. This is especially important when scarce resources are involved.

**$C_{in}$  - Installation costs including the costs of space required for the pumping station**

The possibility of dividing the pumping work among several pumps allows not only the optimisation of the energy costs  $C_e$ , but also of the space requirements for the station and the necessary excavation costs. Another parameter which influences the installation costs  $C_{in}$  is pump rotational speed (see example in Fig.O.2.3). With a rising pump speed  $n$  the pump submergence, and with this the requirements regarding  $NPSH_{av}$ , also increase. Increased submergence means deeper excavation for the pumping station and consequently higher installation costs  $C_{in}$ . On the other hand, raising the pump speed means a smaller pump, and thus reduced initial investment costs  $C_{ic}$  for pumps and motors. The choice of pump speed  $n$  is directly connected with pump specific speed  $nq$  and defines the pump's basic hydraulic design. Each pump type has a region of  $nq$  which is optimal from the efficiency point of view. In this region the energy consumption, and with this the energy costs  $C_e$ , are minimal. Outside this region the energy costs are higher (see Fig. O.2.3).

In addition, installation costs  $C_{in}$  must also include the use of special tools, as well as the necessary equipment for installing and repairing the pump and its auxiliary elements.

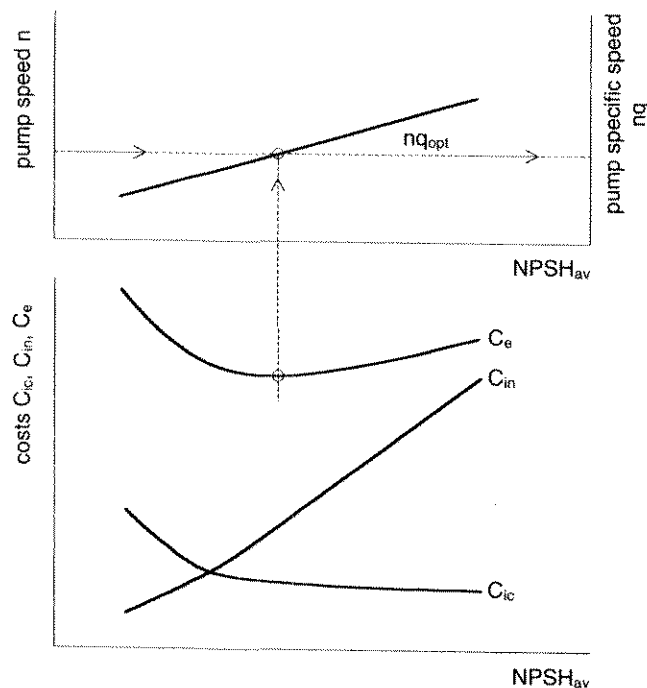


Figure O.2.3 Comparison of installation costs  $C_{in}$ , initial investment costs  $C_{ic}$  and energy costs  $C_e$  for pumping stations with different requirements of  $NPSH_{av}$

### $C_e$ - Predicted energy costs for the pumping system operation

The energy costs  $C_e$ , which also include the costs for possible driver control and auxiliary services, are usually one of the larger cost elements. They have a decisive importance if the pumps are operating for more than 2000 hours per annum. The energy costs are especially relevant when they are of the same magnitude or higher than the initial investment costs:  $C_e \geq C_{ic}$ .

The energy-saving potentials of different pump types and their applications also have to be taken into account when determining the LCC. A high energy-saving potential is presented especially by large pumps with continuous operation: pumps for power plants, water or oil transport, well pumps and cooling system pumps for different processes. An energy-saving potential also exists in small pumps, such as household pumps, even if the power input is low. However, a large number of pumps is involved and consequently absolute energy saving is again large. On the contrary, the energy-saving potential is small for pumps with intermittent operation, such as pumps in sewage and drainage systems.

When the pumping station flow rate varies considerably over time, the influence of the number of pumps in operation has a large effect on the energy consumption. By dividing the total flow over several pumps, the optimum number of pumps in operation can be determined. In such cases the possibility of an additional speed control for the pump drive is often relevant and has to be investigated in order to see whether there is an economic justification. By varying the above-mentioned parameters, a final result can be found for the minimum value of the LCC.

Important elements influencing the energy costs  $C_e$  are: running time per year, specific cost of the energy, head losses in the piping, and pump and driver efficiencies. When analysing costs it also has to be taken into account that the energy costs  $C_e$  are closely linked to the initial investment costs  $C_{ic}$  and installation costs  $C_i$ , as shown in Figs. O.2.2 and O.2.3. The optimal solution can be found by a systematic variation of the parameters until the minimum value for the LCC is reached.

### $C_o$ - Operating labour costs

These costs are the labour costs under normal system supervision, and are basically related to the operation of the whole pumping system, and can be strongly influenced by the complexity of the system. Large reductions in costs can be obtained with a fully automated system. Such a system requires reduced supervision, and normally includes the measurement of pressure, temperature, power consumption, flow, and also in many cases pump vibration. Changes in these data alert the operator and give him the possibility of taking corrective measures. Such automatic supervision increases the initial investment costs  $C_{ic}$ , but also reduces decisively the operating costs  $C_o$ .

### $C_m$ - Routine and preventive maintenance costs, including predicted repairs

Maintenance and repair costs can often be of the same order as the energy costs. These costs are dominated by expenditure on labour and overheads. It is obvious that the pump design, including its auxiliary elements, very much influences the maintenance costs  $C_m$ . The maintenance costs can be reduced by programming in advance the period of annual shutdown, or carrying out overhauls during a changeover of the processes.

As shown in Fig. O.2.4 for the three maintenance philosophies, maintenance planning by the end-user decisively influences the maintenance costs  $C_m$  in the whole pump life cycle.

Different possibilities for carrying out maintenance should be investigated during the planning phase, in order to minimise expenditure. It is obvious that different maintenance philosophies lead to different maintenance costs  $C_m$ ; but on the other hand they also influence the initial investment costs  $C_{ic}$ , due to the costs of instru-

ments and monitoring systems. However, with a higher degree of maintenance, the MTBF (mean time between failures) can be drastically reduced. The trends in the wear in different elements of the pump, extrapolated on the basis of past experience, will make it possible to decide on the most economical time for servicing, thus avoiding unforeseen breakdowns.

requirements	maintenance philosophy	comments
	operate until failure	<ul style="list-style-type: none"> <li>• uncertain availability</li> <li>• only for redundant systems</li> <li>• high repair costs</li> </ul>
maintenance plan →	calendar-driven maintenance	<ul style="list-style-type: none"> <li>• preventive maintenance</li> <li>• bad operation / downtime ratio</li> <li>• high maintenance costs</li> </ul>
monitoring system →	condition-based maintenance	<ul style="list-style-type: none"> <li>• predictive availability</li> <li>• low machine downtime due to diagnostic information</li> </ul>

Fig. O.2.4 Influence of maintenance philosophies on different cost parameters and availability

**C<sub>s</sub> - Downtime costs as a result of production loss**

Unexpected downtime costs, including loss of production, can have a very significant influence on the LCC. This is especially the case, where the costs of the lost energy production (valid for pumps in power plants, and pumping stations for oil and gas) are unacceptably high. For such cases, a back-up pumping system is needed with additional pumps installed in parallel to the pumps in operation. The initial investment costs  $C_{ic}$  then become higher, but the downtime costs  $C_m$  are lower.

Unexpected breakdowns (failures) of a pump or its elements cannot generally be predicted. Based on statistics, the pump manufacturer can estimate the MTBF (mean time between failures) for different types of pump, as well as for the strategic elements of the latter, like seals, bearings, etc. It must be pointed out that the level of failure (breakdown), depends heavily on the phase in which the pump operates within its lifetime (see Fig. O.2.5). In phase I, representing the commissioning phase, the level of failure is high. In phase II, the disturbances in the pump system are practically independent of the running time. They are mostly due to the pump design quality, and should be very low. In phase III, the failure rate has a rising tendency, and is a consequence of wear in the different elements of the pump.

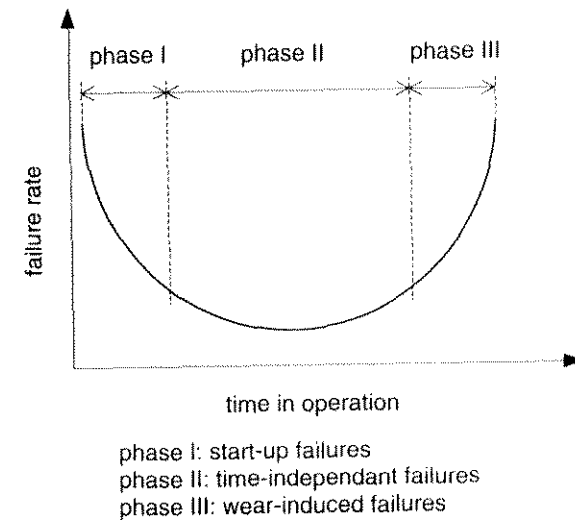


Fig. O.2.5 Operating phases during pump lifetime

**C<sub>env</sub> - Environmental costs**

These costs include the disposal of auxiliary equipment and also of contaminated liquids, the latter varying significantly with the nature of the pumped fluid. In order to reduce the amount of ecologically dangerous contamination, some precautions can be foreseen in the planning stage. However, these measures are connected to a rise in the initial investment costs  $C_{ic}$ , ultimately influencing the LCC.

**C<sub>d</sub> - Decommissioning costs, also including local environmental needs**

When the true total costs of the whole pumping system have to be determined, these costs must be estimated, and the LCC compared for the various alternatives. Usually the results of such investigations show that there is no large difference in LCC between the different alternative pumping systems.

# P. GENERAL TABLES

quantity	name	unit	symbol	quantity	name	unit	symbol
length	metre	m	m	force	newton	N	N
mass	kilogram	kg	kg	torque	newton-metre	Nm	Nm
time	second	s	s	energy	joule	J	J
electric current	ampere	A	A	power	watt	W	W
temperature	kelvin	K	K	pressure	pascal	Pa	Pa
area	square metre	m <sup>2</sup>	m <sup>2</sup>	density		kg/m <sup>3</sup>	kg/m <sup>3</sup>
volume	cubic metre	m <sup>3</sup>	m <sup>3</sup>	kinematic		m <sup>2</sup> /s	m <sup>2</sup> /s
velocity		m/s	m/s	viscosity			
acceleration		m/s <sup>2</sup>	m/s <sup>2</sup>	frequency	hertz	Hz	Hz
				rotational speed		1/s	1/s

Table P.1 SI units

quantity	unit	fps system	SI (mks) system
length	foot	1 ft	1 ft = 0.3048 m
area	square foot	1 ft <sup>2</sup>	1 ft <sup>2</sup> = 0.092903 m <sup>2</sup>
volume	cubic foot	1 ft <sup>3</sup>	1 ft <sup>3</sup> = 0.0283169 m <sup>3</sup>
	US gallon	1 gal (US)	1 gal (US) = 3.785 l
	UK gallon	1 gal (UK)	1 gal (UK) = 4.546 l
velocity	foot per second	1 ft/s	1 ft/s = 0.3048 m/s
acceleration	foot per square second	1 ft/s <sup>2</sup>	1 ft/s <sup>2</sup> = 0.3048 m/s <sup>2</sup>
mass	pound	1 lb	1 lb = 0.453592 kg
force	pound force	1 lbf	1 lbf = 4.44822 N
energy	foot pound	1 ft lb	1 ft lb = 1.35582 J
pressure	pound per square inch	1 lb/in <sup>2</sup>	1 lb/in <sup>2</sup> = 6894.76 N/m <sup>2</sup>
density	pound per cubic foot	1 lb/ft <sup>3</sup>	1 lb/ft <sup>3</sup> = 16.0185 kg/m <sup>3</sup>
temperature	degree fahrenheit	1 °F	°F = 9/5 °C + 32
power	foot pound per second	1 ft lb/s	1 ft lb/s = 1.35582 W
kinematic	square foot per second	1 ft <sup>2</sup> /s	1 ft <sup>2</sup> /s = 0.092903 m <sup>2</sup> /s
viscosity			

Table P.2 Conversion of units

temperature	pressure	density	specific heat at constant pressure	dynamic viscosity	kinematic viscosity
T (°C)	P (bar)	ρ (kg/m <sup>3</sup> )	C <sub>p</sub> (kJ/kg.K)	η (10 <sup>-6</sup> kg/m.s)	ν (10 <sup>-6</sup> m <sup>2</sup> /s)
0.01	0.006112	999.8	4.217	1750	1.75
10	0.012271	999.7	4.193	1300	1.30
20	0.023368	998.3	4.182	1000	1.00
30	0.042417	995.7	4.179	797	0.800
40	0.073749	992.3	4.179	651	0.656
50	0.12334	988.0	4.181	544	0.551
60	0.19919	983.2	4.185	463	0.471
70	0.31161	977.7	4.190	400	0.409
80	0.47359	971.6	4.197	351	0.361
90	0.70108	965.2	4.205	311	0.322
100	1.0132	958.1	4.216	279	0.291
110	1.4326	950.7	4.229	252	0.265
120	1.9854	942.9	4.245	230	0.244
130	2.7012	934.6	4.263	211	0.226
140	3.6136	925.8	4.258	195	0.211
150	4.7597	916.8	4.310	181	0.197
160	6.1804	907.3	4.339	169	0.186
170	7.9202	897.3	4.371	159	0.177
180	10.003	886.9	4.408	149	0.168
190	12.552	876.0	4.449	141	0.161
200	15.551	864.7	4.497	134	0.155
210	19.080	852.8	4.551	127	0.149
220	23.201	840.3	4.614	122	0.145
230	27.979	827.3	4.686	116	0.140
240	33.480	813.6	4.770	111	0.136
250	39.776	799.3	4.869	107	0.134
260	46.940	783.9	4.986	103	0.131
270	55.051	767.8	5.126	99.4	0.129
280	64.191	750.5	5.296	96.1	0.128
290	74.448	732.1	5.507	93.0	0.127
300	85.917	712.2	5.773	90.1	0.127
310	99.697	690.6	6.120	86.5	0.125
320	112.90	666.9	6.586	83.0	0.124
330	128.65	640.5	7.248	79.4	0.124
340	146.08	610.3	8.270	75.4	0.124
350	165.37	574.5	10.08	70.9	0.123
360	186.74	528.3	14.99	65.3	0.124
370	210.53	448.3	53.92	56.0	0.125
374.15	221.20	315.5	∞	45.0	0.143

Table P.3 Characteristic values of water in saturation state

liquid	temperature (°C)	density (kg/m <sup>3</sup> )	liquid	temperature (°C)	density (kg/m <sup>3</sup> )
gasoline			mineral	20	0,88-0,96
- aviation	15	0,72	lubricating oil		
- light	15	0,68-0,72	naphthalene	19	0,76
- normal	15	0,72-0,74	paraffin oil	20	0,90-1,02
- heavy	15	0,75	petroleum	15	0,79-0,82
- premium	15	0,75-0,78	vegetable oil	15	0,90-0,97
beer	15	1,02-1,04	crude oil	20	0,7-1,04
diesel fuel	15	0,82-0,84	- arabian		0,85
gas oil	15	0,85-0,89	- iranian		0,835
gear oil	15	0,92	- kuwaiti		0,87
fuel oil			- libyan		0,83
- extra light	15	0,83-0,85	- romanian		0,854
- light	15	0,86-0,91	- venezuelan		0,935
- medium	15	0,92-0,99	silicone oil	20	0,94
- heavy	15	0,95-1,00	tar	25	1,22-1,24
- from residual oil	20	0,89-0,98	tar oil		
hydraulic oil	20	0,875	- lignite	20	0,88-0,92
kerosene	15	0,78-0,82	- bituminous coal	20	0,9-1,1
machine oil			wine	15	0,99-1,0
- light	15	0,88-0,90	sugar solution		
- medium	15	0,91-0,935	10%	20	1,04
seawater	15	1,02-1,03	20%	20	1,08
milk	15	1,02-1,05	30%	20	1,18
			40%	20	1,28

Table P.4 Density of various liquids

name	chemical formula	density $\rho$ in kg/m <sup>3</sup> (temperature in °C)							
		-75	-50	-25	0	20	50	100	150
acetone	C <sub>3</sub> H <sub>6</sub> O	0,983	0,868	0,840	0,812	0,791	0,756		
ethyl alcohol	C <sub>2</sub> H <sub>6</sub> O				0,806	0,789	0,763	0,716	0,649
formic acid	CH <sub>2</sub> O <sub>2</sub>					1,220	1,184		
aniline	C <sub>6</sub> H <sub>7</sub> N				1,039	1,022	0,996	0,951	
ethyl chloride	C <sub>2</sub> H <sub>5</sub> Cl				0,919	0,892	0,846		
ethylene	C <sub>2</sub> H <sub>4</sub>	0,525	0,482	0,482	0,346				
ethylene glycol	C <sub>2</sub> H <sub>6</sub> O <sub>2</sub>				1,128	1,112			
benzene	C <sub>6</sub> H <sub>6</sub>					0,879	0,847	0,793	0,731
chlorobenzene	C <sub>6</sub> H <sub>5</sub> Cl				1,128	1,106	1,074	1,019	0,960
diethylether	C <sub>4</sub> H <sub>10</sub> O	0,816	0,790	0,764	0,736	0,714	0,676	0,611	0,518
acetic acid	C <sub>2</sub> H <sub>4</sub> O <sub>2</sub>					1,049	1,018	0,960	0,896
glycerol	C <sub>3</sub> H <sub>8</sub> O <sub>3</sub>				1,273	1,261	1,212	1,209	
isobutene	C <sub>4</sub> H <sub>10</sub>			0,611	0,584	0,559	0,520		
hexane	C <sub>6</sub> H <sub>14</sub>	0,742	0,721	0,700	0,678	0,659	0,631	0,580	0,520
methyl alcohol	CH <sub>4</sub> O				0,810	0,792	0,765	0,714	0,650
propane	C <sub>3</sub> H <sub>8</sub>	0,619	0,590	0,560	0,528	0,501	0,450		
propylene	C <sub>3</sub> H <sub>6</sub>				0,590	0,550	0,478		
toluene	C <sub>7</sub> H <sub>8</sub>				0,885	0,868	0,839	0,793	0,737
water	H <sub>2</sub> O				0,999	0,998	0,988	0,958	

Table P.5 Density of pure liquids as a function of temperature

material	density kg/m <sup>3</sup>	modulus of elasticity N/mm <sup>2</sup>	melting point °C
aluminium	2,7	64000	660
antimony	6,62	77400	630
beryllium	1,82	287140	1280
bismuth	9,8	34127	271
brass	8,4	88260	900
bronze			
- Cu Sn 8	8,8	106000	~ 875
- Cu Al 10 Fe 5 Ni 5	7,6	118000	~ 1060
cadmium	8,65	62270	321
chromium	7,2	186330	1890
cobalt	8,9	208685	1495
copper	8,96	122580	1083
gold	19,3	77470	1063
iron (cast - GG 25)	7,2	~ 110000	1300
iron (pure)	7,87	211330	1539
lead	11,34	15690	327
lithium	0,53	11470	186
magnesium	1,74	44280	650
mercury	13,55	-	- 38,9
molybdenum	10,2	329800	2625
monel metal	8,58	155900	1320
nickel	8,9	193000	1455
niobium	8,57	156900	2415
platinum	21,45	169850	1775
red brass	8,7	93160	960
silver	10,47	80020	960
sodium	0,97	8920	98
steel			
- Ck 35	7,85	202000	1500
- 10 Cr Mo 9-10	7,76	211000	1500
- 13 Cr Mo 4-4	7,85	213000	1490
tantalum	16,6	184560	3000
tin	7,30	53940	232
titanium	4,54	103170	1800
tungsten	19,3	407270	3410
vanadium	6,0	147100	1735
zink	7,14	92182	419
zirconium	6,5	68350	1850

Table P.7a Physical properties of metals

material	thermal conductivity W/m.K	coefficient of linear expansion 10 <sup>-6</sup> .K <sup>-1</sup>	specific heat kJ/kg.K
aluminium	203	24	0,83
antimony	21	10	0,21
beryllium	160	12	2,18
bismuth	8,3	12,4	0,14
brass	92	18	0,39
bronze			
- Cu Sn 8	~ 45	20	0,4
- Cu Al 10 Fe 5 Ni 5	37	19	0,38
cadmium	92	30,8	0,23
chromium	67	6,2	0,46
cobalt	69	12,3	0,41
copper	394	16,2	0,39
gold	314	14,2	0,13
iron (cast - GG 25)	48	9,0	0,54
iron (pure)	50	49	0,46
lead	35	28	0,13
lithium	71	58	3,31
magnesium	159	24,5	1,05
mercury	8	61	2,14
molybdenum	146	5	0,26
monel metal	25	14	0,50
nickel	92	13,3	0,44
niobium	-	7	0,27
platinum	71	8,9	0,13
red brass	58	17	-
silver	418	19,7	0,23
sodium	134	72	1,24
steel			
- Ck 35	51	12	0,48
- 10 Cr Mo 9-10	44	12,5	0,46
- 13 Cr Mo 4-4	44	12,5	0,46
tantalum	54	6,6	0,15
tin	67	20,5	0,23
titanium	17	10,8	0,53
tungsten	201	4,5	0,13
vanadium	-	8,5	0,50
zink	113	29,8	0,38
zirconium	-	10	10,22

Table P.7b Physical properties of metals



# NOMENCLATURE

A	area, minimal rolling contact bearing load factor
B	length (hydrodynamic radial bearing)
BEP	best efficiency point
B <sub>2</sub>	impeller outlet width including shrouds
C	rated bearing dynamic load
CNL	cavitation noise level
D	diameter
D <sub>0</sub>	hub diameter
D <sub>1</sub>	eye diameter
E <sub>R</sub>	erosion rate
E	erosion (depth)
F	force, thrust
Fr	Froude number
F <sub>a min</sub>	minimal required rolling contact bearing axial load
F <sub>as</sub>	axial force acting on mechanical seal
F <sub>cor</sub>	corrosion factor
F <sub>mat</sub>	material factor
F <sub>A</sub>	axial thrust
F <sub>R</sub>	radial thrust
I	sound intensity
J	moment of inertia
L	length
LCC	life cycle costs
L <sub>cav</sub>	cavity length
L <sub>i</sub>	sound intensity level
L <sub>p</sub>	sound pressure level (SPL)
L <sub>w</sub>	sound power level
L <sub>10h</sub>	rated rolling contact bearing lifetime (millions of hours)
M	torque
N	pump rotational speed
NPSH	net positive suction head
P	power, power losses, equivalent dynamic rolling contact bearing load
PC = P/A = 4.P/π·D <sub>2</sub> <sup>2</sup>	power concentration
PRE	pitting resistance equivalent
R	radius
Re	Reynolds number
R <sub>m</sub>	tensile strength
S	submergence, relative shaft displacement
S <sub>R</sub>	radial clearance (wear ring, piston)
So	Sommerfeld number
T	temperature
Q	flow rate, volumetric losses, ISO balance grade
V	volume
X	factor of radial force (rolling contact bearing calculation)
Y	specific energy, factor of axial force (rolling contact bearing calculation)

a	sound velocity
c	absolute velocity, sound velocity in air, correction coefficient
c <sub>p</sub>	specific heat of the fluid
d	diameter, thickness
e	eccentricity (hydrodynamic radial bearing)
f	frequency, friction coefficient
g	acceleration due to gravity
h	gap
k	constant, coefficient, hydraulic load factor (mechanical seal)
k <sub>R</sub>	radial thrust coefficient
k <sub>R0</sub>	radial thrust coefficient at Q=0
m	mass, number of diametrical nodes defining pressure pattern
n	speed of rotation
n <sub>q</sub>	specific speed (European)
n <sub>s</sub>	specific speed (American)
n <sub>ss</sub>	suction specific speed
p	pressure, exponent of the rolling contact bearing lifetime equation
r	radius
s	width (stuffing ring)
t	time, tolerance factor
u	peripheral velocity
v	velocity
w	relative velocity, coefficient in efficiency correction formula
w <sub>0</sub>	relative velocity at impeller throat
x	mass concentration of slurry
y	coefficient in efficiency correction formula
z	elevation from the reference plane, number of blades
α	absolute flow angle, gas content in the fluid
β	angle, relative flow angle
β <sub>T</sub>	compressibility coefficient
ν	kinematic viscosity, order number of impeller or diffuser periodicity
ε	relative eccentricity
η	efficiency, pump total efficiency, dynamic viscosity
φ	casing angle, cylindrical coordinates
λ <sub>w</sub>	pressure drop coefficient
π	Ludolf number
ρ	density
ρ'	density of fluid
ρ''	density of saturated steam
τ	shear stress
ω	angular speed
ψ	head coefficient, relative gap (hydrodynamic radial bearing)
Δ	difference

## Indices

a	auxiliary, admissible
av	available
b	barometric
bd	balancing device
bs	back shroud
c	casing
ch	channel
cv	control valve
ct	casing throat
d	pressure (discharge) side, disc, decommissioning
des	design
dp	disc/piston
dyn	dynamic
e	exit, energy
env	environmental
f	friction
fs	front shroud
g	gasket
gas	gas
geo	geodetic
gr	combined motor/pump unit
h	hydraulic, horizontal
i	internal, incidence, implosion, impulse, inner
ic	isentropic compression, initial investment
imp	impeller
in	installation
l	left
liq	liquid
loss	losses
m	meridional, mechanical, model, mean, maintenance
max	maximal
min	minimal
mot	motor
mu	mechanical unbalance
n	noise, pump rotational speed
nc	non-cavitating
o	outer, operation
opt	at optimal duty point (at maximal efficiency)
p	piston, pro
p-p	peak to peak
pip	pipeline
r	right, reaction, riser

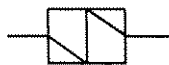
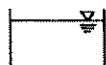
ref	reference
req	required
s	suction side, screw, spring, seal, solid
sb	stuffing box
sh	shaft
sl	slurry
sr	sealing ring
st	static, stage
synh	synchronous
sys	system
t	tightening
te	turning elbow
tr	transition
th	theoretical (finite number of blades)
u	peripheral component of velocity, useful
v	volumetric
vc	vertical can
vis	viscosity
vp	vapour pressure
w	water
A	acceleration, axial, bearing A
B	blade, bearing B
D	diameter, excitation
G	guarantee
H	head
L	leakage
M	motor
N	nominal
P	pump
Q	flow rate
R	reference, radial
T	temperature
Y	star circuit
$\Delta$	delta circuit
$\eta$	efficiency
0	at $Q = 0$ , at $n = 0$
1	impeller inlet, first
2	impeller outlet, impeller, second
2s	between two stages
2R, R	at reduced impeller outlet
3	diffuser inlet or volute tongue, diffuser
3%	at 3% head drop

**Graphical symbols:**

valve

control valve,  
throttling device

check valve

pump,  
pumping unitheat exchanger,  
element symbolising  
pressure loss

open tank



closed tank

**LITERATURE****Books:**

- Anderson, H.H., Centrifugal pumps: Trade&Technical Press Ltd., 1980
- Beitz, W. and Kuettner, K.H., Dubbel – Taschenbuch fuer den Maschinenbau, Springer Verlag, 1995
- Bohl, W., Stroemungsmaschinen 1 and 2, Vogel Buchverlag, 1994/1995
- Florjancic, D., Handbook for pump users (in Slovene), University Ljubljana, 2002
- Guelich, J.F., Kreiselpumpen, Springer Verlag, 1999
- Karassik, I.J. and al., Pump handbook, McGraw-Hill Book Co., 1986
- Neumaier, R., Hermetic pumps, Verlag und Bildarchiv, 2000
- Neumann, B., Interaction between geometry and performance of a centrifugal pump, Mechanical Engineering Publications Ltd., 1991
- Stepanoff, A.J., Centrifugal and axial flow pumps, Wiley, 1957
- Wagner, W., Kreiselpumpen und Kreiselpumpenanlagen, Vogel Buchverlag, 1994

**Conference proceedings, reports:**

- ASME Fluid Engineering Division Summer Meeting, New Orleans, USA, 2001
- International Conference on Pumps and Fans, Beijing, China, 1995
- International Pump Users Symposium, Houston, USA, 2000, 2001
- Pumpentagung, Karlsruhe, Germany, 1996, 2000
- EPRI CS-4204, GS-7398: Suction effects on feed pump performance
- EPRI GS-7405: Rotor dynamic and thermal deformation tests of high-speed boiler feed pumps
- EPRI GS-6398: Guidelines for prevention of cavitation in centrifugal feed pumps
- EPRI TR-102102: Feed pump operation and design guidelines
- Europump: Attainable efficiencies for volute casing pumps, 1999
- Europump: NPSH for rotodynamic pumps, 1999

**Standards:**

- ANSI/HI 1.1-1.5: Centrifugal pumps (ANSI/HI 1.1-1.5), 1994
- ANSI/HI 1.6: Centrifugal pump tests (ANSI/HI 1.6), 1994
- ANSI/HI 2.1-2.5: Vertical pumps (ANSI/HI 2.1-2.5), 1994

- ANSI/HI 2.6: Vertical pump tests (ANSI/HI 2.6), 1994
- ANSI/HI 9.1-9.5: Pumps - General Guidelines (ANSI/HI 9.1-9.5), 1994
- ANSI/HI 9.8: Pump intake design, 1994
- API 610/8: Centrifugal Pumps for General Refinery Service, 1995
- API 670: Vibration, Axial Position, and Bearing Temperature Monitoring Systems, 1993
  
- DIN 1944: Abnahmeversuche an Kreiselpumpen, 1968
  
- EN 10027: Designation systems for steels – Parts 1 and 2, 1992
- EN 12639: Liquid pumps and pumps units - Noise test code - Grades 2 and 3 of accuracy, 2000
  
- EN ISO 3743: Acoustics - Determination of sound power levels of noise sources - Engineering methods for small, movable sources in reverberant fields - Parts 1 and 2, 1995-1996
- EN ISO 3744: Acoustics - Determination of sound power levels of noise sources using sound pressure -Engineering method in an essentially free field over a reflecting plane, 1995
- EN ISO 3746: Acoustics - Determination of sound power levels of noise sources using sound pressure -Survey method using an enveloping measurement surface over a reflecting plane, 1995
- EN ISO 9614: Acoustics - Determination of sound power levels of noise sources using sound intensity - Parts 1 and 2, 1995-1996
  
- ISO 5198: Centrifugal, mixed flow and axial pumps - Code for hydraulic performance tests - Precision class, 1987
- ISO 5199: Technical specifications for centrifugal pumps - Class II, 1986
- ISO 7919: Mechanical vibration of non-reciprocating machines - Measurements on rotating shafts and evaluation criteria - Parts 1-5, 1986-1997
- ISO 9905: Technical specifications for centrifugal pumps - Class I, 1994
- ISO 9906: Rotodynamic pumps - Hydraulic performance acceptance tests - Grades 1 and 2, 1999
- ISO 9908: Technical specifications for centrifugal pumps - Class III
- ISO 10816: Mechanical vibration - evaluation of machine vibration by measurements on non-rotating parts - Parts 1-5, 1995-2000

**Technical catalogues:**

Burgmann, Flender, Flexibox, Glacier, Hermetic, SKF, Thordon, Voith-Turbo

**TERMOMECCANICA  
CENTRIFUGAL PUMP  
HANDBOOK**

Printed in Perugia - Italy, by Grafiche Diemme  
Layout SLF, La Spezia - Italy